BASIC STUDY ON THERMOTOLERANT YEAST *Kluyveromyces marxianus* DMKU 3-1042 TOWARD EFFICIENT CONVERSION OF CELLULOSIC BIOMASS TO ETHANOL

(セルロース系バイオマスの効率的なエタノール変換に向けた耐熱性酵母 *Kluyveromyces marxianus* DMKU 3-1042 の基盤研究)

SUPRAYOGI

GRADUATE SCHOOL OF MEDICINE
YAMAGUCHI UNIVERSITY
JAPAN

2016

BASIC STUDY ON THERMOTOLERANT YEAST

CONTENTS

Pages

LIST OF TABLES vi
LIST OF FIGURES ix
LIST OF ABBREVIATIONS xii

CHAPTER 1
General Introduction and Literature Review 1

1.1 General Introduction 1
1.2 Literature Review 2
1.2.1 Feedstocks for bioethanol production 2
1.2.1.1 The first generation feedstocks 2
1.2.1.2 The second generation feedstocks 2
1.2.1.3 The third generation feedstocks 4
1.2.2 *Kluyveromyces marxianus* 5
1.2.3 Glucose repression 5

CHAPTER 2
A *Kluyveromyces marxianus* 2-deoxyglucose-resistant mutant with enhanced activity of xylose utilization 8

2.1 Abstract 8
2.2 Introduction 8
2.3 Materials and methods 10
2.3.1 Strain and media 10
2.3.2 Cultivation conditions and spotting test 10
2.3.3 Screening and phenotype characterization of 2-DOG-resistant mutants 11
2.3.4 Analytical methods 11

CONTENTS
(Continued)

Pages

2.3.5 Determination of oxidized Nicotinamide Adenine Dinucleotide (NAD^+) and reduced Nicotinamide Adenine Dinucleotide (NADH) concentration 12
2.3.6 Preparation of cell extracts 12
2.3.7 Enzyme assays 13
2.3.8 Nucleotide sequencing and alignment 13
2.4 Results 14
2.4.1 Screening and phenotype characterization of 2-DOG-resistant mutants 14
2.4.2 Cell growth and sugar consumption of 2-DOG-resistant mutants in YP medium containing mixed sugars of Glc and Xyl 17
2.4.3 NAD^+ and NADH concentrations in no. 23 mutant in YP medium containing mixed sugars of Glc and Xyl 20
2.4.4 Weak hexokinase activity in no. 23 mutant 21
2.4.5 Determination of a mutation site on no. 23 mutant. 22
2.5 Discussion 24
2.6 Conclusion 26

CHAPTER 3
Characteristics of *kan*MX4-inserted mutants that exhibit 2-deoxyglucose resistance in thermotolerant yeast *Kluyveromyces marxianus* 27

3.1 Abstract 27
3.2 Introduction 27
3.3 Materials and methods 29
3.3.1 Strain and media 29
3.3.2 Cultivation conditions 29

CONTENTS
(Continued)

Pages

3.3.3 Construction of *kan*MX4-inserted mutants and screening of 2-DOG-resistant mutants 30
3.3.4 Analysis of *kan*MX4-inserted position 30
3.3.5 Complementation of *kan*MX4-inserted mutants with DNA fragments of the target gene and drug-resistance gene 31
3.3.6 Analytical methods 33
3.4 Results 33
3.4.1 Isolation of 2-DOG-resistant mutants by insertion of *kan*MX4 .. 33
3.4.2 Possible functions of genes in which *kan*MX4 was inserted in 2-DOG-resistant mutants 34
3.4.3 Growth phenotype of 2-DOG-resistant mutants in the presence of 2-DOG 35
3.4.4 Comparison of cell growth among 2-DOG-resistant mutants in YP medium containing a single sugar or mixed sugars 39
3.4.5 Cell growth of 2-DOG-resistant mutants in different concentration of Glc 41
3.4.6 Effect of antimycin A on cell growth of 2-DOG-resistant mutants 41
3.4.7 Cell growth and sugar consumption of 2-DOG-resistant mutants in YP medium containing mixed sugars of Glc and Xyl 42
3.5 Discussion 44
3.6 Conclusion 47

CHAPTER 4
Genetic basis of the highly efficient yeast *Kluyveromyces marxianus*: complete genome sequence and transcriptome analyses 48

CONTENTS
(Continued)

Pages

4.1 Abstract 48
4.1.1 Background 48
4.1.2 Results 48
4.1.3 Conclusions 49
4.2 Introduction 49
4.3 Materials and methods 50
4.3.1 Strains, media and culture conditions 50
4.3.2 Genome sequencing, assembly, and annotation 51
4.3.3 Transcriptome analysis in *K. marxianus* 52
4.3.4 Nucleotide sequence accession numbers 53
4.3.5 Quantitative real-time PCR (qPCR) analysis 53
4.4 Results 54
4.4.1 Genomic information and comparative genomics 54
4.4.2 Ribosomal DNA (rDNA) copy number and thermotolerance 57
4.4.3 Genes regulated under a static condition 58
4.4.4 Genes regulated under a high-temperature condition 60
4.4.5 Genes regulated under a xylose-utilizing condition 66
4.5 Discussion 67
4.6 Conclusions 72

CHAPTER 5
Essentiality of respiratory activity for pentose utilization in thermotolerant yeast *Kluyveromyces marxianus* DMKU 3-1042 164

5.1 Abstract 164
5.2 Introduction 164
5.3 Materials and methods 167
5.3.1 Materials 167
5.3.2 Strains, media and culture conditions 167

CONTENTS
(Continued)

Pages

5.3.3 Genetic and molecular biological techniques 167
5.3.4 Untargeted integration mutagenesis, screening and characterization of mutants 168
5.3.5 Complementation of *kan*MX4-insertion mutants with DNA fragments of the target gene and drug-resistance gene 168
5.3.6 Analytical methods 169
5.4 Results 170
5.4.1 Isolation and characterization of pentose utilization-defective mutants 170
5.4.2 Growth and fermentation ability of pentose utilization-defective mutants 171
5.4.3 Effects of respiratory inhibitors on cell growth and ethanol production in the wild-type strain 174
5.4.4 Respiratory activities and low-temperature reduced-minus-oxidized difference spectra 176
5.5 Discussion 179

REFERRENCES 184
ACKNOWLEDGEMENTS 199
SUMMARY 200
LIST OF PUBLICATIONS 202

LIST OF TABLES

Tables Pages

CHAPTER 1

1.1 Reported composition (g/100 g dry matter) of some pentose-rich lignocellulosic feedstocks 4

CHAPTER 2

2.1 Primers used in this study 14

2.2 Hexokinase and glucokinase activities of 2-DOG-resistant no. 23 mutant 22

CHAPTER 3

3.1 Primers used in this study 32

3.2 Orthologues of *S. cerevisiae* and *K. lactis* to the product of gene, which was inserted by *kan*MX4 in mutants 37

CHAPTER 4

4.1 General genome information of nuclear and mitochondrial genomes of *K. marxianus* DMKU 3-1042 54

4.2 General characteristics of 11 hemiascomyceteous yeast genomes 55

4.3 Genes for utilization of sugars at their initial catabolism and genes for alcohol dehydrogenases in *K. marxianus* 58

S1 KOG assignment summary of *K. marxianus* genomic genes 83

S2 Unique genes in *K. marxianus* 83

S3 KOG categories of genes specific for *K. marxianus* 87

S4 Genes shared only between *K. marxianus* and *K. lactis* 87

S5 Ortholog genes shared between *K. marxianus* and *O. parapolymorpha*, which are absent from *K. lactis* 95

S6 Sugar transporters predicted in *K. marxianus* 96

S7 rDNA copy number analysis of several *K. marxianus* strains 96

S8 Numbers of genes significantly changed in expression under different conditions (FDR < 0.05) 97

LIST OF TABLES

(Continued)

Tables Pages

S9 GO terms enriched in significantly up-regulated genes under 30DS condition 97

S10 Summary of significantly up-regulated genes under the 30DS condition 105

S11 GO terms enriched in significantly down-regulated genes under 30DS condition 111

S12 Summary of significantly down-regulated genes under the 30DS conditions..... 113

S13 GO terms enriched in significantly down-regulated genes under 45D condition 120

S14 Summary of significantly down-regulated genes under the 45D condition 122

S15 GO terms enriched in significantly up-regulated genes under 45D condition 143

S16 Summary of significantly up-regulated genes under the 45D condition 146

S17 Subcellular localization of products of significantly expressed genes .. 153

S18 HSP and oxidative stress response genes 153

S19 GO terms enriched in significantly up-regulated genes under 30X condition 155

S20 Summary of significantly up-regulated genes under the 30X condition 156

S21 GO terms enriched in significantly down-regulated genes under 30X condition 159

S22 Summary of significantly down-regulated genes under the 30X condition 161

CHAPTER 5

5.1 Primers used in this study 169

5.2 Identification of *kan*MX4-insertion sites of mutants isolated by TAIL-PCR and nucleotide sequencing 170

LIST OF TABLES

(Continued)

Tables Pages

5.3 Effect of potassium cyanide on respiratory activities in mutants isolated and its parental strain..... 177

LIST OF FIGURES

Figures Pages

CHAPTER 1

1.1 A schematic illustration of the process design for the cellulosic bioethanol production 3

1.2 A model explaining the involvement of Mig1 in the nucleocytoplasmic translocation of Hxk2 7

CHAPTER 2

2.1 Spotting test of 2-DOG-resistant isolates 15

2.2 Growth of 2-DOG-resistant mutants at different concentrations of Glc and effect of antimycin A 16

2.3 Growth and sugar consumption of 2-DOG-resistant mutants in YP medium containing Glc and Xyl 19

2.4 Relative NAD^+/NADH values in 2-DOG-resistant no. 23 mutant in YP medium containing Glc and Xyl 21

2.5 Alignment of amino acid sequences of hexokinases in *K. marxianus, K. lactis and S.cerevisiae* 23

CHAPTER 3

3.1 Resistance of isolated *kan*MX4-inserted mutants to 2-DOG 36

3.2 Comparison of cell growth among 2-DOG-resistant mutants in YP media containing a single sugar of Glc or Xyl or mixed sugars of Glc and Xyl 40

3.3 Cell growth of 2-DOG-resistant mutants in YNB plates containing different concentrations of Glc and effect of antimycin A 41

3.4 Cell growth and sugar consumption of 2-DOG-resistant mutants in YP medium containing mixed sugars of Glc and Xyl 43

LIST OF FIGURES
(Continued)

Figures Pages

CHAPTER 4

4.1 Phylogenetic tree of 11 hemiascomycetous yeast genomes based on 1,361 concatenated amino acid sequences..... 56

4.2 Transcript abundance of genes related to central metabolic pathways under different conditions in *K. marxianus*..... 63

4.3 Transcript abundance of genes related to oxidative stress response in *K. marxianus*..... 65

4.4 Phylogenetic tree of predicted sugar transporters with transcript abundance in *K. marxianus*..... 70

S1 For each chromosome, the upper image represents data from optical mapping while the lower image depicts data from nucleotide sequencing .. 73

S2 Conserved chromosomal segments found between *K. marxianus* and *K. lactis*. Complete genome sequence of *K. lactis* was mapped onto that of *K. marxianus*..... 74

S3 Growth curve comparison among several *K. marxianus* strains under different temperature conditions..... 75

S4 Spot test of several *K. marxianus* strains..... 76

S5 TSS analysis data summarized by logFC/logCPM plot of 30°C xylose shaking (30X)/30°C glucose shaking (30D) (A), 30°C glucose static (30DS)/30D (B) and 45°C glucose shaking (45D)/30D (C)..... 77

S6 Subcellular localization of products from significantly up-regulated or down-regulated genes under different conditions in *K. marxianus*..... 78

S7 Transcript abundance represented by TSS-tag ppm of each genes related to the oxygen-dependent biosynthetic pathways under different conditions in *K. marxianus*..... 79

S8 Transcript abundance represented by TSS-tag ppm of each genes related to the ATP synthase, respiratory chain components and their chaperones under different conditions in *K. marxianus*..... 80

LIST OF FIGURES
(Continued)

Figures Pages

S9 Transcript abundance represented by TSS-tag ppm of each genes related to homologous recombination and non-homologous end-joining under different conditions in *K. marxianus*. 81
S10 Transcript abundance represented by TSS-tag ppm of each genes related to GABA shunt under different conditions in *K. marxianus* 82

CHAPTER 5

5.1 Growth and ethanol productivity of mutants isolated and the parental strain 173
5.2 Growth and ethanol productivity of the wild-type *K. marxianus* in the presence of respiratory inhibitors 175
5.3 Absolute absorption spectra of membrane fractions of mutants isolated and the parental strain 178
5.4 Effects of respiratory inhibitors on cell growth of mutants isolated and the parent..... 180
5.5 A proposed model of the respiratory chain of *K. marxianus* DMKU 3-1042 183

LIST OF ABBREVIATIONS

1,3-DPG	1,3-bisphosphoglycerate
2-DOG	2-deoxyglucose
2PG	2-phosphoglycerate
3PG	3-phosphoglycerate
6P1,5R	6-phospho-D-glucono-1,5-lactone
6PG	6-phosphogluconate
AA	antimycin A
AOX	alternative oxidase
BLAST	Basic local alignment search tool
bp	base pair(s)
CCCP	carbonyl cyanide *m*-chlorophenylhydrazone
Cox	cytochrome *c* oxidase
DHA	dihydroxyacetone
DHAP	dihydroxyacetone phosphate
E4P	erythrose-4-phosphate
F6P	fructose-6-phosphate
FDP	fructose 1,6 bisphosphate
G418	geneticin (antibiotic)
G6-P, G6P	glucose-6-phosphate
Gal	galactose
GAP	glyceraldehyde-3-phosphate
Glc	glucose
HPLC	high performance liquid chromatography
Hsp	heat shock protein
HTF	high temperature fermentation
kanMX4	DNA fragment encoding kanamycin resistance gene
kb	kilo base pair(s) (1,000 bp)
KOG	eukaryotic orthologous groups
LiAc	lithium acetate

LIST OF ABBREVIATIONS
(Continued)

Mb	mega base pair(s)
NAD+	nicotinamide adenine dinucleotide, oxidized form
NADH	nicotinamide adenine dinucleotide, reduced form
NADP+	nicotinamide adenine dinucleotide phosphate, oxidized form
NADPH	nicotinamide adenine dinucleotide phosphate, reduced form
NBRC	NITE biological resource center
NCBI	National center for biotechnology information
Nde1 and 2	external NADH dehydrogenase 1 and 2
Ndh	NADH dehydrogenase
Ndi1	internal NADH dehydrogenase
NR	non-redundant
OD	optical density
OD660	optical density at 660 nm wavelength
PCR	polymerase chain reaction
PEP	phosphoenolpyruvate
PPP	pentose phosphate pathway
PYR	pyruvate
Q	ubiquinone
qPCR	quantitative real-time PCR
R5P	ribose-5-phosphate
rDNA	ribosomal deoxyribonucleic acid
ROS	reactive oxygen species
Ru5P	ribulose-5-phosphate
S7P	sedoheptulose-7-phosphate
SD	standard deviation
Sdh, Sdh1	succinate dehydrogenase 1

LIST OF ABBREVIATIONS
(Continued)

SHAM	salicylhydroxamic acid
SHF	separate of hydrolysis and fermentation
SSF	simultaneous saccharification and fermentation
STO	SHAM-sensitive terminal oxidase
Tm	melting temperature
TSS Seq	transcription start site sequencing
Xul5P	xylulose-5-phosphate
Xyl	xylose
YNB	yeast nitrogen base
YP	yeast extract and peptone
YPA	yeast-peptone-arabinose medium
YPD	yeast-peptone-glucose medium
YPD+Xyl	yeast-peptone-glucose-xylose medium
YPGal	yeast-peptone-galactose medium
YPXyl	yeast-peptone-xylose medium

CHAPTER 1

General Introduction and Literature Review

1.1 General Introduction

Regarding of growth population, increasing demand for fuels, decreasing stocks of natural resources, depletion of fossil fuels, climate change and awareness of carbon dioxide emissions, bioethanol is one of alternative fuels (Popp et al. 2014; Chu and Majumdar 2012; Musatto et al. 2010). Bioethanol has many advantages such as broader flammability limits, less emission of SO_2 and CO_2, higher flame speeds, higher octane number and higher heat of vaporization compared with gasoline (Saxena et al. 2009; Sarkar et al. 2012; Szulczyk et al. 2010). Unlike fossil fuel, bioethanol is renewable and its utilization thus contributes to prevention from emission of greenhouse gas (Farrel et al. 2006) and thus bioethanol becomes very important as an alternative fuel from now to the future. Awareness of global warming and insufficient supply of liquid fuel for transportation has turned to produce a large-scale of ethanol production from forestry residue and agricultural waste (Hahn-Hagerdal et al. 2006).

Most of yeast species are able to utilize sugars extracted from agricultural feedstocks or produced by hydrolyzing starch from edible grains and produce ethanol as a primary metabolite. *Kluyveromyces marxianus* is thermotolerant and ethanologenic yeast which capable to utilize various sugars such as glucose, xylose, galactose, arabinose and sucrose (Rodrussamee et al. 2011). This species is a highly attractive yeast for future developments in producing ethanol at high temperatures. However, glucose repression is a major problem in most yeast species including *K. marxianus* to hamper the utilization of other coexisting sugars. The molecular mechanism of glucose repression in the yeast is thus one of important topics to be studied. In addition to the facilitation of such developments, the genomic information of *K. marxianus* is essential for fundamental and applied researches.

In this study focusing on *K. marxianus* DMKU 3-1042, which is one of the

most thermotolerant and efficiently ethanol-producing yeasts, there are four main objectives: 1) isolation and characterization of glucose repression-defective mutants with enhanced activity of xylose utilization from 2-deoxyglucose (2-DOG) resistant mutants, 2) isolation and characterization of glucose repression-defective mutants from *kan*MX4-inserted mutants, 3) determination of complete genome and analysis of transcriptome and 4) analysis of assimilation of xylose and/or arabinose via a random *kan*MX4 insertion mutagenesis.

1.2 Literature Review

1.2.1 Feedstocks for bioethanol production

1.2.1.1 First generation feedstocks

The production of bioethanol is categorized into the first, second and third generation, depending on feedstocks used (Westman and Franzén, 2015). The first generation bioethanol is produced from sugar or starch, such as sugar cane and cereals (Naik et al. 2010). When starch is used as a raw material, a hydrolysis process is required for fermentation. Whereas, sugar cane juice bearing about 15% sucrose and molasses bearing up to 50% sucrose are directly utilized for fermentation (Walker, 2011). Such feedstocks that contain high concentrations of sugar include relatively low inhibitory compounds are used to produce high concentrations of ethanol (Bothast, 2005).

1.2.1.2 Second generation feedstocks

The second generation bioethanol is made from lignocellulosic materials as feedstocks, which are typically grouped of “biomass”. The biomass such as agricultural residues, municipal solid waste and wood consists of cellulose (40-50%), hemicellulose (25-35) and lignin (15-20%) (Gray, 2006). Due to the high complex of these materials, lignocellulose has to be pretreated before enzymatic hydrolysis, followed by fermentation and the recovery and concentration of

ethanol (Hahn-Hägerdal et al. 2006). There are mainly two methods to perform hydrolysis and fermentation, Separate Hydrolysis and Fermentation (SHF) and Simultaneous Saccharification and Fermentation (SSF). In the both methods, hydrolyzing enzymes are supplied by either microbes or commercial source. The hydrolysis produces pentoses such as xylose and arabinose in addition to hexoses such as glucose, mannose and galactose (Westman and Franzén, 2015; Kim et al. 2013), which are converted to ethanol by fermentation. A summary of ethanol production from lignocellulosic feedstocks is shown in Fig. 1.1. The hemicellulose fractions of many non-food biomass resources like agricultural residues such as corn stover, sugar cane bagasse, wheat straw and rice straw are pentose rich (Table 1).

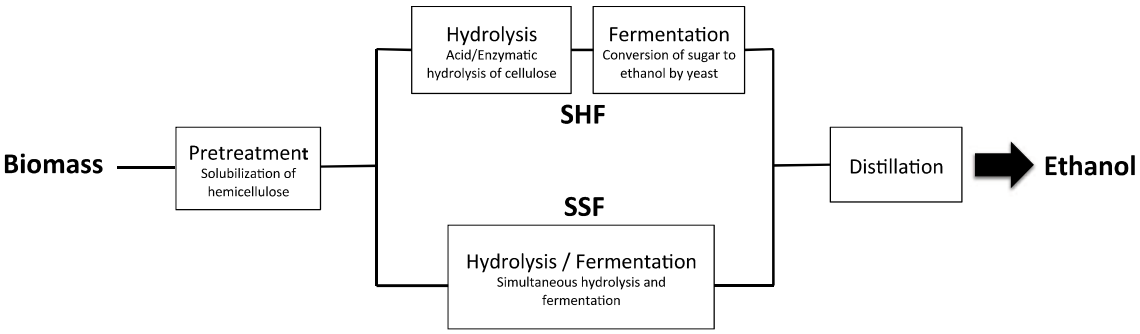

Fig. 1.1 A schematic illustration of the process design of cellulosic bioethanol production. SHF, Separate Hydrolysis and Fermentation; SSF, Simultaneous Saccharification (hydrolysis) and Fermentation. This illustration was reproduced from Hahn-Hägerdal et al. 2007.

Table 1.1 Reported composition (g/100 g dry matter) of some pentose-rich lignocellulosic feedstocks

Material	Glucan	Mannan	Galactan	Xylan	Arabinan	Lignin	Acetyl	Reference
Corn stover (USA)	36.1	1.8	2.5	21.4	3.5	17.2	3.2	Öhgren et al. 2007
Corn stover (Italian)	36.8	0.3	2.9	22.2	5.5	21.2	1.7	Öhgren et al. 2007
Sugar cane bagasse	43.3	NR [a]	NR	24.3	2.0	22.8	2.0	Carrasco et al. 2010
Wheat straw	41.2	NR	NR	26.1[b]	-	19.1	4.2	Remond et al. 210
	32.6		0.8	20.1	3.3	26.5	2.0	Linde et al. 2008
Barley straw	36.8	NR	2.2	17.2	5.3	14.3	NR	Linde et al. 2007
Rice straw	34.2	NR	NR	24.5	NR	11.9	NR	Wiselolgel et al. 1996 Hsu et al. 2010
	36.6	NR	NR	16.1	NR	14.9	NR	
Switch grass	34.2	0.5	1.5	23.3	2.0	19.9	2.4	Faga et al. 2010
Salix	41.5	3.0	2.1	15.0	1.8	25.2	NR	Sassner et al. 2005

This table was reproduced from Almeida et al. 2011
[a] NR, not reported
[b] Including arabinan

1.2.1.3 Third generation feedstocks

The third generation bioethanol is made from algae and seaweeds. Algae utilize CO_2 via photosynthesis and produce oxygen in the atmosphere. Algae contribute to removing N and P from wastewater. Biofuels from algae are made by conversion of algae biomass to biofuels using liquefaction, pyrolysis, gasification, extraction and transesterification, fermentation, and aneorobic digestion processes (Demirbas, 2011; Tsukahara and Sawayama, 2005; Kita et al. 2010; Singh et al. 2011; Singh and Olsen 2011; Demirbas, 2009). On the other hand, microalgae can produce lipids, proteins and carbohydrates as raw materials for production of biofuels.

Some species of algae contained high levels of carbohydrates as energy reserve polymers to produce bioethanol. There are some micro- and macro-algae such as *Chlorococcum* sp., *Prymnesium parvum, Gelidium amansii, Gracilaria* sp., *Laminaria* sp., *Sargassum* sp. and *Spirogyra* sp., which have been used for the bioethanol production (Eshaq et al. 2011; Rajkumar et al. 2014). These algae produce high levels of polysaccharides as feedstocks for bioethanol production.

1.2.2 *Kluyveromyces marxianus*

K. marxianus is homothallic hemiascomycetous yeast, closely related to *S. cerevisiae* and a sister species to *Kluyveromyces lactis* (Lachance, 1998; Llorente et al. 2000). *K. lactis* and *K. marxianus* can utilize lactose as a carbon source but this capability is absent in *S. cerevisiae* (Fukuhara, 2006). *K. marxianus* can produce some enzymes such as inulinase, β-galactosidase, β-glucosidase and endopolygalacturonases (Workman and Day, 1984; Martins et al. 2002; Leclerc et al. 1987).

K. marxianus used by industries for a relatively broad range utilization from biomass production to bioremediation (Fonseca et al. 2008; Lane and Morrissey, 2010) due to advantages of its traits such as thermotolerance, rapid growth, secretion of inulinase and production of ethanol from various carbon sources (Nonklang et al. 2008; Lertwattanasakul et al. 2011; Rodrussamee et al. 2011). The attractive applications of *K. marxianus* are high-temperature fermentation and fermentation with hemicellulose. In addition, its glucose repression effect is not as severe as that of *S. cerevisiae* (Rodrussamee et al. 2011; Lertwattanasakul et al. 2011).

1.2.3 Glucose repression

Most of yeast prefer glucose to other sugars as a carbon source due to the glucose repression that inhibits the utilization of other sugars via the regulation of gene expression. In *Saccharomyces cerevisiae*, the well-known target genes of glucose repression in utilization of galactose are *GAL1* and *GAL4*, *MAL1* through *MAL4* and *MAL6* in utilization of maltose and *SUC1* through *SUC5* and *SUC7* in utilization of sucrose (Nehlin and Ronne 1990; Klein et al. 1998; Carlson 1987; Carlson and Botstein 1983).

As depicted in Fig. 1.2, the glucose repression in *S. cerevisiae* are mediated by Mig1 and Mig2 as DNA-binding zinc finger proteins (Nehlin and Ronne 1990; Luftiyya and Johnston 1996) and Hxk2 (Ahuatzi et al. 2004) that is hexokinase II involved in the catabolism of glucose in the cytoplasm by its phosphorylation at C-

6 (Moreno and Herrero 2002). When glucose is present, Snf1 kinase is inactive (Gancedo 1998; Carlson 1999; Jiang and Carlson 1996; Ashrafi et al. 2000) and the Glc7-Reg1 phosphatase complex dephosphorylates Mig1 (Alms et al. 1999) which causes the translocation of Mig1 and Hxk2 to nucleus. The Hxk2-Mig1 complex binds to the target genes promoters and recruits co-repressor complex Tup1-Cyc8 (Ssn6p) (Keleher et al. 1992; Vallier and Carlson 1994; Treitel and Carlson 1995) to inhibit the transcription of genes related with other sugars. When glucose is depleted, Snf1 protein is activated (Wilson et al. 1996) to phosphorylate Mig1 (Wilson et al. 1996; Treitel et al. 1998; DeVit et al. 1997; Ostling and Ronne 1998). Phosphorylated Mig1 then moves to cytoplasm together with Hxk2 (Ahtuatzi et al. 2004). A Snf1 complex that is a protein kinase complex has a role in transcription of the glucose-repressible genes under derepressing conditions. Snf1 thus changes the kinase complex in response to the limitation of glucose (Jiang and Carlson 1996), and the Snf1 kinase phosphorylates Mig1, by which the phosphorylated Mig1 detaches from the promoters of its target genes and consequently, the target genes are permitted to transcript.

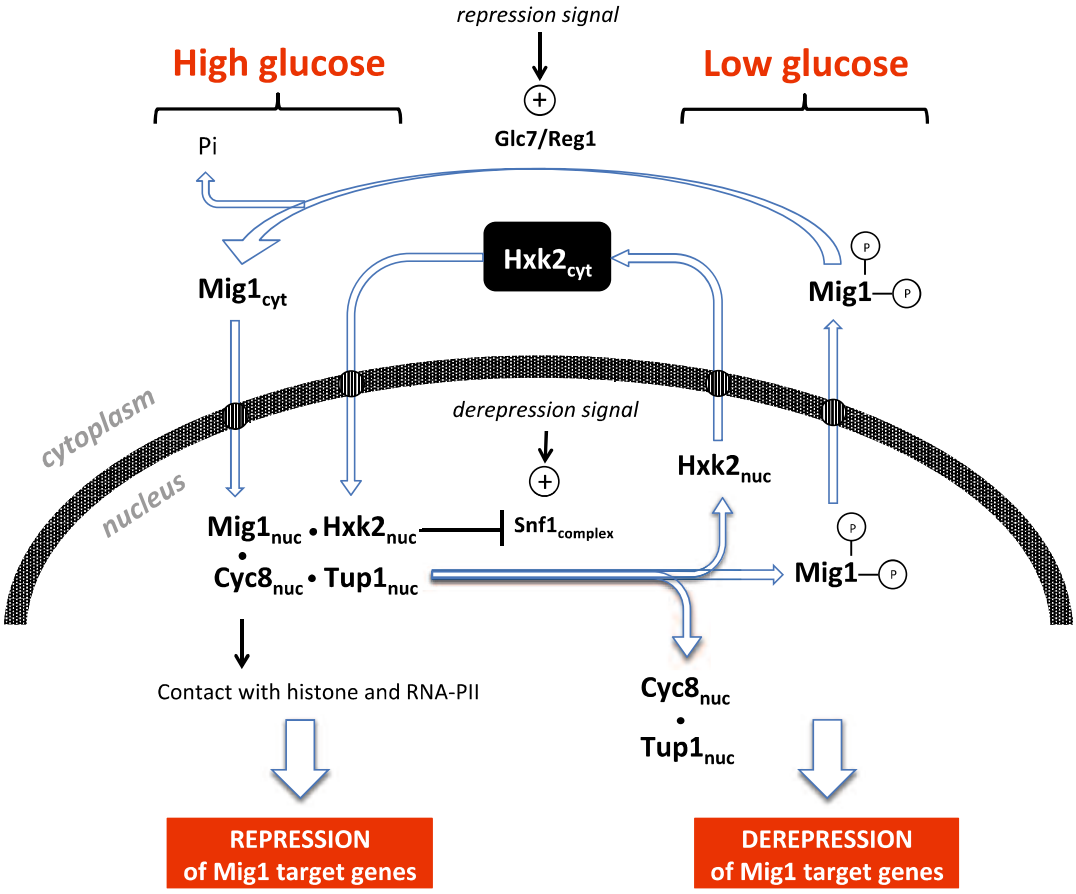

Fig. 1.2 A model explaining the involvement of Mig1 in the nucleocytoplasmic translocation of Hxk2. In the presence of glucose, Mig1 is present in the nucleus to interact with Hxk2 and to repress the transcription of several glucose-regulated genes by direct binding to their promoter regions. In the absence of glucose, Mig1 is phosphorylated and exported out of the nucleus together with Hxk2. The absence of the repressor complex in the nucleus derepresses the transcription of several glucose-regulated genes. *P,* phosphate groups; *cyt,* cytoplasm; *nuc,* nucleus. This picture was reproduced from Ahuatzi et al. 2004.

CHAPTER 2

A *Kluyveromyces marxianus* 2-deoxyglucose-resistant mutant with enhanced activity of xylose utilization

2.1 Abstract

Thermotolerant ethanologenic yeast *Kluyveromyces marxianus* is capable of fermenting various sugars including xylose but exhibits glucose repression to hamper the utilization of other sugars. To acquire glucose repression-defective strains, 33 isolates as 2-deoxyglucose (2-DOG)-resistant mutants were acquired from about 100 colonies grown on plates containing 2-DOG, which were derived from an efficient strain DMKU 3-1042. According to the characteristics of sugar consumption abilities and cell growth and ethanol accumulation along with cultivation time, they were classified into three groups. The first group (3 isolates) utilized glucose and xylose in similar patterns along with cultivation to those of the parental strain, presumably due to reduction of the uptake of 2-DOG or enhancement of its export. The second group (29 isolates) showed greatly delayed utilization of glucose, presumably by reduction of the uptake or initial catabolism of glucose. The last group, only one isolate, showed enhanced utilization ability of xylose in the presence of glucose. Further analysis revealed that the isolate had a single nucleotide mutation to cause amino acid substitution (G270S) in *RAG5* encoding hexokinase and exhibited very low activity of the enzyme. The possible mechanism of defectiveness of glucose repression in the mutant is discussed in this paper.

2.2 Introduction

Compared to *Saccharomyces cerevisiae,* which is used for ethanol fermentation industries, *Kluyveromyces marxianus* has advantageous potentials in application for ethanol production. First, *K. marxianus* is thermotolerant and is able to efficiently produce ethanol around 40° C (Fonseca et al. 2008; Goshima et

al. 2013; Limtong et al. 2007). It is thus applicable for high-temperature fermentation as an economical fermentation, enabling reduction in cooling cost, efficient simultaneous saccharification and fermentation, reduction in contamination, and stable fermentation even in tropical countries (Anderson et al. 1986; Banat et al. 1998; Limtong et al. 2007). Second, the yeast can assimilate various sugars, including xylose, arabinose, sucrose, raffinose and inulin, in addition to several hexoses (Lertwattanasakul et al. 2011; Rodrussamee et al. 2011). This broad spectrum in sugar assimilation capability is beneficial for the conversion to ethanol of biomass including various sugars. Third, the yeast exhibits relatively weak glucose repression of the utilization of sucrose (Lertwattanasakul et al. 2011) and thus is highly preferable to biomass such as sugar cane juice containing glucose, fructose and sucrose as main sugars. Despite such beneficial properties, some crucial problems in the use of *K. marxianus* remain to be solved. One problem is glucose repression of the utilization of other sugars including xylose (Rodrussamee et al. 2011), which is a principal constituent in hemicellulose for second-generation biofuels (Lu et al. 2010).

2-deoxyglucose (2-DOG) is a convenient reagent for screening of mutants defective in glucose repression (Martin and Heredia, 1977; Sreenath and Jeffries, 1999). It is a stable glucose analogue that is taken up into cells by hexose transporters and phosphorylated but cannot be fully metabolized. Accumulation of 2-deoxyglucose-6-phosphate in cells interferes with carbohydrate metabolism by inhibiting the activities of glycolytic enzymes including phosphoglucose isomerase and hexokinase (Chen and Guéron, 1992; Sols and Crane, 1954; Wick et al. 1957). In general, it is assumed that the biological effects of 2-DOG are the consequence of a block in carbohydrate catalysis, implying that 2-DOG-treated cells are unable to metabolize glucose and stop growing as a result of a lack of energy and metabolic intermediates (Ralser et al. 2008).

In order to acquire glucose repression-defective strains, isolation and characterization of 2-DOG-resistant mutants from *K. marxianus* DMKU 3-1042 as one of most thermotolerant strains, which was isolated via an enrichment culture method with samples collected in Thailand (Limtong et al. 2007), were performed. The isolated 2-DOG-resistant mutants were characterized and classified by several

experiments and eventually one mutant was found to have a significantly enhanced activity of xylose utilization. This mutant may be a preferable candidate for ethanol fermentation from biomass containing mixed sugars including glucose. This study thus provided not only a mutant with enhanced activity of xylose utilization in *K. marxianus* but also its metabolic characteristics of conversion of xylose to ethanol under the condition of coexistence of glucose.

2.3 Materials and methods

2.3.1 Strain and media

Yeast strains used in this study were thermotolerant *K. marxianus* DMKU 3-1042 strain isolated in Thailand (Limtong et al. 2007) as a strain that was isolated by an enrichment culture and its derivatives obtained in this study. Pre-culture was carried out in YPGal medium (10 g/l yeast extract, 20 g/l peptone and 20 g/l galactose) for preparation of the inoculum. To examine sugar utilization ability and cell growth, YP medium (10 g/l yeast extract and 20 g/l peptone) supplemented with 20 g/l of glucose (Glc), galactose (Gal) or xylose (Xyl), designated as YPD, YPGal or YPXyl, respectively, was used. YP medium supplemented with 20 g/l Glc and 20 g/l of one of the other sugars was used to examine the effect of glucose on utilization ability of other sugars. YP medium was used for general experiments.

2.3.2 Cultivation conditions and spotting test

Cells were pre-cultured in 5 ml of YPGal medium at 30°C under a shaking condition at 160 rpm overnight. The pre-culture was inoculated into a 300-ml Erlenmeyer flask containing 100 ml fresh medium at an initial optical density at 660 nm (OD_{660}) value of 0.1, and cultivation was performed at 30°C under a shaking condition at 160 rpm for an appropriate time. In experiments for spotting tests, pre-cultured cells were washed with deionized water, suspended in deionized water at 1×10^7 cells/ml, 10-fold sequentially diluted, and then spotted onto agar

plates of YPD, YPGal and YPXyl with or without 0.1% 2-DOG. The plates were incubated at 30°C for 48 h.

2.3.3 Screening and phenotype characterization of 2-DOG-resistant mutants

To screen 2-DOG-tolerant mutants, cells of *K. marxianus* DMKU 3-1042 were grown in 5 ml YPD at 30°C overnight under a shaking condition at 160 rpm, collected by low-speed centrifugation, suspended in 1 ml sterilized water, spread on Yeast Nitrogen Base plates containing 2% Xyl and 0.1% 2-DOG (YNB + 2% Xyl + 0.1% 2-DOG), and incubated at 30°C for 3 days. Colonies on the plates were re-streaked on YPD, YNB + 2% Xyl + 0.1% 2-DOG, YNB + 2% Gal + 0.1% 2-DOG and YNB + 2% Ara + 0.1% 2-DOG and incubated at 30°C for 3 days. The colonies that were able to grow well on the four different plates were selected as 2-DOG-resistant mutants. Growth of all mutants was further examined on YP plates containing different types of sugars; Glc, Gal, Xyl, Gal + 0.1% 2-DOG and Xyl + 0.1% 2-DOG, and on YNB plates containing different concentrations of Glc (0.02, 0.2 and 2%) and the presence of antimycin A. YNB medium was used only for examinations on the first screening of 2-DOG-resistant mutants and effects of glucose concentration on cell growth and antimycin A.

2.3.4 Analytical methods

Cell density was measured turbidimetrically at 660 nm using a spectrophotometer (U-2000A, Hitachi Japan). Cultures were sampled and subjected to low-speed centrifugation. The supernatant was frozen and kept at -20°C until the end of fermentation (96 h) and then analyzed together by using HPLC. Quantitative analysis of sugars, ethanol, glycerol and xylitol was performed by high-performance liquid chromatography (Hitachi Model D-2000 Elite HPLC System Manager) as described previously (Rodrussamee et al. 2011). A GL-C610-S gel pack column (Hitachi) was used together with a refractive index detector (Model L-2490) at 60°C with 0.3ml/min eluent of deionized water.

2.3.5 Determination of oxidized Nicotinamide Adenine Dinucleotide (NAD^+) and reduced Nicotinamide Adenine Dinucleotide (NADH) concentration

Cells were pre-cultured in 5 ml of YPGal medium at 30°C under a shaking condition at 160 rpm overnight. The pre-culture was inoculated into a 300-ml Erlenmeyer flask containing a 100-ml fresh YP medium containing 2% Xyl and 2% Glc, at an initial OD_{660} value of 0.1, and cultivation was performed at 30°C under a shaking condition at 160 rpm for an appropriate time. A sample of the culture (10^6 cells/ml) was subjected to centrifugation at 4°C. The cell pellet was washed with a cold phosphate-buffered saline. Intracellular NAD^+ and NADH concentrations were determined by using EnzyChrom^{TM} NAD^+/NADH Assay Kit (E2ND-100) (BioAssay Systems, USA) according to the instruction manual of the supplier and the reaction mixture was measured in a POWERSCAN HT microplate reader (DS Pharma Biomedical, Osaka, Japan).

2.3.6 Preparation of cell extracts

2-DOG-resistant no. 23 mutant and the parental strains were pre-cultured in 5 ml YPGal at 30°C overnight under a shaking condition at 160 rpm. The pre-culture was inoculated into a 300-ml Erlenmeyer flask containing a 100-ml fresh YP medium containing 2% Xyl and 2% Glc at an initial OD_{660} value of 0.1, and cultivation was performed at 30°C under a shaking condition at 160 rpm. Cells in the exponential growth phase were collected by centrifugation (Himac CR20 Hitachi) at 5,000 rpm and 4°C for 10 min and washed twice with 10 mM potassiume phosphate buffer (pH 7.0). The washed cells were re-suspended in the same buffer. The cells suspension was passed through a French press (Aminico, USA) at 1,000 psi twice and centrifuged at 4°C for 10 min at 9,000 rpm to remove cells debris. The supernatant was further centrifuged at 4°C for 1 h at 44,000 rpm by using a micro-ultracentrifuge (Himac CS 100GXL Hitachi) to remove membrane fraction. The resultant supernatant was used as cell extracts for enzyme assays.

2.3.7 Enzyme assays

Hexokinase activity was measured spectrophotometrically by coupling the reaction to G6-P dehydrogenase (Cáceres et al. 2003). The assay was performed in a reaction mixture containing 0.24 M triethanolamine (pH 7.5), 5.3 mM ATP, 4 mM D-fructose, 0.72 mM $NADP^+$, 5 mM $MgCl_2$, and 2 Uml^{-1} G6-P dehydrogenase from *Leuconostoc sp* (Oriental yeast, Japan) by using a spectrophotometer (U-2000A Hitachi, Japan). Glucokinase activity was determined by the same assay except that 4 mM D-glucose was used as a substrate instead of D-fructose. Protein content was determined by the Lowry method (Lowry et al. 1951).

2.3.8 Nucleotide sequencing and alignment

From cells of 2-DOG resistant no. 23 mutant and parental strains that had been grown in YPD medium, genomic DNA was prepared as described (Sambrook and Russell, 2001). PCR amplification was performed using PRIMESTAR® DNA polymerase (Takara BIO, Japan) with PCR primers listed in Table 2.1. The amplification condition was as follows: one cycle of 10 s denaturation at 98°C, 30 cycles of 10 s denaturation at 98°C, 5 s annealing at 60°C and 2.5 min extension at 72°C and 1 cycle of 5 min extension at 72°C. DNA fragments were purified using a QIAquick PCR purification kit (QIAGEN) and subjected to nucleotide sequencing (Sanger et al. 1977) by using ABI Prism 310 (Perkin Elmer, USA). DNA sequences determined were subjected to BLAST analysis (Altschul et al. 1990). Alignment of amino acid sequences was performed using a clustalW (Thompson et al. 1994).

Table 2.1 Primers used in this study

Name	**Sequence 5' → 3'**
RAG5-I5'[a]	5'CTGTTGCCAGTTGCCAGTTGC3'
RAG5-I3'	5'GGCTGGTGGCTTCTTTGGACC3'
RAG5-II5'	5'CAAGGAACAACTAGTTAAGC3'
RAG5-II3'	5'ATCTTGTTTTGGGAGGCTGGG3'
RAG5-III5'	5'AGTTGTTCTGGTCAAGTTGGG3'
RAG5-III3'	5'AACCGGAAGTCATCTTTTCG3'
RAG5-IV5'	5'CAAGATGGGTATCATCATTGG3'
RAG5-IV3'	5'TCCTTCAAAGCTTGAGCAGCC3'
RAG5-V5'	5'CCATACGTCATGGACACCACC3'
RAG5-V3'	5'TGAGCGATCGTGAATGAATGTC3'

[a] Primers were designed according to the *RAG5* nucleotide sequence (Lertwattanasakul et al. 2015)

2.4 Results

2.4.1 Screening and phenotype characterization of 2-DOG-resistant mutants

About 100 colonies that appeared on YNB plates containing 2% Xyl and 0.1% 2-DOG at the first screening were subjected to re-streaking on the same plates, and 33 independent isolates were obtained. To confirm 2-DOG resistance of the isolates, spotting tests were carried out on YPGal and YPXyl plates supplemented with 2-DOG by using YPD or YPGal and YPXyl without 2-DOG plates as controls (Fig. 2.1). All 33 isolates exhibited sufficient growth at 10^{0}, 10^{-1}, 10^{-2}, 10^{-3} and 10^{-4} fold dilutions on both YPGal and YPXyl plates supplemented with 2-DOG, suggesting that they are resistant to 2-DOG, but the parental strain hardly grew in the presence of 2-DOG. Consequently, the 33 isolates were further analyzed as 2-DOG-resistant mutants.

Fig. 2.1 Spotting test of 2-DOG-resistant isolates. Cells were grown in 2% YPGal medium at 30°C overnight and subjected to a spotting test as described in Methods. After spotting (left to right, 10^{0}, 10^{-1}, 10^{-2}, 10^{-3} and 10^{-4} fold dilutions) on 2% YPD, 2% YPGal, 2% YPXyl, 2% YPGal containing 0.1% 2-DOG, and 2% YPXyl containing 0.1% 2-DOG, plates were incubated at 30°C for 48 h.

It was found that the 33 mutants formed colonies of different sizes on YPD plates (Fig. 2.1). Mutants of no. 1, 5, 9 and 23 as well as the parental strain formed larger colonies than did other mutants on YPD plates at 10^{-3} and 10^{-4}fold dilutions. On the other hand, all mutants exhibited colonies of almost the same sizes on YPGal and YPXyl plates.

To further analyze the Glc utilization ability of the 33 mutants, their growth on YNB plates containing different concentrations of Glc was compared (Fig. 2.2 A-C). Mutants of no. 1, 5, 9 and 23 as well as the parental strain sufficiently grew on 0.2% Glc, but other mutants hardly grew at that low concentration of Glc. All 33 mutants, however, grew well on 2% Glc. These findings suggested that the 33 mutants except for no. 1, 5, 9 and 23 are defective in Glc uptake or in its initial catabolism.

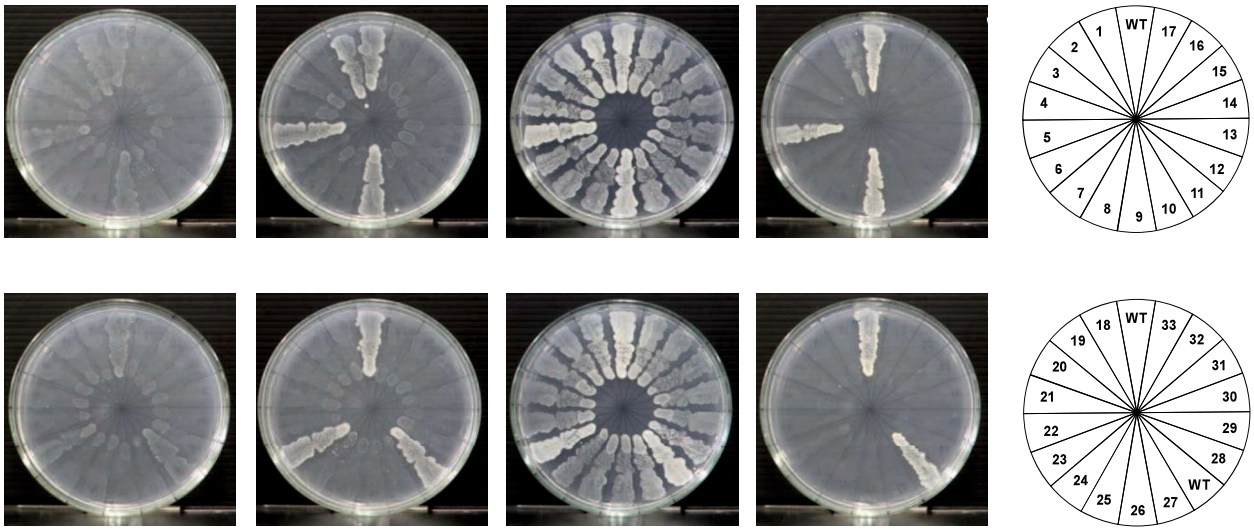

Fig. 2.2 Growth of 2-DOG-resistant mutants at different concentrations of Glc and effect of antimycin A. Cells were grown in 2% YPGal medium at 30°C overnight and streaked on YNB plates containing different concentrations of Glc. The plates were then incubated at 30°C for 48 h. A) 0.02% Glc; B) 0.2% Glc; C) 2% Glc; D) 2% Glc + 5 μM antimycin A.

To examine the effect of the respiratory inhibitor antimycin A on cell growth of 2-DOG-resistant mutants, growth of the mutants was examined on YNB plates containing 5 μM antimycin A at 30°C (Fig. 2.2 D). Mutants of no. 5 and 9 grew well like the parental strain in the presence of antimycin A, and mutants of no. 1 and 23 showed weaker growth than that of the parental strain. In contrast, other mutants did not grow in the presence of antimycin A. These results and the growth phenotype on 0.2% Glc (Fig. 2.2 B) suggest that mutants no. 1, 5, 9 and 23 can support growth on glucose on a fermentative basis, which means that respiration is not induced at this low concentration of glucose, and the uptake of 2g/L glucose into the cells maintains a high enough Glc-6-phosphate concentration inside the cells as to signal a cell growth by fermentation activity. Whereas, the defective growth of other mutants in the presence of the respiratory inhibitor may be due to insufficient metabolic activity of Glc for growth under a fermentation condition.

2.4.2 Cell growth and sugar consumption of 2-DOG-resistant mutants in YP medium containing mixed sugars of Glc and Xyl

To determine whether the 2-DOG-resistant mutants had acquired the phenotype of glucose repression-defective mutants, their Xyl utilization was examined in the presence of Glc. The growth of mutants was examined in YP medium containing both Glc and Xyl, and several parameters including concentrations of Glc, Xyl and ethanol in the medium as well as turbidity of medium were determined. According to the patterns of consumption of both sugars, cell growth and ethanol accumulation along with cultivation time, the 33 mutants were classified into three groups and representative mutants are shown in Fig. 3. One group consisting of no 1, 5 and 9 mutants (no. 5 as a representative) showed similar patterns of the four parameters of turbidity (OD_{660}), Glc, Xyl and ethanol to those of the parental strain (Fig. 2.3 A, B, C and F). This type of mutant started to utilize Xyl after depletion of Glc in the medium. Even after depletion of Glc, their turbidity increased (Fig. 2.3 A, B and C), but ethanol level was slightly reduced during cultivation. The second group consisting of other mutants except for no. 23 (no. 3 as a representative) showed extremely slow Glc and Xyl consumption rates,

and ethanol accumulation in the medium was observed after 24 h (Fig. 2.3 B, C and F). This type of mutant could utilize Glc and Xyl slowly and simultaneously. No. 23 mutant as the third group showed enhancement of Xyl utilization and delay of Glc utilization compared to those of the parental strain (Fig. 2.3 B and C). Notably, both sugars were utilized together after 15 h, indicating suppression of glucose repression. A phenotype similar to that of no. 23 has been reported in an *S. cerevisiae* 2-DOG-resistant mutant that is able to assimilate both sugars of Glc and Xyl together (Kahar et al. 2011). Concentrations of ethanol, glycerol and xylitol in the medium increased after 24 h, and the ethanol level was more than that of the parental strain after 48 h (Fig. 2.3 D, E and F). The ethanol yield of no. 23 mutant was 0.50 g EtOH/g sugars at 24 h, 0.39 g EtOH/g sugars at 48 h, 0.37 g EtOH/g sugars at 72 h and 0.33 g EtOH/g sugars at 96 h. This mutant showed significantly higher ethanol production than that of the parental strain at 48 h ($P<0.05$), 72 h ($P<0.01$) and 96 h ($P<0.05$) (Fig. 2.3 F).

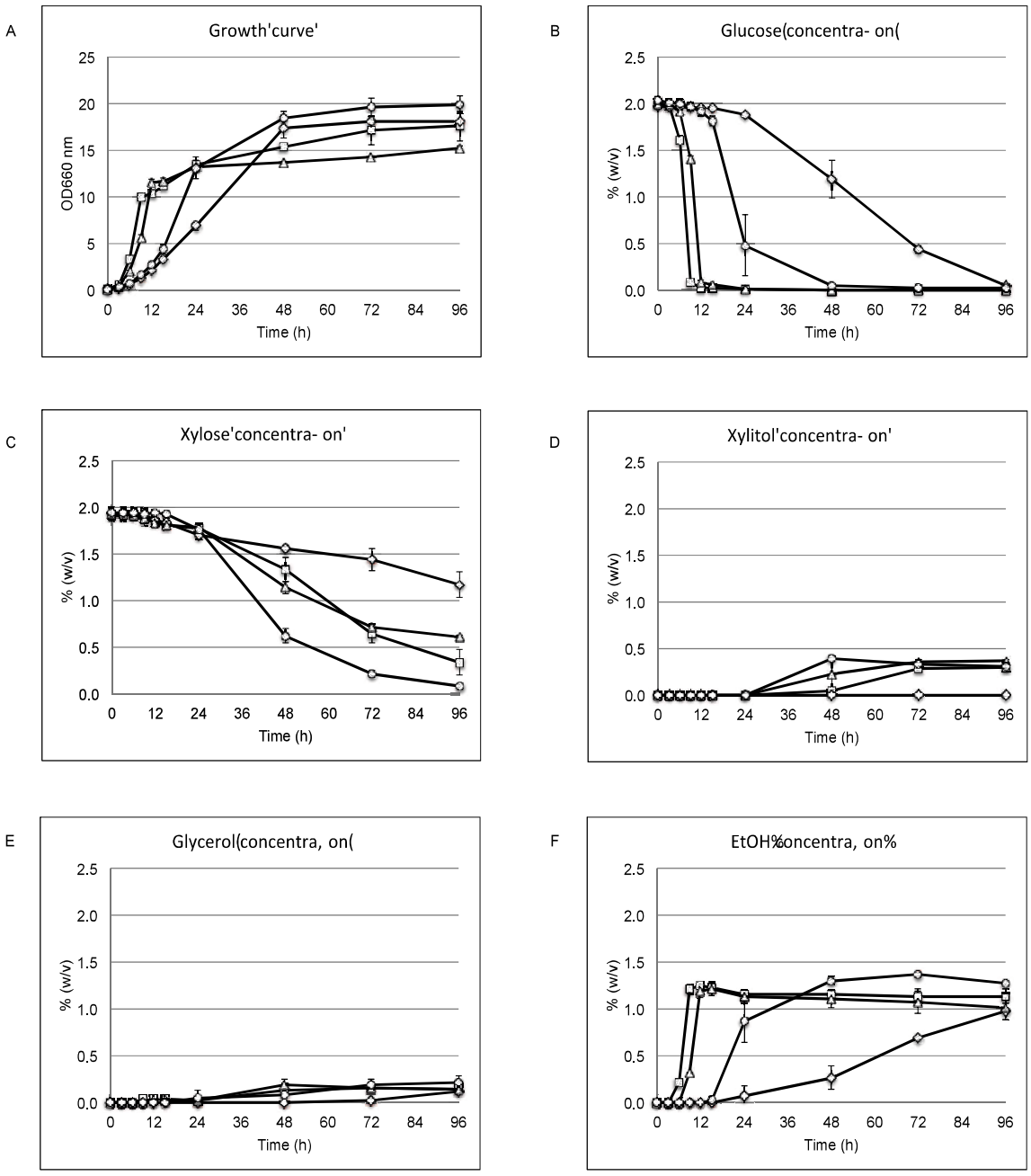

Fig. 2.3 Growth and sugar consumption of 2-DOG-resistant mutants in YP medium containing Glc and Xyl. Cells were grown in 2% YPGal medium at 30°C overnight, transferred to a fresh YP medium containing 2% Xyl and 2% Glc, and cultivated at 30°C under a shaking condition at 160 rpm for 96 h. No. 3 mutant (open diamonds), no. 5 mutant (open triangles), no. 23 mutant (open circles) and their parental strain (open squares) were compared by measuring OD_{660} (A) and concentrations of Glc (B), Xyl (C), xylitol (D), glycerol (E) and ethanol (F) in the medium. Data presented were averages of triplicate experiments and error bars indicate the standard deviations.

2.4.3 NAD^+ and NADH concentrations in no. 23 mutant in YP medium containing mixed sugars of Glc and Xyl

Since no. 23 mutant showed a delay of Glc consumption and almost parallel utilization of Xyl with Glc in contrast to the parental strain, it was guessed to be due to the limitation of NAD^+ for Glc utilization in the mutant. To obtain the clue of the glucose repression-defective phenotype on the mutant, intracellular NAD^+ and NADH concentrations were measured and the relative NAD^+/NADH values between no. 23 mutant and the parental strain were compared (Fig. 2.4). The experiments were performed under the same condition used in Fig. 2.3. The ratio of NAD^+ to NADH concentrations in the mutant was lower than that of the parental strain at all times tested, whereas the relative amount of NAD^+ was gradually reduced after about 6 h. The ratio of NAD^+ to NADH in the mutant was 1.6, 1.4 and 1.2 at 6 h, 12 h and 24 h, respectively, and that in the parental strain was 2.2, 1.7 and 1.4 at 6 h, 12 h and 24 h, respectively. Therefore, it may be possible that the relatively low level of NAD^+ in no. 23 mutant caused its slow utilization of Glc.

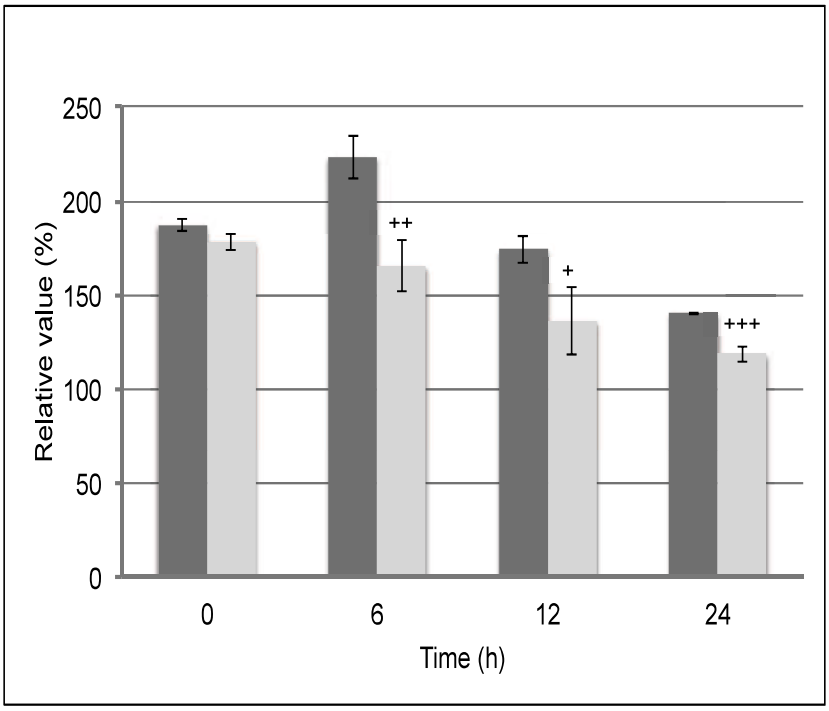

Fig. 2.4 Relative NAD^+/NADH values in 2-DOG-resistant no. 23 mutant in YP medium containing Glc and Xyl. Cells were grown in 2% YPGal medium at 30°C overnight, transferred to a fresh YP medium containing 2% Xyl and 2% Glc, and cultivated at 30°C under a shaking condition at 160 rpm. At the times indicated, cells were harvested and concentrations of NAD^+ and NADH were determined as described in Methods. The relative NAD^+/NADH values of no. 23 mutant (light grey columns) were compared with those of the parental strain (dark grey columns). Data presented were averages of triplicate experiments and error bars indicate the standard deviations. Statistical analysis was performed between no. 23 mutant and the parental strain: +, $P<0.05$; ++, $P<0.01$; +++, $P<0.001$.

2.4.4 Weak hexokinase activity in no. 23 mutant

Two main mechanisms for resistance to 2-DOG have been reported to be either the defect of glucose phosphate kinase (Lobo and Maitra, 1977) or the induction of glucose-6-phosphate phosphatase activity (Heredia and Heredia, 1988). We thus measured activities of hexokinase and glucokinase in no. 23 mutant since *K. marxianus* DMKU 3-1024 bears these two kinases. Cells were grown under the same condition used in Fig. 2.3 and were harvested at the mid-log phase for the enzyme assay. As shown in Table 2.2, the specific activity of fructose kinase corresponding to hexokinase of no. 23 mutant was 16 times lower than that

of the parental strain. Whereas, the specific activity of glucose kinase corresponding to glucokinase in the no. 23 mutant was 3 times lower than that of the parental strain. These results suggest that no. 23 mutant has a defective hexokinase enzyme but retains glucokinase activity almost equivalent to that of the parental strain.

Table 2.2 Hexokinase and glucokinase activities of 2-DOG-resistant no. 23 mutant

Substrate	Enzyme	Specific activity (Umg^{-1})		
		DMKU 3-1042	No. 23	P value
Fructose	Hexokinase	0.497 ± 0.027	0.031 ± 0.003	P<0.001
Glucose	Hexokinase and glucokinase	0.711 ± 0.044	0.220 ± 0.026	P<0.001

2.4.5 Determination of a mutation site on no. 23 mutant

Due to almost no activity of hexokinase in no. 23 mutant, the nucleotide sequence of *RAG5* encoding the enzyme was determined. As a result, there was one nucleotide mutation from G to A at the 270^{th} codon in *RAG5*, causing G270S substitution. Interestingly, G270 is conserved in hexokinases in Fig. 2.5, and is located close to the substrate-binding site (Bergdahl et al. 2013; Kuser et al. 2000). The location of the substitution site might match with the fact that there was a trace amount of hexokinase activity in the no. 23 mutant.

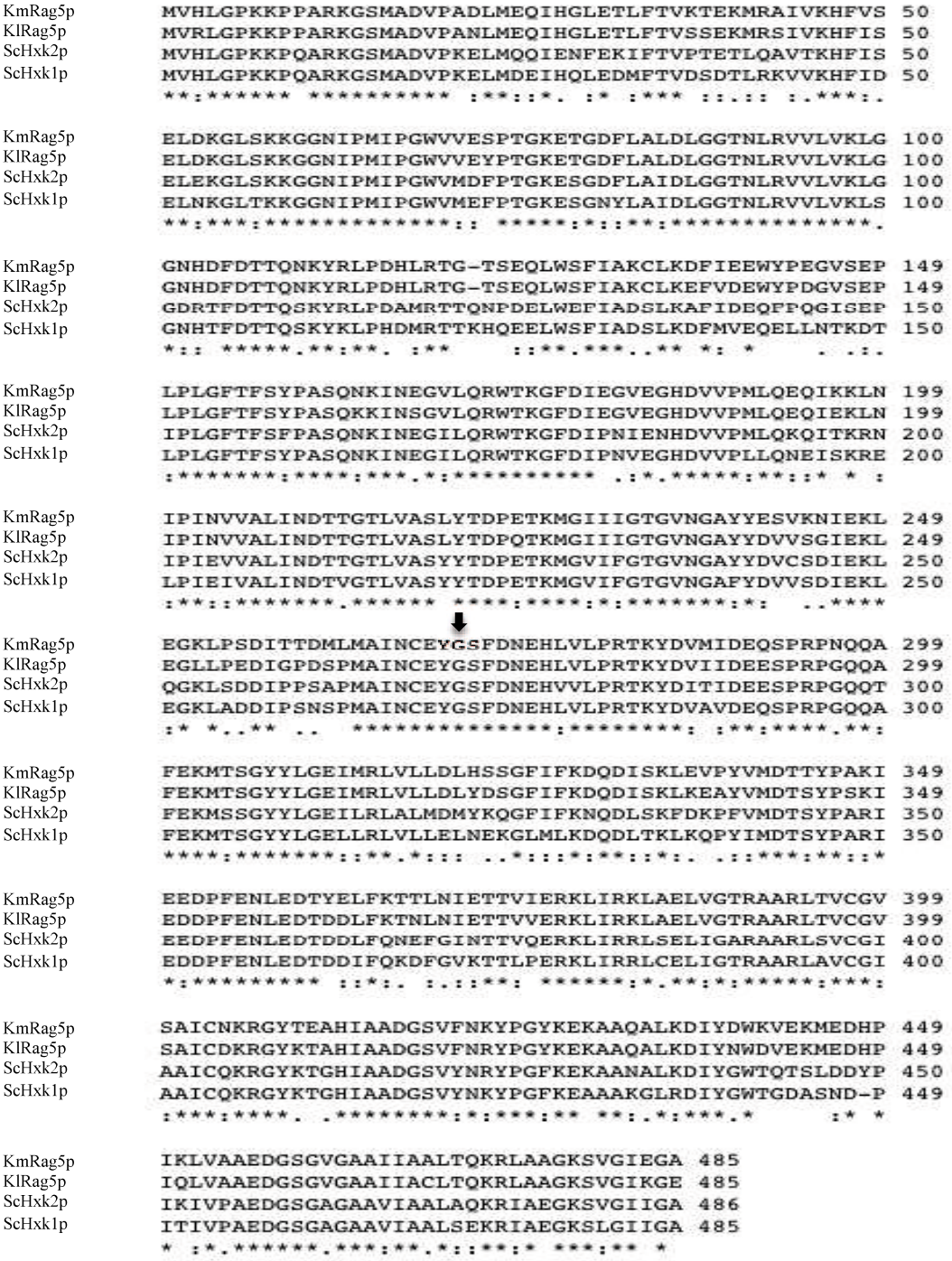

Fig. 2.5 Alignment of amino acid sequences of hexokinases in *K. marxianus, K. lactis* and *S.cerevisiae*. The primary sequences of hexokinases of *K. marxianus* KmRag5p, *K. lactis* KlRag5p, *S. cerevisiae* ScHxk2p and *S. cerevisiae* ScHxk1p were aligned. Stars represent conserved amino acid residues. A vertical arrow represents Gly-270, which was substituted to be serine in no. 23 mutant.

2.5 Discussion

In this study, we attempted to isolate glucose repression-defective strains by screening 2-DOG-resistant mutants in *K. marxianus* as a promising yeast for economical bioethanol production from various types of biomass (Rodrussamee et al. 2011). We compared the growth abilities of the mutants isolated at different concentrations of Glc and in the presence of antimycin A and the consumption patterns of mixed sugars of Xyl and Glc, and we consequently classified them into three groups.

The three groups could be clearly distinguished when compared in liquid culture with YP medium containing mixed sugars of Glc and Xyl (Fig. 2.3). The first group appears to be similar to the parental strain in utilization timing and patterns of Glc and Xyl and in the accumulation profile of ethanol as well as cell growth. The 2-DOG resistance of the first group might be due to blockage of the import of 2-DOG into cells or enhanced export of the drug. They seem to normally import and ferment Glc as indicated by growth in the presence of antimycin A, and they utilize Xyl after depletion of Glc, indicating retainment of the glucose repression of Xyl utilization like the parental strain. The second group might be defective in hexose transporters or initial catabolism of Glc because the group exhibited remarkable retardation of Glc and Xyl utilization compared to that of the parental stain. The retardation of Xyl utilization suggests that hexose transporters are responsible for the Xyl import in *K. marxianus* as reported previously (Hamacher et al. 2002). This group appears to utilize Glc and Xyl together presumably because the intracellular concentration of Glc is too low to evoke glucose repression.

One mutant numbered 23 as the third group exhibited a glucose repression-defective phenotype (Fig. 2.3). This 2-DOG mutant may have acquired the ability of Xyl uptake in the presence of Glc in the medium, though Glc consumption was retarded compared to that of the parental strain. Notably, the utilization of Xyl was much faster than that of the parental strain, and larger amounts of glycerol and xylitol than those in the case of the parental strain were accumulated in the medium. The mutant showed a relatively low ratio of NAD^+ to NADH

concentrations compared to that of the parental strain (Fig. 2.4). The low ratio may be responsible for the utilization of Xyl because its process contains the conversion reaction of NAD^+ to NADH by xylitol dehydrogenase (Ralser et al. 2008), and the limitation of NAD^+ may slow down the glycolysis process, which in turn leads the delay of Glc utilization. Such an effect of NAD^+ limitation on the Glc utilization has been reported in *S. cerevisiae* (Vemuri et al. 2007). Alternatively, the delayed Glc assimilation could be the consequence of low hexokinase activity.

Further analysis revealed that no. 23 mutant exhibited almost no hexokinase activity and had a single nucleotide mutation to cause amino acid substitution (G270S) in *KmRAG5* encoding hexokinase. KmRag5p in *K. marxianus* shares 89.9% and 72.6% identities with KlRag5p in *K. lactis* (Prior et al. 1993) and with ScHxk2p in *S. cerevisiae* (Steizt, 1977), respectively. Amino acid alignment revealed that G270 of KmRag5p corresponds to G271 of ScHxk2p and is located in one of conserved regions (Fig. 2.5), and the amino acid substitution of G271C promotes residue-residue interactions to cause slight changes of backbone conformation (Bergdahl et al. 2013; Kuser et al, 2000). Interestingly, Gly^{271} in ScHxk2p is located close to the glucose-binding site. Therefore, it is assumed that the G270S substitution caused reduction of hexokinase activity in no. 23 mutant.

Considering the function of hexokinase as a transcriptional regulator for the glucose repression in *S. cerevisiae* (Niederacher and Entian, 1991; Peláez et al. 2010; Schuurmans et al. 2008), it may be likely that the amino acid substitution of G270S in hexokinase leads to a glucose repression-defective of no. 23 mutant to permit uptake of Xyl together with Glc. On the other hand, the 2-DOG resistant phenotype of the mutant may be due to reduction in hexokinase-catalyzed formation of 2-DOG-6-phosphate, which hampers glycolysis as an inhibitor of glucose phosphate isomerase (Heredia and Heredia, 1988).

The findings in the experiments using mixed sugars of Glc and Xyl in no. 23 mutant (Fig. 2.3) can be explained as follows. Due to the defect of glucose repression, Xyl was imported at the same time with Glc, and thus NAD^+ would quickly become insufficient for Glc catabolism by its conversion to NADH at the xylitol oxidation step (Richard et al. 1999), which in turn slows down the glycolysis process, consequently suppressing Glc uptake. The defect of hexokinase

may also be responsible for the delay of Glc utilization to some extent. After around 15 h, the glycerol production pathway might be induced to supply NAD^+, which promotes glycolysis to import and catabolize Glc and to further provide NAD^+ by the ethanol production pathway. The amount of NAD^+ provided might be sufficient to assimilate both Glc and Xyl together. This assumption should be experimentally proved.

Unlike gene-engineered *S. cerevisiae* mutants in which foreign genes are introduced (Bera et al. 2011; Demeke et al. 2013; Hector et al. 2011; Tanino et al. 2010), *K. marxianus* strains improved by mutation breeding can be utilized unlimitedly as non-recombinants for the ethanol industry. Therefore, further improvement of no. 23 mutant to be a faster consumer of both sugars of Glc and Xly is expected.

2.6 Conclusion

K. marxianus is a highly competent yeast that can ferment various sugars including Xyl but bears glucose repression to inhibit the utilization of other sugars. This study was thus aimed at developing glucose repression-defective strains from a strongly thermotolerant *K. marxianus* DMKU 3-1042. Via the screening of 2-DOG-resistant mutants, one isolate, no 23 mutant, was acquired, which showed enhanced utilization ability of Xyl in the presence of Glc but delayed utilization of Glc, due to the *RAG5* mutation that largely reduced hexokinase activity. This mutant produced significantly higher ethanol than that of the parental strain after 48 h in the medium containing mixed sugars of Glc and Xyl.

CHAPTER 3

Characteristics of *kan*MX4-inserted mutants that exhibit 2-deoxyglucose resistance in thermotolerant yeast *Kluyveromyces marxianus*

3.1 Abstract

Kluyveromyces marxianus has the attractive potential of utilization capability of various sugars in addition to thermal tolerance and protein productivity. The yeast, however, has an intrinsic system for catabolite repression, by which cells down-regulate the metabolism of alternative sugars when glucose coexists. To acquire glucose-repression-free mutants, we isolated and characterized 2-deoxyglucose-resistant mutants from *kan*MX4-inserted mutants. The insertion site was determined by TAIL-PCR followed by nucleotide sequencing, indicating that the *kan*MX4 cassette was intragenically or intergenically inserted. Further analysis of the sugar utilization ability allowed to classify the intragenically inserted mutants including the *mig1* mutant into two categories. One group showed enhanced utilization of xylose in the presense of glucose, presumably due to a defect in the glucose-repression mechanism, and the other group showed delayed utilization of glucose, probably by reduction of the uptake or initial catabolism of glucose. Considering the possible functions of the disrupted genes in these mutants, it is assumed that *K. marxianus* has undiscovered mechanisms for glucose repression and complex regulation for the uptake or initial catabolism of glucose.

3.2 Introduction

Ethanol as a bioethanol derived from lignocellulose is an environment-friendly alternative to fossil fuels. Since a substantial fraction of lignocellulose material consists of xylose and glucose (Watanabe et al. 2007), efficient bioconversion of xylose to ethanol is expected to make the process cost-effective (Zaldivar et al. 2001).

Kluyveromyces marxianus is expected to become one of the best choices for industrial ethanol production for the following reasons. First, most *K. marxianus* strains are thermotolerant, and they are therefore capable of growing and fermenting at high temperatures, of which the optimal temperature is 10-15 °C higher than that of the traditional alcohol-fermenting yeast *Saccharomyces cerevisiae* (Limtong et al. 2007; Fonseca et al. 2008; Lane and Morrissey, 2010). This thermal character has received much attention for the possibility of cost saving in ethanol production (Gough et al. 1997; Rodrussamee et al. 2011). Second, *K. marxianus* assimilates various sugars including glucose, xylose, arabinose, galactose, sucrose and inulin (Rodrussamee et al. 2011, Lertwattanasakul et al. 2011). Third, its growth is relatively rapid with a typical doubling time of 0.7-2 h (Banat et al. 1998; Singh et al. 1998). Fourth, the yeast has a high capacity of protein production (Fonseca et al. 2007). *K. marxianus* is thus thought to have great promise for industrial applications and has been widely tested in various experiments for biotechnological applications, including ethanol production from whey or lactose (Oda and Nakamura, 2009; Christensen et al. 2011; Zoppellari and Bardi, 2013), production of biomass or single cell protein (Pas et al. 2007), production of endogenous enzymes (Rajoka, 2007) or heterologous enzymes (Hong et al. 2007), food industry (Vasallo et al. 2006) and environmental applications (Pal et al. 2009).

Many microorganisms intrinsically possess rational mechanisms for utilization of carbon sources available in the environment. *S. cerevisiae* prefers glucose or fructose as a carbon source, though it has the ability for assimilation of other sugars (Carlson, 1999). One of the major mechanisms by which cells adapt is via regulation of gene expression, which is achieved primarily but not exclusively (Gancedo, 1998). Analysis of genomic expression has revealed that a great number of genes are differentially transcribed in response to various glucose levels (Derisi et al. 1997). Some genes are induced by glucose, including those encoding low-affinity glucose transporters, glycolytic enzymes and ribosomal proteins. Another large set of genes is repressed by glucose, including genes involved in utilization of alternate carbon sources, gluconeogenesis, respiration and peroxisomal functions (Carlson, 1999).

Though it is attractive to apply the potential for assimilation of various sugars in *K. marxianus* for production of ethanol or other useful materials, the glucose-repression mechanism may hamper such an application when mixed sugars such as molasses or sugarcane juice are utilized as carbon sources. However, information on glucose repression of *K. marxianus* is limited. We thus focused on 2-deoxyglucose (2-DOG) mutants including ones defective in glucose repression in *K. marxianus*. This study is the first extensive study on glucose repression and glucose uptake regulation in the yeast.

3.3 Materials and methods

3.3.1 Strain and media

Yeast strains used in this study were *K. marxianus* DMKU 3-1042 strain, one of the isolates from Thailand (Limtong et al. 2007), and its derivatives. Culture was carried out in YPGal medium (10 g/l yeast extract, 20 g/l peptone and 20 g/l galactose) as used for preparation of the inoculum. To examine sugar utilization ability and cell growth, YP media (10 g/l yeast extract and 20 g/l peptone in each medium) supplemented with 20 g/l of glucose (Glc), galactose (Gal) and xylose (Xyl), designated as YPD, YPGal and YPXyl, respectively, were used. YP medium supplemented with 20 g/l Glc and 20 g/l of one of the other sugars was used to examine the effect of glucose.

3.3.2 Cultivation conditions

For preparation of the pre-culture, cells were grown in 5 ml of YPGal medium at 30°C under a shaking condition at 160 rpm for 18 h. The pre-culture was inoculated into a 100-ml Erlenmeyer flask containing 30 ml fresh medium at an initial OD_{660} value of 0.1, and the cultivation was performed at 30°C under a shaking condition at 160 rpm for an appropriate time. In experiments using spotting tests, pre-cultured cells were washed with deionized water, suspended in deionized water at 1×10^7cells/ml, 10-fold sequentially diluted, and then spotted

onto agar plates of YPD, YPGal and YPXyl with or without 0.01% 2-DOG. The plates were incubated at 30°C for 48 h.

3.3.3 Construction of *kan*MX4-inserted mutants and screening of 2-DOG-resistant mutants

DNA fragments of a *kan*MX4 cassette were prepared by PCR-directed amplification with a specific set of primers (Table 3.1) and pUG6 as a template DNA (Lertwattanasakul et al. 2013) and introduced into *K. marxianus* cells by the lithium acetate method (Antunes et al. 2000). After 60-min incubation at 30°C in YPD medium, the cells were spread on plates of YPXyl supplemented with 0.01% 2-DOG and 150 μg/ml of geneticin G418 and then incubated at 30°C for 72 h. Each colony on the plates was re-streaked on the same plates. Colonies capable of growing in the presence of 2-DOG and G418 were selected as candidates for glucose-repression-free mutants.

3.3.4 Analysis of *kan*MX4-inserted position

The insertion site of the cassette on the genome of each 2-DOG mutant was determined by TAIL-PCR followed by nucleotide sequencing as described previously (Lertwattanasakul et al. 2013). Six primers specific for *kan*MX4 and random primers were used for the TAIL-PCR (Charoensuk et al. 2011) to amplify DNA fragments from the genomic DNA of each mutant, which was isolated as described previously (Lertwattanasakul et al. 2007). Nucleotide sequencing was performed by using one of the *kan*MX4 primers and DNA fragments amplified by TAIL-PCR. The nucleotide sequence determined was then compared with the genome sequence of *K. marxianus* DMKU 3-1042 to identify the disrupted gene in each mutant.

3.3.5 Complementation of *kan*MX4-inserted mutants with DNA fragments of the target gene and drug-resistance gene

For the complementation test of *kan*MX4-inserted mutant strains, double transformation with amplified DNA fragments of the corresponding target gene and the *ble* gene encoding zeomycin resistance gene was performed. Primers were designed to anneal at approximately 1,000 bp away from each coding region of the target genes. Target genes were amplified by PCR using the genomic DNA of the parental strain as a template with corresponding primer sets (Table 3.1). The *ble* gene was amplified by PCR from pSH65 (Gueldener et al. 2002) DNA as a template with a primer set (Table 3.1). The PCR products were recovered by ethanol precipitation, and 50−400 ng of the products of each target gene and *ble* were mixed and transformed using the lithium acetate method (Antunes et al. 2000) into the corresponding disrupted-mutant strain. Transformants were then obtained on 2% YPD agar plates containing 100 μg/ml of zeomycin after incubation at 30°C. For the complementation test, the independent colonies were cultivated in 2% YPGal medium at 30°C for 18 h and subjected to a spot test using agar plates of 2% YPD and 2 % YPXyl containing 0.01% 2-DOG. The plates were incubated at 30°C for 48 h. Colonies that were sensitive to 2-DOG and grew well like the parental strain in YPD were distinguished to be complemented ones.

Table 3.1 Primers used in this study

Name	Sequence	Remark
bleF	5'-TCTGTACAGACGCGTGTACG-3'	Primer for *ble* amplification
bleR	5'-AACTAATTACATGATATCGA-3'	Primer for *ble* amplification
kanMX-KpnI5'	5'-GATGGTACCCAGCTGAAGCTTCGTACGC-3'	Primer for *kan*MX4 amplification
kanMX-KpnI3'	5'-CATGGTACCGCATAGGCCACTAGTGGATCTG-3'	Primer for *kan*MX4 amplification
kanMX-100-IV	5'-AGGAGGGTATTCTGGGC-3'	[a]
kanMX-1381-IV	5'-TGCGAAGTTAAGTGCGC-3'	[a]
kanMX-322-IV	5'-TGCTCGCAGGTCTGCAGCGAGGA-3'	[a]
kanMX-216-IV	5'-ACGGGCGACAGTCACATCATGCC-3'	[a]
kanMX-1135-IV	5'-AGTCGGAATCGCAGACCGATACC-3'	[a]
kanMX-1485-IV	5'-GGTCGCTATACTGCTGTCGATTC-3'	[a]
mig1-F	5'-ACAACCAACTATCCCGGTGC-3'	[b]
mig1-R	5'-AGAGATGGCATCATCAGTTCGT-3'	[b]
wtm2-F	5'-GCAGCAGGAATAACAGGACC-3'	[b]
wtm2-R	5'-TTTTCTCTGGGACAGAGTGT-3'	[b]
dfg16-F	5'-GGACAGAAAAGTCACGCAGC-3'	[b]
dfg16-R	5'-TGAGTTCTGCAACGCAGTCT-3'	[b]
ctm1-F	5'-TCGCTAAGTCATGCTGCTCC-3'	[b]
ctm1-R	5'- GTTGGAGTAGGTGGGTTCGG -3'	[b]
dig1-F	5'-CGAATTGAAGGCCACTTCGT-3'	[b]
dig1-R	5'-TGGCCGTGACCAAAGAAAGG-3'	[b]
msn5-F	5'-GGCCATGGTAGACCAACGAG-3'	[b]
msn5-R	5'-CGAACCTTTTCCCCCGGTAT-3'	[b]
alg10-F	5'-GATGCGTAAGTTCCGCCTGA-3'	[b]
alg10-R	5'-GAATCGCGCAAGTTGAGAGT-3'	[b]
nnk1-F	5'-TGGACTTGATAACGGCACCT-3'	[b]
nnk1-R	5'-ACCTAGATGAGTGGATGAGTGGA-3'	[b]
zip2-F	5'-TCGAAGGATTCCGTCTGCATT-3'	[b]
zip2-R	5'-CTCCTATCTAAAGGGCGAGGC-3'	[b]
rgi2-F	5'-ACAGTGCAGGTAGAAAAACCAT-3'	[b]
rgi2-R	5'-GTTGCATCATTTGAGGTGCAG-3'	[b]
mdj2-F	5'-ATGCAACCGCTCAGACAAGA-3'	[b]

Name	Sequence	Remark
mdj2-R	5'-CTCTGTTGGGACAGGTTCAGT-3'	[b]
arg3-F	5'-AGGAGCTTGGAATAACCGCC-3'	[b]
arg3-R	5'-GCACCAGACAGCCAATTTGA-3'	[b]

[a] Primers for amplification and sequencing of flanking regions of *kan*MX4 inserted.
[b] Primers for amplification of a corresponding gene to complement the *kan*MX4-inserted mutation.

3.3.6 Analytical methods

Cell density was measured turbidimetrically at 660 nm. Cultures were sampled and subjected to a low-speed centrifugation. The supernatant was frozen and kept at -20°C until used for analysis. Quantitative analysis of sugars, ethanol, glycerol and xylitol was performed by high-performance liquid chromatography (Hitachi, Japan) as described previously (Rodrussamee et al. 2011). A GL-C610-S gel pack column (Hitachi, Japan) was used together with a refractive index detector (Model L-2490, Hitachi) at 60°C with 0.3 ml/min eluent of deionized water.

3.4. Results

3.4.1 Isolation of 2-DOG-resistant mutants by insertion of *kan*MX4

In general, 2-DOG as a glucose analogue was used for screening mutants defective in glucose repression (Kahar et al. 2011). We thus introduced PCR-amplified DNA fragments of a *kan*MX4 cassette into *K. marxianus* DMKU3-1402 and isolated G418- and 2-DOG-resistant strains. From about 6,000 G418-resistant strains, 125 2-DOG-resistant strains were isolated and subjected to TAIL-PCR to determine the nucleotide sequence flanking the inserted *kan*MX4 cassette. Of these, the nucleotide sequences of about 110 mutants tested were found to be mixtures of sequences due to more than one *kan*Max4 cassette at one or more than one of the insertion sites of the cassette on the genome. Only 17 mutants showed a

clear single sequence at both flanking regions of *kan*MX4, and both flanking sequences were a continous sequence on the parental genome, indicating a single insertion of the *kan*MX4 cassette on the genome. Of the 17 mutants, 11 and 6 mutants were found to have intragenic and intergenic insertions, respectively, of the casette.

To further verify the disrupted genes of the 11 intragenically inserted mutants, we performed complementation experiments by introduction of DNA fragments of the wild-type gene, which were PCR-amplified from the genomic DNA of the parental *K. marxianus*, and DNA fragments of the zeomycin resistance gene as a selective marker. As expected, all mutants became sensitive to 2-DOG similarly to the parental strain after successful introduction of the intact gene. These results clearly suggest a single integration of the *kan*MX4 fragment in the 11 mutants. In the same screening, an intragenically *kan*MX4-inserted *mig1* mutant was also obtained as a 2-DOG-resistant mutant, which had an additional insertion of the *kan*MX4 cassette into 26S rDNA gene. Since the 2-DOG-resistant phenotype of the *mig1* mutation was complemented with the wild-type gene, *MIG1*, we used the mutant strain as a positive control for the glucose repression-free mutant, because Mig1p is well known as a key regulator of glucose repression in *S. cerevisiae* (Nehlin et al. 1990; Nehlin et al. 1991; Cassart et al. 1995).

3.4.2 Possible functions of genes in which *kan*MX4 was inserted in 2-DOG-resistant mutants

*kan*MX4-inserted genes of the 11 mutants and the *mig1* mutant are shown in Table 3.2 with the *S. cerevisiae* and *K. lactis* orthologues of these gene products and their function (14%-68% identity in 41%-100% coverage). We compared the product of the gene, which was disrupted by the *kan*MX4 insertion in mutants isolated, with the orthologue of *S. cerevisiae.* KmWtm2p shares 35% identity with ScWtm2p, which functions as a transcriptional modulator for meiotic regulation and silencing (Pemberton and Blobel, 1997). KmDfg16p shares 25% identity with ScDfg16p, which is a multiple transmembrane protein involved in diploid invasive and pseudohyphal growth upon nitrogen starvation (Rothfels et al. 2005).

KmCtm1p shares 27% identity with ScCtm1p, which functions as a cytochrome *c* lysine methyltransferase (Polevoda et al. 2000). KmDig1p shares 14% identity with ScDig1p, which is a MAP kinase-responsive inhibitor of the Ste12p transcription factor, involved in the regulation of mating-specific genes and the invasive growth pathway (Bardwell et al. 1998). KmMsn5p shares 67% identity with ScMsn5p, which is a karyopherin involved in the nuclear import and export of proteins (Yoshida and Blobel, 2001). KmAlg10p shares 56% identity with ScAlg10p, which is a dolichyl-phosphoglucose-dependent □-1,2 glucosyltransferase in the endoplasmic reticulum (Burda and Aebi, 1998). KmNnk1p shares 31% identity with ScNnk1p, which is a protein kinase involved in proteasome function (Breitkreutz et al. 2010). KmZip2p shares 25% identity with ScZip2p, which is a meiosis-specific protein involved in normal synaptonemal complex formation and pairing between homologous chromosomes during meiosis (Chua and Roeder, 1998). KmRgi2p shares 68% identity with ScRgi2p, which is involved in energy metabolism under respiratory conditions (Domitrovic et al. 2010). KmMdj2p shares 49% identity with ScMdj2p, which participates in the mitochondrial import of proteins (Mokranjac et al. 2005). KmArg3p shares 72% identity with ScArg3p, which is an ornithine carbamoyltransferase (Crabeel et al. 1981).

3.4.3 Growth phenotype of 2-DOG-resistant mutants in the presence of 2-DOG

To confirm 2-DOG resistance of the 11 mutants, spot tests were carried out on YPGal and YPXyl plates supplemented with or without 2-DOG by using YPD as a control (Fig. 1). Compared to the parental strain, these mutants exhibited efficient growth at 10^3- and 10^4-fold dilutions on both YPGal and YPXyl plates supplemented with 2-DOG, suggesting that they are resistant to 2-DOG. Interestingly, colony sizes in 10^4-fold dilution of *zip2, rgi2* and *arg3* mutants in addition to the *mig1* mutant were larger than those of other mutants in YPD, indicating variation in mutants isolated. On the other hand, all mutants similarly grew on YPGal and YPXyl plates in the absence of 2-DOG.

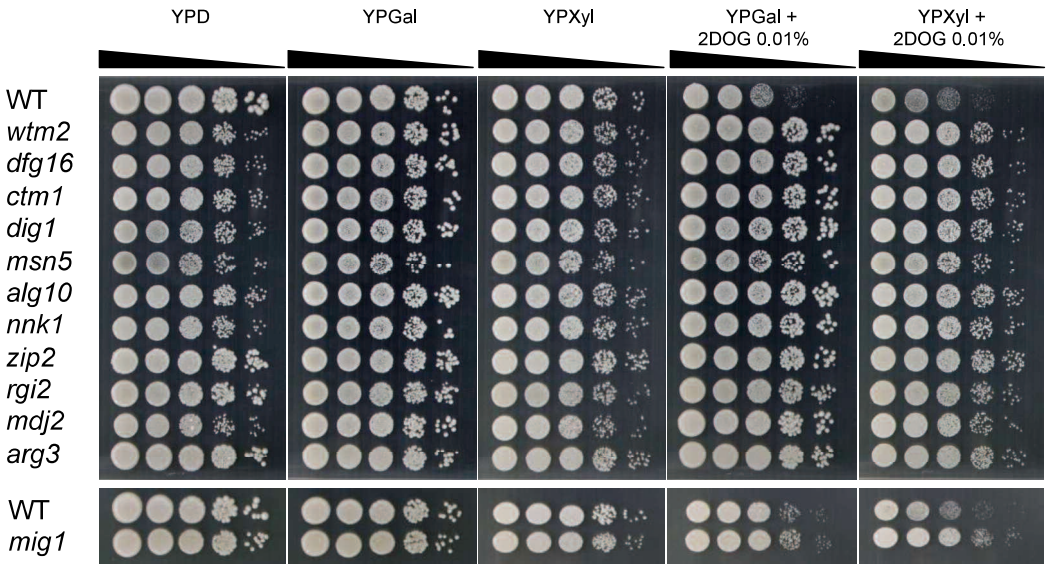

Fig. 3.1 Resistance of isolated *kan*MX4-inserted mutants to 2-DOG. Cells were grown in 2% YPGal medium at 30°C for 18 h and subjected to a spot test as described in Materials and methods. After spotting (left to right, 10^{0}, 10^{-1}, 10^{-2}, 10^{-3} and 10^{-4} fold dilutions) on 2% YPD, 2% YPGal, 2% YPXyl, 2% YPGal containing 0.01% 2-DOG and 2% YPXyl containing 0.01% 2-DOG, plates were incubated at 30°C for 48 h

Table 3.2 Orthologues of *S. cerevisiae* and *K. lactis* to the product of gene, which was inserted by *kan*MX4 in mutants

Mutant	Disrupted gene	Source organism	Accession number	Orthologue	Function and description [a]	Query length	Target length	E-value	Target coverage	Alignment coverage	Identity	Positive
DG2	KLMA_20059	*Saccharomyces cerevisiae* S288c	NP_011480	Mig1p	Transcription factor involved in glucose repression; sequence specific DNA binding protein containing two Cys2His2 zinc finger motifs; regulated by the SNF1 kinase and the GLC7 phosphatase; regulates filamentous growth along with Mig2p in response to glucose depletion	556	504	1.9E-38	91%	41%	18%	23%
		Kluyveromyces lactis NRRL Y-1140	XP_454446	Hypothetical protein	Uniprot|P50898 *K. lactis* MIG1 Regulatory protein MIG1	556	474	5.57E-132	85%	100%	50%	62%
DG4	KLMA_20787	*Saccharomyces cerevisiae* S288c	NP_014872	Wtm2p	Transcriptional modulator involved in regulation of meiosis, silencing, and expression of RNR genes; involved in response to replication stress; contains WD repeats	455	467	7.51E-77	100%	100%	35%	51%
		Kluyveromyces lactis NRRL Y-1140	XP_453386	Hypothetical protein	Similar to gnl|GLV|CAGL0M02563g *Candida glabrata* CAGL0M02563g and weakly similar to uniprot|Q12206 YOR229W *S. cerevisiae* WTM2	455	450	1.7E-170	99%	100%	56%	72%
DG6	KLMA_60099	*Saccharomyces cerevisiae* S288c	NP_014673	Dfg16p	Probable multiple transmembrane protein; involved in diploid invasive and pseudohyphal growth upon nitrogen starvation; is glycosylated and phosphorylated; interacts with Rim21p and Rim9p in the plasma membrane to form a pH-sensing complex in the Rim101 pathway and is required to maintain Rim21p levels; required for accumulation of processed Rim101p	479	619	4.1E-59	100%	81%	25%	44%
		Kluyveromyces lactis NRRL Y-1140	XP_454708	Hypothetical protein	Some similarities with uniprot|Q99234 *S. cerevisiae* YOR030W DFG16	479	482	1.42E-178	100%	100%	56%	74%
DG9	KLMA_20447	*Saccharomyces cerevisiae* S288c	NP_011977	Ctm1p	Cytochrome *c* lysine methyltransferase, trimethylates residue 72 of apo-cytochrome *c* (Cyc1p) in the cytosol; not required for normal respiratory growth	511	585	1.32E-44	100%	100%	27%	49%
		Kluyveromyces lactis NRRL Y-1140	XP_454919	Hypothetical protein	Weakly similar to uniprot|P38818 YHR109W *S. cerevisiae* CTM1	511	503	4.65E-175	98%	99%	50%	67%
DG41	KLMA_60404	Saccharomyces cerevisiae S288c	NP_015276	Dig1p	MAP kinase-responsive inhibitor of the Ste12p transcription factor, involved in the regulation of mating-specific genes and the invasive growth pathway; related regulators Dig1p and Dig2p bind to Ste12p	376	452	4.00E-07	100%	43%	14%	23%
		Kluyveromyces lactis NRRL Y-1140	XP_453577	Hypothetical protein	Conserved hypothetical protein	376	372	4.3E-132	99%	100%	58%	70%
DG50	KLMA_40242	*Saccharomyces cerevisiae* S288c	NP_010622	Msn5p	Karyopherin involved in nuclear import and export of proteins, including import of replication protein A and export of Swi6p, Far1p, and Pho4p; required for re-export of mature tRNAs after their retrograde import from the cytoplasm	1221	1224	0	100%	100%	67%	84%
		Kluyveromyces lactis NRRL Y-1140	XP_456046	Hypothetical protein	Highly similar to uniprot|P52918 *S. cerevisiae* YDR335W MSN5	1221	1221	0	100%	100%	91%	97%
DG54	KLMA_60055	*Saccharomyces cerevisiae* S288c	NP_011743	Alg10p	Dolichyl-phosphoglucose-dependent alpha-1,2 glucosyltransferase of the ER, functions in the pathway that synthesizes the dolichol-linked oligosaccharide precursor for N-linked protein glycosylation, has a role in regulation of ITR1 and INO1	509	525	0	100%	100%	56%	73%
		Kluyveromyces lactis NRRL Y-1140	XP_454662	Hypothetical protein	Similar to uniprot|P50076 *S. cerevisiae* YGR227W DIE2	509	533	0	100%	100%	80%	89%
DG68	KLMA_10391	*Saccharomyces cerevisiae* S288c	NP_012750	Nnk1p	Protein kinase; implicated in proteasome function; interacts with TORC1, Ure2 and Gdh2; overexpression leads to hypersensitivity to rapamycin and nuclear accumulation of Gln3; epitope-tagged protein localizes to the cytoplasm	806	928	8.04E-103	100%	93%	31%	46%
		Kluyveromyces lactis NRRL Y-1140	XP_451302	Hypothetical protein	Similar to uniprot|Q757Y0 *Ashbya gossypii* AEL120W AEL120Wp and some similarities with YKL171W uniprot|P36003 *S. cerevisiae* YKL171W	806	800	0	99%	100%	69%	82%
DG71	KLMA_60409	*Saccharomyces cerevisiae* S288c	NP_011265	Zip2p	Meiosis-specific protein; involved in normal synaptonemal complex formation and pairing between homologous chromosomes during meiosis; relocalizes from mitochondrion to cytoplasm upon DNA replication stress	678	704	1.06E-19	104%	100%	25%	45%
		Kluyveromyces lactis NRRL Y-1140	XP_453570	Hypothetical protein	Weakly similar to uniprot|P53061 *S. cerevisiae* YGL249W ZIP2: Required for 'ZIPpering' up meiotic chromosomes during chromosome synapsis involved in meiotic recombination and disjunction	678	675	2.29E-157	100%	100%	40%	62%

Mutant	Disrupted gene	Source organism	Accession number	Orthologue	Function and description [a]	Query length	Target length	E-value	Target coverage	Alignment coverage	Identity	Positive
DG72	KLMA_70178	*Saccharomyces cerevisiae* S288c	NP_010990	Rgi2p	Hypothetical protein; involved in energy metabolism under respiratory conditions; protein abundance is increased upon intracellular iron depletion; protein abundance increases in response to DNA replication stress	161	161	1.12E-70	100%	99%	68%	79%
		Kluyveromyces lactis NRRL Y-1140	XP_452559	Hypothetical protein	Highly similar to uniprot|P40188 *S. cerevisiae* YIL057C Hypothetical ORF	161	163	2.25E-105	100%	100%	91%	94%
DG79	KLMA_20626	*Saccharomyces cerevisiae* S288c	NP_014071	Mdj2p	Constituent of the mitochondrial import motor associated with the presequence translocase; function overlaps with that of Pam18p; stimulates the ATPase activity of Ssc1p to drive mitochondrial import; contains a J domain	148	146	4.81E-48	99%	100%	49%	75%
		Kluyveromyces lactis NRRL Y-1140	XP_454039	Hypothetical protein	Similar to uniprot|P42834 *S. cerevisiae* YNL328C MDJ2: Protein of the mitochondrial inner membrane function partially overlaps that of Mdj1p which is a chaperone involved in folding of mitochondrially synthesized proteins in the mitochondrial matrix member of the DnaJ family	148	146	9.36E-78	99%	99%	76%	92%
DG80	KLMA_30168	*Saccharomyces cerevisiae* S288c	NP_012447	Arg3p	Ornithine carbamoyltransferase (carbamoylphosphate: L-ornithine carbamoyltransferase), catalyzes the sixth step in the biosynthesis of the arginine precursor ornithine	340	338	0	99%	98%	72%	83%
		Kluyveromyces lactis NRRL Y-1140	XP_455725	Hypothetical protein	Similar to uniprot|P05150 YJL088W *S. cerevisiae* ARG3	340	334	0	98%	94%	85%	90%

[a)] The function of genes was derived on inferred from the NCBI on Swiss-Prot database

3.4.4 Comparison of cell growth among 2-DOG-resistant mutants in YP medium containing a single sugar or mixed sugars

Since the 11 mutants formed colonies of different sizes on YPD plates, their cell growth was compared in YPD and YPXyl liquid media under a shaking condition (circles and squares, respectively, in Fig. 2). In YPD medium, the cell growth of the *zip2* and *arg3* mutants was similar to those of the *mig1* mutant and parental stains. The *rgi2* mutant showed the similar pattern of growth to that of the parental stain, but relatively low maximum growth. Other mutants showed extended lag phases. In YPXyl medium, almost all of the mutants grew similarly to the parent strain. These growth characteristics in liquid culture may be thus nearly consistent with those in plate culture.

To further investigate the effect of glucose, the cell growth of 2-DOG-resistant mutants was compared with those of the parental and *mig1* mutant strains in YPD, YPXyl and YPD + Xyl liquid media as shown in Fig. 2. As a result, all mutants except for *zip2, rgi2* and *arg3* mutants grew very slowly compared to the *mig1* mutant and parental strains in both YPD and YPD+Xyl media. The *rig2* and *arg3* mutants showed similar patterns of growth to that of the parental strain in the three different media tested, though *rgi2* showed slightly slower growth in both YPD and YPD+YPXyl media. Notably, the cell growth of *zip2* and *mig1* mutants in the YPD+Xyl medium was found to be more than that in the YPD medium after around12 h, indicating derepression of the glucose repression on the utilization of Xyl. On the other hand, other mutants showed lower cell growth in YPD+Xyl medium than that in YPXyl medium, indicating the existence of glucose repression on the utilization of Xyl.

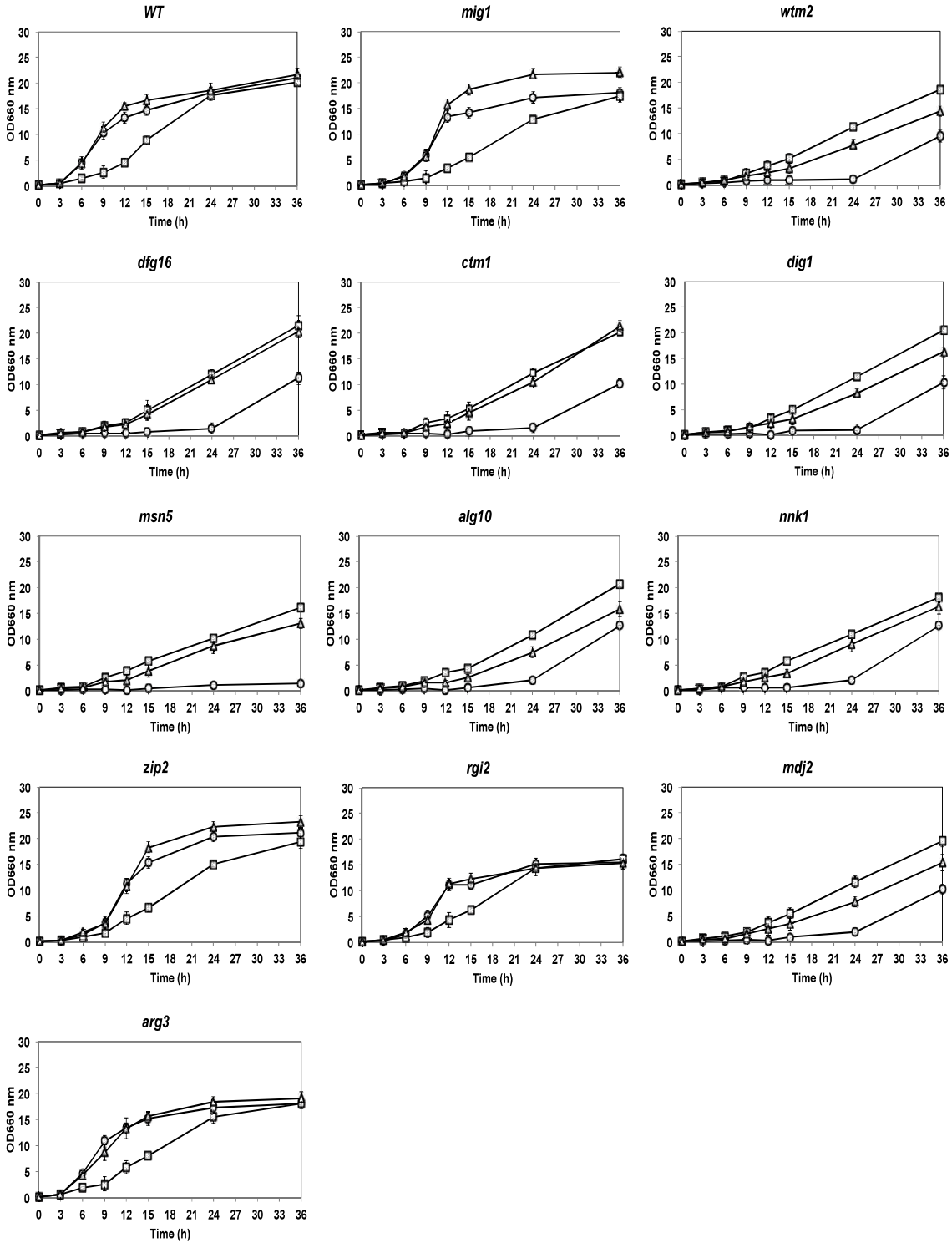

Fig. 3.2 Comparison of cell growth among 2-DOG-resistant mutants in YP media containing a single sugar of Glc or Xyl or mixed sugars of Glc and Xyl. Cells were grown in 2% YPGal medium at 30°C for 18 h, transferred to fresh 2% YP media containing 2% Glc (circles), 2% Xyl (squares) or 2% Glc + 2% Xyl (triangles) and cultivated at 30°C for 36 h. Cell growth of mutants and the parental strain was compared by measuring OD_{660}. Data presented were averages of triplicate experiments and error bars indicate the standard deviations

3.4.5 Cell growth of 2-DOG-resistant mutants in different concentration of Glc

To further analyze the Glc utilization ability of the 11 mutants and the *mig1* mutant, we compared their growth in YNB plates containing different concentrations of Glc (Fig. 3). Mutants of *zip2* and *rgi2* were found to grow well like the parental strain at 0.2%. The *arg3* and *ctm1*mutants also grew at 0.2%, but their growth was lower than that of the parental strain. Other mutants hardly grew at the low concentration of Glc. All eleven mutants, however, grew at 2% Glc. Notably, growth of the *arg3* mutant did not increase at 2% Glc compared to that at 0.2% Glc, indicating that its growth was repressed by some extent by Glc. These findings suggest that the eight mutants *wtm2, dfg16, ctm1, dig1, msn5, alg10, nnk1* and *mdj2* are defective in Glc uptake or in its initial catabolism.

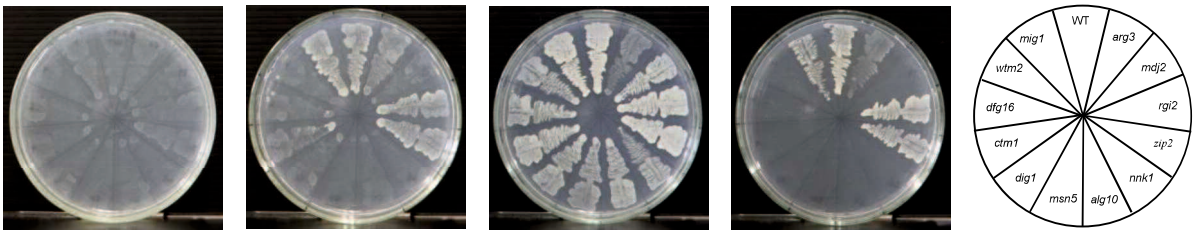

a 0.02% Glc **b 0.2% Glc** **c 2 % Glc** **d 2 %Glc + antimycin A**

Fig. 3.3 Cell growth of 2-DOG-resistant mutants in YNB plates containing different concentrations of Glc and effect of antimycin A. Cells were grown in 2% YPGal medium at 30°C for 18 h and streaked on YNB plates containing different concentrations of Glc. The plates were then incubated at 30°C for 48 h. a, 0.02% Glc; b, 0.2% Glc; c, 2% Glc; d, 2% Glc + 5 μM antimycin A

3.4.6 Effect of antimycin A on cell growth of 2-DOG-resistant mutants

To examine the effect of a respiratory inhibitor, antimycin A, on cell growth of 2-DOG-resistant mutants, the mutants were grown on YNB plates containing 2% Glc and 5 μM antimycin A at 30 °C (Fig. 3d). The mutants *zip2* and

rgi2 as well as the *mig1* mutant grew well like the parental strain in the presence of antimycin A and the *arg3* mutant showed weaker growth than that of the parental strain, but other mutants did not grow. These results and growth of mutants on 0.2% Glc (Fig. 3b) suggest that *zip2, rgi2* and *mig1* mutants can sufficiently uptake and catabolize Glc to support cell growth by fermentation activity. On the other hand, the defective growth of other mutants in the presence of the respiratory inhibitor may be due to too weak import activity of Glc to grow under a fermentation condition.

3.4.7 Cell growth and sugar consumption of 2-DOG-resistant mutants in YP medium containing mixed sugars of Glc and Xyl

To determine whether the 2-DOG-resistant mutants had acquired the phenotype of glucose-repression-free mutation, their Xyl utilization ability was examined in the presence of Glc. The 11 intragenically *kan*MX4-inserted mutants were grown in YP medium containing Glc and Xyl and their consumption patterns of both sugars were compared with those of the parental and *mig1* mutant strains (Fig. 4). The sugar utilization features in the figure allow them to be classified into two groups. One group of *zip2, rgi2* and *arg3* mutants as well as *mig1* mutant exhibited slower Glc and faster Xyl consumption rates than those of the parental strain. Values of OD_{660} suggest that cell growth at 24 h and 36 h of *zip2, rgi2* and *mig1* mutants was higher than or similar to that of the parental strain. However, cell growth of the *rgi2* mutant at all of the times tested was slightly lower than that in the parental strain. Among these mutants and the parent, however, there was no significant difference in ethanol concentration in media after 15 h. The other group of the remaining mutants showed extremely slow Glc and Xyl consumption rates and almost no ethanol accumulation in the medium. The former group may be mutants that can utilize Glc and Xyl simultaneously since their sugar utilization features were similar to those of a *S. cerevisiae* 2-DOG-resistant mutant that is able to assimilate both sugars together (Kahar et al. 2011). The reduction in Xyl concentration after 24 h in the parental strain may be due to derepression of the glucose repression after consumption of Glc.

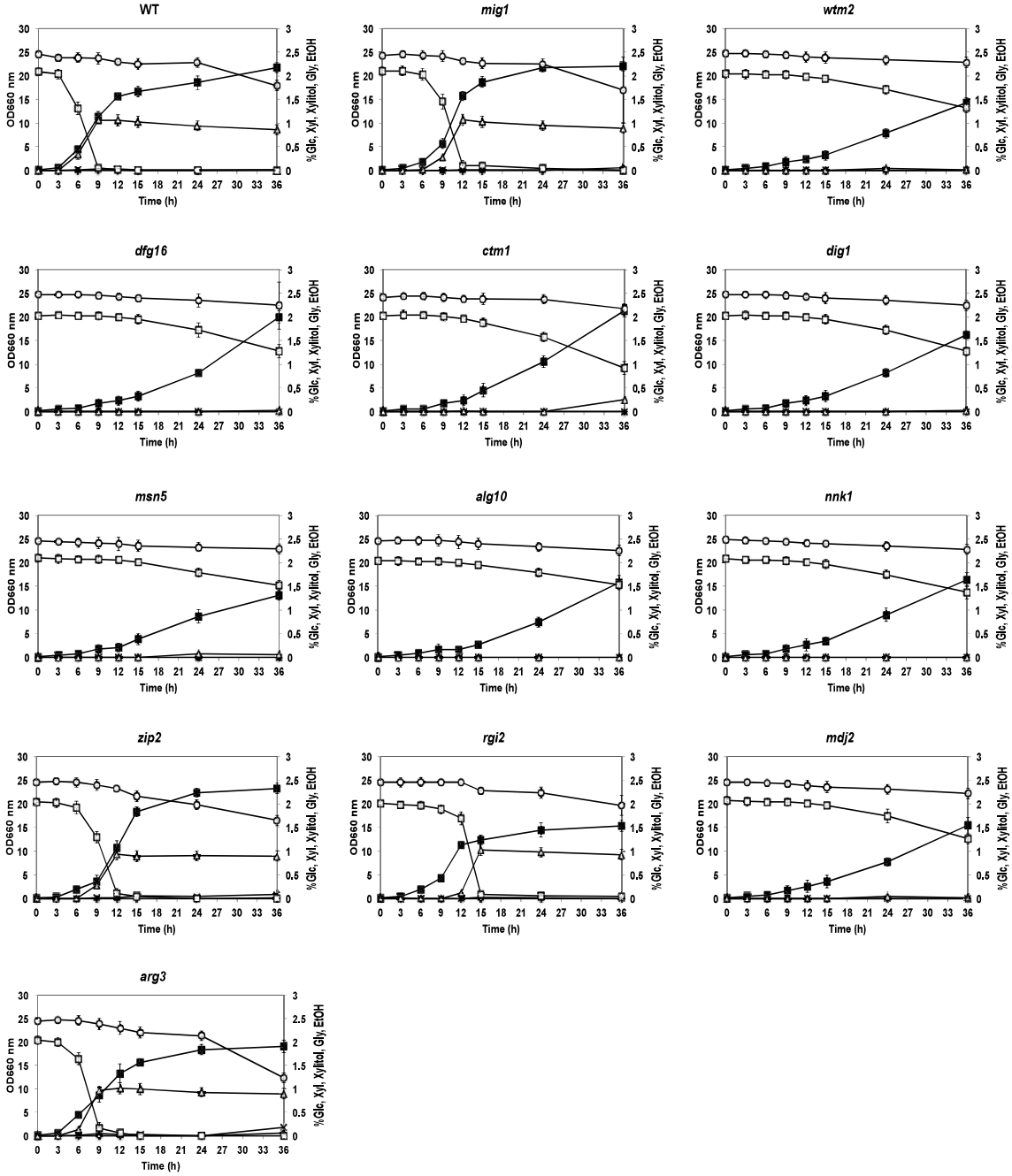

Fig. 3.4 Cell growth and sugar consumption of 2-DOG-resistant mutants in YP medium containing mixed sugars of Glc and Xyl. Cells were grown in 2% YPGal medium at 30°C for 18 h, transferred to fresh YP medium containing 2% Xyl and 2% Glc and cultivated at 30°C for 36 h. Cell growth of mutants and the parental strain (close squares) was compared by measuring OD_{660}. Concentration of Glc (open squares), Xyl (circles), ethanol (triangles), glycerol (crosses) and xylitol (diamonds) in media were measured. Data presented were averages of triplicate experiments and error bars indicate the standard deviations.

3.5 Discussion

In general, microbes possess mechanisms of preferential uptake and catabolism of Glc (Carlson, 1999) including the glucose repression as a catabolite repression that may be crucial for microorganisms to survive by utilizing available sugars (Gancedo, 1998). Since the uptake of Glc has a negative impact on the metabolism of other sugars (Klein et al. 1998), efficient glucose-repression-free mutants are expected to be developed for the utilization of mixed sugars, such as those in lignocellulosic biomass, to produce useful materials including ethanol.

In this study, as the first trial to elucidate the glucose repression in *K. marxianus*, we characterized intragenically *kan*MX4-inserted mutants isolated as 2-DOG-resistant mutants, which were derived by the random integration mutagenesis. Analysis of consumption ability of a single sugar or mixed sugars revealed that these mutants could be classified into two groups. One group of mutants, *zip2, rgi2* and *arg3* acquired significantly better growth ability on Xyl and Gal in the presence of 2-DOG than that of the parental strain (Fig. 1), and their consumption of Glc and Xyl was delayed and slightly faster, respectively, in a medium containing mixed sugars, Xyl plus Glc (Fig. 4). These characteristics resemble those of the *mig1* mutant. The *zip2* and *mig1* mutants exhibited higher growth in the mixed-sugars medium of Xyl plus Glc than that in the single-sugar medium of Glc or Xyl (Fig. 2). Whereas, the growth of *rgi2* and *arg3* mutants as well as the parental strain in a medium containing Xyl and Glc was found to be similar to that in a medium containing only Glc. The *rgi2* and *arg3* mutants thus seem to retain partial glucose repression. Judging from these findings, it is suggested that Zip2p like Mig1p is directly involved in the glucose repression of *K. marxianus* and that Rgi2p and Arg3p are closely related to the repression. Mig1p is a zinc finger protein that mediates glucose repression in *S. cerevisiae* (Nehlin and Ronne, 1990) and functions as a repressor to down-regulate a large number of genes involved in carbohydrate catabolism, gluconeogenesis and respiration (Entian, 1986; Gancedo and Gancedo, 1986; Carlson, 1987). KlMig1p shares 55% similarity (10% identity) with ScMig1p (Cassart et al. 1995) and high similarity (50% identity) with KmMig1p (Table 3.2). KlMig1p has been shown to

heterologously complement the *S. cerevisiae mig1* mutant (Cassart et al. 1995). When glucose is present, ScMig1p is dephosphorylated by phosphatase (probably the Reg1-Glc7 complex), imported into the nucleus by the aid of importin (DeVit and Johnston, 1999), binds target genes and recruits Ssn6 and Tup1 to repress their transcription (Treitel and Carlson, 1995; Tzamarias and Struhl, 1994; Tzamarias and Struhl, 1995). KmZip2p, which is similar (25% identity) to ScZip2p, a protein required for the initiation of meiotic chromosome synapsis (Chua and Roeder, 1998), may participate in the Mig1p-mediated glucose repression. It is thus possible that Zip2p is involved in Mig1p-mediated glucose repression under the condition of a high level of glucose and involved in meiosis under the condition of a limited level of glucose. ScRgi2p is important for cell growth in non-fermentable carbon sources (Domitrovic et al. 2010), and ScArg3p is an ornithine carbamoyltransferase catalyzing step 6 of arginine biosynthesis (Crabeel et al. 1985). The evidence that *RGI2* and *ARG3* mutations weakened the Mig1-mediated glucose repression suggests that there is some regulatory interaction between the glucose repression mechanism and respiratory or amino acid metabolism.

The other group of mutants, *wtm2, dfg16, ctm1, dig1, msn5, alg10, nnk1* and *mdj2*, seem to be defective in uptake or initial catabolism of Glc, resulting in very slow growth in Glc medium (Fig. 2) and no growth in Glc medium in the presence of antimycin A (Fig. 3). These mutants, however, appear to retain the regulation of glucose repression (Fig. 2). Due to dysfunction of the uptake or initial catabolism of Glc, these mutants may import 2-DOG very limitedly, resulting in being resistant to the drug. They exhibited inability of growth at a low concentration of Glc (Fig. 3), which may be unlikely due to the disruption of genes for specific high-affinity glucose transporters because *K. marxianus* possesses more than 16 putative sugar transporters (Lertwattanasakul et al. 2015). Functions of these mutated genes were deduced from those of the corresponding genes in *S. cerevisiae* that have been characterized: *WTM2* encoding for a transcriptional modulator for several loci (Pemberton and Blobel, 1997), *DIG1* encoding for a presumable negative regulator of Ste12 for invasive growth (Cook et al. 1996), *DFG16* encoding for a corepressor for *DIT1* as the mid-late class of the sporulation-specific gene (Rothfels et al. 2005), and *NNK1* encoding for a protein

kinase (Breitkreutz et al. 2010). Their possible functions allow us to speculate that their related transcriptional regulation or signal transduction somehow stimulate the uptake or initial catabolism of Glc in *K. marxianus*.

Disrupted mutants of *MDJ2* and *CTM1* that encode mitochondrial DnaJ homologue and cytochrome c methyltransferease, respectively, do not exhibit any growth defect in Glc medium in *S. cerevisiae* (Polevoda et al. 2000; Westermann and Neupert, 1997), but the corresponding disrupted mutants in *K. marxianus* exhibited defective growth in Glc medium. *ALG10* encodes the α-1,2 glucosyltransferease in the endoplasmic reticulum in *S. cerevisiae*, and its mutation leads to underglycosylation of N-linked glycoproteins (Burda and Aebi, 1998). Therefore, it is possible that the abnormality of these organelles has some kind of feedback effect on the initial stage of Glc assimilation in *K. marxianus*. Interestingly, Msn5p, which mediates the nuclear import and nuclear export of different cargo proteins, is required for the nuclear export of Mig1p in *S. cerevisiae* (Yoshida and Blobel, 2001; DeVit and Johnston, 1999). If this is the case in *K. marxianus*, it is assumed that dysfunction of the control of Mig1p nuclear localization prevents the initial stage of Glc assimilation. Of course, there are alternative explanations to these possibilities and assumption. Further experiments on individual mutants should thus be performed to clarify physiological functions of these genes and the complicated control systems of glucose utilization including glucose repression in *K. marxianus*.

At the beginning of this study, we thought to obtain *K. marxianus* mutants that can efficiently and simultaneously utilize two sugars of Glc and Xyl. The mutants obtained, however, exhibited faster Xyl utilization but slower Glc utilization than those of the parental strain even in the *mig1* mutant. The enhancement of Xyl utilization may be due to impairment of the glucose-repression mechanism. The unexpected phenotype of reduction of Glc utilization might be due to the cofactor imbalance caused by Xyl catabolism (Bakker et al. 2001). Our next target is thus improvement of the cofactor imbalance and the ethanol producibility from Xyl in the yeast.

3.6 Conclusion

Glucose repression, which is a ubiquitous mechanism in microbes to inhibit the utilization of other sugars, hampers the conversion of biomass including various sugars to useful materials. In this study, to avoid the negative effect in *K. marxianus* that possesses an attractive potential in conversion of biomass, we screened the yeast mutants defective in glucose repression from 2-DOG resistant mutants that had been mutagenized by random insertion of the *kan*MX4 cassette into the genome. Isolated 11 intragenically *kan*MX4-inserted mutants were further analyzed and classified on sugar utilization ability to two categories: one group showed the phenotype of enhanced utilization of xylose in the presence of glucose and the other group showed largely delayed utilization of glucose. The former may be due to a defect in the glucose-repression mechanism and the latter may be due to reduction of the uptake or initial catabolism of glucose. Considering the possible functions of the disrupted genes in these mutants, it is likely that *K. marxianus* has undiscovered mechanisms for glucose repression and complex regulation for glucose uptake.

CHAPTER 4

Genetic basis of the highly efficient yeast *Kluyveromyces marxianus*: complete genome sequence and transcriptome analyses

4.1 Abstract

4.1.1 Background

High-temperature fermentation technology with thermotolerant microbes has been expected to reduce the cost of bioconversion of cellulosic biomass to fuels or chemicals. Thermotolerant *Kluyveromyces marxianus* possesses intrinsic abilities to ferment and assimilate a wide variety of substrates including xylose and to efficiently produce proteins. These capabilities have been found to exceed those of the traditional ethanol producer *Saccharomyces cerevisiae* or lignocellulose-bioconvertible ethanologenic *Scheffersomyces stipitis*.

4.1.2 Results

The complete genome sequence of *K. marxianus* DMKU 3-1042 as one of the most thermotolerant strains in the same species has been determined. A Comparison of its genomic information with those of other yeasts and transcriptome analysis revealed that the yeast bears beneficial properties of temperature resistance, wide-range bioconversion ability and production of recombinant proteins. The transcriptome analysis clarified distinctive metabolic pathways under three different growth conditions, static culture, high temperature and xylose medium, in comparison to the control condition of glucose medium under a shaking condition at 30°C. Interestingly, the yeast appears to overcome the issue of reactive oxygen species, which tend to accumulate under all three conditions.

4.1.3 Conclusions

This study reveals many gene resources for the ability to assimilate various sugars in addition to species-specific genes in *K. marxianus*, and the molecular basis of its attractive traits for industrial applications including high-temperature fermentation. Especially, the thermotolerance trait may be achieved by an integrated mechanism consisting of various strategies. Gene resources and transcriptome data of the yeast are particularly useful for fundamental and applied researches for innovative applications.

4.2 Introduction

Along with rising concern about global warming and the rapid increase in fuel consumption, there is worldwide interest in the production of bioethanol from renewable resources (Hahn-Hägerdal et al. 2006). For economically sustainable production of bioethanol, it is necessary to increase the types of biomass such as lignocellulosic materials that can be used without competing with food supplies. Accordingly, microbes that can efficiently convert various sugars in these kinds of biomass to ethanol must be developed.

A high-temperature fermentation (HTF) technology is expected to help reduce cooling cost, efficiently achieve simultaneous saccharification and fermentation, reduce the risk of contamination, and offer stable fermentation even in tropical countries (Banat et al. 1998; Limtong et al. 2007). Thermotolerant yeast *K. marxianus*, which is able to ferment various sugars, may be a suitable microbe for HTF with lignocellulosic hydrolysates (Rodrussamee et al. 2011; Nonklang et al. 2008).

K. marxianus is a haploid, homothallic, thermotolerant, hemiascomycetous yeast (Lachance 2011; Llorente et al. 2000) and a close relative of *Kluyveromyces lactis*, a model Crabtree-negative yeast (Fukuhara 2006; Schaffrath and Breunig 2000; González-Siso et al. 2000; Rodicio and Heinisch 2013). Both yeasts share the assimilating capability of lactose, which is absent from *Saccharomyces cerevisiae*. *K. marxianus* has a number of advantages over *K. lactis* or *S. cerevisiae*,

including the intrinsic fermentation capability of various sugars at high temperatures (Rodrussamee et al. 2011; Lertwattanasakul et al. 2011; Fonseca et al. 2008), weak glucose repression that is preferable for mixed sugars such as hemicellulose hydrolysate, and fermentability of inulin (Fonseca et al. 2008; dos Santos et al. 2013). However, its fermentation activity from xylose is extremely low compared to that of glucose. Recently, we developed a procedure that improves this disadvantageous trait (unpublished data) and increases the fermentation activity to slightly less than that of *Scheffersomyces stipitis* at around 30°C and much higher activity at higher temperatures. Many biotechnological applications of *K. marxianus* have so far been achieved: production of various enzymes including heterologous proteins, aroma compounds or bioingredients, reduction of lactose content in food products, production of ethanol or single-cell protein and bioremediation (Fonseca et al. 2008). In addition, novel methods and genetic tools for genetic engineering have been developed on the basis of its high nonhomologous end-joining activity (Abdel-Banat et al. 2010; Hoshida et al. 2014). *K. marxianus* is thus a highly competent yeast for future developments. In order to facilitate such developments, its genomic information is essential. Draft genome sequences of three *K. marxianus* strains have been published (Llorente et al. 2000; Jeong et al. 2012; Suzuki et al. 2014) but no detailed analysis is available.

This study provides core information on *K. marxianus* DMKU 3-1042, which is one of the most thermotolerant strains in the same species isolated (Limtong et al. 2007; unpublished data), including its ability to assimilate various sugars and the molecular basis of its thermotolerance and efficient protein productivity, in addition to the complete genome sequence.

4.3 Materials and methods

4.3.1 Strains, media and culture conditions

The yeast strain used in this work was *K. marxianus* DMKU 3-1042 strain, which has been deposited in the NITE Biological Resource Center (NBRC) under the deposit numbers NITE BP-283 and NBRC 104275. Media used were YP (1%

w/v yeast extract and 2% w/v peptone) supplemented with one of two different carbon sources: YPD, with 2% w/v glucose, or YPX, with 2% w/v xylose.

4.3.2 Genome sequencing, assembly, and annotation

Two plasmid libraries with average insert sizes of 3 and 5 kb were generated in pTS1 (Nippon Gene, Tokyo, Japan) and pUC118 (TaKaRa Bio. Inc., Otsu, Shiga, Japan) plasmid vectors, respectively, while a fosmid library with an average insert size of 40 kb was constructed in pCC1FOS (EPICENTRE, Illumina Inc., San Diego, CA, USA). Shotgun sequencing was performed on an ABI 3730*xl* DNA Analyzer (Applied Biosystems Co., Thermo Fisher Scientific, Inc., Foster City, CA, USA). Gaps were closed by the sequencing of gap-spanning PCR products. Telomeric regions were further analyzed by transposon-insertion sequencing of corresponding fosmid clones with Template Generation System II (Finnzymes, Thermo Fisher Scientific, Inc., Foster City, CA, USA). Genome assemblies were validated by optical mapping (OpGen, Gaithersburg, MD, USA). The genome was finally assembled into nine ungapped contigs corresponding to eight chromosomes and a mitochondrion with and average coverage of 11.1x. The mean error rate was estimated to be less than 6×10^{-8}.

The rRNA-encoding regions were identified by a BLASTN program using the ribosomal sequences of *K. marxianus*, while the tRNA-coding regions were predicted by the ARAGORN program (Laslett and Canback 2004). Proteins-coding gene prediction was performed by combining the Glimmer 3.02 program with a self-training dataset and six frames prediction by using *in silico* Molecular Cloning (in silico Biology, Inc., Yokohama, Kanagawa, Japan) and manually identification (Salzberg et al. 1998; Delcher et al. 2007). Intron prediction was performed by the AUGUSTUS program using the coding DNA sequences (CDSs) of *Ashbya gossypii* as the reference for pattern learning and manual correction of each CDS (Stanke and Waack 2003; Stanke et al. 2006). Functional annotation of the predicted CDSs was performed by BLASTP searching against the nonredundant (nr) database (Altschul et al. 1997) with an E-value threshold of 10^{-10}. Protein domains were predicted using the InterProScan program against various

domain libraries (Prints, Prosite, PFAM, ProDom, SMART). Protein functions were assigned by KOG database (Tatusov et al. 2003). Assignment of UniProt number was performed by a BLASTP program against the UniProt database (Apweiler et al. 2012) with an E-value threshold of 10^{-10}. UniProt gene name, cellular localization and Gene Ontology were assigned based on UniProt database information. The assignment of KO number of KEGG Orthology was performed by the KAAS program (Moriya et al. 2007; Aoki-Kinoshita and Kanehisa 2007). Individual annotations were then summarized according to KEGG Orthology and KEGG metabolic pathways.

4.3.3 Transcriptome analysis in *K. marxianus*

Cells grown in 100-ml Erlenmeyer flasks in 30 ml YPD medium at 30ºC, 160 rpm for 18 h were inoculated at the initial OD_{660} of about one into sequential batch culture, which was conducted in 300-ml Erlenmeyer flasks with 100 ml YPD at 30ºC or 45ºC under the shaking condition (30D and 45D) or the static condition at 30ºC (30DS) or with 100 ml YPX at 30ºC under the shaking condition (30X). The cells were further cultivated under each condition for 6 h and immediately subjected to RNA isolation. Each culture condition for TSS Seq experiments is under the same condition as performed previously (Rodrussamee et al. 2011). Total RNA from cells was isolated by the hot phenol method (Aiba et al. 1981) and was purified using an RNeasy Midi Kit (QIAGEN, Hilden, Germany) with RNase free DNase I (QIAGEN) according to the manufacturer's instructions. Transcriptional starting site (TSS) Seq analysis was performed using the extracted total RNA, providing precise information on TSSs and their expression levels in a high-throughput manner (Tsuchihara et al. 2009). TSS-tag counts were divided by the total number of uniquely and perfectly (with no mismatch) mapped TSS-tags to calculate TSS-tag ppm (parts per million). Experiments on each culture condition and TSS Seq analysis were performed in triplicate. Statistical testing was performed by edgeR of R package using the TSS-tag counts data of TSS analysis with a cutoff value as false discovery rate smaller than 0.05 indicating significantly changed genes (Robinson et al. 2010). The GO enrichment test was performed by

topGO of R package (Alexa and Rahnenfuhrer 2000). The TSS was submitted to the Gene Expression Omnibus database (GEO, http://www.ncbi.nlm.nih.gov/geo/under the accession number GSE 66600.

4.3.4 Nucleotide sequence accession numbers

The complete genome sequence of *K. marxianus* DMKU 3-1042 has been deposited in DDBJ/EMBL/GenBank under accession no. AP012213-AP012221.

4.3.5 Quantitative real-time PCR (qPCR) analysis

Primers for qPCR were designed by using Primer Express software version 3.0 (Applied Biosystem Co.). A pair of primers, Km-rDNA-F1: 5′-GATCGGGTGGTGTTTTTCTTATG-3′ and Km-rDNA-R1: 5′-TCCCCCCAGAACCCAAAG-3′, was designed to amplify the 18S rDNA gene. The reaction produced a 71bp PCR product. Probe for 18S rDNA, Km-rDNA-probe1: 5′-CCCACTCGGCACCTTACGAGAAATCA-3′ was labeled at the 5′-end with 6-carboxyfluorescein (FAM) as a reporter and at the 3′-end with dihydrocyclopyrroloindole tripeptide minor groove binder (MGB) as a quencher. Real-time PCR was performed using a TaqMan® Universal Master Mix II (Applied Biosystem Co.) and Applied Biosystems 7300 Real-Time PCR system (Applied Biosystem Co.). The 18S rDNA was amplified using genomic DNA isolated from 10 strains of *K. marxianus*. The C_T value was determined by the instrument's software and adjusted manually as necessary. Concentration and DNA quality were measured by using Qubit™ dsDNA HS Assay Kits (Invitrogen Ltd., Paisley, UK) with Qubit® Fluorometer and by gel electrophoresis and converted to the number of copies by using the molecular weight of the DNA. The equation $C_T = m$ (log quantity) + b from the equation for a line (y = mx + b) was constructed by plotting the standard curve of log quantity versus its corresponding C_T value. The 18S rDNA copy numbers were determined by the absolute quantitation method, by which total copies were first calculated using the following equation: total 18S rDNA copies = $10^{([CT-b]/m)}$. The number of 18S rDNA copies per genome was then

determined by the following equation: 18S rDNA copies per genome = (Total copies of 18S rDNA)/ (Total copy of genomic DNA). The genome size of 11 Mb of *K. marxianus* DMKU 3-1042 was used for all calculations.

4.4 Results

4.4.1 Genomic information and comparative genomics

The genome sequence of *K. marxianus* DMKU 3-1042 was precisely determined (less than one estimated error per chromosome) by nucleotide sequencing with three different sizes of shotgun libraries. Telomeric regions were further analyzed by transposon-insertion sequencing of corresponding fosmid clones. This strategy allowed us to determine the complete genome sequence of 11.0 Mb including all centromeric regions and boundary regions containing up to one to several sequence repeats (GGTGTACGGATTTGATTAGTTATGT) of telomeres. Optical mapping confirmed the genome organization except for three inverted regions, which were fixed in the final complete sequences (Figure S1). There are eight chromosomes ranging in size from 0.9 to 1.7 Mb and a mitochondrial genome of 46 kb. The annotation process predicted 4,952 genes (Table 4.1), of which 98.0% were predicted to consist of a single exon. The average gene density is 68.0% (Table 4.2). The average gene and protein lengths are 1.5 kb and 501 amino acids, respectively (Table 4.1).

Table 4.1 General genomes information of nuclear and mitochondrial genomes of *K. marxianus* DMKU 3-1042

	length	CDS	Intron-containing CDS	tRNA	rDNA	na_length avg.	na_length max	aa_length avg.	aa_length max.
Total	10,966,467	4,952	172	202	8[b]				
Average						1,505		501	
Chromosome									
1	1,745,387	803	25	31	0	1,473	12,174	491	4,058
2	1,711,476	808	29	28	0	1,440	6,168	480	2,056
3	1,588,169	706	21	24	0	1,553	8,004	517	2,668

	length	CDS	Intron-containing CDS	tRNA	rDNA	na_length avg.	na_length max	aa_length avg.	aa_length max.
4	1,421,472	624	26	25	0	1,593	14,742	531	4,914
5	1,353,011[a]	611	20	30	6[b]	1,529	9,018	509	3,006
6	1,197,921	537	18	17	0	1,500	8,709	500	2,903
7	963,005	438	19	10	0	1,454	8,310	484	2,770
8	939,718	414	12	15	0	1,523	9,381	507	3,127
Mitochondrion	46,308	11	2	22	2	978	1,491	326	497

[a]The length does not include that of most of rDNA. [b]Six rDNA copies in the genome sequence in database, but 140 rDNA copies by optical mapping. CDS, coding DNA sequence.

Table 4.2 General characteristics of 11 hemiascomyceteous yeast genomes

Species	Genome size (Mb)	Avg. G+C content (%)	Total CDS	Total tRNA genes	Avg. gene density (%)	Avg. G+C in CDS (%)	Source
Kluyveromyces marxianus	10.97	40.12	4,954	202	68.58	41.67	This study
Kluyveromyces lactis	10.60	38.70	5,329	162	71.60	40.10	[20]
Saccharomyces cerevisiae	12.10	38.30	5,807	274	70.30	39.60	[20]
Candida glabrata	12.30	38.80	5,283	207	65.00	41.00	[20]
Debaryomyces hansenii	12.20	36.30	6,906	205	79.20	37.50	[20]
Yarrowia lipolytica	20.50	49.00	6,703	510	46.30	52.90	[20]
Scheffersomyces stipitis	15.40	41.10	5,841	-	55.90	42.70	[21]
Ashbya gossypii	9.12	51.70	4,776	220	77.10	52.80	[19]
Ogataea parapolymorpha	8.87	47.83	5,325	80	84.58	49.13	This study[a]
Debaryomyces hansenii	12.18	36.34	6,290	225	74.31	37.45	[20]
Clavispora lusitaniae	12.11	44.50	5,936	217	68.07	46.80	[22]
Schizosaccharomyces pombe	12.59	36.04	5,133	195	57.17	39.63	[23]

[a]Values were summarized by us using data from Joint Genome Institute (JGI, http://jgi.doe.gov). G + C, guanine + cytosine; CDS, coding DNA sequence.

Eukaryotic orthologous groups (KOG) database analysis led to the assignment of protein functions of about 72.4% of predicted genes (Table S1) and protein domains were predicted in 3,584 gene models. UniProt and KAAS assignments led to the assignment of homologous genes of about 86.4% of predicted genes and KEGG Orthology number of 50.5%, respectively. The yeast shares 1,552 genes with *K. lactis*, *Ashby gossypii*, *Candida glabrata*, *S. cerevisiae*, *Ogataea parapolymorpha*, *Debaryomyces hansenii*, *S. stipitis*, *Clavispora lusitaniae*, *Yarrowia lipolytica* and *Schizosaccharomyces pombe* as hemiascomycetous yeasts (Dietrich et al. 2004; Dujon et al. 2004; Jeffries et al. 2007; Butler et al. 2009; Wood et al. 2002). The phylogenetic tree exhibits the closest location of *K. marxianus* to *K. lactis* and closer to *A. gossypii*, *C. glabrata* and *S. cerevisiae* in the eleven yeasts (Figure 4.1). Consistent with this, *K.*

marxianus shares 4,676; 3,826; 3,672 and 3,853 genes with *K. lactis*, *A. gossypii*, *C. glabrata* and *S. cerevisiae*, respectively. On the other hand, there are 193 genes specific for *K. marxianus* (Table S2), which may be responsible for its species-specific characteristics, of which two thirds of the genes could not be assigned by the KOG database (Table S3). There are 422 genes shared only between *K. marxianus* and *K. lactis* (Table S4), which may be related to their genus-specific characteristics, such as production of β-galactosidase (Rubio-Texeira, 2006), assimilation of a wide variety of inexpensive substrates (Lane and Morrisey 2010), efficient productivity of heterologous proteins (Rocha et al. 2011; Rocha et al. 2010; van Ooyen et al. 2006) and synthesis of a killer toxin against certain ascomycetous yeasts (Abranches et al. 1997; Jablonowski and Schaffrath 2007).

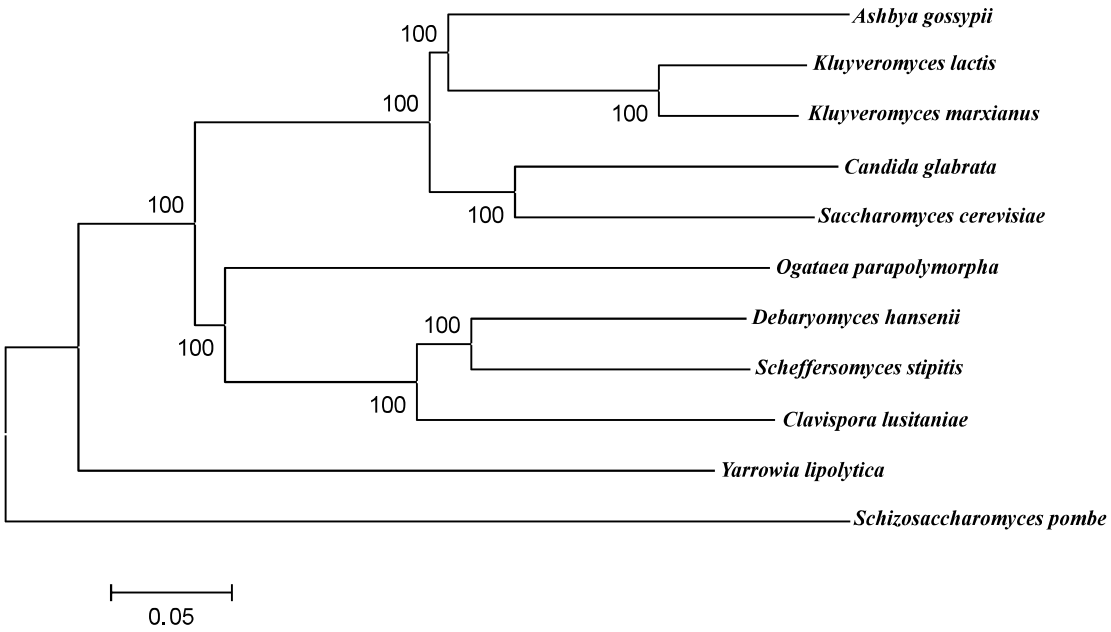

Fig. 4.1 Phylogenetic tree of 11 hemiascomycetous yeast genomes based on 1,361 concatenated amino acid sequences. *K. marxianus* shares 1,552 genes with *K. lactis* NRRL Y-1140 (CR382121-CR382126), *Ashbya gossypii* (*Eremothecium gossypii*) ATCC 10895 (AE016814-AE016821), *Candida glabrata* CBS 138 (CR380947-CR380959), *S. cerevisiae* S288c (BK006934-BK006949), *Ogataea parapolymorpha* DL-1 (AEOI00000000), *Debaryomyces hansenii* CBS 767 (CR382133-CR382139), *S. stipitis* CBS 6054 (AAVQ00000000), *Clavispora lusitaniae* ATCC 42720 (AAFT00000000), *Yarrowia lipolytica* CLIB122 (CR382127-CR382132) and *Schizosaccharomyces pombe* 972h- (CU329670-CU329672) as hemiascomycetous yeasts, of which complete or draft genome

sequences are available (Dietrich et al. 2004; Dujon et al. 2004; Jeffries et al. 2007; Butler et al. 2009; Wood et al. 2002). A whole genome-wide phylogenetic tree with amino acid sequences deduced from the conserved 1,361 genes was constructed using the neighbor-joining algorithm of MEGA5.05 as previously reported (Matsutani et al. 2010). The numbers at each branch indicate bootstrap values.

The two most attractive traits of *K. marxianus* for fermentation applications are thermotolerance and pentose assimilation capability, which are also found in *O. parapolymorpha* and *S. stipitis*, respectively. The number of genes that are shared between the two thermotolerant yeasts but absent from *K. lactis* is 30, including genes for three siderophore-iron transporters and three vacuolar proteins (Table S5). Notably, there are 27 putative sugar transporters in the *K. marxianus* genome (Table S6). Like *S. stipitis*, the initial xylose catabolism after its uptake in *K. marxianus* is accomplished by three genes, *XYL1*, *XYL2* and *XKS1*, which are involved in conversion of xylose to xylulose-5-phosphate as an intermediate in the pentose phosphate pathway (PPP). Genes for utilization of various other sugars and alcohol dehydrogenases are listed (Table 4.3).

Chromosomal segments including 4,277 genes, which retain the ancestral gene groupings, were found between *K. marxianus* and *K. lactis* (Figure S2). The average of mapped segments to the chromosome is 57.9% and the *K. marxianus* chromosome best covered by *K. lactis* chromosomal segments is chromosome 6, with 60.8% coverage.

4.4.2 Ribosomal DNA (rDNA) copy number and thermotolerance

Optical mapping allowed us to estimate at least 140 copies of the rDNA gene as a cluster on chromosome 5 (Figure S1), which occupies 67.5% (0.9 Mb) of the chromosome. To examine the relationship between the rDNA copy number and its thermotolerance among *K. marxianus* strains, strains exhibiting different growth at different temperatures (Figs. S3, S4) were subjected to a test to determine the copy number of rDNA (Table S7). As a result, the rDNA copy number is not correlated to the thermotolerance of the yeast, and at least 31 copies of rDNA are sufficient to support its thermotolerance.

Table 4.3 Genes for utilization of sugars at their initial catabolism and genes for alcohol dehydrogenases in *K. marxianus*

	Product	UniProt gene	Sugar
KMLA_60412	Hexokinase	HXK2 (RAG5)	Glucose, fructose, mannose
KLMA_10763	Glucose-6-phosphate dehydrogenase	RAG2	
KLMA_50384	Mannose 6-phosphate isomerase	PMI40	Mannose
KLMA_20333	Galactokinase	GAL1	Galactose
KLMA_20331	Galactose-1-phosphate uridylyltransferase	GAL7	
KLMA_30099	Phosphoglucomutase	GAL5 (PGM2)	
KLMA_10683	Xylose reductase	XYL1	Xylose
KLMA_70044	Xylitol dehydrogenase	XYL2	
KLMA_80066	Xylulokinase	XKS1	
KLMA_30577	Arabinose dehydrogenase [$NADP^+$ dependent]	ARA1	Arabinose
KLMA_40310	Arabinose dehydrogenase [NAD dependent]	ARA2	
KLMA_80176	Xylose/Arabinose reductase	YJR096W	
KLMA_10558	D-arabitol-2-dehydrogenase	ARD2	
KLMA_10157	Probable ribokinase	RBK1	D-ribose
KLMA_10176	ribose-phosphate pyrophosphokinase 5	PRS5	
KLMA_10783	Sorbose reductase	SOU1	Mannitol, glucitol, L-sorbose
KLMA_10649	D-lactate dehydrogenase [cytochrome], mitochondrial	DLD1	Lactate
KLMA_40583	D-lactate dehydrogenase [cytochrome] 1, mitochondrial	DLD1	
KLMA_50301	D-lactate dehydrogenase [cytochrome], mitochondrial	DLD1	
KLMA_60482	D-lactate dehydrogenase [cytochrome] 2, mitochondrial	DLD2	
KLMA_10179	Glycerol-3-phosphate dehydrogenase [NAD(+)] 1	GPD1	Glycerol
KLMA_30722	Glycerol-3-phosphate dehydrogenase, mitochondrial	GUT2	
KLMA_60361	Glycerol uptake protein 1	GUP1	
KLMA_80411	Glycerol uptake/efflux facilitator protein	FPS1	
KLMA_80412	Glycerol kinase	GUT1	
KLMA_10427	Galactose/lactose metabolism regulatory protein GAL80	GAL80	Lactose
KLMA_20830	Lactose permease	LAC12	
KLMA_30010	Lactose permease	LAC12	
KLMA_30728	Lactose permease	LAC12	
KLMA_30011	beta-glucosidase	-	Cellobiose
KLMA_20184	Endo-1,3(4)-beta-glucanase 1	DSE4	1,3-β- D-glucan
KLMA_50517	Endo-1,3(4)-beta-glucanase 2	ACF2	
KLMA_10518	Inulinase	INU1	Sucrose, raffinose, inulin
KLMA_40102	Alcohol dehydrogenase 1	ADH1	
KLMA_40220	Alcohol dehydrogenase 2	ADH2	
KLMA_80306	Alcohol dehydrogenase 3	ADH3	
KLMA_20005	Alcohol dehydrogenase 4a	ADH4a	
KLMA_20158	Alcohol dehydrogenase 4b	ADH4b	
KLMA_40624	Alcohol dehydrogenase	ADH	
KLMA_80339	Alcohol dehydrogenase 6	ADH6	

NAD, nicotinamide adenine dinucleotide; NADP, nicotinamide adenine dinucleotide phosphate.

4.4.3 Genes regulated under a static condition

The alteration of genome-wide gene expression was analyzed by transcription start site sequencing (TSS Seq) under four different conditions: shaking condition in yeast extract peptone dextrose (YPD) medium at 30°C (30D) or 45°C (45D), static condition in YPD medium at 30°C (30DS) and shaking condition in yeast extract peptone xylose (YPX) medium at 30°C (30X) and was expressed as the ratio of 30DS/30D, 45D/30D and 30X/30D using 30D as a control

condition, which was evaluated by a statistical test (FDR < 0.05) (Table S8) and summarized (Figure S5).

The growth of *K. marxianus* under the static condition is much slower than that under the shaking condition (Rodrussamee et al. 2011; Lertwattanasakul et al. 2011). Under the 30DS condition, there were 159 significantly upregulated genes (Table S8), and the top-five significantly enriched GO terms were ribosome biogenesis, ribonucleoprotein complex biogenesis, rRNA processing, rRNA metabolic process and noncoding RNA processing (Table S9); their individual gene details are shown in Table S10. Interestingly, 55% of upregulated gene products are located in the nucleus (Figure S6), some of which are factors for ribosome biogenesis, ATP-dependent RNA helicases, RNA polymerases subunits, nucleolar complex proteins, components of exosome complex, DNA polymerase subunits and chromatin assembly factor 1 subunit. Conversely, there were 154 significantly downregulated genes (Table S8) and their most significantly enriched GO terms were ascospore formation, sexual sporulation, sexual sporulation resulting in the formation of a cellular spore, cell development and reproductive process in single-celled organisms (Tables S11, S12). The largest population consists of 43 genes for membrane proteins including 15 transporters for amino acids and other metabolites. Taken together, under the static condition, *K. marxianus* may increase the turnover of RNAs and proteins in addition to suppression of transporters and spore formation that depends on mitochondrial respiration activity (Codón et al. 1995).

Under the static condition, the oxygen level in cells may become low as cells proliferate so that the condition may affect oxygen-requiring biosynthetic pathways, such as those for heme, sterols, unsaturated fatty acids, pyrimidine and deoxyribonucleotides (Snoek and Steensma 2006). As expected, almost all genes related to ergosterol biosynthesis, sterol biosynthesis, unsaturated fatty acids production, pyrimidine synthesis and ribonucleotide reductase were largely upregulated under the 30DS condition (Figure S7). However, unlike *S. cerevisiae*, the expression of *MDL1* for a putative mitochondrial heme carrier was not significantly altered (Kwast et al. 2002). In addition, *NPT1* for nicotinate phosphoribosyl transferase (Npt1) involved in the nicotinamide adenine

dinucleotide phosphate (NAD) salvage pathway, *CYC7* for cytochrome *c* and *AAC* for ADP/ATP carrier in mitochondrial inner membrane were upregulated. The ADP/ATP carrier functions to exchange cytoplasmic adenosine diphosphate (ADP) for mitochondorial ATP under aerobic conditions and vice versa under anaerobic conditions (Snoek and Steensma 2006). Taken together, these results suggest that the enhanced expression of most genes for several oxygen-dependent biosynthetic pathways or some genes related to the production and management of energy is crucial for the cellular metabolism of *K. marxianus* under the static condition. Notably, almost all genes described above were upregulated not only under the 30DS condition but also under the 45D conditions, suggesting that cells suffer from oxygen deficiency under the two conditions.

Metabolic changes were further analyzed by KEGG assignment. A number of genes for glycolysis after 1,3-bisphosphoglycerate, PPP and tricarboxylic acid (TCA) cycle were relatively upregulated (Figure 4.2A,B). Enhanced PPP may provide nicotinamide adenine dinucleotide phosphate (NADPH) to cope with reactive oxygen species (ROS) generated under the condition, consistent with upregulation of ROS-scavenging genes (see Figure 4.3). Enhancement of expression of genes related to the pathway from 2-phosphoglycerate to acetyl-CoA via acetaldehyde may indicate the possibility that cells under a static condition tend to increase in acetyl-CoA and NADPH production in the process of oxidation of acetaldehyde. The oxaloacetate-malate shuttle may contribute to the oxidation of NADH in cytoplasm. Many genes for the respiratory chain were downregulated, though compensatorily most of the chaperone-coding genes for cytochrome *c* oxidase were upregulated (Figure S8).

4.4.4 Genes regulated under a high-temperature condition

To clarify the thermotolerant mechanism of *K. marxianus*, it is necessary to consider the expressional alteration of whole genomic genes at high temperature. Under the 45D condition, 508 genes were significantly downregulated (Table S8) and the top-five significant GO terms were carbohydrate metabolic process, isoleucine biosynthetic process, small molecule metabolic process,

monosaccharide metabolic process and branched chain family amino acid biosynthetic process (Tables S13, S14). Conversely, in 199 upregulated genes (Table S8), the most significant GO terms were noncoding RNA processing, ribosome biogenesis, rRNA processing, ribonucleoprotein complex biogenesis and rRNA metabolic process (Tables S15, S16) and 45 genes were related to translation, transcription, DNA replication and repair and protein and RNA degradations. Interestingly, *LYS21* for homocitrate synthase, which is linked to the key process of DNA damage repair in a nucleus (Scott and Pillus 2010) in addition to its involvement in lysine biosynthesis in the cytoplasm, was upregulated. Several genes for homologous recombination and nonhomologous end joining, which function in the repair of DNA double-stranded breaks, were also upregulated (Figure S9). Therefore, it is assumed that *K. marxianus* copes with high temperatures by reducing central metabolic activities and reinforcing the synthesis and degradation of proteins and DNA repair.

In further analysis of the subcellular localization of products (Figure S6), 21% of all upregulated genes are located in the nucleolus or nucleus (Table S17), and are related to 18S rRNA preprocessing, 60S ribosomal subunit biogenesis, transcription process and pre-rRNA processing (Tables S15, S16). Conversely, products of several downregulated genes exist in the nucleolus, which are involved in 40S ribosomal subunit biogenesis and pre-18S rRNA processing (Tables S13, S14). Notably, seven genes for mitochondrial ribosome subunits were downregulated. In addition, genes for DNA repair in nuclei and mitochondria, including a DNA damage sensor or chromosome transmission fidelity protein, were significantly upregulated (Table S16).

Genes for glycolysis were remarkably downregulated, except for *GLK1* and *FBP1*, under the 45D condition (Figure 4.2A), which is consistent with relatively slow growth speed and low ethanol productivity at high temperatures (Rodrussamee et al. 2011). Conversely, *ZWF* and *SOL1* in PPP in addition to *GLK1* were upregulated, indicating an increase in NADPH amount. In TCA cycle, downregulation of *CIT1*, *LSC2*, *FUM1* and *MDH1* and upregulation of *IDH1*, *IDH2*, *KGD1* and *KGD2* were found, which might lead to the accumulation of intermediates (Figure 4.2B and Table S16). Most mitochondrial genomic genes

were selectively expressed (Figure S8). Additionally, some genes for succinate dehydrogenase (Sdh) and *bc*1 complex were upregulated, whereas some genes for NADH dehydrogenase (Ndh), Coenzyme Q biosynthesis and cytochrome *c* oxidase including heme *a* synthesis were downregulated (Figure S8). These findings allow us to speculate that *K. marxianus* scavenges H_2O_2 by the pathway of Sdh-*bc*1 complex-cytochrome *c* peroxidase and prevents the production of ROS by reduction of gene expression for Ndh and Coenzyme Q biosynthesis at high temperatures.

Heat shock proteins (Hsps) and chaperones are expected to be crucial for survival at high temperatures. The transcription of *HSP26*, *HSP60*, *HSP78*, *HSP82*, *SSA3* and *CPR6* was enhanced under the 45D condition (Figure 4.3A and Table S18), suggesting that both mitochondrial and cytoplasmic compartments need such Hsps at that temperature.

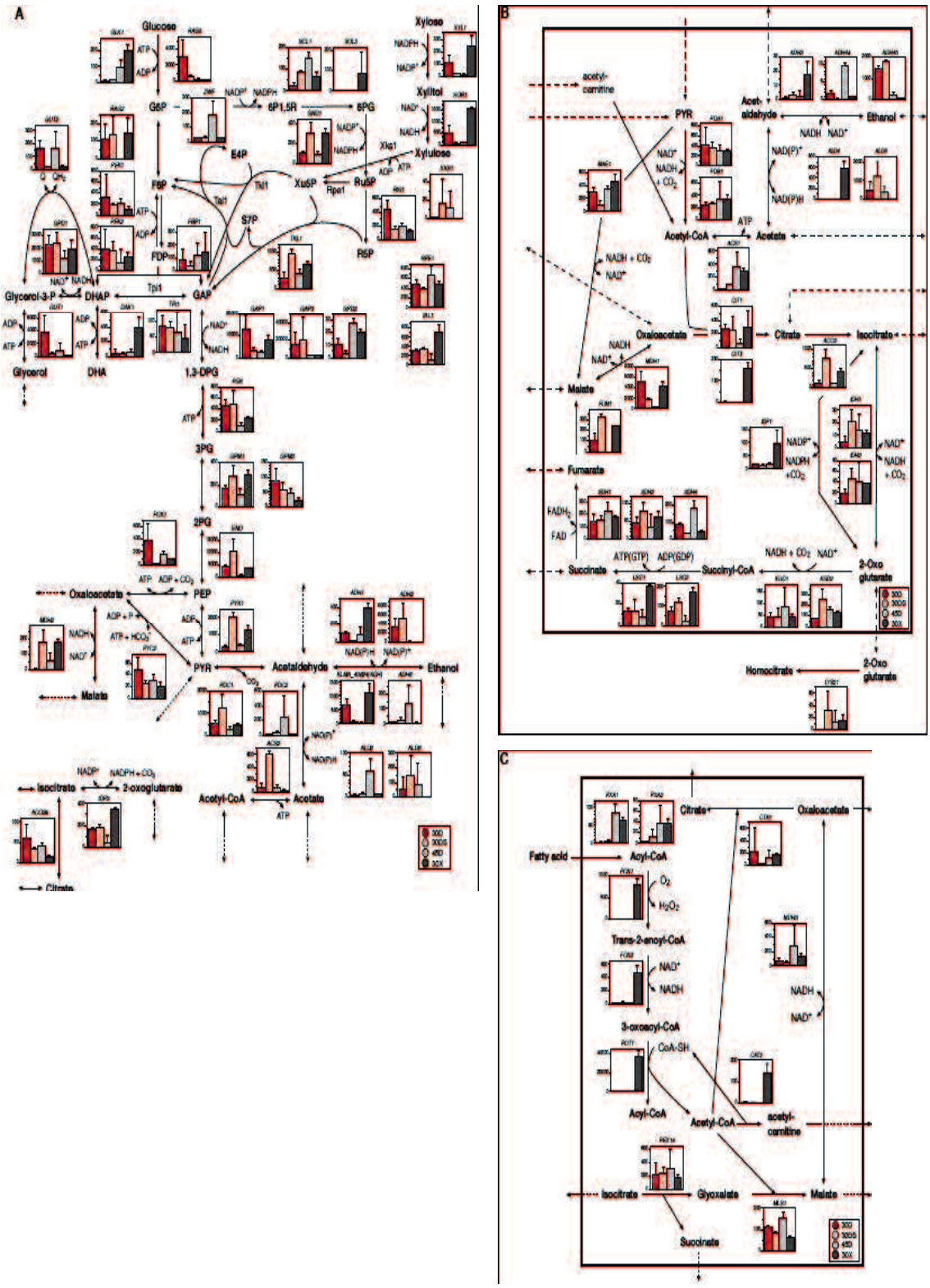

Fig. 4.2 Transcript abundance of genes related to central metabolic pathways under different conditions in *K. marxianus*. The transcript abundance was determined by TSS analysis. Y axis of each column graph shows the transcript abundance of each gene as TSS-tag ppm. Columns from left to right in each graph represent 30D (strong red), 30DS (soft orange), 45D (gray) and 30X (dark gray).

Empty columns mean gene expression below the detectable level. (A) Central metabolic pathway. (B) Mitochondrial metabolic pathway. (C) Peroxisomal metabolic pathway. Abbreviations are as follows: G6P, glucose-6-phosphate; F6P, fructose-6-phosphate; FDP, fructose 1,6 bisphosphate; DHAP, dihydroxyacetone phosphate; DHA, dihydroxyacetone; GAP, glyceraldehyde-3-phosphate; 1,3-DPG, 1,3-bisphosphoglycerate; 3PG, 3-phosphoglycerate; 2PG, 2-phosphoglycerate; PEP, phosphoenolpyruvate; PYR, pyruvate; 6P1,5R, 6-phospho-D-glucono-1,5-lactone; 6PG, 6-phosphogluconate; Ru5P, ribulose-5-phosphate; R5P, ribose-5-phosphate; Xul5P, xylulose-5-phosphate; E4P, erythrose-4-phosphate; S7P, sedoheptulose-7-phosphate; NAD, nicotinamide adenine dinucleotide; NADP, nicotinamide adenine dinucleotide phosphate; ATP, adenosine triphosphate; ADP, adenosine diphosphate.

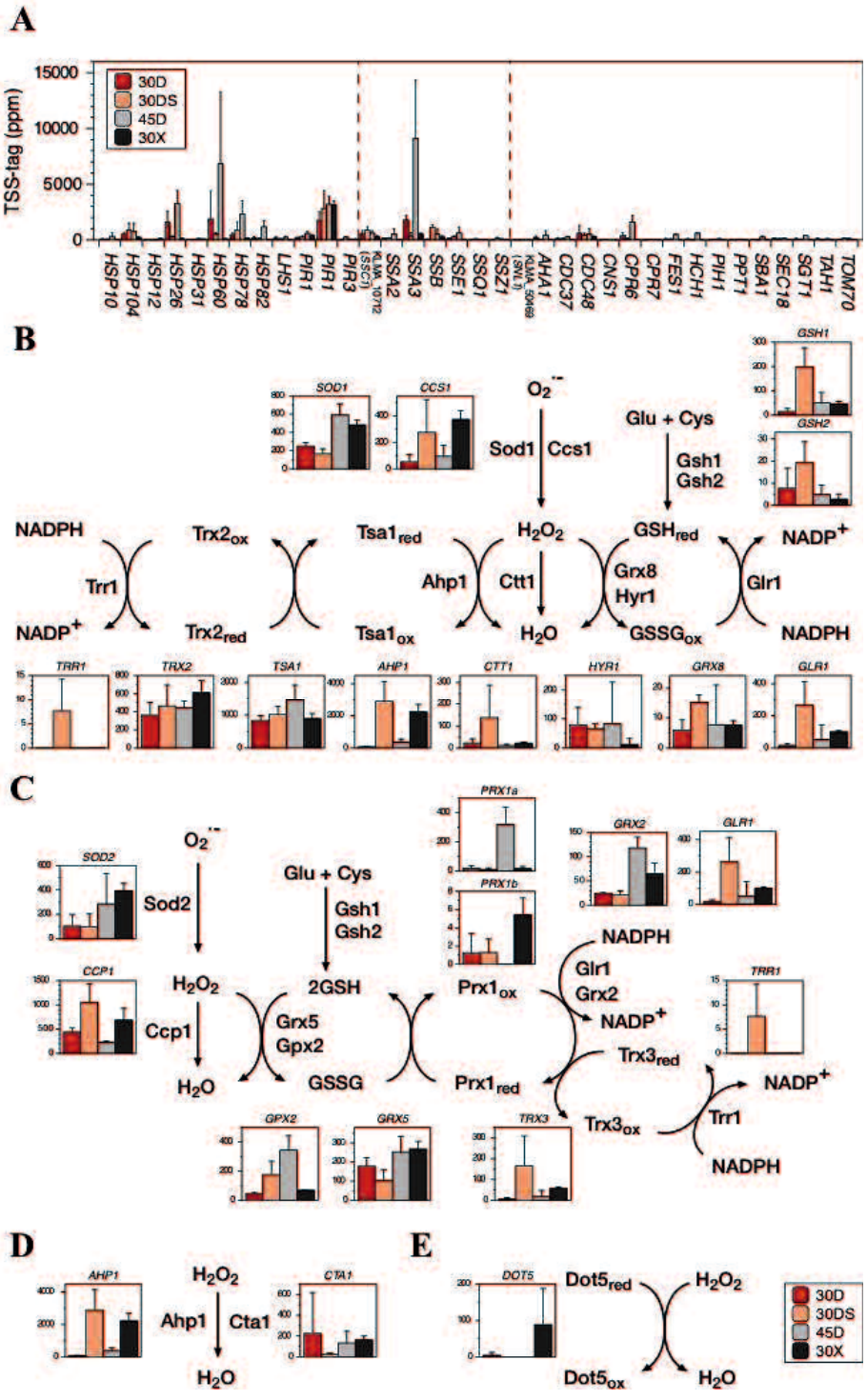

Fig. 4.3 Transcript abundance of genes related to oxidative stress response in *K. marxianus*. (A) Transcript abundance of heat shock genes and related genes listed in Table S18 is represented as TSS-tag ppm. Enzyme reactions to scavenge ROS in cytoplasm (B), mitochondria (C) peroxisome (D) and nucleus (E) are shown. Each column in the graph shows the transcript abundance of each gene as described in Figure 2.

4.4.5 Genes regulated under a xylose-utilizing condition

Under the 30X condition, the top-five significant GO terms of significantly upregulated genes were fatty acid catabolic process, monocarboxylic acid catabolic process, cellular lipid catabolic process, fatty acid β-oxidation and fatty acid oxidation (Tables S19, S20). Conversely, the most significant GO terms of significantly downregulated genes were α-amino acid metabolic process, carboxylic acid metabolic process, lysine biosynthetic process, small molecule biosynthetic process and oxoacid metabolic process (Tables S21, S22). Therefore, the 30X condition may stimulate the degradation of lipid in peroxisome and keep a low level of amino acid synthesis, which is consistent with the slow growth of the yeast in xylose (Rodrussamee et al. 2011).

The phylogenetic tree of sugar transporters revealed that KLMA_50360, KLMA_50361, KLMA_50362, KLMA_50363 and KLMA_50364 share high similarity with xylose transporters predicted in *S. stipitis* (Figure 4.3) (Jeffries et al. 2007). Unlike *S. stipitis*, however, these genes were not induced specifically under the 30X condition. Genes of several transporters exhibited specific induction under the 30X or 30D condition, suggesting that KLMA_60073, KLMA_80101 and KLMA_70145 are involved in xylose uptake.

Genes for the initial catabolism of xylose, PPP, the conversion of PEP to ethanol, the mitochondrial conversion of acetaldehyde to acetyl-CoA and TCA cycle were relatively upregulated (Figure 4.2A,B). A part of the ethanol produced in cytoplasm may thus be consumed by conversion to acetyl-CoA in mitochondria through the ethanol-acetaldehyde shuttle followed by TCA cycle, which is consistent with low ethanol productivity in xylose medium (Rodrussamee et al. 2011). In contrast, *ADH2* and *ADH4b* for alcohol dehydrogenases, *GUT1* for glycerol kinase and *GUT2* for the glycerol-3-phosphate shuttle were down-regulated. TSS results also indicate the generation of acetyl-CoA from the fatty acids through the peroxisomal β-oxidation pathway (Figure 4.2C), indicating the possibility that fatty acids could be a subsidiary intracellular carbon source in xylose medium. Such supply of acetyl-CoA in xylose medium might result in more NADH production and generate more ATP, which is required for phosphorylation

of xylulose and dihydroxyacetone. Additional ATP may also be supplied as a result of the *DAK1* upregulation in the cytoplasm (Figure 4.2A).

4.5 Discussion

As the first step to understanding the genetic basis of the highly efficient yeast *K. marxianus*, complete genome sequence and transcriptome analyses of its most thermotolerant strain were performed. The former analysis revealed many gene resources for the ability to assimilate various sugars in addition to species-specific genes. The latter clarified the molecular basis of attractive traits of the yeast. All information obtained here about the yeast will be useful for fundamental and applied research for innovative applications.

The thermotolerance as an attractive trait was investigated under the 45D condition, which revealed that *K. marxianus* seems to drastically change metabolic pathways from those under the 30D condition, that is, the enhancement of PPP and the attenuation of TCA cycle after the fumarate-producing step. The changes lead to the speculation that the former provides NADPH for scavenging ROS and that the latter deals with H_2O_2 via the electron transfer from Sdh to cytochrome *c* peroxidase (Figs. 4.2 and 4.3). Consistent with these conjectures, a higher temperature generates more ROS, which causes DNA damage (Hori et al. 2009). Notably, the findings of upregulation of genes for DNA double-stranded break repair and removal of uracil in DNA molecules suggest the occurrence of enhancement of double-stranded break or deamination of cytosines in DNA at high temperatures. In addition, ATP synthesis via oxidative phosphorylation may be greatly reduced due to the repression of *ATP3* for the gamma subunit of ATP synthase. The existence of additional strategies is guessed from the TSS analysis data for survival at high temperature: alteration of ribosome biogenesis including pre-rRNA processing presumably for stable and efficient protein synthesis, reduction of mitochondrial ribosome biogenesis probably for saving energy, reinforcement of checkpoints of DNA replication and spindle assembly, minimization of electron leakage in respiratory chain by reduction of NADH dehydrogenase and Coenzyme Q or enhanced expression of Hsps and chaperones.

Taken together, the thermotolerance of *K. marxianus* is likely achieved by systematic mechanisms consisting of various strategies. Especially, the yeast would mainly acquire ATP from glycolysis rather than TCA cycle at high temperatures, which could prevent the generation of ROS by minimization of mitochondrial activity.

Under a static condition, the growth and ethanol production of *K. marxianus* were low compared to those under a shaking condition (Rodrussamee et al. 2011), probably due to low ATP yield in mitochondria, which may be related to the enhanced expression of *AAC*. *K. lactis* bearing a null mutation of *AAC2* exhibits growth defect on glycerol, galactose, maltose and raffinose (Flores et al. 2000). In addition, the expression of *RAG5* for hexokinase was relatively low. In *K. lactis*, *RAG5* mutations (Prior et al. 1993) abolish the expression of *RAG1* for low-affinity glucose transporter (Chen et al. 1992) and decrease the level of the 2.0-kb mRNA species of *HGT1* for a high-affinity glucose transporter (Billard et al. 1996). Furthermore, NADH would be accumulated in the cytoplasm because of the downregulation of *GAP1* for glyceraldehyde-3-phosphate dehydrogenase. Contrarily, respiratory genes kept their transcriptional levels similar to those under the 30D condition (Figure S8). Such situations may raise reactive oxygen species from the respiratory chain to cause oxidative stress. Consistently, cytoplasmic oxidative stress response genes were relatively strongly expressed (Fig. 4.3B), especially glutathione-related genes depicted at the cytoplasm side were highly induced. Almost *HSP*s, however, were not upregulated under the 30DS condition as under the 30D (Fig. 4.3A). These metabolic activities may lead the low level of cell proliferation under a static condition.

Regulation of gene expression in response to the level of oxygen is achieved via several transcription factors. Under a static condition, *K. marxianus* seems to increase glucose metabolism and shift to fermentation, implying a connection between the oxygen- and glucose-sensing pathways. In *S. cerevisiae* and *K. lactis*, the transcription factor Hap1 mediates the induction of genes involved in their respiration, lipid metabolism and oxidative stress response (Rodicio and Heinisch 2013). *K. lactis* Hap1 negatively regulates fermentation (Bao et al. 2008). In contrast, the *HAP1* expression in *K. marxianus* was

upregulated under the 30DS condition, and consistently, several genes related to ATP synthase and chaperones for respiratory chain components were upregulated (Figure S8). These lines of evidence and the enhanced expression of genes for glycolytic pathway suggest differences in regulation of oxygen-responsive genes from those in *S. cerevisiae* and *K. lactis*.

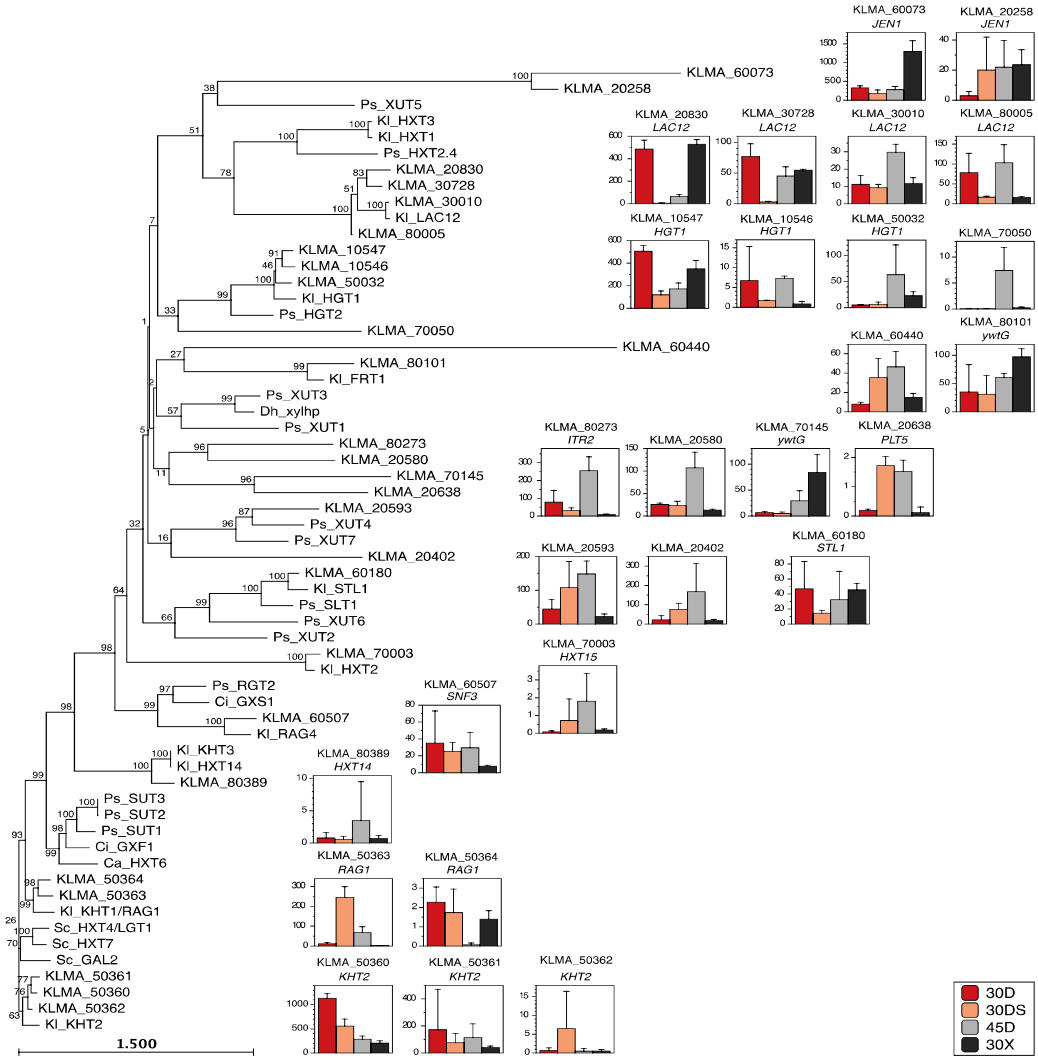

Fig. 4.4 Phylogenetic tree of predicted sugar transporters with transcript abundance in *K. marxianus*. The phylogenetic tree was constructed with amino acid sequences of predicted sugar transporters by the neighbor-joining algorithm using CLC Sequence Viewer. Each column in the graph shows the transcript abundance of each gene as described in Figure 2. The accession numbers of amino acid sequences of sugar transporters are as follows: Ps_HGT2, XP_001382755; Sc_HXT7, NP_010629; Sc_GAL2, NP_013182; Dh_xylhp, AY347871; Ci_GXS1, GN107181; Ci_GXF1, GN107179; Ps_SUT1, XP_001387898; Ps_SUT2, XP_001384295; Ps_SUT3, XP_001386019; Ps_HXT2.4, XP_001387757; Ps_XUT1, XP_001385583; Ps_XUT2, XP_001387242; Ps_XUT3, XP_001387138; Ps_XUT4, XP_001386715; Ps_XUT5, XP_001385962; Ps_XUT6, XP_001386589; Ps_XUT7, XP_001387067; Ps_RGT2, XP_001386588; Ps_SLT1, XP_001383774; Kl_KHT1/RAG1, XP_453656; Kl_KHT2, GN107317; Kl_KHT3, XP_454897; Kl_FRT1, XP_454356; Kl_HGT1, XP_451484; Kl_HXT1, XP_455078; Kl_HXT14, XP_454897; Kl_HXT2, XP_453960; Kl_HXT3, XP_453088; Sc_HXT4/LGT1, NP_011960; Kl_STL1, XP_456249; Kl_RAG4, XP_455315; Kl_LAC12, XP_452193; Ca_HXT6, XP_719472.

The oxidative stress-response genes were found to be highly induced under the three conditions tested (Figs. 4.2C and 4.4B,C,D,E), indicating that ROS is accumulated in cytoplasm, mitochondria and peroxisome under the 30DS and 30X conditions and in cytoplasm and mitochondria under the 45D condition. Notably, Ahp1 in addition to Cta1 and Dot5 may be responsible for H_2O_2 detoxification in the peroxisome and nucleus, respectively.

Xylose assimilation capability as the second trait was examined under the 30X condition. It is known that *K. marxianus* tends to suffer from cofactor imbalance in xylose medium (Zhang et al. 2011; Lulu et al. 2003), and thus, its growth strongly depends on mitochondrial respiratory activity (Lertwattanasakul et al. 2013). Inter-convertibility of NAD^+ species for maintaining the redox balance is essential for growth efficiency and metabolite excretion (Marres et al. 1991), but the yeast is incapable of directly converting NAD^+ and NADPH into $NADP^+$ and NADH owing to lack of transhydrogenases (van Dijken and Scheffers 1986). Instead, redox-balancing mechanisms between cytoplasm and mitochondria are probably used to resolve the NADH/NADPH imbalance. Reoxidation of cytosolic NADPH and its strong connection to oxidative stress in *K. lactis* have been reported (Tarrio et al. 2006; Gonzalez-Siso et al. 2009). In *S. cerevisiae*, five cytosolic-mitochondrial redox shuttles have been proposed (Bakker et al. 2001). Of these, genes for enzymes related to ethanol-acetaldehyde, citrate-oxoglutarate and oxaloacetate-malate shuttles were relatively upregulated under the 30X condition (Fig. 4.2A,B). The GABA shunt from 2-oxoglutarate to succinate that has been proposed in *S. cerevisiae* and *S. stipitis* (Cao et al. 2013; Jeffries et al. 2007) may not be so important due to the low expression of related genes (Fig. S10), suggesting that *K. marxianus* uses different shuttles for resolving the cofactor imbalance from those of the two yeasts. In addition to TCA cycle intermediates by these shuttles, acetyl-CoA might be transferred from peroxisome on the basis of TSS data. Eventually, mitochondrial activity may be enhanced, which tends to increase the leakage of electrons to generate ROS, which is consistent with elevation of expression of oxidative stress-response genes.

The last trait is efficient protein productivity, which meets the demand for fast growth and high yield biomass (Groeneveld et al. 2009). The yeast has been exploited as a cell factory to obtain valuable enzymes, showing retention of activity over a large temperature range (Foukis et al. 2012). TSS results under the 30D and 30X conditions reveal high expression of *INU1* for inulinase, which is useful for the production of recombinant proteins in culture medium, as described in previous studies (Rocha et al. 2010; Rocha et al. 2011; Raimondi et al. 2010). These useful characteristics may allow simultaneous production of ethanol and valuable proteins, thus, reducing the cost of ethanol production.

4.6 Conclusions

The complete sequences of *K. marxianus* DMKU 3-1042 nuclear and mitochondrial genomes have been determined, which reveal many genes for the cells to cope with high temperature and to assimilate a wide variety of sugars including xylose and arabinose in addition to species-specific genes. The present study thus provides the molecular basis of attractive traits of the yeast for industrial applications including high-temperature fermentation and information of its gene resources and transcriptome data, which are particularly useful for fundamental and applied researches for innovative applications.

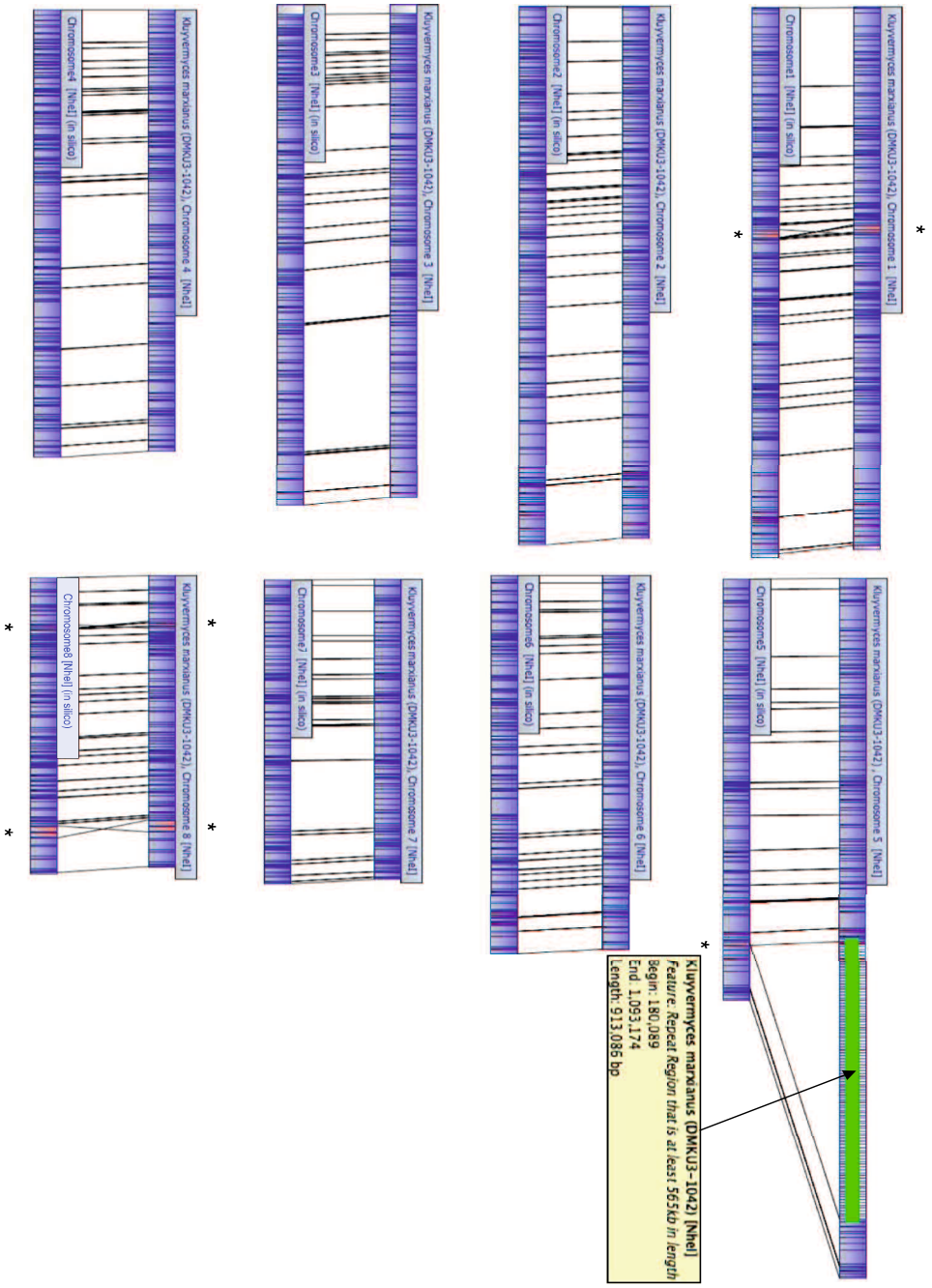

Figure S1 For each chromosome, the upper image represents data from optical mapping while the lower image depicts data from nucleotide sequencing. Asterisks indicate inverted regions. The green highlighting on Chromosome 5 represents the highly repetitive rDNA region.

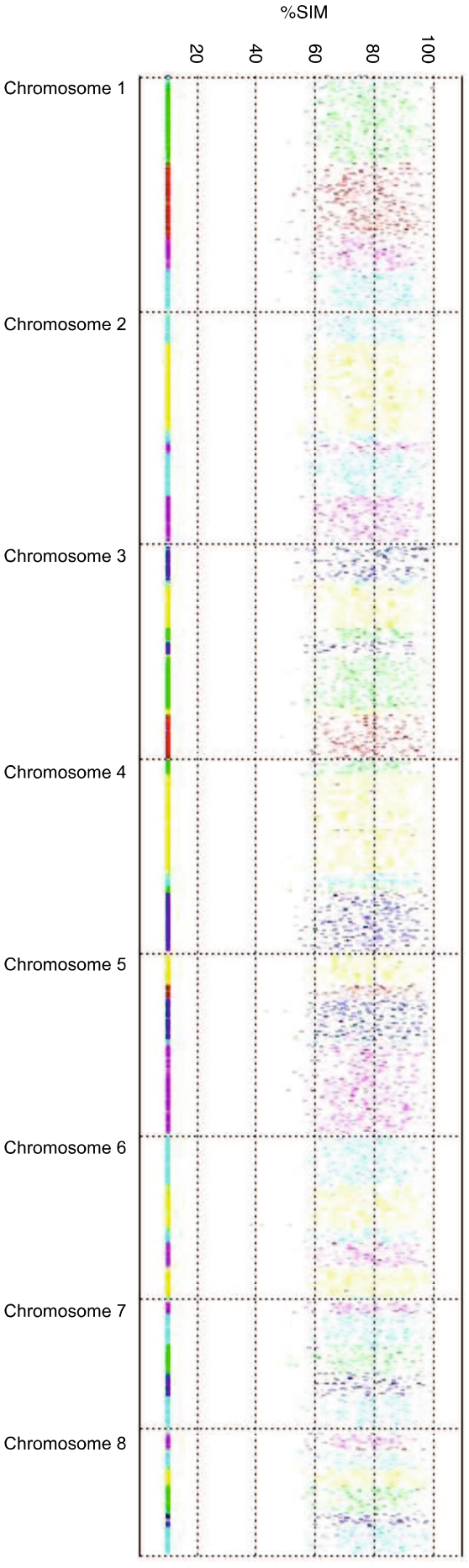

Fig. S2 Conserved chromosomal segments found between *K. marxianus* and *K. lactis*. Complete genome sequence of *K. lactis* was mapped onto that of *K. marxianus*. Alignment against whole chromosomes was done using the Promer from the MUMmer package (Kurtz et al. *Genome Biology*, 5:R12, 2004). Color bars represent the *K. lactis* chromosomes: red, chromosome 1; blue, chromosome 2; green, chromosome 3; magenta, chromosome 4; light blue, chromosome 5; yellow, chromosome 6.

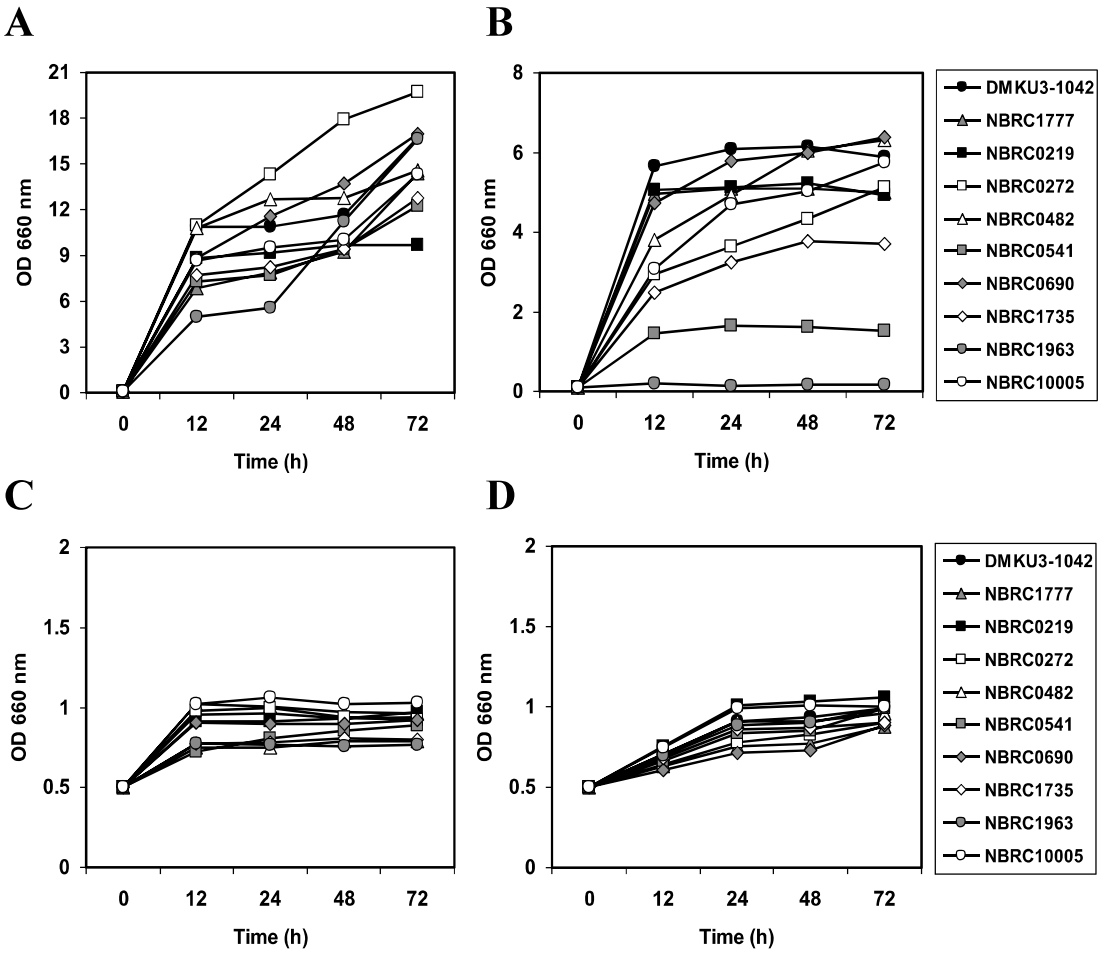

Figure S3 Growth curve comparison among several *K. marxianus* strains under different temperature conditions. Strains tested are DMKU 3-1042, NBRC 1777, NBRC 0219, NBRC 0272, NBRC 0482, NBRC 0541, NBRC 0690, NBRC 1735, NBRC 1963 and NBRC 10005. Cells were grown in YPD medium at 40°C (A), 45°C (B), 46°C (C) and 47°C (D) under a shaking condition (160 rpm).

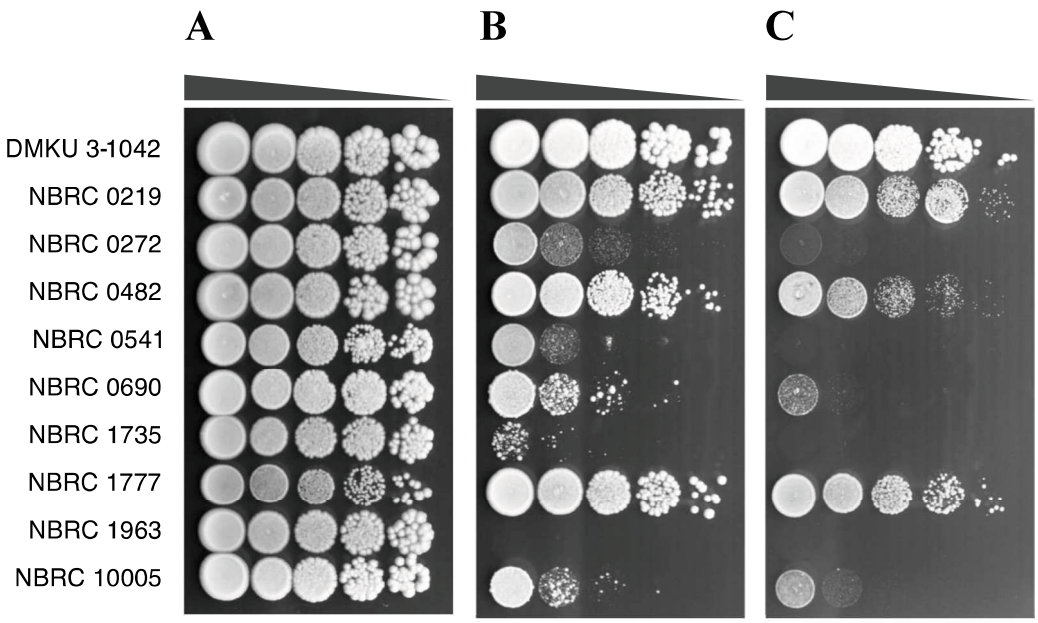

Figure S4 Spot test of several *K. marxianus* strains. Cells were grown in YPD medium to about 10^7 cells/ml, aliquots of 10-fold serial dilutions of cells were spotted onto YPD agar plates and the plates were incubated at 30°C (A), 45°C (B) and 48°C (C) for 3 days.

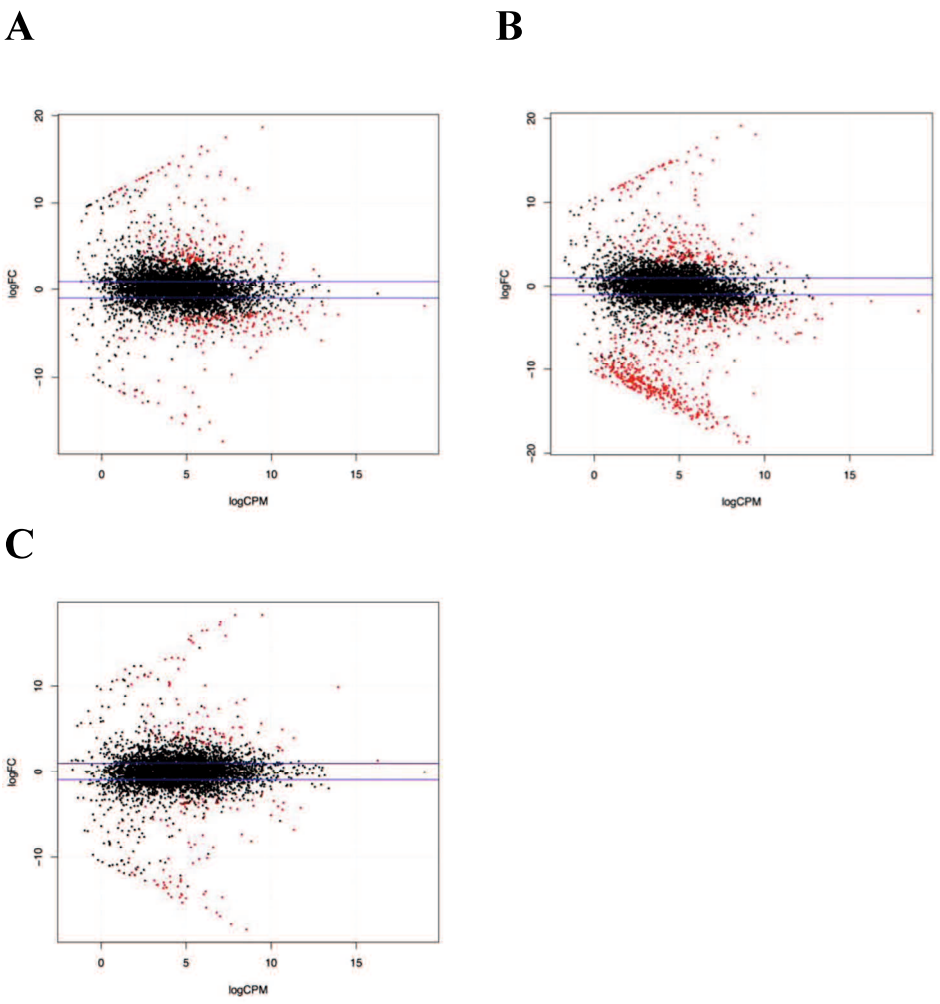

Figure S5 TSS analysis data summarized by logFC/logCPM plot of 30°C xylose shaking (30X)/30°C glucose shaking (30D) (A), 30°C glucose static (30DS)/30D (B) and 45°C glucose shaking (45D)/30D (C). logFC is legalistic value of fold change (FC). logCPM is legalistic value of count per million (CPM). Each spot indicates one gene. Red spots are genes that were significantly changed in expression. Yellow spots are outlier genes. Blue lines represent $\log_2 = 1$ or -1.

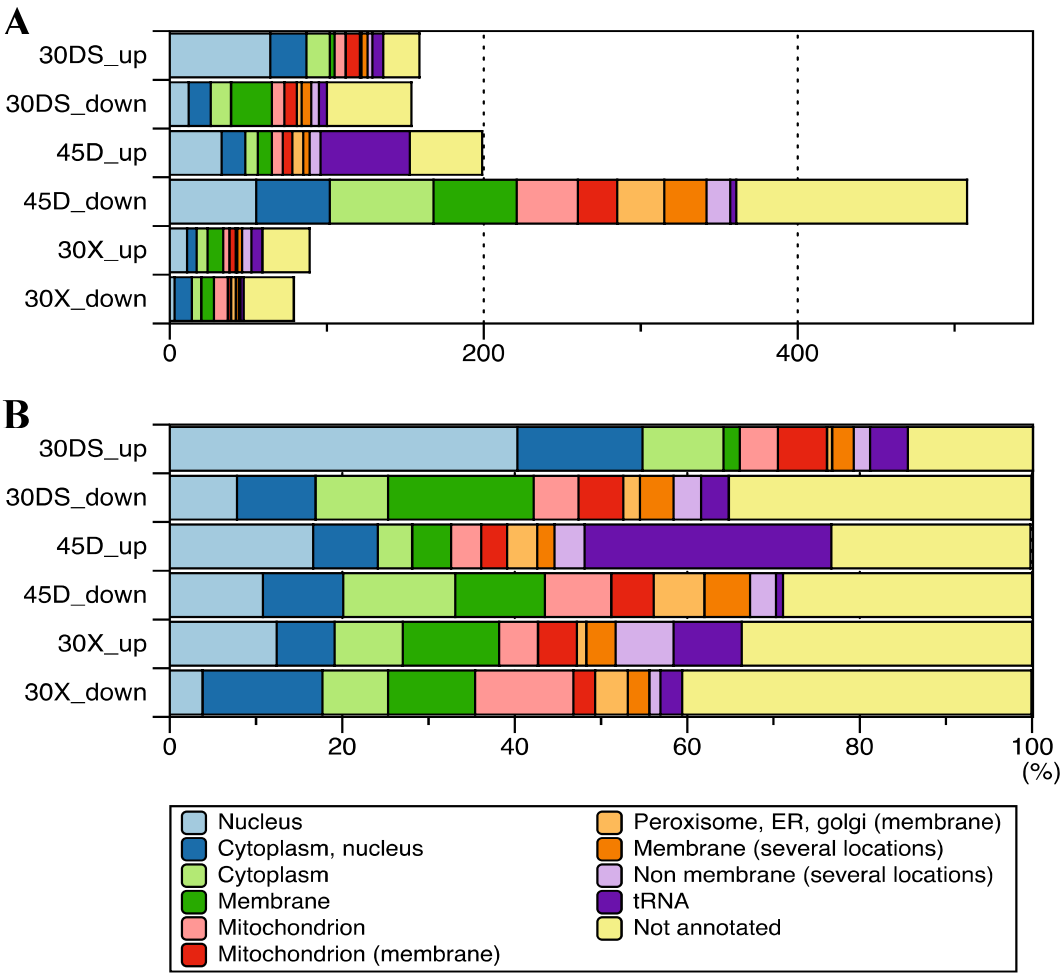

Figure S6 Subcellular localization of products from significantly up-regulated or down-regulated genes under different conditions in *K. marxianus*. Total RNA was prepared from cells grown batch-wise on YPD or YPX medium under four conditions. (A) The up-regulated or down-regulated genes are classified according to subcellular localizations of their products. (B) The number in (A) is expressed as a percentage. The precise numbers and percentages of (A) and (B) are listed in Table S17. The remaining minor subcellular locations are combined and expressed as membrane (several locations) and non-membrane (several locations). Up and down indicate significantly up- and down-regulated genes, respectively, under these conditions compared to 30D. The subcellular localization of each gene product was assigned by UniProt and listed in Tables S10, S12, S14, S16, S20 and S22.

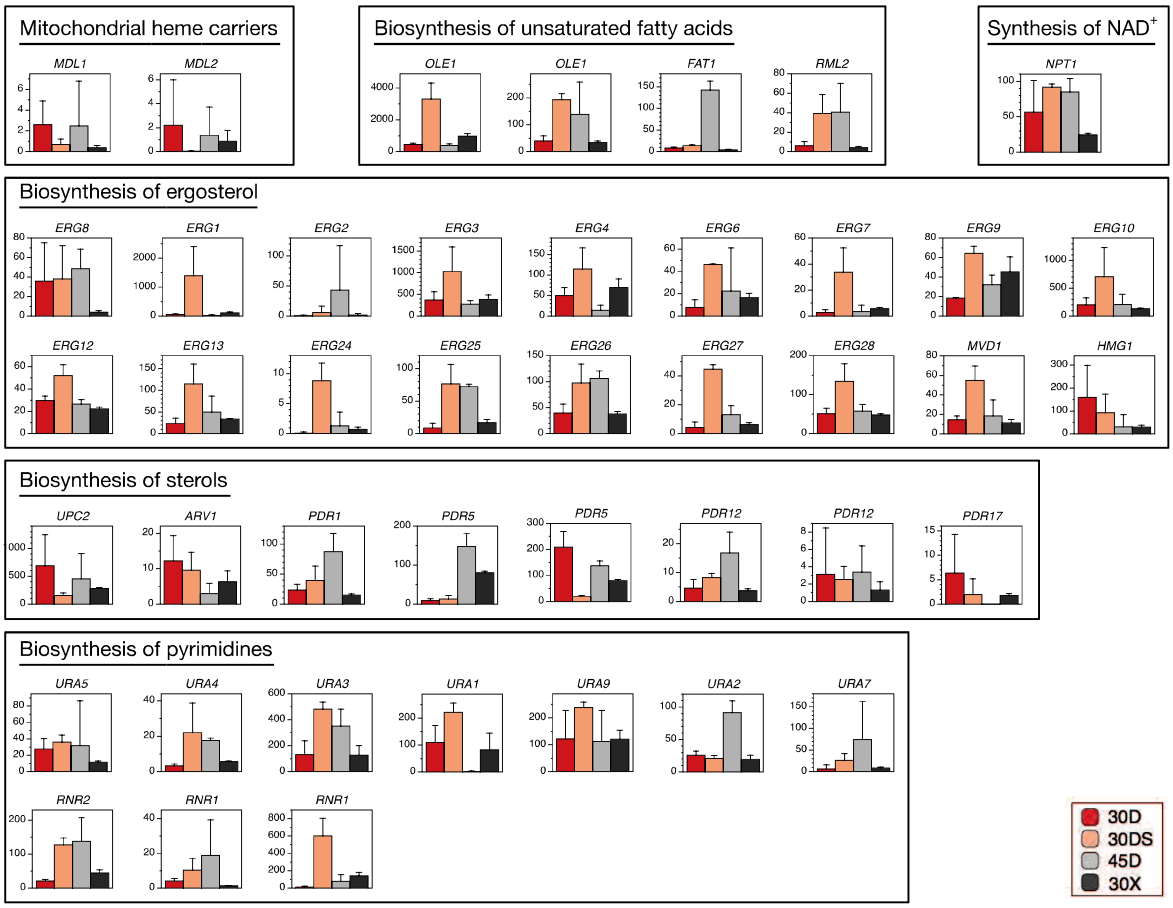

Figure S7 Transcript abundance represented by TSS-tag ppm of each genes related to the oxygen-dependent biosynthetic pathways under different conditions in *K. marxianus*. Empty column means the gene expression below detectable level.

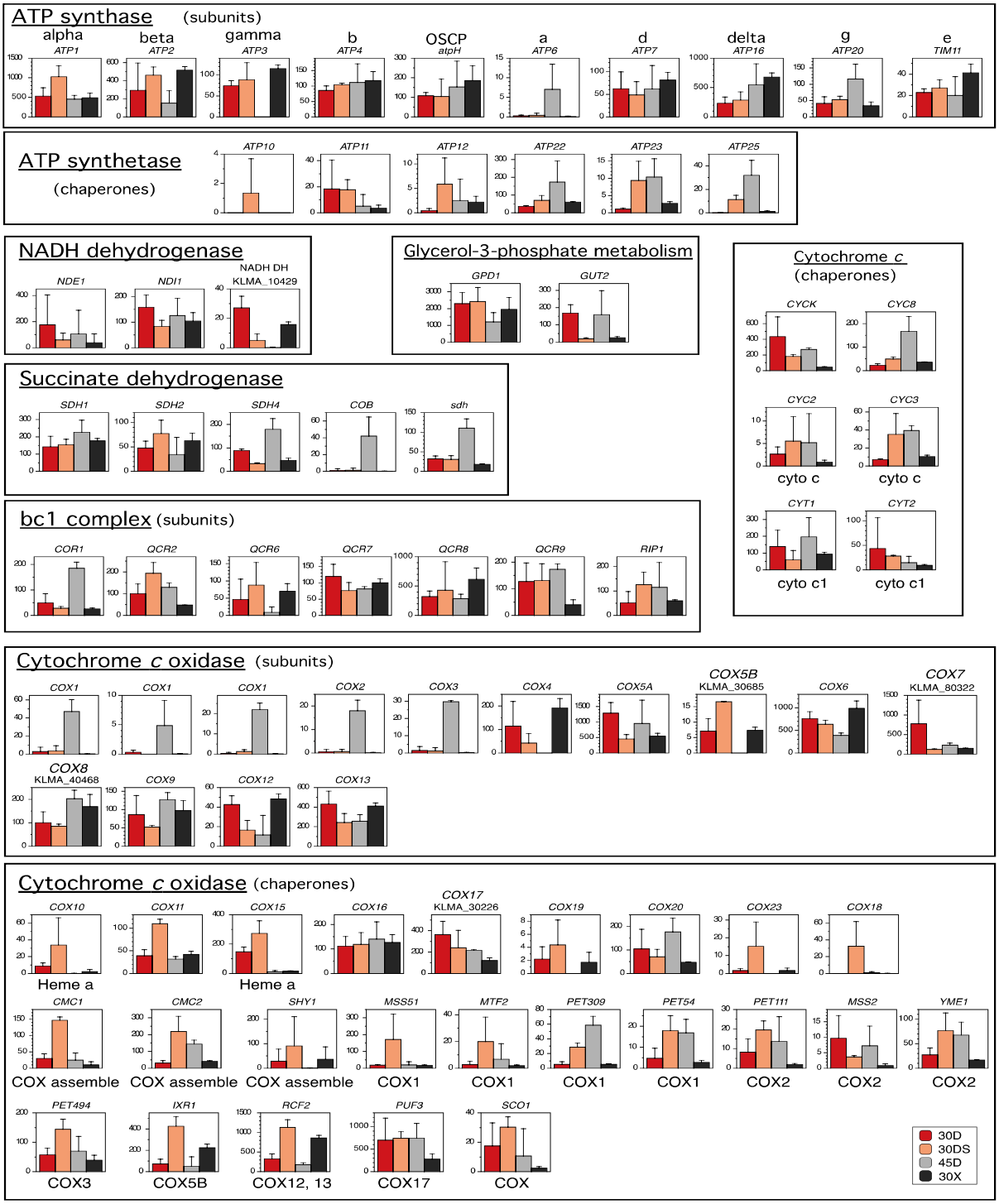

Figure S8 Transcript abundance represented by TSS-tag ppm of each genes related to the ATP synthase, respiratory chain components and their chaperones under different conditions in *K. marxianus*. Empty column means the gene expression below detectable level.

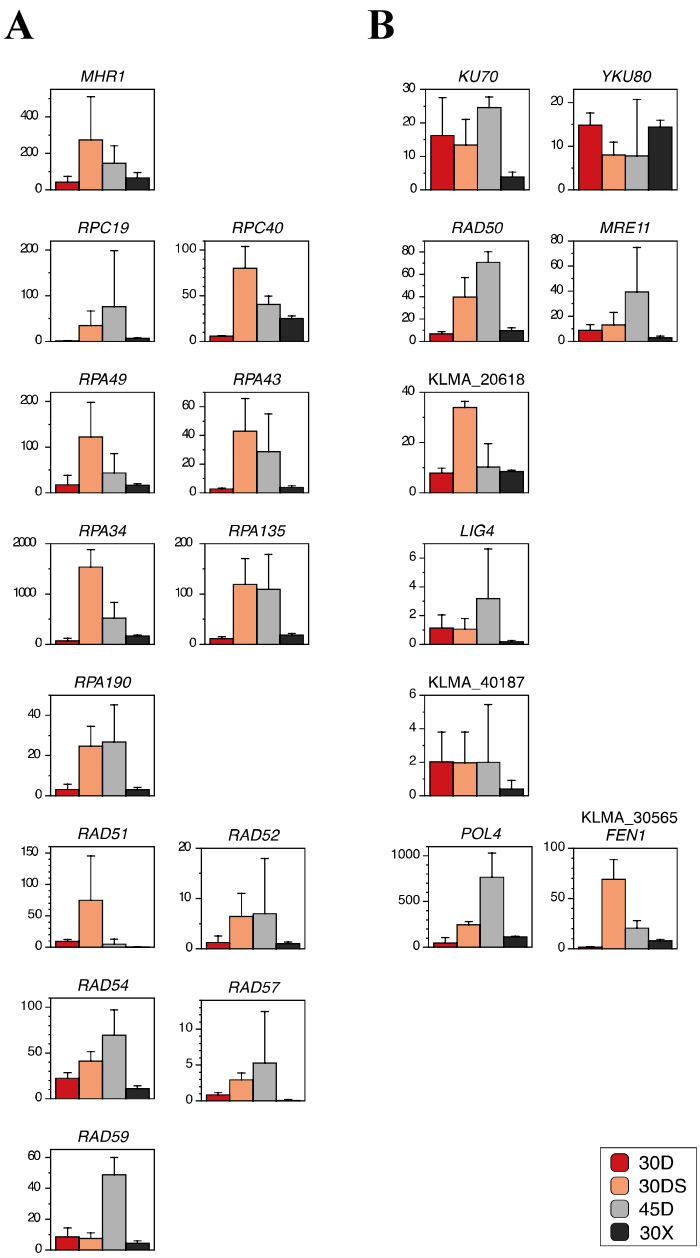

Figure S9 Transcript abundance represented by TSS-tag ppm of each genes related to homologous recombination and non-homologous end-joining under different conditions in *K. marxianus*. The transcript abundance by TSS-tag ppm of genes related to homologous recombination (A) and non-homologous end-joining (B) under different conditions were shown. Empty column means the gene expression below detectable level.

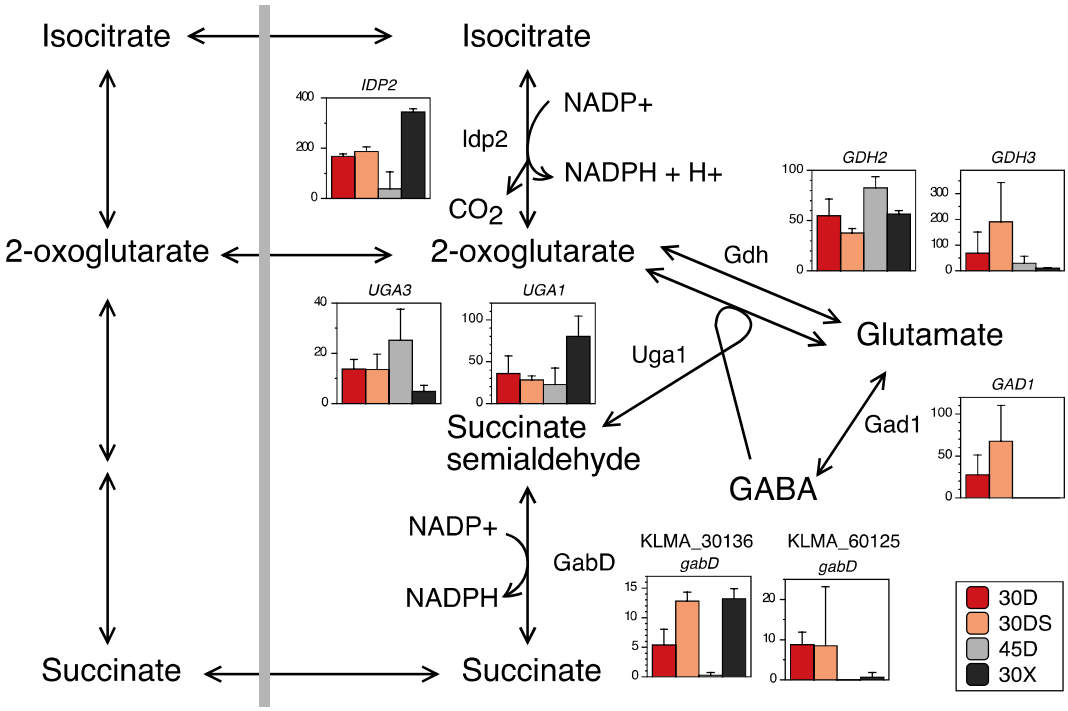

Figure S10 Transcript abundance represented by TSS-tag ppm of each genes related to GABA shunt under different conditions in *K. marxianus.* Empty column means the gene expression below detectable level.

Table S1 KOG assignment summary of *K. marxianus* genomic genes

Total CDS	4954
assigned KOG	3587
assigned KOG percent (%)	72.4
assigned KOG function	2893
assigned KOG function percent (%)	58.4
KOG categories	
Amino acid transport and metabolism	179
Carbohydrate transport and metabolism	151
Cell cycle control	116
Cell motility	6
Cell wall/membrane/envelope biogenesis	33
Chromatin structure and dynamics	76
Coenzyme transport and metabolism	63
Cytoskeleton	60
Defense mechanisms	25
Energy production and conversion	175
Extracellular structures	6
Inorganic ion transport and metabolism	94
Intracellular trafficking	217
Lipid transport and metabolism	127
Nuclear structure	29
Nucleotide transport and metabolism	71
Posttranslational modification	331
Replication	137
RNA processing and modification	196
Secondary metabolites biosynthesis	60
Signal transduction mechanisms	251
Transcription	205
Translation	285
Function unknown	263
General function prediction only	431
no hit	1367

Table S2 Unique genes in *K. marxianus*

Locus_tag	Product
KLMA_10002	hypothetical protein
KLMA_10003	hypothetical protein
KLMA_10013	hypothetical protein
KLMA_10017	hypothetical protein
KLMA_10019	hypothetical protein
KLMA_10040	uncharacterized protein YDR524C-B
KLMA_10041	hypothetical protein
KLMA_10061	DUF3128 super family
KLMA_10067	SCP super family
KLMA_10146	Zn2/Cys6 DNA-binding domain
KLMA_10217	proline-rich protein LAS17
KLMA_10233	hypothetical protein
KLMA_10242	RRM
KLMA_10314	silent chromatin protein ESC1
KLMA_10355	hypothetical protein
KLMA_10376	ribosomal_L22
KLMA_10423	hypothetical protein
KLMA_10432	NADB_Rossmann super family

Locus_tag	Product
KLMA_10443	hypothetical protein
KLMA_10466	erv26 super family
KLMA_10529	hypothetical protein
KLMA_10574	chromatin modification-related protein EAF7
KLMA_10637	hypothetical protein
KLMA_10652	hypothetical protein
KLMA_10664	smg4_UPF3 super family
KLMA_10676	zinc finger
KLMA_10696	GAL4
KLMA_10701	ribosomal_L13e super family
KLMA_10770	hypothetical protein
KLMA_10773	hypothetical protein
KLMA_10806	hypothetical protein
KLMA_10829	hypothetical protein
KLMA_10837	hypothetical protein
KLMA_20001	conserved hypothetical membrane protein
KLMA_20002	flocculation protein FLO5
KLMA_20055	hypothetical protein
KLMA_20103	hypothetical protein
KLMA_20104	hypothetical protein
KLMA_20154	uncharacterized protein YMR086W
KLMA_20163	hypothetical protein
KLMA_20219	BNI1-related protein 1
KLMA_20261	hypothetical protein
KLMA_20328	hypothetical protein
KLMA_20349	SWR1-complex protein 3
KLMA_20369	mediator of RNA polymerase II transcription subunit 15
KLMA_20380	hypothetical protein
KLMA_20393	zinc finger protein STP4
KLMA_20428	flocculation protein FLO11
KLMA_20441	cell wall integrity and stress response component 4
KLMA_20465	chitin biosynthesis protein CHS5
KLMA_20496	hypothetical protein
KLMA_20538	protein CAF130
KLMA_20567	hypothetical protein
KLMA_20572	flocculation suppression protein
KLMA_20606	hypothetical protein
KLMA_20625	hypothetical protein
KLMA_20633	hypothetical protein
KLMA_20689	protein FYV8
KLMA_20758	protein DSE2
KLMA_20782	hypothetical protein
KLMA_20820	hypothetical protein
KLMA_30002	chol_sulfatase
KLMA_30003	transposon Ty1-NL1 Gag polyprotein
KLMA_30005	transposon Ty1-NL1 Gag polyprotein
KLMA_30007	transposon Ty1-NL1 Gag polyprotein
KLMA_30020	AP-1 accessory protein LAA1
KLMA_30079	centromere DNA-binding protein complex CBF3 subunit
KLMA_30115	guanine nucleotide-binding protein subunit beta-like
KLMA_30116	hypothetical protein
KLMA_30122	DASH complex subunit HSK3
KLMA_30178	myosin tail region-interacting protein MTI1
KLMA_30208	c reductase complex
KLMA_30226	cytochrome c oxidase copper chaperone

Locus_tag	Product
KLMA_30239	plasma membrane proteolipid 3
KLMA_30309	protein SPA2
KLMA_30317	hypothetical protein
KLMA_30330	homeodomain super family
KLMA_30368	dentin matrix acidic phosphoprotein 1
KLMA_30382	nuclear localization sequence-binding protein
KLMA_30502	putative guanine nucleotide-exchange factor SED4
KLMA_30555	conserved hypothetical transmembrane protein
KLMA_30609	cell wall integrity sensor MID2
KLMA_30667	herpes_gp2
KLMA_40001	TY2B-F
KLMA_40049	hansenula MRAKII killer toxin-resistant protein
KLMA_40079	uncharacterized endoplamic reticulum membrane
KLMA_40106	uncharacterized protein YDR210W
KLMA_40116	hypothetical protein
KLMA_40117	transcriptional regulator NRG1
KLMA_40132	transcription activator
KLMA_40149	hypothetical protein
KLMA_40192	translation machinery-associated protein 7
KLMA_40200	probable inorganic polyphosphate/ATP-NAD kinase
KLMA_40213	MOG interacting and ectopic P-granules protein
KLMA_40227	POU domain
KLMA_40240	H/ACA ribonucleoprotein complex subunit 1
KLMA_40299	transposon Ty2-LR1 Gag-Pol polyprotein
KLMA_40304	hypothetical protein
KLMA_40308	hypothetical protein
KLMA_40366	hypothetical protein
KLMA_40374	negative regulator of RAS-cAMP pathway
KLMA_40377	hypothetical protein
KLMA_40389	conserved hypothetical membrane protein
KLMA_40446	conserved hypothetical membrane protein
KLMA_40557	PHO85 cyclin-8
KLMA_40626	flocculation protein FLO9
KLMA_40631	hypothetical protein
KLMA_50002	choline-sulfatase conserved domain
KLMA_50003	hypothetical protein
KLMA_50198	nested antisense gene NAG1
KLMA_50203	verprolin
KLMA_50264	40S ribosomal protein S14
KLMA_50320	conserved hypothetical protein
KLMA_50324	uncharacterized protein YPL250W-A
KLMA_50335	transposon Ty1-H Gag-Pol polyprotein
KLMA_50343	tubulin-specific chaperone C
KLMA_50397	gti1_Pac2 super family conserved domain
KLMA_50409	flo11 super family
KLMA_50423	transposon Ty2-LR1 Gag-Pol polyprotein
KLMA_50425	uncharacterized membrane protein YPR109W
KLMA_50456	hypothetical protein
KLMA_50460	mediator of RNA polymerase II transcription subunit 22
KLMA_50515	hypothetical protein
KLMA_50521	hypothetical protein
KLMA_50529	Hyaluronic acid-binding protein 4
KLMA_50597	dolichyl-diphosphooligosaccharide--protein glycosyltransferase
KLMA_50598	subunit OST4
KLMA_60035	serine/threonine-protein kinase ste20

Locus_tag	Product
KLMA_60043	hypothetical protein
KLMA_60045	conserved hypothetical membrane protein
KLMA_60069	40S ribosomal protein S0
KLMA_60084	mer2 super family protein
KLMA_60123	RCR super family protein
KLMA_60124	RCR super family protein
KLMA_60142	N-glycosylation protein EOS1
KLMA_60169	hypothetical protein
KLMA_60215	hypothetical protein
KLMA_60244	protein RTM1
KLMA_60269	lysine-rich arabinogalactan protein 19
KLMA_60270	hypothetical protein
KLMA_60341	SWI/SNF chromatin-remodeling complex subunit SNF5
KLMA_60363	hypothetical protein
KLMA_60368	hypothetical protein
KLMA_60458	mediator of RNA polymerase II transcription subunit
KLMA_70008	conserved hypothetical protein
KLMA_70009	flocculation protein FLO9
KLMA_70019	protein PET20
KLMA_70030	protein SIC1
KLMA_70089	conserved hypothetical membrane protein
KLMA_70107	hypothetical protein
KLMA_70112	conserved hypothetical protein
KLMA_70156	conserved hypothetical protein
KLMA_70220	conserved hypothetical protein
KLMA_70233	uncharacterized protein YLR211C
KLMA_70275	hypothetical protein
KLMA_70309	conserved hypothetical protein
KLMA_70361	conserved hypothetical protein
KLMA_70364	conserved hypothetical protein
KLMA_70390	suppressor protein SRP40
KLMA_70391	hypothetical protein
KLMA_70402	succinate dehydrogenase assembly factor 2
KLMA_70408	zinc finger protein YPR022C
KLMA_70421	DNA-directed RNA polymerase III subunit RPC8
KLMA_70425	uncharacterized protein MBB1
KLMA_70428	conserved hypothetical protein
KLMA_70453	ice-structuring glycoprotein
KLMA_70458	uncharacterized protein ywnB
KLMA_70461	YKL222C
KLMA_70463	hypothetical protein
KLMA_70464	conserved hypothetical membrane protein
KLMA_80001	hypothetical protein
KLMA_80053	DNA-directed RNA polymerase II subunit RPB1
KLMA_80069	alpha-agglutinin
KLMA_80115	transcriptional regulator CRZ1
KLMA_80162	vacuolar segregation protein 7
KLMA_80187	conserved hypothetical protein containing HMG-box super family
KLMA_80191	meiotically up-regulated gene 70 protein
KLMA_80192	conserved hypothetical membrane brotien
KLMA_80223	hypothetical protein
KLMA_80289	uncharacterized protein YBR108W
KLMA_80297	general transcriptional corepressor CYC8
KLMA_80304	hypothetical protein
KLMA_80326	hypothetical protein

Locus_tag	Product
KLMA_80378	hypothetical protein
KLMA_80394	protein KRE1
KLMA_80423	flocculation protein FLO9
KLMA_80424	uncharacterized oligopeptide transporter C1840.12
KLMA_80428	hypothetical protein
KLMA_80429	hypothetical protein
KLMA_90005	probable intron-encoded endonuclease aI5
KLMA_90006	Intron-encoded DNA endonuclease aI4
KLMA_90008	cytochrome c oxidase subunit 1
KLMA_90009	ATP synthase protein 8

Table S3 KOG categories of genes specific for *K. marxianus*

KOG category	Number
Carbohydrate transport and metabolism, Posttranslational modification, protein turnover, chaperones	1
Cell cycle control, cell division, chromosome partitioning	1
Cell cycle control, cell division, chromosome partitioning, Posttranslational modification, protein turnover, chaperones	1
Cell wall/membrane/envelope biogenesis	1
Chromatin structure and dynamics, Transcription	1
Cytoskeleton	2
Energy production and conversion	3
Function unknown	5
General function prediction only	4
Intracellular trafficking, secretion, and vesicular transport	2
Nuclear structure	1
Posttranslational modification, protein turnover, chaperones	2
RNA processing and modification	3
Signal transduction mechanisms	11
Signal transduction mechanisms, Carbohydrate transport and metabolism	1
Signal transduction mechanisms, Cytoskeleton	2
Signal transduction mechanisms, Lipid transport and metabolism	1
Transcription	13
Translation, ribosomal structure and biogenesis	4
non-categorized gene (KOG)	134
Total	193

Table S4 Genes shared only between *K. marxianus* and *K. lactis*

Locus_tag	Product
KLMA_10001	RVT_2 super family
KLMA_10014	mating-type protein ALPHA1
KLMA_10015	mating-type protein ALPHA2
KLMA_10016	mating-type protein ALPHA3
KLMA_10023	hypothetical protein
KLMA_10026	hypothetical protein
KLMA_10027	hypothetical protein
KLMA_10028	hypothetical protein

Locus_tag	Product
KLMA_10033	hypothetical protein
KLMA_10056	dnaQ_like_exo super family
KLMA_10057	hypothetical protein
KLMA_10076	protein PSP1
KLMA_10100	G1/S-specific cyclin CLN1
KLMA_10104	FH2 super family
KLMA_10119	GYF super family
KLMA_10128	hypothetical protein
KLMA_10141	ANTH_AP180_CALM
KLMA_10142	hypothetical protein
KLMA_10143	mating-type protein A2
KLMA_10144	hypothetical protein
KLMA_10147	RNase_H2_suC super family
KLMA_10160	probable DNA-binding protein SNT1
KLMA_10170	SMC_prok_B
KLMA_10171	CRT10 super family[
KLMA_10174	hypothetical protein
KLMA_10183	zinc finger
KLMA_10197	flocculation protein FLO5
KLMA_10226	hypothetical protein
KLMA_10232	rhoGAP_fMSB1
KLMA_10236	SNF2_N
KLMA_10239	hypothetical protein
KLMA_10246	hypothetical protein
KLMA_10249	cylicin-2
KLMA_10277	hypothetical protein
KLMA_10318	RRM
KLMA_10327	hypothetical protein
KLMA_10329	RRM
KLMA_10346	hypothetical protein
KLMA_10366	hypothetical protein
KLMA_10367	hypothetical protein
KLMA_10379	RSC chromatin remodeling complex subunit RSC8
KLMA_10430	RRM
KLMA_10438	hypothetical protein
KLMA_10469	hypothetical protein
KLMA_10472	hypothetical protein
KLMA_10502	rtt102p super family
KLMA_10525	atg31 super family
KLMA_10528	pH-response regulator protein palI/RIM9
KLMA_10538	hypothetical protein
KLMA_10539	inorganic pyrophosphatase
KLMA_10544	glycoside hydrolase
KLMA_10555	hypothetical protein
KLMA_10567	hypothetical protein
KLMA_10579	protein ZDS2
KLMA_10584	hypothetical protein
KLMA_10596	hemocyanin
KLMA_10603	increased rDNA silencing protein 4
KLMA_10608	hypothetical protein
KLMA_10646	AFT super family
KLMA_10647	hypothetical protein
KLMA_10697	hypothetical protein
KLMA_10738	PH domain-containing protein YHR131C
KLMA_10740	esterase_lipase super family

Locus_tag	Product
KLMA_10743	F-box protein COS111
KLMA_10750	hypothetical protein
KLMA_10756	hypothetical protein
KLMA_10759	hypothetical protein
KLMA_10779	hypothetical protein
KLMA_10784	MADS_MEF2_like
KLMA_10820	hypothetical protein
KLMA_10826	hypothetical protein
KLMA_10828	hypothetical protein
KLMA_10835	flocculation protein FLO5
KLMA_20003	conserved hypothetical membrane protein
KLMA_20010	protein crtK
KLMA_20014	hypothetical protein
KLMA_20016	PCI super family
KLMA_20027	hypothetical protein
KLMA_20036	transcriptional activator HAP3
KLMA_20059	regulatory protein MIG1
KLMA_20064	hypothetical conserved protein
KLMA_20065	DUF2410 super family
KLMA_20071	DUP super family
KLMA_20072	hypothetical conserved protein
KLMA_20073	hypothetical conserved protein
KLMA_20080	crossover junction endonuclease EME1
KLMA_20117	regulatory protein ADR1
KLMA_20118	rad9_Rad53_bind super family
KLMA_20128	ribosome assembly protein 3
KLMA_20144	hap4 transcription factor
KLMA_20157	probable serine/threonine-protein kinase HSL1
KLMA_20160	hypothetical protein
KLMA_20164	hypothetical protein
KLMA_20166	hypothetical protein
KLMA_20177	hypothetical protein
KLMA_20178	hypothetical protein
KLMA_20183	conserved hypothetical protein
KLMA_20186	conserved hypothetical protein
KLMA_20238	uncharacterized protein YGL108C
KLMA_20266	hypothetical protein
KLMA_20271	zinc finger DNA binding domain
KLMA_20287	hypothetical protein
KLMA_20302	oligoribonuclease
KLMA_20303	basic-leucine zipper (bZIP) transcription factor
KLMA_20315	hypothetical protein
KLMA_20334	hypothetical protein
KLMA_20338	hypothetical protein
KLMA_20357	sds3 super family
KLMA_20361	hypothetical protein
KLMA_20365	hypothetical protein
KLMA_20371	hypothetical protein
KLMA_20381	hypothetical protein
KLMA_20384	hypothetical protein
KLMA_20416	hypothetical protein
KLMA_20426	p-loop NTPase super family
KLMA_20456	conserved hypothetical protein
KLMA_20458	putative uncharacterized protein YAL004W
KLMA_20477	chromosome segregation ATPases

Locus_tag	Product
KLMA_20506	hypothetical protein
KLMA_20516	hypothetical protein
KLMA_20522	pheromone-regulated membrane protein 3
KLMA_20524	bZIP_1 super family
KLMA_20533	protein SAN1
KLMA_20550	DUF3020 super family
KLMA_20557	SMC_prok_A
KLMA_20588	hypothetical protein
KLMA_20599	GAL4-like Zn2Cys6 binuclear cluster DNA-binding domain
KLMA_20601	rho-type GTPase-activating protein 1
KLMA_20641	transcription activator MSS11
KLMA_20668	transcription initiation factor TFIID subunit 13
KLMA_20684	hypothetical protein
KLMA_20686	hypothetical protein
KLMA_20697	hypothetical protein
KLMA_20700	serine/threonine-protein kinase PAK1
KLMA_20704	CBM_21 super family
KLMA_20705	hypothetical protein
KLMA_20716	ATPase
KLMA_20730	hypothetical protein
KLMA_20746	hypothetical protein
KLMA_20749	uncharacterized protein YHR146W
KLMA_20754	CRE-binding bZIP protein SKO1
KLMA_20756	bud neck protein 5
KLMA_20772	hypothetical protein
KLMA_20776	hypothetical protein
KLMA_20780	chaperone_DMP super family
KLMA_20819	hypothetical protein
KLMA_20838	hypothetical protein
KLMA_30004	transposon Ty2-F/Ty2-GR2 Gag-Pol polyprotein
KLMA_30006	transposon Ty2-F/Ty2-GR2 Gag-Pol polyprotein
KLMA_30008	transposon Ty2-F/Ty2-GR2 Gag-Pol polyprotein
KLMA_30021	mating-type protein A2
KLMA_30022	mating-type protein A1
KLMA_30023	protein SLA2
KLMA_30036	UDP-N-acetylenolpyruvoylglucosamine reductase
KLMA_30055	bZIP_1 super family
KLMA_30058	serine/threonine-protein kinase STE20
KLMA_30077	vacuolar protein sorting-associated protein 38
KLMA_30121	probable kinetochore protein SPC24
KLMA_30129	hypothetical protein
KLMA_30144	negative regulator of sporulation MDS3
KLMA_30166	protein SIP4
KLMA_30167	hypothetical protein
KLMA_30186	mediator of RNA polymerase II transcription subunit 2
KLMA_30194	phosphatidylserine decarboxylase proenzyme 2
KLMA_30200	central kinetochore subunit OKP1
KLMA_30217	mRNA-binding protein PUF3
KLMA_30218	ADIPOR-like receptor IZH3
KLMA_30296	protein BCK2
KLMA_30315	hypothetical protein
KLMA_30320	glyco_transf_15 super family protein
KLMA_30338	protein ICY2
KLMA_30339	ATP synthase subunit b
KLMA_30343	central kinetochore subunit MCM21

Locus_tag	Product
KLMA_30345	hypothetical protein
KLMA_30351	INCENP_ARK-bind super family protein
KLMA_30353	hypothetical protein
KLMA_30354	YTH1[COG5084]
KLMA_30356	transcriptional regulatory protein LGE1
KLMA_30369	hypothetical protein
KLMA_30381	hypothetical protein
KLMA_30399	conserved hypothetical membrane protein
KLMA_30445	conserved hypothetical protein
KLMA_30462	protein NIP100
KLMA_30474	nucleolar protein NET1
KLMA_30481	glyoxalase super family protein
KLMA_30482	glyoxalase super family protein
KLMA_30538	hypothetical protein
KLMA_30544	suppressor of mar1-1 protein
KLMA_30566	transcription factor BAF1
KLMA_30572	meiosis induction protein kinase IME2/SME1
KLMA_30576	halotolerance protein 9
KLMA_30614	hypothetical protein
KLMA_30616	transcriptional activator HAA1
KLMA_30624	conserved hypothetical transmembrane protein
KLMA_30630	conserved hypothetical membrane protein
KLMA_30633	conserved hypothetical membrane protein
KLMA_30635	GAL4
KLMA_30637	bud site selection protein 8
KLMA_30642	conserved hypothetical transmembrane protein
KLMA_30651	e3 SUMO-protein ligase SIZ1
KLMA_30665	ACBP super family protein
KLMA_30682	nitrogen regulatory protein GLN3
KLMA_30688	conserved hypothetical protein
KLMA_30702	hypothetical protein
KLMA_30718	hypothetical protein
KLMA_30730	hypothetical protein
KLMA_40017	protein MSO1
KLMA_40024	probable serine/threonine-protein kinase YNR047W
KLMA_40058	hypothetical protein
KLMA_40061	cell wall protein YLR040C
KLMA_40077	uncharacterized protein YMR124W
KLMA_40100	meiotic activator RIM4
KLMA_40108	hypothetical protein
KLMA_40112	serine/threonine-protein kinase ppk29
KLMA_40127	chaperone protein htpG
KLMA_40136	protein CSF1
KLMA_40146	hypothetical protein
KLMA_40174	uncharacterized cell wall protein YDR134C
KLMA_40187	non-homologous end-joining protein 1
KLMA_40201	zinc finger protein YPR013C
KLMA_40204	transcriptional regulatory protein UME6
KLMA_40209	hypothetical protein
KLMA_40211	protein WHI3
KLMA_40212	solute carrier family 2
KLMA_40215	cell division control protein 13
KLMA_40226	pre-mRNA-splicing factor SPP381
KLMA_40230	hypothetical protein
KLMA_40232	protein GZF3

Locus_tag	Product
KLMA_40250	hypothetical protein
KLMA_40260	hypothetical protein
KLMA_40271	zinc finger protein
KLMA_40272	v-type proton ATPase catalytic subunit A
KLMA_40292	hypothetical protein
KLMA_40311	RNA polymerase II transcriptional coactivator SUB1
KLMA_40314	hypothetical protein
KLMA_40315	hypothetical protein
KLMA_40317	m-phase inducer phosphatase
KLMA_40326	hypothetical protein
KLMA_40341	hypothetical protein
KLMA_40345	ubiquitin-like-specific protease 2
KLMA_40348	hypothetical protein
KLMA_40352	hypothetical protein
KLMA_40358	protein ASI2
KLMA_40370	hypothetical protein
KLMA_40383	hypothetical protein
KLMA_40386	hypothetical protein
KLMA_40421	hypothetical protein
KLMA_40447	weak acid resistance protein 1
KLMA_40457	zinc finger protein SFP1
KLMA_40464	beta tubulin
KLMA_40469	hypothetical protein
KLMA_40484	hypothetical protein
KLMA_40514	hypothetical protein
KLMA_40541	hypothetical protein
KLMA_40564	hypothetical protein
KLMA_40582	hypothetical protein
KLMA_40613	zinc-regulated protein 8
KLMA_40617	putaive regulatory protein
KLMA_40621	hypothetical protein
KLMA_40622	hypothetical protein
KLMA_40629	transposon Ty1-H Gag-Pol polyprotein
KLMA_40630	transposon Ty2-F/Ty2-GR2 Gag-Pol polyprotein
KLMA_50004	transposon Ty2-F/Ty2-GR2 Gag-Pol polyprotein
KLMA_50006	peroxisome assembly protein 22
KLMA_50010	nuclear division defective protein 1
KLMA_50027	kinetochore protein SLK19
KLMA_50064	target of rapamycin complex 2 subunit BIT61,HbrB super family conserved domain
KLMA_50066	hypothetical protein
KLMA_50078	DNA polymerase epsilon subunit C
KLMA_50091	COG5647 (Cullin
KLMA_50092	hypothetical protein
KLMA_50097	hypothetical protein
KLMA_50111	protein SCD5
KLMA_50114	ras_like_GTPase super family
KLMA_50125	sterol regulatory element-binding protein ECM22
KLMA_50129	probable phosphatidylinositol-4-phosphate 5-kinase MSS4
KLMA_50138	zinc finger
KLMA_50158	chromatin structure-remodeling complex protein RSC14
KLMA_50171	THO complex subunit MFT1
KLMA_50180	hypothetical protein
KLMA_50199	hypothetical protein
KLMA_50218	protein MBR1
KLMA_50238	inositol hexakisphosphate kinase 1

Locus_tag	Product
KLMA_50251	J protein JJJ2
KLMA_50252	mitochondrial membrane protein FMP33
KLMA_50256	cyclin-dependent kinase inhibitor FAR1
KLMA_50268	hypothetical protein
KLMA_50275	F-box domain
KLMA_50292	conserved hypothetical membrane protein
KLMA_50298	DSL1 super family conserved domain
KLMA_50300	hypothetical protein
KLMA_50307	predicted solute binding protein
KLMA_50330	lactose regulatory protein LAC9
KLMA_50359	hypothetical protein
KLMA_50372	uncharacterized protein YIR003W
KLMA_50386	nuclear localization sequence-binding protein
KLMA_50392	protein VAB2
KLMA_50427	pre-mRNA-processing factor 31
KLMA_50451	acyl-coenzyme A:6-aminopenicillanic-acid-acyltransferase 40 kDa form
KLMA_50461	kinetochore-associated protein DSN1
KLMA_50463	conserved hypothetical membrane protein
KLMA_50479	hypothetical protein
KLMA_50481	uncharacterized protein YGR130C
KLMA_50494	structure-specific endonuclease subunit SLX4
KLMA_50509	SH3 super family
KLMA_50512	RNA polymerase I-specific transcription initiation factor RRN5
KLMA_50541	conserved hypothetical membrane protein
KLMA_50545	conserved hypothetical membrane protein
KLMA_50555	something about silencing protein 4
KLMA_50561	protein ATC1/LIC4
KLMA_50594	conserved hypothetical protein
KLMA_50599	vacuolar import and degradation protein 27
KLMA_50602	PAPA-1 super family conserved domain
KLMA_50623	protein BNI4
KLMA_60001	DUP super family
KLMA_60007	flocculation protein FLO9
KLMA_60016	histone chaperone ASF1
KLMA_60030	hypothetical protein
KLMA_60044	kelch repeat-containing protein 1
KLMA_60049	hypothetical protein
KLMA_60053	spo12 super family protein
KLMA_60081	mvb12 super family protein
KLMA_60097	probable transcription factor HMS1
KLMA_60105	hypothetical protein
KLMA_60161	hypothetical protein
KLMA_60162	flavoprotein super family protein
KLMA_60170	UBX domain-containing protein 4
KLMA_60190	splicing factor MUD2
KLMA_60199	H2A super family protein
KLMA_60202	hypothetical protein
KLMA_60205	conserved hypothetical phospatase and actin regulator 2
KLMA_60207	ISWI one complex protein 3
KLMA_60217	HLH[cd00083]
KLMA_60242	E3 ubiquitin-protein ligase DMA2
KLMA_60245	mRNA-decapping enzyme subunit 2
KLMA_60254	H/ACA ribonucleoprotein complex non-core subunit NAF1
KLMA_60266	NDT80_PhoG super family protein
KLMA_60267	protein FYV6

Locus_tag	Product
KLMA_60273	hypothetical protein
KLMA_60299	GCR1_C super family protein
KLMA_60316	uncharacterized transcriptional regulatory protein YKL038W
KLMA_60329	HMGB-UBF_HMG-box containing protein
KLMA_60330	hypothetical protein
KLMA_60332	transcriptional activator/repressor MOT3
KLMA_60345	target of rapamycin complex 1 subunit TCO89
KLMA_60352	hypothetical protein
KLMA_60355	ULP1-interacting protein 4
KLMA_60367	hypothetical membrane protein
KLMA_60404	hypothetical protein
KLMA_60453	hypothetical protein
KLMA_60456	transcription factor NRM1
KLMA_60460	inheritance of peroxisomes protein 1
KLMA_60466	uncharacterized protein YMR206W
KLMA_60467	hypothetical protein
KLMA_60490	uncharacterized protein YDL129W
KLMA_60498	uncharacterized protein YDL186W
KLMA_60525	kilA-N super family protein
KLMA_60545	hypothetical protein
KLMA_70004	conserved hypothetical protein
KLMA_70023	pheromone-regulated membrane protein 4
KLMA_70035	hypothetical protein
KLMA_70036	hypothetical protein
KLMA_70062	covalently-linked cell wall protein 14
KLMA_70066	conserved hypothetical membrane protein
KLMA_70085	central kinetochore subunit MCM16
KLMA_70090	conserved hypothetical protein
KLMA_70094	hypothetical protein
KLMA_70109	bud site selection protein 4
KLMA_70121	assembly-complementing factor 4
KLMA_70133	retrograde regulation protein 3
KLMA_70151	37S ribosomal protein MRP21
KLMA_70164	protein DAL82
KLMA_70181	hypothetical protein
KLMA_70187	PHO85 cyclin-6
KLMA_70198	54S ribosomal protein IMG2
KLMA_70204	conserved hypothetical protein
KLMA_70208	hypothetical protein
KLMA_70221	hypothetical protein
KLMA_70230	hypothetical protein
KLMA_70242	conserved hypothetical protein
KLMA_70267	hypothetical protein
KLMA_70294	hypothetical protein
KLMA_70303	probable 6-phosphofructo-2-kinase/fructose-2,6-biphosphatase
KLMA_70323	uncharacterized protein YOL036W
KLMA_70324	transcriptional activator of sulfur metabolism
KLMA_70352	mitotic spindle-associated protein SHE1
KLMA_70356	hypothetical protein
KLMA_70379	nucleus export protein BRR6
KLMA_70393	hypothetical protein
KLMA_70394	paxillin-like protein 1
KLMA_70420	conserved hypothetical membrane protein
KLMA_70430	hypothetical protein
KLMA_70431	hypothetical protein

Locus_tag	Product
KLMA_70460	hypothetical protein
KLMA_80002	transposon Ty2-LR1 Gag-Pol polyprotein
KLMA_80003	transposon Ty2-DR2 Gag-Pol polyprotein
KLMA_80008	conserved hypothetical protein
KLMA_80012	conserved hypothetical protein
KLMA_80040	aminoglycoside antibiotic sensitivity protein 3
KLMA_80056	conserved hypothetical protein
KLMA_80078	conserved hypothetical protein
KLMA_80082	hypothetical protein
KLMA_80136	conserved hypothetical protein containing PIG-H super family
KLMA_80143	hypothetical protein
KLMA_80164	nucleoporin NUP159
KLMA_80194	protein PXR1
KLMA_80209	stress response protein NST1
KLMA_80231	[PSI+] induction protein 2
KLMA_80257	uncharacterized protein YKL054C
KLMA_80266	hypothetical protein
KLMA_80274	conserved hypothetical protein
KLMA_80284	vacuolar import and degradation protein 24
KLMA_80288	hypothetical protein
KLMA_80303	protein OPY2
KLMA_80307	hypothetical protein
KLMA_80320	conserved hypothetical protein
KLMA_80338	RNA-binding protein PIN4
KLMA_80341	transcriptional regulatory protein DOT6
KLMA_80376	uncharacterized protein YBL081W
KLMA_80402	probable 26S proteasome complex subunit SEM1
KLMA_80409	autophagy-related protein 10
KLMA_80426	flocculation protein FLO5

Table S5 Ortholog genes shared between *K. marxianus* and *O. parapolymorpha*, which are absent from *K. lactis*

K. marxianus	*O. parapolymorpha*	product
KLMA_10011	HPODL_1713	probable transporter SEO1
KLMA_10012	HPODL_1714	uncharacterized protein C11D3.14c
KLMA_10060	HPODL_2230	selR super family
KLMA_10319	HPODL_2009	serine/threonine-protein kinase SKY1
KLMA_10342	HPODL_4082	dihydrosphingosine 1-phosphate phosphatase LCB3
KLMA_10592	HPODL_3133	enoate reductase 1
KLMA_10631	HPODL_3986	26S proteasome regulatory subunit RPN13
KLMA_10824	HPODL_1198	Sit1p
KLMA_10834	HPODL_0821	repressible acid phosphatase
KLMA_30012	HPODL_0089	siderophore iron transporter mirA
KLMA_30276	HPODL_2565	siderophore iron transporter 1
KLMA_40279	HPODL_1232	hypothetical protein
KLMA_40364	HPODL_2244	uncharacterized oxidoreductase YIR035C
KLMA_40424	HPODL_0230	uncharacterized MFS-type transporter C530.15c
KLMA_40491	HPODL_3179	homoserine dehydrogenase
KLMA_50087	HPODL_2310	sec sixty-one protein homolog
KLMA_50190	HPODL_3676	acyl-CoA-binding protein, ACBP
KLMA_50243	HPODL_2732	DNA replication complex GINS protein PSF1
KLMA_50379	HPODL_1677	high affinity potassium transporter
KLMA_50391	HPODL_2886	prefoldin subunit 2
KLMA_50447	HPODL_2932	vacuolar ATPase assembly integral membrane protein VMA21

K. marxianus	*O. parapolymorpha*	product
KLMA_60004	HPODL_1024	arylsulfotrans
KLMA_60156	HPODL_2503	actin-related protein 2/3 complex subunit 4
KLMA_60402	HPODL_3431	pisatin demethylase
KLMA_60497	HPODL_3764	v-type proton ATPase catalytic subunit A
KLMA_60558	HPODL_1717	aminotriazole resistance protein
KLMA_70012	HPODL_4148	1-aminocyclopropane-1-carboxylate oxidase
KLMA_70013	HPODL_1025	vacuolar basic amino acid transporter 2
KLMA_70310	HPODL_0880	mitochondrial respiratory chain complexes assembly protein AFG3
KLMA_80201	HPODL_3639	ubiquitin carboxyl-terminal hydrolase 15

Table S6 Sugar transporters predicted in *K. marxianus*

Locus_tag	Product	UniProt number	UniProt gene	KEGG Orthology
KLMA_10546	high-affinity glucose transporter	P49374	HGT1	
KLMA_10547	high-affinity glucose transporter	P49374	HGT1	
KLMA_20258	putative sialic acid transporter	P36035	JEN1	K08178
KLMA_20402	probable metabolite transport protein YBR241C	P38142		
KLMA_20580	probable metabolite transport protein YDR387C	Q04162		
KLMA_20593	uncharacterized mitochondrial outer membrane protein YDR381C-A	Q3E6R5		
KLMA_20638	putative polyol transporter 2	Q8VZ80	PLT5	
KLMA_20830	lactose permease	P07921	LAC12	
KLMA_30010	lactose permease	P07921	LAC12	
KLMA_30728	lactose permease	P07921	LAC12	
KLMA_50032	high-affinity glucose transporter	P49374	HGT1	
KLMA_50360	hexose transporter 2	P53387	KHT2	K08139
KLMA_50361	hexose transporter 2	P53387	KHT2	K08139
KLMA_50362	hexose transporter	P53387	KHT2	
KLMA_50363	low-affinity glucose transporter	P18631	RAG1	K08139
KLMA_50364	low-affinity glucose transporter	P18631	RAG1	K08139
KLMA_60073	carboxylic acid transporter protein homolog	P36035	JEN1	K08178
KLMA_60180	sugar transporter STL1	P39932	STL1	
KLMA_60440	uncharacterized membrane protein YJR124C	P47159		
KLMA_60507	high-affinity glucose transporter SNF3	P10870	SNF3	K08139
KLMA_70003	hexose transporter HXT9	P54854	HXT15	
KLMA_70050	probable metabolite transport protein YFL040W	P43562		
KLMA_70145	conserved hypothetical membrane protein	C0SPB2	ywtG	
KLMA_80005	high-affinity glucose transporter	P07921	LAC12	
KLMA_80101	conserved hypothetical protein containing the Major Facilitator Superfamily (MFS) domain	C0SPB2	ywtG	K06609
KLMA_80273	myo-inositol transporter 2	P30606	ITR2	K08150
KLMA_80389	hexose transporter HXT14	P42833	HXT14	

Table S7 rDNA copy number analysis of several *K. marxianus* strains

Strain	rDNA copy number (per genome)	Spot test	
		45°C	48°C
DMKU 3-1042	205	+ + + + +	+ + + + +
NBRC 0219	31	+ + + + +	+ + + + +
NBRC 0272	56	+ + +	+
NBRC 0482	50	+ + + + +	+ + + +
NBRC 0541	90	+ +	-

Strain	rDNA copy number (per genome)	Spot test	
		45°C	48°C
NBRC 0690	80	+ + +	-
NBRC 1735	88	+	-
NBRC 1777	89	+ + + + +	+ + + + +
NBRC 1963	276	-	-
NBRC 10005	149	+ +	+

+, the level of growth (see Figure S4)

-, no growth

Table S8 Numbers of genes significantly changed in expression under different conditions (FDR < 0.05)

Condition	30DS/30D	45D/30D	30X/30D
Total gene number (4,839)	313	707	168
Up-regulated	159	199	89
Down-regulated	154	508	79

Table S9 GO terms enriched in significantly up-regulated genes under 30DS condition

GO.ID	Term	Annotated gene[a]	Significant[b]	Expected[c]	P-value[d]	Genes
GO:0042254	ribosome biogenesis	270	59	9.67	< 1e-30	ALB1, BMS1, BRX1, BUD23, CAM1, CBF5, CGR1, CIC1, DBP10, DBP3, DBP7, DHR2, DIP2, DRS1, EFG1, ESF1, FUN12, IMP4, KRI1, LCP5, MAK5, MRT4, NMD3, NOC2, NOC3, NOG2, NOP1, NOP15, NOP2, NOP4, NOP56, NOP7, NSA1, NSA2, NSR1, PNO1, PUF6, PXR1, REI1, REX4, RLI1, RPF2, RPL8B, RRP14, RRP4, RRP42, RRP45, RRP5, RRP8, RSA3, SAS10, SDO1, SKI6, SPB1, SSF1, TIF6, TSR2, UTP15, UTP25
GO:0022613	ribonucleoprotein complex biogenesis	317	59	11.35	4.7e-30	ALB1, BMS1, BRX1, BUD23, CAM1, CBF5, CGR1, CIC1, DBP10, DBP3, DBP7, DHR2, DIP2, DRS1, EFG1, ESF1, FUN12, IMP4, KRI1, LCP5, MAK5, MRT4, NMD3, NOC2, NOC3, NOG2, NOP1, NOP15, NOP2, NOP4, NOP56, NOP7, NSA1, NSA2, NSR1, PNO1, PUF6, PXR1, REI1, REX4, RLI1, RPF2, RPL8B, RRP14, RRP4, RRP42, RRP45, RRP5, RRP8, RSA3, SAS10, SDO1, SKI6, SPB1, SSF1, TIF6, TSR2, UTP15, UTP25
GO:0006364	rRNA processing	191	43	6.84	1.1e-24	BMS1, BUD23, CBF5, CGR1, DBP10, DBP3, DBP7, DHR2, DIP2, EFG1, ESF1, FUN12, IMP4, KRI1, LCP5, MAK5, MRT4, NOC3, NOP1, NOP15, NOP2,

GO.ID	Term	Annotated gene[a]	Significant[b]	Expected[c]	P-value[d]	Genes
						NOP4, NOP56, NOP7, NSA1, NSA2, NSR1, PXR1, REX4, RLI1, RPF2, RRP14, RRP4, RRP42, RRP45, RRP5, SAS10, SKI6, SPB1, TIF6, TSR2, UTP15, UTP25
GO:0016072	rRNA metabolic process	196	43	7.02	3.3e-24	BMS1, BUD23, CBF5, CGR1, DBP10, DBP3, DBP7, DHR2, DIP2, EFG1, ESF1, FUN12, IMP4, KRI1, LCP5, MAK5, MRT4, NOC3, NOP1, NOP15, NOP2, NOP4, NOP56, NOP7, NSA1, NSA2, NSR1, PXR1, REX4, RLI1, RPF2, RRP14, RRP4, RRP42, RRP45, RRP5, SAS10, SKI6, SPB1, TIF6, TSR2, UTP15, UTP25
GO:0034470	ncRNA processing	259	46	9.28	7.5e-22	BMS1, BUD23, CBF5, CGR1, DBP10, DBP3, DBP7, DHR2, DIP2, EFG1, ELP6, ESF1, FUN12, IMP4, KRI1, LCP5, MAK5, MRT4, NOC3, NOP1, NOP15, NOP2, NOP4, NOP56, NOP7, NSA1, NSA2, NSR1, PUS4, PXR1, REX4, RLI1, RPF2, RRP14, RRP4, RRP42, RRP45, RRP5, SAS10, SKI6, SPB1, TIF6, TRM82, TSR2, UTP15, UTP25
GO:0034660	ncRNA metabolic process	305	47	10.92	1.2e-19	BMS1, BUD23, CBF5, CGR1, DBP10, DBP3, DBP7, DHR2, DIP2, EFG1, ELP6, ESF1, FUN12, ILS1, IMP4, KRI1, LCP5, MAK5, MRT4, NOC3, NOP1, NOP15, NOP2, NOP4, NOP56, NOP7, NSA1, NSA2, NSR1, PUS4, PXR1, REX4, RLI1, RPF2, RRP14, RRP4, RRP42, RRP45, RRP5, SAS10, SKI6, SPB1, TIF6, TRM82, TSR2, UTP15, UTP25
GO:0044085	cellular component biogenesis	685	63	24.53	5.8e-15	ALB1, BMS1, BRX1, BUD23, CAC2, CAM1, CBF5, CGR1, CIC1, DBP10, DBP3, DBP7, DHR2, DIP2, DRS1, EFG1, ESF1, FUN12, IMP4, KLMA_60262, KRI1, LCP5, MAK5, MRT4, NMD3, NOC2, NOC3, NOG2, NOP1, NOP15, NOP2, NOP4, NOP56, NOP7, NSA1, NSA2, NSR1, PNO1, PTP2, PUF6, PXR1, REI1, REX4, RLF2, RLI1, RPF2, RPL8B, RRP14, RRP4, RRP42, RRP45, RRP5, RRP8, RSA3, SAS10, SDO1, SKI6, SPB1, SSF1, TIF6, TSR2, UTP15, UTP25
GO:0006396	RNA processing	405	47	14.5	1.6e-14	BMS1, BUD23, BUD31, CBF5, CGR1, DBP10, DBP3, DBP7, DHR2, DIP2, EFG1, ELP6, ESF1, FUN12, IMP4, KRI1, LCP5, MAK5, MRT4, NOC3, NOP1, NOP15, NOP2, NOP4, NOP56, NOP7, NSA1, NSA2, NSR1, PUS4, PXR1, REX4, RLI1, RPF2, RRP14, RRP4, RRP42, RRP45, RRP5, SAS10, SKI6, SPB1, TIF6, TRM82, TSR2, UTP15, UTP25
GO:0042273	ribosomal large subunit biogenesis	45	14	1.61	1.8e-10	ALB1, BRX1, CIC1, MRT4, NOP15, PUF6, REI1, RLI1, RPF2, RRP14, RRP5, RRP8, SSF1, TIF6
GO:0071840	cellular component organization or biogenesis	1424	79	51	3.6e-07	ALB1, BMS1, BRX1, BUD23, CAC2, CAM1, CBF5, CGR1, CIC1, COX18, CTF4, DBP10, DBP3, DBP7, DHR2, DIP2, DNA2, DRS1, EFG1, ESF1, FUN12, HIR1, IMP4, KAP123, KLMA_50458, KLMA_60262, KRI1, LCP5, MAK5, MDH2, MDJ2, MRPL35,

GO.ID	Term	Annotated gene[a]	Significant[b]	Expected[c]	P-value[d]	Genes
						MRT4, NMD3, NOC2, NOC3, NOG2, NOP1, NOP15, NOP2, NOP4, NOP56, NOP7, NPR3, NSA1, NSA2, NSR1, PDS5, PNO1, POL12, PTP2, PUF6, PXR1, REI1, REX4, RFA1, RLF2, RLI1, RPF2, RPL8B, RRP14, RRP4, RRP42, RRP45, RRP5, RRP8, RSA3, RSM22, SAS10, SDO1, SKI6, SPB1, SPC105, SSF1, TIF6, TIM17, TSR2, UTP15, UTP25
GO:0000466	maturation of 5.8S rRNA from tricistronic rRNA transcript (SSU-rRNA, 5.8S rRNA, LSU-rRNA)	46	11	1.65	3.7e-07	BUD23, DIP2, KRI1, RPF2, RRP4, RRP42, RRP45, RRP5, SAS10, SKI6, TIF6
GO:0042255	ribosome assembly	29	9	1.04	4.0e-07	BMS1, BRX1, MRT4, NOC2, NSR1, RPF2, SDO1, SSF1, TIF6
GO:0000460	maturation of 5.8S rRNA	47	11	1.68	4.7e-07	BUD23, DIP2, KRI1, RPF2, RRP4, RRP42, RRP45, RRP5, SAS10, SKI6, TIF6
GO:0016070	RNA metabolic process	923	58	33.06	1.0e-06	BMS1, BUD23, BUD31, CAM1, CBF5, CGR1, DBP10, DBP3, DBP7, DHR2, DIP2, EFG1, ELP6, ESF1, FEN1, FUN12, HIR1, ILS1, IMP4, KLMA_20616, KRI1, LCP5, MAK5, MRT4, NOC3, NOP1, NOP15, NOP2, NOP4, NOP56, NOP7, NSA1, NSA2, NSR1, POL1, PUS4, PXR1, RBA50, REX4, RLI1, RPA34, RPC25, RPC37, RPF2, RRP14, RRP4, RRP42, RRP45, RRP5, SAS10, SKI6, SPB1, SPT6, TIF6, TRM82, TSR2, UTP15, UTP25
GO:0090304	nucleic acid metabolic process	1152	66	41.26	3.4e-06	BMS1, BUD23, BUD31, CAC2, CAM1, CBF5, CGR1, CTF4, DBP10, DBP3, DBP7, DHR2, DIP2, DNA2, EFG1, ELP6, ESF1, FEN1, FUN12, HIR1, ILS1, IMP4, KLMA_20616, KRI1, LCP5, MAK5, MRT4, NOC3, NOP1, NOP15, NOP2, NOP4, NOP56, NOP7, NSA1, NSA2, NSR1, PDS5, POL1, POL12, PUS4, PXR1, RBA50, REX4, RFA1, RLF2, RLI1, RNR1, RPA34, RPC25, RPC37, RPF2, RRP14, RRP4, RRP42, RRP45, RRP5, SAS10, SKI6, SPB1, SPT6, TIF6, TRM82, TSR2, UTP15, UTP25
GO:0000469	cleavage involved in rRNA processing	39	9	1.4	6.3e-06	BUD23, DIP2, KRI1, RRP4, RRP42, RRP45, RRP5, SAS10, SKI6
GO:0006139	nucleobase-containing compound metabolic process	1330	72	47.63	7.3e-06	BMS1, BUD23, BUD31, CAC2, CAM1, CBF5, CDC21, CGR1, CTF4, DAS2, DBP10, DBP3, DBP7, DCD1, DHR2, DIP2, DNA2, DUT1, EFG1, ELP6, ESF1, FEN1, FUN12, HIR1, ILS1, IMP4, KLMA_20616, KRI1, LCP5, MAK5, MEF2, MRT4, NOC3, NOP1, NOP15, NOP2, NOP4, NOP56, NOP7, NSA1, NSA2, NSR1, PDS5, POL1, POL12, PUS4, PXR1, RBA50, REX4, RFA1, RLF2, RLI1, RNR1, RPA34, RPC25, RPC37, RPF2, RRP14, RRP4, RRP42, RRP45, RRP5, SAS10, SKI6, SPB1, SPT6, TIF6, TRM82, TSR2, URK1, UTP15, UTP25
GO:0090501	RNA phosphodiester bond hydrolysis	40	9	1.43	7.8e-06	BUD23, DIP2, KRI1, RRP4, RRP42, RRP45, RRP5, SAS10, SKI6

GO.ID	Term	Annotated gene[a]	Significant[b]	Expected[c]	P-value[d]	Genes
GO:0000462	maturation of SSU-rRNA from tricistronic rRNA transcript (SSU-rRNA, 5.8S rRNA, LSU-rRNA)	44	9	1.58	1.8e-05	BUD23, DHR2, DIP2, FUN12, KRI1, RRP5, SAS10, TSR2, UTP15
GO:0042274	ribosomal small subunit biogenesis	67	11	2.4	1.9e-05	BUD23, DHR2, DIP2, FUN12, KRI1, NSR1, RRP14, RRP5, SAS10, TSR2, UTP15
GO:0030490	maturation of SSU-rRNA	48	9	1.72	3.8e-05	BUD23, DHR2, DIP2, FUN12, KRI1, RRP5, SAS10, TSR2, UTP15
GO:0009157	deoxyribonucleoside monophosphate biosynthetic process	3	3	0.11	4.5e-05	CDC21, DCD1, DUT1
GO:0009162	deoxyribonucleoside monophosphate metabolic process	3	3	0.11	4.5e-05	CDC21, DCD1, DUT1
GO:0009176	pyrimidine deoxyribonucleoside monophosphate metabolic process	3	3	0.11	4.5e-05	CDC21, DCD1, DUT1
GO:0009177	pyrimidine deoxyribonucleoside monophosphate biosynthetic process	3	3	0.11	4.5e-05	CDC21, DCD1, DUT1
GO:0006725	cellular aromatic compound metabolic process	1395	72	49.96	4.9e-05	BMS1, BUD23, BUD31, CAC2, CAM1, CBF5, CDC21, CGR1, CTF4, DAS2, DBP10, DBP3, DBP7, DCD1, DHR2, DIP2, DNA2, DUT1, EFG1, ELP6, ESF1, FEN1, FUN12, HIR1, ILS1, IMP4, KLMA_20616, KRI1, LCP5, MAK5, MEF2, MRT4, NOC3, NOP1, NOP15, NOP2, NOP4, NOP56, NOP7, NSA1, NSA2, NSR1, PDS5, POL1, POL12, PUS4, PXR1, RBA50, REX4, RFA1, RLF2, RLI1, RNR1, RPA34, RPC25, RPC37, RPF2, RRP14, RRP4, RRP42, RRP45, RRP5, SAS10, SKI6, SPB1, SPT6, TIF6, TRM82, TSR2, URK1, UTP15, UTP25
GO:0009147	pyrimidine nucleoside triphosphate metabolic process	7	4	0.25	5.1e-05	CDC21, DAS2, DUT1, URK1
GO:0009129	pyrimidine nucleoside monophosphate metabolic process	13	5	0.47	5.6e-05	CDC21, DAS2, DCD1, DUT1, URK1
GO:0009130	pyrimidine nucleoside monophosphate biosynthetic process	13	5	0.47	5.6e-05	CDC21, DAS2, DCD1, DUT1, URK1
GO:0034641	cellular nitrogen compound metabolic process	1463	74	52.39	7.2e-05	ASP1, BMS1, BUD23, BUD31, CAC2, CAM1, CBF5, CDC21, CGR1, CTF4, DAS2, DBP10, DBP3, DBP7, DCD1, DHR2, DIP2, DNA2, DUT1, EFG1, ELP6, ESF1, FEN1, FUN12, HIR1, ILS1, IMP4, KLMA_20616, KRI1, LCP5, MAK5, MEF2, MRT4, NOC3, NOP1, NOP15, NOP2, NOP4, NOP56, NOP7, NSA1, NSA2, NSR1, PDS5, POL1, POL12, PSD1, PUS4, PXR1, RBA50, REX4, RFA1, RLF2, RLI1, RNR1, RPA34, RPC25, RPC37, RPF2, RRP14, RRP4, RRP42, RRP45, RRP5, SAS10, SKI6, SPB1, SPT6, TIF6, TRM82, TSR2, URK1,

GO.ID	Term	Annotated gene[a]	Significant[b]	Expected[c]	P-value[d]	Genes
						UTP15, UTP25
GO:0046483	heterocycle metabolic process	1414	72	50.64	8.2e-05	BMS1, BUD23, BUD31, CAC2, CAM1, CBF5, CDC21, CGR1, CTF4, DAS2, DBP10, DBP3, DBP7, DCD1, DHR2, DIP2, DNA2, DUT1, EFG1, ELP6, ESF1, FEN1, FUN12, HIR1, ILS1, IMP4, KLMA_20616, KRI1, LCP5, MAK5, MEF2, MRT4, NOC3, NOP1, NOP15, NOP2, NOP4, NOP56, NOP7, NSA1, NSA2, NSR1, PDS5, POL1, POL12, PUS4, PXR1, RBA50, REX4, RFA1, RLF2, RLI1, RNR1, RPA34, RPC25, RPC37, RPF2, RRP14, RRP4, RRP42, RRP45, RRP5, SAS10, SKI6, SPB1, SPT6, TIF6, TRM82, TSR2, URK1, UTP15, UTP25
GO:0009262	deoxyribonucleotide metabolic process	8	4	0.29	9.8e-05	CDC21, DCD1, DUT1, RNR1
GO:0009263	deoxyribonucleotide biosynthetic process	8	4	0.29	9.8e-05	CDC21, DCD1, DUT1, RNR1
GO:1901360	organic cyclic compound metabolic process	1454	73	52.07	0.00012	BMS1, BUD23, BUD31, CAC2, CAM1, CBF5, CDC21, CGR1, CTF4, DAS2, DBP10, DBP3, DBP7, DCD1, DHR2, DIP2, DNA2, DUT1, EFG1, ELP6, ESF1, FEN1, FUN12, HIR1, ILS1, IMP4, KLMA_20616, KRI1, LCP5, MAK5, MEF2, MRT4, NCP1, NOC3, NOP1, NOP15, NOP2, NOP4, NOP56, NOP7, NSA1, NSA2, NSR1, PDS5, POL1, POL12, PUS4, PXR1, RBA50, REX4, RFA1, RLF2, RLI1, RNR1, RPA34, RPC25, RPC37, RPF2, RRP14, RRP4, RRP42, RRP45, RRP5, SAS10, SKI6, SPB1, SPT6, TIF6, TRM82, TSR2, URK1, UTP15, UTP25
GO:0009219	pyrimidine deoxyribonucleotide metabolic process	4	3	0.14	0.00017	CDC21, DCD1, DUT1
GO:0009221	pyrimidine deoxyribonucleotide biosynthetic process	4	3	0.14	0.00017	CDC21, DCD1, DUT1
GO:0009265	2'-deoxyribonucleotide biosynthetic process	4	3	0.14	0.00017	CDC21, DCD1, DUT1
GO:0009394	2'-deoxyribonucleotide metabolic process	4	3	0.14	0.00017	CDC21, DCD1, DUT1
GO:0019692	deoxyribose phosphate metabolic process	4	3	0.14	0.00017	CDC21, DCD1, DUT1
GO:0046385	deoxyribose phosphate biosynthetic process	4	3	0.14	0.00017	CDC21, DCD1, DUT1
GO:0090305	nucleic acid phosphodiester bond hydrolysis	101	12	3.62	0.00021	BUD23, DIP2, DNA2, FEN1, KRI1, REX4, RRP4, RRP42, RRP45, RRP5, SAS10, SKI6
GO:0070925	organelle assembly	60	9	2.15	0.00023	BMS1, BRX1, MRT4, NOC2, NSR1, RPF2, SDO1, SSF1, TIF6
GO:0006220	pyrimidine nucleotide metabolic process	17	5	0.61	0.00024	CDC21, DAS2, DCD1, DUT1, URK1
GO:0006221	pyrimidine nucleotide biosynthetic process	17	5	0.61	0.00024	CDC21, DAS2, DCD1, DUT1, URK1
GO:0006807	nitrogen compound metabolic process	1621	78	58.05	0.00025	ARG1, ASP1, BMS1, BUD23, BUD31, CAC2, CAM1, CBF5, CDC21, CGR1, CTF4, CYS3, DAS2, DBP10, DBP3,

GO.ID	Term	Annotated gene[a]	Significant[b]	Expected[c]	P-value[d]	Genes
						DBP7, DCD1, DHR2, DIP2, DNA2, DUT1, EFG1, ELP6, ESF1, FEN1, FUN12, HIR1, ILS1, IMP4, KLMA_20616, KRI1, LCP5, LYS21, MAK5, MEF2, MRT4, NIT3, NOC3, NOP1, NOP15, NOP2, NOP4, NOP56, NOP7, NSA1, NSA2, NSR1, PDS5, POL1, POL12, PSD1, PUS4, PXR1, RBA50, REX4, RFA1, RLF2, RLI1, RNR1, RPA34, RPC25, RPC37, RPF2, RRP14, RRP4, RRP42, RRP45, RRP5, SAS10, SKI6, SPB1, SPT6, TIF6, TRM82, TSR2, URK1, UTP15, UTP25
GO:0071042	nuclear polyadenylation-dependent mRNA catabolic process	12	4	0.43	0.00062	RRP4, RRP42, RRP45, SKI6
GO:0071047	polyadenylation-dependent mRNA catabolic process	12	4	0.43	0.00062	RRP4, RRP42, RRP45, SKI6
GO:0009148	pyrimidine nucleoside triphosphate biosynthetic process	6	3	0.21	0.00083	CDC21, DAS2, URK1
GO:0016078	tRNA catabolic process	13	4	0.47	0.00087	RRP4, RRP42, RRP45, SKI6
GO:0070651	nonfunctional rRNA decay	13	4	0.47	0.00087	RRP4, RRP42, RRP45, SKI6
GO:0071038	nuclear polyadenylation-dependent tRNA catabolic process	13	4	0.47	0.00087	RRP4, RRP42, RRP45, SKI6
GO:0071051	polyadenylation-dependent snoRNA 3'-end processing	13	4	0.47	0.00087	RRP4, RRP42, RRP45, SKI6
GO:0010467	gene expression	1331	65	47.67	0.00106	ATP25, BMS1, BUD23, BUD31, CAM1, CBF5, CGR1, CIC1, DBP10, DBP3, DBP7, DHR2, DIP2, EFG1, ELP6, ESF1, FUN12, HIR1, ILS1, IMP4, KRI1, LCP5, MAK5, MEF2, MRPL35, MRT4, NMA111, NOC3, NOP1, NOP15, NOP2, NOP4, NOP56, NOP7, NSA1, NSA2, NSR1, PUS4, PXR1, RBA50, REX4, RLI1, RPA34, RPC25, RPC37, RPF2, RPL28, RPL8B, RRP14, RRP4, RRP42, RRP45, RRP5, RSM22, SAS10, SKI6, SPB1, SPT6, SSM4, TAE1, TIF6, TRM82, TSR2, UTP15, UTP25
GO:0000447	endonucleolytic cleavage in ITS1 to separate SSU-rRNA from 5.8S rRNA and LSU-rRNA from tricistronic rRNA transcript (SSU-rRNA, 5.8S rRNA, LSU-rRNA)	23	5	0.82	0.00109	BUD23, DIP2, KRI1, RRP5, SAS10
GO:0000478	endonucleolytic cleavage involved in rRNA processing	23	5	0.82	0.00109	BUD23, DIP2, KRI1, RRP5, SAS10
GO:0000479	endonucleolytic cleavage of tricistronic rRNA transcript (SSU-rRNA, 5.8S rRNA, LSU-rRNA)	23	5	0.82	0.00109	BUD23, DIP2, KRI1, RRP5, SAS10
GO:0043633	polyadenylation-dependent RNA catabolic process	14	4	0.5	0.00119	RRP4, RRP42, RRP45, SKI6
GO:0043634	polyadenylation-dependent ncRNA catabolic process	14	4	0.5	0.00119	RRP4, RRP42, RRP45, SKI6
GO:0070481	nuclear-transcribed mRNA catabolic process, non-stop	14	4	0.5	0.00119	RRP4, RRP42, RRP45, SKI6

GO.ID	Term	Annotated gene[a]	Significant[b]	Expected[c]	P-value[d]	Genes
	decay					
GO:0071029	nuclear ncRNA surveillance	14	4	0.5	0.00119	RRP4, RRP42, RRP45, SKI6
GO:0071046	nuclear polyadenylation-dependent ncRNA catabolic process	14	4	0.5	0.00119	RRP4, RRP42, RRP45, SKI6
GO:0006226	dUMP biosynthetic process	2	2	0.07	0.00127	DCD1, DUT1
GO:0006231	dTMP biosynthetic process	2	2	0.07	0.00127	CDC21, DCD1
GO:0044211	CTP salvage	2	2	0.07	0.00127	DAS2, URK1
GO:0046073	dTMP metabolic process	2	2	0.07	0.00127	CDC21, DCD1
GO:0046078	dUMP metabolic process	2	2	0.07	0.00127	DCD1, DUT1
GO:0090502	RNA phosphodiester bond hydrolysis, endonucleolytic	24	5	0.86	0.00134	BUD23, DIP2, KRI1, RRP5, SAS10
GO:0000459	exonucleolytic trimming involved in rRNA processing	15	4	0.54	0.00158	RRP4, RRP42, RRP45, SKI6
GO:0000467	exonucleolytic trimming to generate mature 3'-end of 5.8S rRNA from tricistronic rRNA transcript (SSU-rRNA, 5.8S rRNA, LSU-rRNA)	15	4	0.54	0.00158	RRP4, RRP42, RRP45, SKI6
GO:0006273	lagging strand elongation	15	4	0.54	0.00158	DNA2, FEN1, POL1, POL12
GO:0031125	rRNA 3'-end processing	15	4	0.54	0.00158	RRP4, RRP42, RRP45, SKI6
GO:0090503	RNA phosphodiester bond hydrolysis, exonucleolytic	15	4	0.54	0.00158	RRP4, RRP42, RRP45, SKI6
GO:0022618	ribonucleoprotein complex assembly	79	9	2.83	0.00180	BMS1, BRX1, MRT4, NOC2, NSR1, RPF2, SDO1, SSF1, TIF6
GO:0072528	pyrimidine-containing compound biosynthetic process	26	5	0.93	0.00196	CDC21, DAS2, DCD1, DUT1, URK1
GO:0034427	nuclear-transcribed mRNA catabolic process, exonucleolytic, 3'-5'	16	4	0.57	0.00204	RRP4, RRP42, RRP45, SKI6
GO:0043928	exonucleolytic nuclear-transcribed mRNA catabolic process involved in deadenylation-dependent decay	16	4	0.57	0.00204	RRP4, RRP42, RRP45, SKI6
GO:0070478	nuclear-transcribed mRNA catabolic process, 3'-5' exonucleolytic nonsense-mediated decay	16	4	0.57	0.00204	RRP4, RRP42, RRP45, SKI6
GO:0071826	ribonucleoprotein complex subunit organization	82	9	2.94	0.00235	BMS1, BRX1, MRT4, NOC2, NSR1, RPF2, SDO1, SSF1, TIF6
GO:0009451	RNA modification	53	7	1.9	0.00251	BUD23, CBF5, ELP6, LCP5, NOP56, PUS4, SPB1
GO:0000291	nuclear-transcribed mRNA catabolic process, exonucleolytic	17	4	0.61	0.00260	RRP4, RRP42, RRP45, SKI6
GO:0034475	U4 snRNA 3'-end processing	9	3	0.32	0.00322	RRP4, RRP45, SKI6
GO:0006335	DNA replication-dependent nucleosome assembly	3	2	0.11	0.00373	CAC2, RLF2
GO:0009211	pyrimidine deoxyribonucleoside triphosphate metabolic process	3	2	0.11	0.00373	CDC21, DUT1
GO:0034723	DNA replication-dependent nucleosome organization	3	2	0.11	0.00373	CAC2, RLF2
GO:0000027	ribosomal large subunit assembly	19	4	0.68	0.00401	BRX1, MRT4, RPF2, SSF1

GO.ID	Term	Annotated gene[a]	Significant[b]	Expected[c]	P-value[d]	Genes
GO:0016075	rRNA catabolic process	19	4	0.68	0.00401	RRP4, RRP42, RRP45, SKI6
GO:0072527	pyrimidine-containing compound metabolic process	31	5	1.11	0.00438	CDC21, DAS2, DCD1, DUT1, URK1
GO:0000154	rRNA modification	10	3	0.36	0.00448	BUD23, LCP5, NOP56
GO:0071025	RNA surveillance	20	4	0.72	0.00487	RRP4, RRP42, RRP45, SKI6
GO:0071027	nuclear RNA surveillance	20	4	0.72	0.00487	RRP4, RRP42, RRP45, SKI6
GO:0034661	ncRNA catabolic process	21	4	0.75	0.00585	RRP4, RRP42, RRP45, SKI6
GO:0000463	maturation of LSU-rRNA from tricistronic rRNA transcript (SSU-rRNA, 5.8S rRNA, LSU-rRNA)	11	3	0.39	0.00600	RPF2, RRP5, TIF6
GO:0031126	snoRNA 3'-end processing	22	4	0.79	0.00696	RRP4, RRP42, RRP45, SKI6
GO:0006241	CTP biosynthetic process	4	2	0.14	0.00728	DAS2, URK1
GO:0009208	pyrimidine ribonucleoside triphosphate metabolic process	4	2	0.14	0.00728	DAS2, URK1
GO:0009209	pyrimidine ribonucleoside triphosphate biosynthetic process	4	2	0.14	0.00728	DAS2, URK1
GO:0010138	pyrimidine ribonucleotide salvage	4	2	0.14	0.00728	DAS2, URK1
GO:0032262	pyrimidine nucleotide salvage	4	2	0.14	0.00728	DAS2, URK1
GO:0034473	U1 snRNA 3'-end processing	4	2	0.14	0.00728	RRP45, SKI6
GO:0042256	mature ribosome assembly	4	2	0.14	0.00728	SDO1, TIF6
GO:0044206	UMP salvage	4	2	0.14	0.00728	DAS2, URK1
GO:0046036	CTP metabolic process	4	2	0.14	0.00728	DAS2, URK1
GO:0000054	ribosomal subunit export from nucleus	35	5	1.25	0.00746	BUD23, NMD3, NOC2, RLI1, TIF6
GO:0000288	nuclear-transcribed mRNA catabolic process, deadenylation-dependent decay	35	5	1.25	0.00746	KLMA_20616, RRP4, RRP42, RRP45, SKI6
GO:0033750	ribosome localization	35	5	1.25	0.00746	BUD23, NMD3, NOC2, RLI1, TIF6
GO:0033753	establishment of ribosome localization	35	5	1.25	0.00746	BUD23, NMD3, NOC2, RLI1, TIF6
GO:0071166	ribonucleoprotein complex localization	35	5	1.25	0.00746	BUD23, NMD3, NOC2, RLI1, TIF6
GO:0071426	ribonucleoprotein complex export from nucleus	35	5	1.25	0.00746	BUD23, NMD3, NOC2, RLI1, TIF6
GO:0071428	rRNA-containing ribonucleoprotein complex export from nucleus	35	5	1.25	0.00746	BUD23, NMD3, NOC2, RLI1, TIF6
GO:0000470	maturation of LSU-rRNA	12	3	0.43	0.00779	RPF2, RRP5, TIF6
GO:0034472	snRNA 3'-end processing	12	3	0.43	0.00779	RRP4, RRP45, SKI6
GO:0000184	nuclear-transcribed mRNA catabolic process, nonsense-mediated decay	23	4	0.82	0.00819	RRP4, RRP42, RRP45, SKI6
GO:0043170	macromolecule metabolic process	1877	81	67.22	0.00854	ATP25, BMS1, BUD23, BUD31, CAC2, CAM1, CBF5, CGR1, CIC1, CTF4, DBP10, DBP3, DBP7, DHR2, DIP2, DNA2, DPH2, EFG1, ELP6, ESF1, FAS2, FEN1, FUN12, HIR1, HPM1, ILS1, IMP4, KLMA_20616, KRI1, LCP5, MAK5, MEF2, MRPL35, MRT4, NMA111, NOC3, NOP1, NOP15, NOP2, NOP4, NOP56, NOP7, NSA1, NSA2, NSR1, PDS5, PGU1, POL1, POL12, PTP2, PUS4, PXR1, RBA50, REX4, RFA1, RLF2,

GO.ID	Term	Annotated gene[a]	Significant[b]	Expected[c]	P-value[d]	Genes
						RLI1, RNR1, RPA34, RPC25, RPC37, RPF2, RPL28, RPL8B, RRP14, RRP4, RRP42, RRP45, RRP5, RSM22, SAS10, SKI6, SPB1, SPT6, SSM4, TAE1, TIF6, TRM82, TSR2, UTP15, UTP25
GO:0016180	snRNA processing	13	3	0.47	0.00986	RRP4, RRP45, SKI6

[a]The number of GO term annotated genes in the *K. marxianus* genome.
[b]The number of GO term annotated genes, which were significantly (FDR < 0.05) expressed under the condition.
[c]The expected value of Fisher's exact test.
[d]The P-value of Fisher's exact test.

Table S10 Summary of significantly up-regulated genes under the 30DS condition

Locus_tag	logFC	logCPM	FDR	Product	UniProt gene	KO number	Localization	Specific[a]
KLMA_80413	18.7	9.5	0.000	60S ribosomal protein L8-B	RPL8B	K02936	Cytoplasm.	C
KLMA_10180	17.4	7.3	0.006	argininosuccinate synthase	ARG1	K01940	Cytoplasm.	30X
KLMA_10496	16.4	5.9	0.000	rRNA-processing protein EFG1	EFG1		Nucleus, nucleolus (By similarity).	S
KLMA_70354	15.9	6.2	0.002	ADP,ATP carrier protein	AAC	K05863	Mitochondrion inner membrane; Multi-pass membrane protein.	45D
KLMA_30371	15.5	5.8	0.030	calcium/calmodulin-dependent protein kinase II	CMK2	K00908		45D
KLMA_80051	15.3	4.8	0.002	phosphoglucomutase YMR278W	PGM3	K01835	Cytoplasm. Nucleus.	S
KLMA_10353	14.4	3.9	0.000	mitochondrial import inner membrane translocase subunit TIM17	TIM17		Mitochondrion inner membrane; Multi-pass membrane protein.	S
KLMA_10516	14.4	4.0	0.000	polygalacturonase	PGU1	K01184		C
KLMA_60474	14.2	4.5	0.001	putative methyltransferase BUD23	BUD23		Cytoplasm. Nucleus.	C
KLMA_10225	14.1	5.3	0.000	GTP-binding nuclear protein GSP1/Ran	GSP1	K07936	Nucleus (By similarity).	30X
KLMA_50396	14.0	3.6	0.005	uncharacterized mitochondrial carrier YIL006W	YIA6	K15115	Mitochondrion inner membrane; Multi-pass membrane protein.	S
KLMA_50089	13.7	3.3	0.014	methyltransferase-like protein YBR261C	TAE1		Cytoplasm.	S
KLMA_40373	13.5	7.0	0.006	hypothetical protein	OM45		Mitochondrion outer membrane.	30X
KLMA_20354	13.4	2.9	0.023	cystathionine gamma-lyase	CYS3	K01758	Cytoplasm.	S
KLMA_20381	13.4	2.9	0.019	hypothetical protein	OSW5		Membrane; Multi-pass membrane protein (By similarity).	S
KLMA_10783	13.1	7.0	0.005	sorbose reductase SOU1	SOU1			C
KLMA_60493	13.1	3.8	0.026	homocitrate synthase	LYS21	K01655	Mitochondrion (Potential).	C
KLMA_10267	13.1	5.2	0.000	SAP super family	AIM34		Mitochondrion membrane; Single-pass membrane protein (By similarity).	30X

Locus_tag	logFC	logCPM	FDR	Product	UniProt gene	KO number	Localization	Specific[a]
KLMA_50281	13.1	2.6	0.017	mitochondrial inner membrane protein COX18	COX18		Mitochondrion inner membrane; Multi-pass membrane protein.	S
KLMA_30641	13.0	6.2	0.013	probable hydrolase NIT3	NIT3			C
KLMA_70421	12.9	2.4	0.047	DNA-directed RNA polymerase III subunit RPC8	RPC25	K03022	Nucleus.	S
KLMA_40101	12.8	2.4	0.002	protein RMD11	NPR3			S
KLMA_50217	12.7	2.2	0.008	serine hydrolase YJU3	YJU3		Cytoplasm. Endoplasmic reticulum. Lipid droplet. Mitochondrion outer membrane.	S
KLMA_30482	12.7	7.9	0.000	glyoxalase super family protein				30X
KLMA_40309	12.5	2.0	0.011	endoplasmic reticulum transmembrane protein 1	YET1		Endoplasmic reticulum membrane; Multi-pass membrane protein.	S
KLMA_20616	11.9	4.4	0.019	uncharacterized protein YDR370C			Cytoplasm.	45D
KLMA_10226	11.9	1.4	0.022	hypothetical protein				S
KLMA_R308	11.7	8.6	0.005	Lys-tRNA				45D
KLMA_30499	11.6	1.1	0.027	bud site selection protein 31	BUD31	K12873	Nucleus (Potential).	S
KLMA_20496	11.5	2.5	0.013	hypothetical protein		K11098		C
KLMA_80158	11.5	1.0	0.027	mitotic exit network interactor 1	HPM1		Cytoplasm. Nucleus.	S
KLMA_30167	11.4	2.1	0.001	hypothetical protein				C
KLMA_20730	11.3	0.8	0.042	hypothetical protein				S
KLMA_40347	11.1	1.4	0.032	protein SSM4	SSM4		Endoplasmic reticulum membrane; Multi-pass membrane protein. Nucleus inner membrane; Multi-pass membrane protein.	S
KLMA_10682	11.0	0.5	0.041	thioredoxin reductase	TRR1	K00384	Mitochondrion (Potential).	S
KLMA_R416	10.6	4.5	0.000	Val-tRNA				C
KLMA_R519	10.5	7.2	0.013	Gly-tRNA				45D
KLMA_80091	10.3	5.9	0.011	exosome complex component RRP42	RRP42	K12589	Cytoplasm. Nucleus, nucleolus.	45D
KLMA_20617	10.1	0.9	0.007	SAM50-like protein SpAC17C9.06				30X
KLMA_R127	10.0	4.9	0.010	Val-tRNA				C
KLMA_R322	9.8	4.0	0.027	Gln-tRNA				C
KLMA_60403	9.7	6.1	0.001	putative elongation factor 1 gamma homolog	CAM1	K03233	Cytoplasm. Nucleus.	C
KLMA_R608	8.9	1.7	0.015	Met-tRNA				45D
KLMA_R602	8.5	2.8	0.017	Ala-tRNA				C
KLMA_30511	8.0	4.1	0.002	ATP-dependent RNA helicase DBP3	DBP3	K14811	Nucleus, nucleolus (By similarity).	30X
KLMA_70304	7.8	6.3	0.000	transcription elongation factor SPT6	SPT6	K11292	Nucleus (By similarity).	C
KLMA_60031	7.7	2.5	0.026	tRNA (adenine-N(1)-)-methyltransferase catalytic subunit TRM61	TRM61	K07442	Nucleus (By similarity).	S
KLMA_10038	7.7	2.8	0.006	RNA polymerase II-associated protein RBA50	RBA50		Cytoplasm.	S

Locus_tag	logFC	logCPM	FDR	Product	UniProt gene	KO number	Localization	Specific[a]
KLMA_70323	7.5	6.8	0.026	uncharacterized protein YOL036W				S
KLMA_20051	7.2	4.3	0.000	rRNA-processing protein CGR1	CGR1	K14822	Nucleus, nucleolus (By similarity).	C
KLMA_50459	6.7	2.2	0.042	deoxyuridine 5'-triphosphate nucleotidohydrolase	DUT1	K01520		S
KLMA_30139	6.7	5.9	0.027	tRNA (cytosine-5-)-methyltransferase NCL1	NCL1	K15334	Nucleus, nucleolus.	S
KLMA_50586	6.7	3.8	0.031	serine/threonine-protein phosphatase 4 regulatory subunit 3	PSY2		Nucleus (By similarity).	S
KLMA_70414	6.6	8.3	0.007	ribosome biogenesis protein NSA2	NSA2	K14842	Nucleus, nucleolus (By similarity).	S
KLMA_20626	6.4	2.9	0.002	mitochondrial DnaJ homolog 2	MDJ2		Mitochondrion inner membrane.	C
KLMA_60025	6.3	5.0	0.004	ribosome biogenesis protein ALB1	ALB1	K14814	Cytoplasm (By similarity). Nucleus (By similarity).	S
KLMA_60179	6.3	4.5	0.001	probable ATP-dependent RNA helicase DHR2	DHR2	K14781	Nucleus, nucleolus.	45D
KLMA_70346	6.2	3.1	0.010	DNA polymerase alpha subunit B	POL12	K02321	Nucleus.	30X
KLMA_30593	6.2	5.1	0.001	spindle pole component SPC72				S
KLMA_60204	6.2	7.2	0.000	ribosomal RNA-processing protein 8	RRP8	K14850	Nucleus, nucleolus. Chromosome, telomere (Potential).	30X
KLMA_80272	6.1	2.1	0.023	pumilio homology domain family member 6	PUF6	K14844	Bud tip. Nucleus, nucleolus.	S
KLMA_40391	6.1	6.9	0.000	malate dehydrogenase	MDH2	K00026	Cytoplasm.	C
KLMA_70395	6.1	4.5	0.000	tRNA pseudouridine synthase 4	PUS4	K03177	Nucleus. Mitochondrion.	C
KLMA_70273	6.0	3.9	0.022	WD repeat-containing protein JIP5	JIP5		Nucleus, nucleolus (By similarity).	S
KLMA_60172	6.0	7.2	0.000	ribosomal RNA-processing protein 14	RRP14		Nucleus, nucleolus.	30X
KLMA_60262	6.0	3.0	0.005	UPF0195 protein YHR122W				30X
KLMA_40375	5.9	4.3	0.004	U3 small nucleolar ribonucleoprotein protein IMP4	IMP4	K14561	Nucleus, nucleolus.	45D
KLMA_30060	5.8	5.2	0.003	mRNA turnover protein 4	MRT4	K14815	Nucleus, nucleolus.	S
KLMA_70415	5.7	8.2	0.000	U3 small nucleolar ribonucleoprotein protein LCP5	LCP5	K14765	Nucleus, nucleolus.	45D
KLMA_30567	5.7	2.8	0.005	uncharacterized protein YMR098C	ATP25		Mitochondrion inner membrane; Peripheral membrane protein; Matrix side (By similarity).	45D
KLMA_10595	5.7	6.6	0.017	eukaryotic translation initiation factor 6	TIF6	K03264	Cytoplasm. Nucleus, nucleolus.	S
KLMA_70374	5.7	4.5	0.018	tRNA (guanine-N(1)-)-methyltransferase	TRM5	K15429	Mitochondrion matrix. Nucleus. Cytoplasm.	S
KLMA_50152	5.5	2.5	0.025	protein HIR1	HIR1	K11293	Nucleus (By similarity).	S
KLMA_80380	5.5	5.3	0.000	importin subunit beta-4	KAP123		Cytoplasm. Nucleus. Nucleus, nuclear pore	S

Locus_tag	logFC	logCPM	FDR	Product	UniProt gene	KO number	Localization	Specific[a]
							complex.	
KLMA_20725	5.4	5.6	0.007	NADPH--cytochrome P450 reductase	NCP1	K00327	Endoplasmic reticulum membrane; Single-pass membrane protein. Mitochondrion outer membrane; Single-pass membrane protein. Cell membrane; Single-pass membrane protein. Microsome.	45D
KLMA_70219	5.4	6.9	0.011	fatty acid synthase subunit alpha	FAS2	K00667		S
KLMA_20345	5.2	9.4	0.008	protein FUN14				30X
KLMA_80369	5.2	6.4	0.032	isoleucyl-tRNA synthetase	ILS1	K01870	Cytoplasm.	S
KLMA_50229	5.2	5.6	0.039	putative uridine kinase YDR020C	DAS2		Cytoplasm. Nucleus.	45D
KLMA_10031	5.0	4.2	0.001	adoMet-dependent rRNA methyltransferase SPB1	SPB1	K14857	Nucleus, nucleolus (By similarity).	45D
KLMA_30382	5.0	7.7	0.000	nuclear localization sequence-binding protein	NSR1	K11294	Nucleus. Nucleus, nucleolus (Potential).	S
KLMA_80194	5.0	3.2	0.039	protein PXR1	PXR1	K11135	Nucleus, nucleolus (By similarity).	S
KLMA_20128	4.9	8.1	0.032	ribosome assembly protein 3	RSA3	K14854	Nucleus, nucleolus (By similarity).	S
KLMA_10418	4.8	5.2	0.001	ribosome biogenesis protein RPF2	RPF2	K14847	Nucleus, nucleolus.	45D
KLMA_50291	4.8	2.8	0.018	rRNA biogenesis protein RRP5	RRP5	K14792	Nucleus, nucleolus.	45D
KLMA_70170	4.8	7.6	0.002	ribonucleoside-diphosphate reductase large chain 1	RNR1	K10807	Cytoplasm.	30X
KLMA_60324	4.8	3.7	0.019	sister chromatid cohesion protein PDS5	PDS5	K11267	Nucleus.	S
KLMA_60349	4.7	4.5	0.003	spindle pole body component SPC105	SPC105	K11563	Cytoplasm, cytoskeleton, spindle pole body. Nucleus membrane; Peripheral membrane protein; Nucleoplasmic side. Chromosome, centromere, kinetochore.	C
KLMA_80234	4.7	5.1	0.014	DNA polymerase alpha catalytic subunit A	POL1	K02320	Nucleus.	S
KLMA_50445	4.7	4.7	0.025	pescadillo homolog	NOP7	K14843	Nucleus, nucleolus (By similarity). Nucleus, nucleoplasm (By similarity).	S
KLMA_60396	4.6	5.8	0.001	nucleolar protein 4	NOP4	K14573	Nucleus, nucleolus.	S
KLMA_20139	4.5	5.0	0.037	ATP-dependent RNA helicase DBP7	DBP7	K14806	Nucleus, nucleolus (By similarity).	S
KLMA_30565	4.4	4.4	0.004	structure-specific endonuclease RAD27	FEN1	K04799	Nucleus, nucleolus (By similarity). Nucleus, nucleoplasm (By similarity). Mitochondrion (By similarity).	S
KLMA_70291	4.4	2.5	0.018	DNA polymerase alpha-binding protein	CTF4	K11274	Nucleus.	S
KLMA_70238	4.4	7.5	0.002	something about	SAS10	K14767	Nucleus, nucleolus.	S

Locus_tag	logFC	logCPM	FDR	Product	UniProt gene	KO number	Localization	Specific[a]
				silencing protein 10				
KLMA_60250	4.4	4.8	0.048	pro-apoptotic serine protease NMA111	NMA111		Nucleus (By similarity).	S
KLMA_20683	4.3	4.1	0.007	nucleolar complex-associated protein 3	NOC3	K14834	Nucleus, nucleolus.	S
KLMA_50072	4.3	4.1	0.050	pre-60S factor REI1	REI1	K14816	Cytoplasm.	S
KLMA_20233	4.3	5.4	0.009	hypothetical protein	NSA1	K14841	Nucleus, nucleolus (By similarity).	S
KLMA_10597	4.2	2.5	0.026	chromatin assembly factor 1 subunit p90	RLF2		Nucleus.	S
KLMA_50045	4.2	7.2	0.002	nucleolar complex protein 2	NOC2	K14833	Nucleus, nucleolus.	S
KLMA_50181	4.2	6.5	0.005	pre-rRNA-processing protein TSR2	TSR2	K14800	Cytoplasm. Nucleus.	S
KLMA_40173	4.2	10.7	0.000	peroxiredoxin type-2	AHP1	K14171	Cytoplasm.	30X
KLMA_50201	4.1	4.8	0.026	ribonucleases P/MRP protein subunit POP6		K14524		C
KLMA_40397	4.1	7.5	0.004	protein KRI1	KRI1	K14786	Nucleus, nucleolus.	S
KLMA_30592	4.0	5.2	0.036	eukaryotic translation initiation factor 3 subunit B	PRT1	K03253	Cytoplasm (By similarity).	S
KLMA_10634	4.0	5.4	0.010	diphthamide biosynthesis protein 2	DPH2		Cytoplasm (By similarity).	S
KLMA_40544	4.0	4.6	0.006	ATP-dependent RNA helicase MRH4	MRH4		Mitochondrion (By similarity).	S
KLMA_50458	3.9	6.8	0.006	uncharacterized protein YGR111W				45D
KLMA_20136	3.9	3.6	0.017	ribosome-releasing factor 2	MEF2	K02355	Mitochondrion (By similarity).	S
KLMA_10082	3.9	5.1	0.007	protein PLM2	PLM2		Nucleus (Probable).	C
KLMA_80170	3.8	5.3	0.011	putative ribosomal RNA methyltransferase Nop2	NOP2	K14835	Nucleus, nucleolus.	S
KLMA_60277	3.8	5.2	0.008	ATP-dependent RNA helicase DBP10	DBP10	K14808	Nucleus, nucleolus (By similarity).	45D
KLMA_20751	3.7	5.5	0.013	phosphatidylserine decarboxylase proenzyme 1	PSD1	K01613	Mitochondrion inner membrane.	45D
KLMA_10282	3.7	3.3	0.041	pre-rRNA-processing protein PNO1	PNO1	K11884	Cytoplasm. Nucleus, nucleolus (By similarity).	S
KLMA_60232	3.7	9.4	0.004	ribosome biogenesis protein 15	NOP15	K14838	Cytoplasm. Nucleus, nucleolus.	S
KLMA_10451	3.7	7.0	0.010	replication factor A protein 1	RFA1	K07466	Nucleus.	S
KLMA_10328	3.6	5.7	0.020	DNA replication ATP-dependent helicase DNA2	DNA2	K10742	Nucleus. Chromosome.	45D
KLMA_30223	3.6	5.6	0.014	phosphatase PSR1	PSR1	K15731	Cell membrane.	S
KLMA_30301	3.6	5.0	0.010	translation initiation factor RLI1	RLI1	K06174	Cytoplasm. Nucleus.	S
KLMA_10509	3.6	6.5	0.031	elongator complex protein 6	ELP6	K11377	Cytoplasm. Nucleus.	S
KLMA_10414	3.6	3.8	0.032	thymidylate synthase	CDC21	K00560	Nucleus.	45D
KLMA_10361	3.6	8.9	0.005	DNA-directed RNA polymerase I subunit RPA34	RPA34	K03003	Nucleus, nucleolus.	S
KLMA_30400	3.6	5.6	0.014	exosome complex component RRP45	RRP45	K03678	Cytoplasm. Nucleus, nucleolus.	S
KLMA_30432	3.5	5.9	0.012	protein BFR2	BFR2	K14782	Nucleus, nucleolus (By similarity).	S
KLMA_50363	3.5	5.9	0.015	low-affinity glucose	RAG1	K08139	Membrane; Multi-pass	S

Locus_tag	logFC	logCPM	FDR	Product	UniProt gene	KO number	Localization	Specific[a]
				transporter			membrane protein.	
KLMA_20092	3.5	4.0	0.048	37S ribosomal protein S22	RSM22		Mitochondrion.	S
KLMA_20752	3.5	6.5	0.037	deoxycytidylate deaminase	DCD1	K01493		45D
KLMA_60210	3.5	6.4	0.019	eukaryotic translation initiation factor 5B	FUN12	K03243		S
KLMA_20478	3.5	5.8	0.026	centromere/microtubule-binding protein CBF5	CBF5	K11131	Nucleus, nucleolus (By similarity). Chromosome, centromere (By similarity). Cytoplasm, cytoskeleton (By similarity).	S
KLMA_40079	3.4	10.7	0.000	uncharacterized endoplamic reticulum membrane				30X
KLMA_50520	3.4	5.5	0.039	tRNA (guanine-N(7)-)-methyltransferase subunit TRM82	TRM82	K15443	Nucleus (By similarity).	S
KLMA_30219	3.4	5.5	0.033	ribosome maturation protein SDO1	SDO1	K14574	Cytoplasm. Nucleus.	S
KLMA_30229	3.4	4.3	0.026	ATP-dependent RNA helicase DRS1	DRS1	K13181	Nucleus, nucleolus (By similarity).	S
KLMA_70394	3.4	3.6	0.036	paxillin-like protein 1	PXL1			S
KLMA_40555	3.4	5.2	0.020	ribosome biogenesis protein BMS1	BMS1	K14569	Cytoplasm. Nucleus, nucleolus.	S
KLMA_30549	3.4	3.7	0.041	ribosome biogenesis protein SSF2	SSF1	K14859	Nucleus, nucleolus.	S
KLMA_40251	3.3	5.5	0.019	proteasome-interacting protein CIC1	CIC1	K14783	Nucleus, nucleolus.	S
KLMA_20688	3.3	5.1	0.026	exosome complex component SKI6	SKI6	K11600	Cytoplasm. Nucleus, nucleolus.	S
KLMA_40432	3.3	5.1	0.028	60S ribosomal export protein NMD3	NMD3	K07562	Cytoplasm. Nucleus, nucleoplasm.	45D
KLMA_20327	3.3	3.7	0.047	uncharacterized protein YOR305W	RRG7		Mitochondrion (By similarity).	S
KLMA_30393	3.3	5.0	0.027	ATP-dependent RNA helicase MAK5	MAK5	K14805	Nucleus, nucleolus (By similarity).	S
KLMA_80399	3.3	6.6	0.027	pre-rRNA-processing protein ESF1	ESF1		Nucleus, nucleolus.	S
KLMA_60140	3.2	5.8	0.028	RNA exonuclease 4	REX4	K01175	Nucleus (By similarity).	S
KLMA_80126	3.2	8.1	0.017	uncharacterized protein YIL091C	UTP25	K14774	Nucleus, nucleolus (By similarity).	45D
KLMA_60136	3.2	4.3	0.046	ribosome biogenesis protein BRX1	BRX1	K14820	Nucleus, nucleolus.	45D
KLMA_50487	3.1	5.2	0.030	U3 small nucleolar RNA-associated protein 12	DIP2	K14556	Nucleus, nucleolus.	S
KLMA_50345	3.1	8.3	0.042	L-asparaginase 1	ASP1	K01424	Cytoplasm.	S
KLMA_40012	3.1	6.9	0.043	nucleolar GTP-binding protein 2	NOG2	K14537	Nucleus, nucleolus (By similarity).	S
KLMA_20147	3.0	4.6	0.049	U3 small nucleolar RNA-associated protein 15	UTP15	K14549	Nucleus, nucleolus.	S
KLMA_70373	3.0	7.0	0.039	exosome complex component RRP4	RRP4	K03679	Cytoplasm. Nucleus, nucleolus.	S
KLMA_10199	2.9	7.8	0.034	rRNA 2'-O-methyltransferase fibrillarin	NOP1	K14563	Nucleus, nucleolus (By similarity).	S
KLMA_20138	2.9	5.2	0.046	DNA-directed RNA	RPC37	K14721	Nucleus.	S

Locus_tag	logFC	logCPM	FDR	Product	UniProt gene	KO number	Localization	Specific[a]
				polymerase III subunit rpc5				
KLMA_60464	2.9	5.2	0.042	uridine kinase	URK1	K00876	Cytoplasm. Nucleus.	S
KLMA_20067	2.9	7.6	0.042	chromatin assembly factor 1 subunit p60	CAC2	K10751	Nucleus.	S
KLMA_50311	2.9	9.0	0.033	nucleolar protein 56	NOP56	K14564	Nucleus, nucleolus.	S
KLMA_20813	2.7	8.9	0.042	tyrosine-protein phosphatase 2	PTP2	K01104	Cytoplasm. Nucleus.	C
KLMA_50350	2.5	10.5	0.026	54S ribosomal protein L35	MRPL35		Mitochondrion.	S
KLMA_20403	2.4	12.5	0.003	ribosomal_L18e super family	RPL28	K02900	Cytoplasm (By similarity).	S

[a]Gene expression was significantly (FDR < 0.05) altered under the following conditions: S, 30DS-specific up-regulation; C, commonly up-regulated under 30DS, 45D and 30X conditions; 45D, up-regulated under 45D and 30DS conditions; 30X, up-regulated under 30X and 30DS conditions.

Table S11 GO terms enriched in significantly down-regulated genes under 30DS condition

GO.ID	Term	Annotated gene[a]	Significant[b]	Expected[c]	P-value[d]	Genes
GO:0030437	ascospore formation	50	9	1.38	6.2e-06	CPR1, DIT1, FKS3, FMP45, GLC7, KLMA_50101, OSW2, SPS19, UBI4
GO:0034293	sexual sporulation	51	9	1.4	7.4e-06	CPR1, DIT1, FKS3, FMP45, GLC7, KLMA_50101, OSW2, SPS19, UBI4
GO:0043935	sexual sporulation resulting in formation of a cellular spore	51	9	1.4	7.4e-06	CPR1, DIT1, FKS3, FMP45, GLC7, KLMA_50101, OSW2, SPS19, UBI4
GO:0048468	cell development	51	9	1.4	7.4e-06	CPR1, DIT1, FKS3, FMP45, GLC7, KLMA_50101, OSW2, SPS19, UBI4
GO:0022413	reproductive process in single-celled organism	75	10	2.07	3.0e-05	CPR1, DIT1, DPB11, FKS3, FMP45, GLC7, KLMA_50101, OSW2, SPS19, UBI4
GO:0003006	developmental process involved in reproduction	77	10	2.12	3.8e-05	CPR1, DIT1, DPB11, FKS3, FMP45, GLC7, KLMA_50101, OSW2, SPS19, UBI4
GO:0044702	single organism reproductive process	78	10	2.15	4.2e-05	CPR1, DIT1, DPB11, FKS3, FMP45, GLC7, KLMA_50101, OSW2, SPS19, UBI4
GO:0019953	sexual reproduction	107	11	2.95	0.00014	CPR1, DIT1, FAR1, FKS3, FMP45, GLC7, KLMA_50101, OSW2, RVS161, SPS19, UBI4
GO:0044703	multi-organism reproductive process	107	11	2.95	0.00014	CPR1, DIT1, FAR1, FKS3, FMP45, GLC7, KLMA_50101, OSW2, RVS161, SPS19, UBI4
GO:0022414	reproductive process	127	12	3.5	0.00015	CPR1, DIT1, DPB11, FAR1, FKS3, FMP45, GLC7, KLMA_50101, OSW2, RVS161, SPS19, UBI4
GO:0009081	branched-chain amino acid metabolic process	20	5	0.55	0.00016	ARO10, BAT1, ILV6, LEU4, MMF1
GO:0051704	multi-organism process	140	12	3.86	0.00038	CPR1, DIT1, FAR1, FKS3, FMP45, GLC7, KLMA_50101, MUC1, OSW2, RVS161, SPS19, UBI4
GO:0009082	branched-chain amino acid biosynthetic process	14	4	0.39	0.00044	BAT1, ILV6, LEU4, MMF1
GO:0016054	organic acid catabolic process	68	8	1.87	0.00047	ARO10, BAT1, BNA3, CIT3, KLMA_60382, PDH1, POT1, SPS19
GO:0046395	carboxylic acid catabolic process	68	8	1.87	0.00047	ARO10, BAT1, BNA3, CIT3, KLMA_60382, PDH1, POT1, SPS19
GO:0030435	sporulation resulting in	86	9	2.37	0.00050	CPR1, DIT1, FKS3, FMP45, GLC7,

GO.ID	Term	Annotated gene[a]	Significant[b]	Expected[c]	P-value[d]	Genes
	formation of a cellular spore					KLMA_50101, OSW2, SPS19, UBI4
GO:0048610	cellular process involved in reproduction	233	16	6.42	0.00051	CDC15, CPR1, DIT1, DPB11, FAR1, FKS3, FMP45, GAC1, GLC7, KLMA_50101, OSW2, REC8, RMI1, RVS161, SPS19, UBI4
GO:0008643	carbohydrate transport	26	5	0.72	0.00060	HGT1, LAC12, MTH1
GO:0043934	sporulation	89	9	2.45	0.00065	CPR1, DIT1, FKS3, FMP45, GLC7, KLMA_50101, OSW2, SPS19, UBI4
GO:0030154	cell differentiation	108	10	2.98	0.00066	CPR1, DIT1, DPB11, FKS3, FMP45, GLC7, KLMA_50101, OSW2, SPS19, UBI4
GO:0048646	anatomical structure formation involved in morphogenesis	90	9	2.48	0.00071	CPR1, DIT1, FKS3, FMP45, GLC7, KLMA_50101, OSW2, SPS19, UBI4
GO:0032505	reproduction of a single-celled organism	109	10	3	0.00071	CPR1, DIT1, DPB11, FKS3, FMP45, GLC7, KLMA_50101, OSW2, SPS19, UBI4
GO:0005975	carbohydrate metabolic process	247	16	6.8	0.00098	ARDH, CIT3, DLD1, DOG2, FKS3, GAC1, GAL1, GAP1, GLC7, INU1, KLMA_60382, MDH1, PCK1, RAG5, SIP4, SOR1
GO:0072329	monocarboxylic acid catabolic process	29	5	0.8	0.00101	CIT3, KLMA_60382, PDH1, POT1, SPS19
GO:0006551	leucine metabolic process	8	3	0.22	0.00103	ARO10, BAT1, LEU4
GO:0009097	isoleucine biosynthetic process	9	3	0.25	0.00151	BAT1, ILV6, MMF1
GO:0044262	cellular carbohydrate metabolic process	100	9	2.75	0.00151	ARDH, CIT3, DLD1, FKS3, GAC1, GLC7, KLMA_60382, MDH1, SIP4
GO:0000003	reproduction	265	16	7.3	0.00207	CDC15, CPR1, DIT1, DPB11, FAR1, FKS3, FMP45, GAC1, GLC7, KLMA_50101, OSW2, REC8, RMI1, RVS161, SPS19, UBI4
GO:0048869	cellular developmental process	126	10	3.47	0.00217	CPR1, DIT1, DPB11, FKS3, FMP45, GLC7, KLMA_50101, OSW2, SPS19, UBI4
GO:0019541	propionate metabolic process	3	2	0.08	0.00221	CIT3, PDH1
GO:0019543	propionate catabolic process	3	2	0.08	0.00221	CIT3, PDH1
GO:0019626	short-chain fatty acid catabolic process	3	2	0.08	0.00221	CIT3, PDH1
GO:0019629	propionate catabolic process, 2-methylcitrate cycle	3	2	0.08	0.00221	CIT3, PDH1
GO:0009062	fatty acid catabolic process	21	4	0.58	0.00226	CIT3, PDH1, POT1, SPS19
GO:0019752	carboxylic acid metabolic process	345	19	9.5	0.00226	ARO10, ARO3, ARO8, BAT1, BIO3, BIO4, BNA3, CIT3, ILV6, KLMA_60382, LEU4, LYS12, MDH1, MMF1, PDH1, PDX3, POT1, SPS19, STR3
GO:0009653	anatomical structure morphogenesis	106	9	2.92	0.00228	CPR1, DIT1, FKS3, FMP45, GLC7, KLMA_50101, OSW2, SPS19, UBI4
GO:0048856	anatomical structure development	107	9	2.95	0.00243	CPR1, DIT1, FKS3, FMP45, GLC7, KLMA_50101, OSW2, SPS19, UBI4
GO:0044282	small molecule catabolic process	89	8	2.45	0.00280	ARO10, BAT1, BNA3, CIT3, KLMA_60382, PDH1, POT1, SPS19
GO:0006549	isoleucine metabolic process	11	3	0.3	0.00285	BAT1, ILV6, MMF1
GO:0043436	oxoacid metabolic process	354	19	9.75	0.00305	ARO10, ARO3, ARO8, BAT1, BIO3, BIO4, BNA3, CIT3, ILV6, KLMA_60382, LEU4, LYS12, MDH1, MMF1, PDH1, PDX3, POT1, SPS19, STR3
GO:0032787	monocarboxylic acid metabolic process	111	9	3.06	0.00313	BIO3, BIO4, BNA3, CIT3, KLMA_60382, PDH1, PDX3, POT1, SPS19
GO:0006082	organic acid metabolic	356	19	9.81	0.00325	ARO10, ARO3, ARO8, BAT1, BIO3, BIO4,

GO.ID	Term	Annotated gene[a]	Significant[b]	Expected[c]	P-value[d]	Genes
	process					BNA3, CIT3, ILV6, KLMA_60382, LEU4, LYS12, MDH1, MMF1, PDH1, PDX3, POT1, SPS19, STR3
GO:0071265	L-methionine biosynthetic process	12	3	0.33	0.00372	ARO8, BAT1, STR3
GO:0019318	hexose metabolic process	74	7	2.04	0.00387	DOG2, GAL1, GAP1, PCK1, RAG5, SIP4, SOR1
GO:0000076	DNA replication checkpoint	4	2	0.11	0.00435	DPB11, GLC7
GO:0046459	short-chain fatty acid metabolic process	4	2	0.11	0.00435	CIT3, PDH1
GO:0006790	sulfur compound metabolic process	97	8	2.67	0.00479	ARO10, ARO8, BAT1, BIO3, BIO4, OPT1, PHO3, STR3
GO:0044283	small molecule biosynthetic process	263	15	7.25	0.00496	ARO10, ARO3, ARO8, BAT1, BIO3, BIO4, BNA3, ILV6, LEU4, LYS12, MMF1, PDX3, RIB3, STR3, UPC2
GO:0005996	monosaccharide metabolic process	81	7	2.23	0.00639	DOG2, GAL1, GAP1, PCK1, RAG5, SIP4, SOR1
GO:0044767	single-organism developmental process	171	11	4.71	0.00673	CPR1, DIT1, DPB11, FKS3, FMP45, GLC7, KLMA_50101, MDH1, OSW2, SPS19, UBI4
GO:0009099	valine biosynthetic process	5	2	0.14	0.00712	BAT1, ILV6
GO:0006091	generation of precursor metabolites and energy	149	10	4.1	0.00726	CIT3, COX5A, DLD1, FRE1, GAC1, GAP1, GLC7, MDH1, RAG5, RIB3
GO:0032502	developmental process	174	11	4.79	0.00765	CPR1, DIT1, DPB11, FKS3, FMP45, GLC7, KLMA_50101, MDH1, OSW2, SPS19, UBI4
GO:0007093	mitotic cell cycle checkpoint	30	4	0.83	0.00857	BAT1, DPB11, GAC1, GLC7
GO:1901988	negative regulation of cell cycle phase transition	30	4	0.83	0.00857	BAT1, DPB11, GAC1, GLC7
GO:1901991	negative regulation of mitotic cell cycle phase transition	30	4	0.83	0.00857	BAT1, DPB11, GAC1, GLC7
GO:0044723	single-organism carbohydrate metabolic process	202	12	5.56	0.00874	ARDH, DOG2, FKS3, GAC1, GAL1, GAP1, GLC7, KLMA_60382, PCK1, RAG5, SIP4, SOR1
GO:0006766	vitamin metabolic process	48	5	1.32	0.00961	BIO3, BIO4, PDX3, PHO3, RIB3
GO:0006767	water-soluble vitamin metabolic process	48	5	1.32	0.00961	BIO3, BIO4, PDX3, PHO3, RIB3

[a]The number of GO term annotated genes in the *K. marxianus* genome.

[b]The number of GO term annotated genes, which were significantly (FDR < 0.05) expressed under the condition.

[c]The expected value of Fisher's exact test.

[d]The P-value of Fisher's exact test.

Table S12 Summary of significantly down-regulated genes under the 30DS conditions

Locus_tag	logFC	logCPM	FDR	Product	UniProt gene	KO number	Localization	Specific[a]
KLMA_80303	-17.4	7.1	0.017	protein OPY2				S
KLMA_40392	-15.9	5.8	0.000	uncharacterized vacuolar membrane protein YNL305C	BXI1	K06890	Endoplasmic reticulum membrane; Multi-pass membrane protein. Vacuole membrane; Multi-pass membrane protein. Mitochondrion membrane; Multi-pass membrane	30X

Locus_tag	logFC	logCPM	FDR	Product	UniProt gene	KO number	Localization	Specific[a]
							protein.	
KLMA_20536	-15.3	4.8	0.000	yjgF_YER057c_UK 114_family				C
KLMA_80089	-15.1	6.3	0.002	translation machinery-associated protein 17	TMA17		Cytoplasm. Nucleus.	45D
KLMA_50500	-14.6	4.1	0.006	epsin-like protein	ENT5		Cytoplasm. Endosome membrane; Peripheral membrane protein.	C
KLMA_50088	-14.4	5.0	0.000	uncharacterized protein YBR262C	AIM5		Mitochondrion inner membrane; Single-pass membrane protein (By similarity).	45D
KLMA_10139	-14.3	4.9	0.002	pre-mRNA-splicing factor CWC25	CWC25		Nucleus (By similarity).	45D
KLMA_80058	-13.4	5.7	0.007	UPF0103 protein YJR008W		K06990		S
KLMA_10732	-13.0	3.3	0.049	mitochondrial import inner membrane translocase subunit TIM9	TIM9		Mitochondrion inner membrane; Peripheral membrane protein; Intermembrane side (By similarity).	45D
KLMA_20820	-12.9	2.4	0.004	hypothetical protein				45D
KLMA_40601	-12.2	2.0	0.016	UBX domain-containing protein 2	UBX2	K14013	Endoplasmic reticulum membrane; Multi-pass membrane protein (Potential).	S
KLMA_50270	-11.8	2.4	0.024	3,4-dihydroxy-2-butanone 4-phosphate synthase	RIB3	K02858		S
KLMA_50256	-11.8	1.3	0.007	cyclin-dependent kinase inhibitor FAR1	FAR1	K06652		45D
KLMA_50406	-11.8	5.4	0.025	peroxiredoxin DOT5	DOT5	K03564	Nucleus. Chromosome, telomere (Potential).	45D
KLMA_20344	-11.6	1.1	0.025	mRNA 3'-end-processing protein YTH1	YTH1	K14404	Nucleus (By similarity).	45D
KLMA_40301	-11.6	1.0	0.004	UPF0067 GAF domain-containing protein YKL069W		K08968	Cytoplasm. Nucleus.	C
KLMA_70331	-11.5	2.0	0.012	mitochondrial import inner membrane translocase subunit TIM12	TIM12		Mitochondrion inner membrane; Peripheral membrane protein.	45D
KLMA_30346	-11.1	4.9	0.011	pre-mRNA-splicing factor CWC21	CWC21		Cytoplasm (By similarity). Nucleus (By similarity).	S
KLMA_60382	-10.7	1.3	0.038	probable gluconokinase		K00851	Cytoplasm.	45D
KLMA_R420	-10.4	3.3	0.005	His-tRNA				S
KLMA_50501	-9.7	7.7	0.001	peptidyl-prolyl cis-trans isomerase	CPR1	K01802	Cytoplasm.	S
KLMA_70444	-9.1	6.1	0.001	citrate synthase 3	CIT3	K01647		45D
KLMA_10008	-8.9	-0.1	0.029	siderophore iron transporter ARN2	ARN2		Endosome membrane; Multi-pass membrane protein (By similarity).	S
KLMA_20830	-7.7	8.8	0.000	lactose permease	LAC12		Membrane; Multi-pass membrane protein.	45D

Locus_tag	logFC	logCPM	FDR	Product	UniProt gene	KO number	Localization	Specific[a]
KLMA_30142	-7.2	6.0	0.000	serine/threonine-protein phosphatase PP1-2	GLC7	K06269	Cytoplasm. Nucleus.	C
KLMA_50531	-7.0	9.1	0.000	uncharacterized transporter YLR152C		K07088	Membrane; Multi-pass membrane protein.	45D
KLMA_60047	-6.6	9.4	0.003	uncharacterized protein YGR235C	MOS2		Mitochondrion inner membrane; Multi-pass membrane protein.	45D
KLMA_70355	-6.5	8.4	0.019	uncharacterized protein YBL029C-A			Cell membrane; Peripheral membrane protein.	45D
KLMA_10829	-6.5	5.6	0.003	hypothetical protein				45D
KLMA_20832	-6.2	5.9	0.000	dethiobiotin synthetase	BIO4	K01935		45D
KLMA_30728	-5.8	6.0	0.000	lactose permease	LAC12		Membrane; Multi-pass membrane protein.	S
KLMA_10518	-5.8	12.9	0.000	inulinase	INU1	K01193	Secreted.	45D
KLMA_30719	-5.8	7.7	0.000	phosphoenolpyruvate carboxykinase [ATP]	PCK1	K01610		45D
KLMA_40260	-5.6	3.1	0.004	hypothetical protein				30X
KLMA_10299	-5.6	1.2	0.036	spore wall maturation protein DIT1	DIT1			S
KLMA_30399	-5.5	5.7	0.008	conserved hypothetical membrane protein				S
KLMA_70433	-5.5	1.5	0.025	conserved hypothetical protein				S
KLMA_20831	-5.5	1.1	0.039	adenosylmethionine-8-amino-7-oxononanoate aminotransferase	BIO3	K00833		30X
KLMA_40583	-5.3	5.3	0.005	D-lactate dehydrogenase [cytochrome] 1	DLD1	K00102	Mitochondrion inner membrane.	S
KLMA_60263	-5.3	5.5	0.026	cholinephosphotransferase 1	CPT1	K00993	Microsome membrane; Multi-pass membrane protein. Endoplasmic reticulum membrane; Multi-pass membrane protein. Mitochondrion outer membrane; Multi-pass membrane protein.	S
KLMA_60492	-5.2	9.0	0.017	ATPase inhibitor				45D
KLMA_20333	-5.2	9.4	0.000	galactokinase	GAL1	K00849		45D
KLMA_70303	-5.1	4.9	0.040	probable 6-phosphofructo-2-kinase/fructose-2,6-biphosphatase				45D
KLMA_30619	-5.0	9.7	0.000	meiotic recombination protein REC8	REC8	K12780	Nucleus. Chromosome. Chromosome, centromere.	S
KLMA_R606	-5.0	7.7	0.043	Thr-tRNA				S
KLMA_50151	-5.0	6.1	0.025	aromatic amino acid aminotransferase 1	ARO8		Cytoplasm.	30X
KLMA_30148	-5.0	6.2	0.032	acetolactate synthase small subunit	ILV6	K01653	Mitochondrion.	45D
KLMA_40214	-5.0	2.6	0.049	SUR7 family protein FMP45	FMP45		Cell membrane; Multi-pass membrane protein.	S
KLMA_40132	-4.9	9.4	0.014	transcription				S

Locus_tag	logFC	logCPM	FDR	Product	UniProt gene	KO number	Localization	Specific[a]
				activator				
KLMA_40371	-4.8	10.0	0.000	protein TMA108	TMA108		Cytoplasm.	S
KLMA_30398	-4.8	8.5	0.015	2-deoxyglucose-6-phosphate phosphatase 2	DOG2	K01111		45D
KLMA_20829	-4.8	3.7	0.042	repressible acid phosphatase	PHO3			S
KLMA_10121	-4.8	8.4	0.001	metal homeostasis factor ATX1	ATX1	K07213	Cytoplasm.	S
KLMA_30672	-4.7	6.0	0.029	probable metabolite transport protein C1271.09			Membrane; Multi-pass membrane protein (Potential).	30X
KLMA_30166	-4.7	4.9	0.004	protein SIP4	SIP4		Nucleus (Probable).	S
KLMA_10827	-4.7	5.6	0.001	MFS_1			Membrane; Multi-pass membrane protein.	45D
KLMA_R205	-4.7	5.7	0.013	Leu-tRNA				S
KLMA_50449	-4.6	7.6	0.006	fungal_trans super family conserved domain				C
KLMA_70178	-4.5	12.0	0.000	uncharacterized protein YIL057C	RGI1		Cell membrane; Peripheral membrane protein (By similarity).	45D
KLMA_40244	-4.4	7.1	0.001	ATP-dependent permease PDR15	PDR5		Cell membrane; Multi-pass membrane protein.	S
KLMA_70044	-4.3	9.8	0.000	sorbitol dehydrogenase 1	SOR1	K00008		45D
KLMA_70189	-4.3	8.6	0.027	protein MMF1	MMF1		Mitochondrion matrix.	45D
KLMA_60300	-4.3	2.6	0.023	outer spore wall protein 2	OSW2		Cytoplasm. Prospore membrane.	S
KLMA_70134	-4.3	6.8	0.005	protein transport protein SFT2	SFT2		Golgi apparatus membrane; Multi-pass membrane protein.	30X
KLMA_80174	-4.2	8.9	0.004	probable transporter AQR1	AQR1		Membrane; Multi-pass membrane protein.	C
KLMA_30325	-4.2	6.6	0.044	cystathionine beta-lyase	STR3	K01760	Cytoplasm. Nucleus.	S
KLMA_30497	-4.1	6.4	0.004	1,3-beta-glucan synthase component GSC2	FKS3		Mitochondrion. Membrane; Multi-pass membrane protein (Potential).	S
KLMA_60171	-4.1	4.1	0.044	protein SOV1	SOV1		Mitochondrion.	S
KLMA_60042	-4.1	8.2	0.002	peroxisomal membrane protein PEX21	PEX21		Cytoplasm (By similarity). Peroxisome membrane; Peripheral membrane protein; Cytoplasmic side (By similarity).	45D
KLMA_20007	-4.1	5.5	0.027	putative monooxygenase yxeK	yxeK			S
KLMA_30718	-4.0	5.2	0.005	hypothetical protein				S
KLMA_80322	-4.0	8.9	0.006	cytochrome c oxidase subunit 7		K02269		45D
KLMA_30331	-4.0	6.5	0.006	hypothetical protein				45D
KLMA_40622	-4.0	11.7	0.000	hypothetical protein				C
KLMA_60413	-4.0	6.3	0.006	uncharacterized esterase/lipase C417.12			Cytoplasm. Nucleus.	S
KLMA_70459	-4.0	5.2	0.010	probable transporter MCH2	MCH2		Membrane; Multi-pass membrane protein.	S
KLMA_10440	-3.9	5.4	0.007	hypothetical protein			Membrane; Multi-pass membrane protein (Potential).	S

Locus_tag	logFC	logCPM	FDR	Product	UniProt gene	KO number	Localization	Specific[a]
KLMA_20004	-3.9	5.7	0.009	oligopeptide transporter 1	OPT1		Cell membrane; Multi-pass membrane protein.	S
KLMA_20489	-3.8	9.0	0.008	GAL4-like Zn2Cys6 binuclear cluster DNA-binding domain				C
KLMA_30496	-3.8	6.0	0.010	TPR repeat-containing protein associated with Hsp90	TAH1		Cytoplasm. Nucleus.	30X
KLMA_50409	-3.8	7.4	0.008	flo11 super family	MUC1	K01178	Secreted, cell wall (Probable). Membrane; Lipid-anchor, GPI-anchor (Potential).	45D
KLMA_60412	-3.8	10.7	0.001	hexokinase	RAG5	K00844		C
KLMA_80275	-3.8	7.2	0.006	non-disjunction protein 1				S
KLMA_70443	-3.8	3.9	0.044	probable 2-methylcitrate dehydratase	PDH1	K01720		C
KLMA_30246	-3.7	8.6	0.005	sphingoid long-chain base transporter RSB1	RSB1		Cell membrane (By similarity); Multi-pass membrane protein.	S
KLMA_20704	-3.7	9.8	0.001	CBM_21 super family	GAC1			45D
KLMA_40201	-3.7	8.0	0.007	zinc finger protein YPR013C				S
KLMA_20222	-3.6	4.4	0.017	GAL4				S
KLMA_30072	-3.6	5.0	0.025	poly(A) polymerase	PAP1	K14376	Nucleus.	S
KLMA_30640	-3.5	8.3	0.043	D-amino-acid oxidase	dao1			C
KLMA_20822	-3.5	5.2	0.019	dnaJ-like chaperone JEM1		K09523		S
KLMA_20442	-3.5	11.6	0.000	ubiquitin	UBI4	K08770	Cytoplasm (By similarity). Nucleus (By similarity).	S
KLMA_R128	-3.5	6.0	0.014	Ser-tRNA				S
KLMA_30237	-3.5	7.7	0.030	protein MTH1	MTH1			S
KLMA_20010	-3.5	4.4	0.050	protein crtK				S
KLMA_R530	-3.5	5.1	0.039	Gln-tRNA				30X
KLMA_40341	-3.5	8.3	0.008	hypothetical protein				S
KLMA_60520	-3.4	7.8	0.017	ferric/cupric reductase transmembrane component 1	FRE1		Cell membrane; Multi-pass membrane protein.	S
KLMA_40128	-3.4	10.1	0.001	heat shock protein 26	HSP26	K13993		30X
KLMA_70213	-3.4	7.1	0.026	dilute domain-containing protein YPR089W		K06867	Golgi apparatus.	S
KLMA_50067	-3.4	6.2	0.024	probable kynurenine--oxoglutarate transaminase BNA3	BNA3	K14264	Cytoplasm. Mitochondrion.	S
KLMA_30165	-3.4	4.8	0.018	DNA replication regulator DPB11	DPB11	K03507	Nucleus.	S
KLMA_60392	-3.4	9.4	0.003	uncharacterized protein YPL039W				C
KLMA_40294	-3.3	6.4	0.039	protein SYM1	SYM1	K13348	Mitochondrion inner membrane; Multi-pass membrane protein (By similarity).	S

Locus_tag	logFC	logCPM	FDR	Product	UniProt gene	KO number	Localization	Specific[a]
KLMA_30729	-3.3	6.1	0.026	putative uncharacterized oxidoreductase YGL039W				S
KLMA_60379	-3.3	6.5	0.025	recQ-mediated genome instability protein 1	RMI1	K15364	Cytoplasm. Nucleus.	45D
KLMA_80130	-3.3	6.8	0.020	homoisocitrate dehydrogenase	LYS12	K05824	Mitochondrion.	C
KLMA_10187	-3.3	5.0	0.025	cell division control protein 15	CDC15	K06683	Cytoplasm, cytoskeleton, spindle pole.	S
KLMA_60414	-3.3	4.1	0.040	allantoate permease	DAL5		Membrane; Multi-pass membrane protein.	S
KLMA_70042	-3.3	5.9	0.025	uncharacterized protein YFL042C			Cytoplasmic vesicle membrane; Single-pass membrane protein (Potential).	S
KLMA_10514	-3.3	10.4	0.002	branched-chain-amino-acid aminotransferase	BAT1	K00826	Mitochondrion matrix.	C
KLMA_30689	-3.3	7.4	0.037	SIT4-associating protein SAP155	SAP155	K15457	Cytoplasm.	S
KLMA_50241	-3.3	7.4	0.018	pyridoxamine 5'-phosphate oxidase	PDX3	K00275		C
KLMA_20597	-3.3	5.7	0.027	transaminated amino acid decarboxylase	ARO10	K12732	Cytoplasm.	30X
KLMA_40372	-3.2	10.5	0.002	J domain-containing protein APJ1	APJ1		Cytoplasm. Nucleus.	S
KLMA_30644	-3.2	4.4	0.038	protein PNS1	PNS1		Cell membrane; Multi-pass membrane protein (By similarity).	S
KLMA_20826	-3.2	5.0	0.027	pantothenate transporter FEN2	FEN2	K03448	Cell membrane; Multi-pass membrane protein.	S
KLMA_10547	-3.2	8.7	0.012	high-affinity glucose transporter	HGT1		Membrane; Multi-pass membrane protein.	45D
KLMA_40126	-3.2	6.9	0.026	UDP-N-acetylglucosamine transferase subunit ALG14	ALG14	K07441	Endoplasmic reticulum membrane; Single-pass membrane protein (By similarity).	S
KLMA_20326	-3.2	6.6	0.026	riboflavin transporter MCH5	MCH5		Cell membrane; Multi-pass membrane protein (Potential).	S
KLMA_40057	-3.1	7.7	0.033	interstrand crosslink repair protein	PSO2	K15340	Nucleus (Probable).	S
KLMA_80005	-3.1	5.7	0.028	high-affinity glucose transporter	LAC12		Membrane; Multi-pass membrane protein.	S
KLMA_40149	-3.1	9.1	0.011	hypothetical protein				45D
KLMA_50587	-3.1	5.3	0.046	peroxisomal 2	SPS19	K13237	Peroxisome.	S
KLMA_60268	-3.1	7.8	0.019	uncharacterized protein YNL134C				S
KLMA_50482	-3.1	11.5	0.001	non-classical export protein 2	NCE102		Cell membrane; Multi-pass membrane protein.	45D
KLMA_40045	-3.1	11.5	0.000	ATPase-stabilizing factor 15 kDa protein	STF2		Mitochondrion.	45D
KLMA_80246	-3.1	8.7	0.036	nuclear polyadenylated RNA-binding protein 4	HRP1	K14411	Cytoplasm. Nucleus.	S
KLMA_10558	-3.0	9.6	0.008	D-arabinitol 2-dehydrogenase	ARDH			45D

Locus_tag	logFC	logCPM	FDR	Product	UniProt gene	KO number	Localization	Specific[a]
				[ribulose-forming]				
KLMA_30715	-3.0	8.2	0.026	LCB5				S
KLMA_10036	-3.0	5.5	0.045	pantothenate kinase	CAB1	K09680	Cytoplasm. Nucleus.	C
KLMA_40107	-3.0	8.2	0.023	phospho-2-dehydro-3-deoxyheptonate aldolase	ARO3	K01626		S
KLMA_50125	-3.0	8.8	0.039	sterol regulatory element-binding protein ECM22	UPC2		Nucleus.	S
KLMA_20615	-3.0	8.9	0.017	YCII super family		K09780		S
KLMA_50402	-2.9	8.5	0.032	2-isopropylmalate synthase	LEU4	K01649	Isoform Cytoplasmic: Cytoplasm.Isoform Mitochondrial: Mitochondrion.	45D
KLMA_20515	-2.9	6.7	0.047	protein ISD11	ISD11		Mitochondrion.	45D
KLMA_50101	-2.9	7.0	0.046	SWIRM domain-containing protein YOR338W				S
KLMA_20220	-2.9	13.9	0.000	3-ketoacyl-CoA thiolase	POT1	K00632	Peroxisome.	45D
KLMA_20042	-2.8	8.7	0.026	acetyl-CoA hydrolase	ACH1	K01067	Cytoplasm (By similarity).	45D
KLMA_10487	-2.8	9.6	0.023	probable serine/threonine-protein kinase YMR291W	TDA1	K08286	Cytoplasm. Nucleus.	S
KLMA_40218	-2.8	13.1	0.000	glyceraldehyde-3-phosphate dehydrogenase 1	GAP1	K00134	Cytoplasm (By similarity).	45D
KLMA_20503	-2.8	10.0	0.026	DNA polymerase epsilon subunit B	DPB2	K02325	Nucleus (By similarity).	S
KLMA_40270	-2.8	9.1	0.026	dual specificity protein kinase KNS1	KNS1	K08287		S
KLMA_20475	-2.8	7.4	0.049	protein ROD1	ROD1		Membrane; Peripheral membrane protein.	S
KLMA_50537	-2.7	11.2	0.002	eukaryotic peptide chain release factor GTP-binding subunit	SUP35	K03267	Cytoplasm (Probable).	S
KLMA_20100	-2.6	8.8	0.043	reduced viability upon starvation protein 161	RVS161		Cytoplasm, cytoskeleton.	45D
KLMA_80119	-2.6	11.8	0.008	histone H3	HHT1	K11253	Nucleus (By similarity). Chromosome (By similarity).	45D
KLMA_60167	-2.6	12.1	0.002	malate dehydrogenase	MDH1	K00026	Mitochondrion matrix.	45D
KLMA_50289	-2.6	9.2	0.042	vacuolar membrane protein YOR292C			Vacuole membrane; Multi-pass membrane protein.	45D
KLMA_80159	-2.5	9.9	0.037	cytochrome c oxidase polypeptide 5A	COX5A	K02263	Mitochondrion inner membrane.	S
KLMA_20440	-2.3	10.5	0.023	pH-response transcription factor pacC/RIM101	RIM101		Cytoplasm (By similarity). Nucleus (By similarity).	S
KLMA_10040	-1.9	19.0	0.000	uncharacterized protein YDR524C-B				45D
KLMA_10830	-1.9	12.3	0.017	ribosyldihydronicotinamide dehydrogenase	Nqo2		Cytoplasm (By similarity).	S

Locus_tag	logFC	logCPM	FDR	Product	UniProt gene	KO number	Localization	Specific[a]
KLMA_60129	-1.8	13.0	0.010	[quinone] histone H3	HHT1	K11253	Nucleus (By similarity). Chromosome (By similarity).	45D

[a]Gene expression was significantly (FDR < 0.05) altered under the following conditions: S, 30DS-specific down-regulation; C, commonly down-regulated under 30DS, 45D and 30X conditions; 45D, down-regulated under 45D and 30DS conditions; 30X, down-regulated under 30X and 30DS conditions.

Table S13 GO terms enriched in significantly down-regulated genes under 45D condition

GO.ID	Term	Annotated gene[a]	Significant[b]	Expected[c]	P-value[d]	Genes
GO:0005975	carbohydrate metabolic process	247	44	25.86	0.0002	ACN9, ALG3, ARDH, BUD32, BUD7, CAT5, CIT3, CRH1, DFG5, DOG2, ENO, EOS1, GAC1, GAL1, GAP1, GAP3, GAS5, GID8, GLC7, GLO4, GPD1, INU1, KLMA_20548, KLMA_30562, KLMA_40105, KLMA_60382, KTR1, KTR5, MDH1, MIOX5, OCH1, PCK1, PCM1, PGK, PKP2, RAG2, RAG5, RER2, RKI1, RMD5, SOR1, STT3, SVP26, XYL1
GO:0009097	isoleucine biosynthetic process	9	5	0.94	0.0011	BAT1, ILV1, ILV2, ILV6, MMF1
GO:0044281	small molecule metabolic process	645	90	67.52	0.0012	ACP1, ADI1, ALA1, APA2, ARDH, ARO7, ATF1, ATP3, BAT1, BDH1, BIO4, CAB1, CAT2, CAT5, CIT3, COQ1, COQ5, CYB5, DTD1, DUG3, EFT1, FAA2, FMN1, FOL2, FUM1, FUR1, GAD1, GCV1, GDI1, GID8, GLO4, GRS1, HAM1, HIS1, HIS7, IDI1, ILS1, ILV1, ILV2, ILV6, IOC2, IOC4, ISN1, IZH2, KLMA_10627, KLMA_10805, KLMA_30357, KLMA_40483, KLMA_40623, KLMA_60382, LEU4, LYS12, LYS9, MDH1, MEF1, MET17, MET22, MIOX5, MMF1, MRS6, MST1, OCA5, PCD1, PCM1, PDH1, PDR17, PDX3, PHA2, POT1, PRO2, PRS3, RDI1, RER2, RIB4, RKI1, RMD5, SAM4, SER2, SNZ3, TEF, THI20, TRP3, TYR1, URA1, URE2, YFH1, YRB2, gabD, gcp
GO:0005996	monosaccharide metabolic process	81	18	8.48	0.0014	ACN9, CAT5, DOG2, ENO, GAL1, GAP1, GAP3, GID8, MIOX5, PCK1, PGK, PKP2, RAG2, RAG5, RKI1, RMD5, SOR1, XYL1

GO.ID	Term	Annotated gene[a]	Significant[b]	Expected[c]	P-value[d]	Genes
GO:0009082	branched-chain amino acid biosynthetic process	14	6	1.47	0.0018	BAT1, ILV1, ILV2, ILV6, LEU4, MMF1
GO:0006549	isoleucine metabolic process	11	5	1.15	0.0033	BAT1, ILV1, ILV2, ILV6, MMF1
GO:0019318	hexose metabolic process	74	16	7.75	0.0034	ACN9, CAT5, DOG2, ENO, GAL1, GAP1, GAP3, GID8, PCK1, PGK, PKP2, RAG2, RAG5, RKI1, RMD5, SOR1
GO:0042822	pyridoxal phosphate metabolic process	4	3	0.42	0.0042	BUD17, KLMA_70278, SNZ3
GO:0042823	pyridoxal phosphate biosynthetic process	4	3	0.42	0.0042	BUD17, KLMA_70278, SNZ3
GO:0046184	aldehyde biosynthetic process	4	3	0.42	0.0042	BUD17, KLMA_70278, SNZ3
GO:0019752	carboxylic acid metabolic process	345	51	36.12	0.0053	ACP1, ADI1, ALA1, ARO7, BAT1, BIO4, CAT2, CIT3, DTD1, DUG3, FAA2, FOL2, FUM1, GAD1, GCV1, GLO4, GRS1, HIS1, HIS7, ILS1, ILV1, ILV2, ILV6, IZH2, KLMA_10627, KLMA_10805, KLMA_30357, KLMA_40623, KLMA_60382, LEU4, LYS12, LYS9, MDH1, MET17, MET22, MIOX5, MMF1, MST1, PDH1, PDR17, PDX3, PHA2, POT1, PRO2, SAM4, SER2, TRP3, TYR1, YFH1, gabD
GO:0006006	glucose metabolic process	64	14	6.7	0.0053	ACN9, CAT5, DOG2, ENO, GAP1, GAP3, GID8, PCK1, PGK, PKP2, RAG2, RAG5, RKI1, RMD5
GO:0044723	single-organism carbohydrate metabolic process	202	33	21.15	0.0054	ACN9, ALG3, ARDH, BUD32, BUD7, CAT5, DOG2, ENO, EOS1, GAC1, GAL1, GAP1, GAP3, GID8, GLC7, KLMA_60382, KTR1, KTR5, MIOX5, OCH1, PCK1, PCM1, PGK, PKP2, RAG2, RAG5, RER2, RKI1, RMD5, SOR1, STT3, SVP26, XYL1
GO:0043436	oxoacid metabolic process	354	52	37.06	0.0055	ACP1, ADI1, ALA1, ARO7, BAT1, BIO4, CAT2, CIT3, DTD1, DUG3, FAA2, FOL2, FUM1, GAD1, GCV1, GLO4, GRS1, HIS1, HIS7, ILS1, ILV1, ILV2, ILV6, IZH2, KLMA_10627, KLMA_10805, KLMA_30357, KLMA_40623, KLMA_60382, LEU4, LYS12, LYS9, MDH1, MET17, MET22, MIOX5, MMF1, MST1, PDH1, PDR17, PDX3, PHA2, POT1, PRO2, SAM4, SER2, TRP3, TYR1, URE2, YFH1, gabD
GO:0006082	organic acid metabolic process	356	52	37.27	0.0062	ACP1, ADI1, ALA1, ARO7, BAT1, BIO4, CAT2, CIT3, DTD1, DUG3, FAA2, FOL2, FUM1, GAD1, GCV1, GLO4, GRS1, HIS1,

GO.ID	Term	Annotated gene[a]	Significant[b]	Expected[c]	P-value[d]	Genes
						HIS7, ILS1, ILV1, ILV2, ILV6, IZH2, KLMA_10627, KLMA_10805, KLMA_30357, KLMA_40623, KLMA_60382, LEU4, LYS12, LYS9, MDH1, MET17, MET22, MIOX5, MMF1, MST1, PDH1, PDR17, PDX3, PHA2, POT1, PRO2, SAM4, SER2, TRP3, TYR1, URE2, YFH1, gabD
GO:0051188	cofactor biosynthetic process	80	16	8.37	0.0075	ACP1, BUD17, CAB1, CAT5, COQ1, COQ5, COX10, COX15, FMN1, FOL2, HEM12, HEM4, KLMA_70278, SNZ3, THI20, YFH1
GO:0044283	small molecule biosynthetic process	263	40	27.53	0.0082	ACP1, ADI1, ARO7, BAT1, BDH1, BIO4, CAT5, COQ1, COQ5, CYB5, FMN1, FOL2, GLO4, HIS1, HIS7, IDI1, ILV1, ILV2, ILV6, KLMA_30357, KLMA_40623, LEU4, LYS12, LYS9, MET17, MET22, MIOX5, MMF1, PDR17, PDX3, PHA2, PRO2, RER2, RIB4, SAM4, SER2, SNZ3, THI20, TRP3, TYR1
GO:0009095	aromatic amino acid family biosynthetic process, prephenate pathway	5	3	0.52	0.0097	ARO7, PHA2, TYR1
GO:0009099	valine biosynthetic process	5	3	0.52	0.0097	BAT1, ILV2, ILV6

[a]The number of GO term annotated genes in the *K. marxianus* genome.
[b]The number of GO term annotated genes, which were significantly (FDR < 0.05) expressed under the condition.
[c]The expected value of Fisher's exact test.
[d]The P-value of Fisher's exact test.

Table S14 Summary of significantly down-regulated genes under the 45D condition

Locus_tag	logFC	logCPM	FDR	Product	UniProt gene	KO number	Localization	Specific[a]
KLMA_60492	-18.7	9.0	0.000	ATPase inhibitor				30DS
KLMA_50402	-18.6	8.5	0.000	2-isopropylmalate synthase	LEU4	K01649	Isoform Cytoplasmic: Cytoplasm.Isoform Mitochondrial: Mitochondrion.	30DS
KLMA_50016	-18.0	9.0	0.000	(2R,3R)-2,3-butanediol dehydrogenase	BDH1	K00004	Cytoplasm.	S
KLMA_70355	-17.9	8.4	0.000	uncharacterized protein YBL029C-A			Cell membrane; Peripheral membrane protein.	30DS
KLMA_20783	-17.6	8.2	0.000	60S ribosomal protein L33-B	RPL33B	K02917	Cytoplasm.	S
KLMA_60402	-17.1	6.6	0.000	pisatin demethylase	PDAT9	K00493		30X
KLMA_60530	-16.9	6.9	0.000	mitochondrial import receptor subunit TOM7				S

Locus_tag	logFC	logCPM	FDR	Product	UniProt gene	KO number	Localization	Specific[a]
KLMA_50407	-16.8	7.0	0.000	UPF0662 protein YPL260W			Cytoplasm. Nucleus.	S
KLMA_60022	-16.7	7.9	0.000	protein PET10	PET10		Lipid droplet. Membrane; Peripheral membrane protein.	S
KLMA_30148	-16.5	6.2	0.000	acetolactate synthase small subunit	ILV6	K01653	Mitochondrion.	30DS
KLMA_40593	-16.5	7.2	0.000	uncharacterized vacuolar membrane protein YML018C		K15289	Vacuole membrane; Multi-pass membrane protein.	S
KLMA_20491	-16.3	7.2	0.000	cytochrome c oxidase subunit 4	COX4	K02265	Mitochondrion inner membrane.	S
KLMA_20726	-15.9	5.7	0.000	D-tyrosyl-tRNA(Tyr) deacylase	DTD1	K07560	Cytoplasm (By similarity).	S
KLMA_50231	-15.9	6.6	0.000	aminomethyltransferase	GCV1	K00605	Mitochondrion.	S
KLMA_50143	-15.8	5.7	0.001	26S protease regulatory subunit 8 homolog	RPT6	K03066	Cytoplasm (Potential). Nucleus (Potential).	S
KLMA_80028	-15.8	7.7	0.000	fumarate hydratase	FUM1	K01679	Mitochondrion matrix. Cytoplasm.	S
KLMA_30554	-15.7	6.0	0.000	cell wall protein ECM33	ECM33		Cell membrane; Lipid-anchor, GPI-anchor. Secreted, cell wall.	S
KLMA_10763	-15.7	7.0	0.000	glucose-6-phosphate isomerase	RAG2	K01810	Cytoplasm.	S
KLMA_80057	-15.7	7.8	0.000	eukaryotic translation initiation factor 2 subunit alpha	SUI2	K03237		S
KLMA_40016	-15.6	6.0	0.000	saccharopine dehydrogenase [NADP+	LYS9	K00293		S
KLMA_30643	-15.6	5.6	0.000	IMP-specific 5'-nucleotidase 1	ISN1			S
KLMA_80241	-15.6	5.8	0.000	jmjC domain-containing protein 4				S
KLMA_50237	-15.5	6.6	0.000	ATP synthase subunit gamma	ATP3	K02136	Mitochondrion. Mitochondrion inner membrane; Peripheral membrane protein (Probable).	S
KLMA_60233	-15.5	6.1	0.009	cytochrome b5	CYB5		Endoplasmic reticulum membrane; Single-pass membrane protein; Cytoplasmic side (By similarity). Microsome membrane; Single-pass membrane protein; Cytoplasmic side (By similarity).	S
KLMA_30515	-15.5	6.5	0.000	pre-mRNA-splicing factor CWC2	CWC2		Nucleus (By similarity).	S
KLMA_30259	-15.4	6.1	0.000	altered inheritance rate of mitochondria protein 29	AIM29		Cytoplasm.	S
KLMA_70435	-15.4	6.0	0.000	probable electron transfer flavoprotein subunit alpha	AIM45	K03522	Mitochondrion matrix (By similarity).	S
KLMA_40572	-15.3	6.1	0.000	HIG1 domain-containing protein YML030W	RCF1		Mitochondrion membrane; Multi-pass membrane protein (By similarity).	S
KLMA_70351	-15.3	6.9	0.004	KH domain-containing protein YBL032W	HEK2		Cytoplasm (By similarity). Cytoplasm, P-body (By similarity). Nucleus (By similarity). Chromosome, telomere (By similarity).	S
KLMA_20536	-15.3	4.8	0.000	yjgF_YER057c_UK1				C

Locus_tag	logFC	logCPM	FDR	Product	UniProt gene	KO number	Localization	Specific[a]
				14_family				
KLMA_40148	-15.3	6.6	0.001	putative aryl-alcohol dehydrogenase YPL088W				S
KLMA_50202	-15.2	4.9	0.000	DUF3445 super family conserved domain				S
KLMA_80089	-15.1	6.3	0.000	translation machinery-associated protein 17	TMA17		Cytoplasm. Nucleus.	30DS
KLMA_10819	-15.1	6.1	0.000	prephenate dehydrogenase [NADP+]	TYR1	K00211		S
KLMA_80363	-15.1	5.3	0.000	protein AST1	AST1		Membrane; Peripheral membrane protein.	S
KLMA_20756	-15.0	6.7	0.000	bud neck protein 5	BNI5		Cytoplasm. Bud.	S
KLMA_10322	-14.9	5.5	0.000	hypothetical protein	CAF20	K03261	Cytoplasm (By similarity).	S
KLMA_60026	-14.9	6.3	0.000	UPF0615 protein YJL123C	MTC1		Cytoplasm. Cytoplasmic vesicle, COPI-coated vesicle.	S
KLMA_80182	-14.8	5.7	0.003	ER-derived vesicles protein ERV29	ERV29		Endoplasmic reticulum membrane; Multi-pass membrane protein.	S
KLMA_50566	-14.8	5.5	0.000	methionine aminopeptidase 1	MAP1	K01265		S
KLMA_50134	-14.7	6.2	0.000	GTP-binding nuclear protein GSP1/Ran	GSP1	K07936	Nucleus (By similarity).	S
KLMA_10811	-14.7	5.3	0.000	translocation protein SEC66	SEC66	K12273	Endoplasmic reticulum membrane; Single-pass type II membrane protein.	S
KLMA_30093	-14.7	5.7	0.000	mitochondrial oxaloacetate transport protein	OAC1	K15117	Mitochondrion inner membrane; Multi-pass membrane protein (Potential).	S
KLMA_80332	-14.7	5.1	0.000	chorismate mutase	ARO7	K01850		S
KLMA_70093	-14.6	4.6	0.000	carboxypeptidase S	CPS1		Vacuole membrane; Single-pass membrane protein.	30X
KLMA_50500	-14.6	4.1	0.001	epsin-like protein	ENT5		Cytoplasm. Endosome membrane; Peripheral membrane protein.	C
KLMA_20534	-14.5	5.0	0.000	aspartic proteinase 3	YPS1	K06009	Cell membrane; Lipid-anchor, GPI-anchor.	S
KLMA_60542	-14.5	5.4	0.000	NADPH-dependent 1-acyldihydroxyacetone phosphate reductase	AYR1	K06123	Lipid droplet. Endoplasmic reticulum.	S
KLMA_30030	-14.5	6.6	0.000	cell division control protein 11	CDC11		Membrane. Bud neck.	S
KLMA_20071	-14.4	4.8	0.000	DUP super family				S
KLMA_60505	-14.4	4.8	0.011	ADP-ribosylation factor	ARF1	K07977	Golgi apparatus (By similarity).	S
KLMA_30617	-14.3	6.0	0.000	plasma membrane iron permease	FTR1	K07243	Membrane; Multi-pass membrane protein (Potential).	S
KLMA_10139	-14.3	4.9	0.000	pre-mRNA-splicing factor CWC25	CWC25		Nucleus (By similarity).	30DS
KLMA_50247	-14.3	6.8	0.000	54S ribosomal protein MRP49	MRP49		Mitochondrion.	S
KLMA_30556	-14.2	4.7	0.000	glutamate decarboxylase	GAD1	K01580		30X
KLMA_40015	-14.2	4.0	0.000	protein OCA4	OCA4			S
KLMA_R701	-14.2	5.1	0.000	Gly-tRNA				S
KLMA_60501	-14.1	6.3	0.000	rho GDP-dissociation inhibitor	RDI1	K12462	Cytoplasm.	S
KLMA_50335	-14.1	6.7	0.000	transposon Ty1-H Gag-Pol polyprotein				S

Locus_tag	logFC	logCPM	FDR	Product	UniProt gene	KO number	Localization	Specific[a]
KLMA_60028	-14.0	4.8	0.004	sm-like protein LSm1	LSM1	K12620	Nucleus. Cytoplasm. Cytoplasm, P-body.	S
KLMA_30420	-13.9	4.4	0.001	v-type proton ATPase subunit G	VMA10	K02152		S
KLMA_60175	-13.9	5.1	0.000	v-type proton ATPase subunit C	VMA5	K02148	Vacuole membrane; Peripheral membrane protein.	S
KLMA_70356	-13.9	5.3	0.000	hypothetical protein				S
KLMA_30069	-13.9	4.9	0.000	DOA4-independent degradation protein 4	DID4	K12191	Cytoplasm. Endosome membrane; Peripheral membrane protein.	S
KLMA_60169	-13.8	5.4	0.000	hypothetical protein	AVO2		Cell membrane; Peripheral membrane protein; Cytoplasmic side. Vacuole membrane; Peripheral membrane protein; Cytoplasmic side.	S
KLMA_70260	-13.8	6.7	0.000	tubulin alpha-1 chain	TUB1	K07374	Cytoplasm, cytoskeleton.	S
KLMA_40390	-13.7	4.6	0.000	tRNA guanosine-2'-O-methyltransferase TRM13	TRM13	K15446	Cytoplasm (By similarity). Nucleus, nucleolus (By similarity).	S
KLMA_70023	-13.6	4.9	0.000	pheromone-regulated membrane protein 4	PRM4		Membrane; Single-pass membrane protein (Potential).	S
KLMA_80042	-13.6	4.7	0.000	ADIPOR-like receptor IZH2	IZH2	K07036	Membrane; Multi-pass membrane protein.	S
KLMA_50307	-13.6	5.8	0.001	predicted solute binding protein				S
KLMA_50599	-13.6	4.1	0.000	vacuolar import and degradation protein 27	VID27		Cytoplasm.	S
KLMA_80414	-13.6	3.7	0.005	single-stranded nucleic acid-binding protein	SBP1		Cytoplasm. Nucleus, nucleolus.	30X
KLMA_20413	-13.5	3.1	0.001	imidazole glycerol phosphate synthase hisHF	HIS7	K01663		S
KLMA_80030	-13.4	3.9	0.000	rRNA-processing protein UTP23	UTP23	K14773	Mitochondrion. Nucleus, nucleolus.	S
KLMA_30067	-13.4	4.0	0.001	inositol phosphorylceramide synthase	AUR1		Golgi apparatus, Golgi stack membrane; Multi-pass membrane protein.	S
KLMA_10233	-13.4	4.5	0.000	hypothetical protein				30X
KLMA_10389	-13.4	5.1	0.016	farnesyl pyrophosphate synthetase	FPS1	K00787	Cytoplasm.	S
KLMA_70400	-13.4	6.4	0.000	coatomer subunit gamma	SEC21		Cytoplasm. Golgi apparatus membrane; Peripheral membrane protein; Cytoplasmic side. Cytoplasmic vesicle, COPI-coated vesicle membrane; Peripheral membrane protein; Cytoplasmic side. Endosome.	S
KLMA_40287	-13.4	6.0	0.000	probable glycosidase CRH1	CRH1		Secreted, cell wall. Membrane; Lipid-anchor, GPI-anchor.	S
KLMA_20050	-13.3	3.1	0.001	inositol oxygenase 1	MIOX5	K00469	Cytoplasm (Probable).	S
KLMA_20280	-13.3	3.9	0.000	zinc finger transcription factor YRR1	YRM1		Cytoplasm. Nucleus.	S
KLMA_70403	-13.2	3.3	0.006	40S ribosomal protein MRP10	MRP10		Mitochondrion (By similarity).	30X
KLMA_20712	-13.2	3.1	0.001	protein OPY1	OPY1			S
KLMA_10713	-13.2	5.4	0.007	vacuolar protein sorting-associated protein 55	VPS55		Endosome membrane; Multi-pass membrane protein (Potential).	S

Locus_tag	logFC	logCPM	FDR	Product	UniProt gene	KO number	Localization	Specific[a]
KLMA_20238	-13.2	4.3	0.007	uncharacterized protein YGL108C				S
KLMA_50299	-13.2	4.3	0.000	peroxisomal membrane protein PAS20	PEX13	K13344	Peroxisome membrane; Single-pass membrane protein.	S
KLMA_70031	-13.1	4.5	0.000	protein transport protein BOS1	BOS1	K08496	Golgi apparatus membrane; Single-pass type IV membrane protein (By similarity). Endoplasmic reticulum membrane; Single-pass type IV membrane protein (By similarity).	S
KLMA_80316	-13.1	3.6	0.002	protein phosphatase 2C homolog 4	PTC4	K01090		S
KLMA_20441	-13.0	6.6	0.000	cell wall integrity and stress response component 4				S
KLMA_10677	-13.0	3.3	0.000	protein MET17	MET17	K01740	Cytoplasm (By similarity).	S
KLMA_20181	-13.0	3.9	0.000	uroporphyrinogen decarboxylase	HEM12	K01599	Nucleus. Cytoplasm.	S
KLMA_50480	-13.0	4.7	0.000	mitochondrial import inner membrane translocase subunit TIM44	TIM44		Mitochondrion inner membrane.	S
KLMA_10732	-13.0	3.3	0.018	mitochondrial import inner membrane translocase subunit TIM9	TIM9		Mitochondrion inner membrane; Peripheral membrane protein; Intermembrane side (By similarity).	30DS
KLMA_80017	-13.0	5.0	0.002	APC/C-CDH1 modulator 1				S
KLMA_60156	-12.9	4.3	0.000	actin-related protein 2/3 complex subunit 4	ARC19	K05755	Cytoplasm, cytoskeleton, actin patch.	S
KLMA_30042	-12.9	4.3	0.007	protein HAM1	HAM1	K01519	Cytoplasm (By similarity). Nucleus (By similarity).	S
KLMA_60047	-12.9	9.4	0.000	uncharacterized protein YGR235C	MOS2		Mitochondrion inner membrane; Multi-pass membrane protein.	30DS
KLMA_60068	-12.9	4.1	0.006	mitochondral 37S ribosomal protein S27	RSM27		Mitochondrion.	30X
KLMA_20608	-12.8	4.2	0.000	catabolite repression protein CAT5	CAT5	K06134	Mitochondrion inner membrane.	S
KLMA_50563	-12.8	3.3	0.000	palmitoyltransferase ERF2	ERF2		Endoplasmic reticulum membrane; Multi-pass membrane protein (By similarity).	S
KLMA_70152	-12.8	3.8	0.007	vacuolar amino acid transporter 6	AVT6		Vacuole membrane; Multi-pass membrane protein.	S
KLMA_10466	-12.8	4.7	0.000	erv26 super family	SVP26		Golgi apparatus, cis-Golgi network membrane; Multi-pass membrane protein.	S
KLMA_10735	-12.8	3.8	0.000	uracil phosphoribosyltransferase	FUR1	K00761		S
KLMA_40106	-12.8	4.7	0.000	uncharacterized protein YDR210W				30X
KLMA_50627	-12.8	3.1	0.000	protein YTP1	YTP1		Membrane; Multi-pass membrane protein.	S
KLMA_60318	-12.8	3.1	0.000	transmembrane E3 ubiquitin-protein ligase 1	TUL1		Golgi apparatus membrane; Multi-pass membrane protein.	S
KLMA_50080	-12.8	3.5	0.005	putative carboxypeptidase	CPS1	K01293	Vacuole membrane; Single-pass membrane protein.	S

Locus_tag	logFC	logCPM	FDR	Product	UniProt gene	KO number	Localization	Specific[a]
				YOL153C				
KLMA_30665	-12.8	2.7	0.021	ACBP super family protein				S
KLMA_10064	-12.7	3.8	0.016	acetate non-utilizing protein 9	ACN9		Mitochondrion intermembrane space (By similarity).	S
KLMA_60473	-12.7	2.6	0.008	54S ribosomal protein IMG1	IMG1		Mitochondrion.	S
KLMA_10588	-12.7	4.4	0.000	signal recognition particle SEC65 subunit	SEC65	K03105	Cytoplasm (By similarity).	S
KLMA_70126	-12.7	3.1	0.002	uncharacterized protein YJR080C	AIM24		Mitochondrion (By similarity).	30X
KLMA_70046	-12.7	3.6	0.000	elongation factor G	MEF1	K02355	Mitochondrion (By similarity).	S
KLMA_30439	-12.6	3.3	0.000	peptidyl-prolyl cis-trans isomerase D	CPR5	K03768	Endoplasmic reticulum lumen.	S
KLMA_30444	-12.5	3.4	0.002	vacuolar membrane protein YPL162C			Vacuole membrane; Multi-pass membrane protein.	S
KLMA_40044	-12.5	4.7	0.001	ethanolamine-phosphate cytidylyltransferase	ECT1	K00967	Cytoplasm. Nucleus.	30X
KLMA_30367	-12.5	4.8	0.000	uncharacterized protein YLR257W			Cytoplasm.	S
KLMA_70027	-12.5	3.9	0.005	protein EMP47	EMP47		Golgi apparatus membrane; Single-pass type I membrane protein. Endoplasmic reticulum membrane; Single-pass type I membrane protein.	S
KLMA_60487	-12.5	4.1	0.001	vacuolar calcium ion transporter	VCX1	K07300	Vacuole membrane; Multi-pass membrane protein.	S
KLMA_70056	-12.5	4.2	0.000	tubulin beta chain	TUB2	K07375	Cytoplasm, cytoskeleton.	S
KLMA_10671	-12.5	2.4	0.003	uncharacterized protein YHL029C	OCA5		Cytoplasm (By similarity).	S
KLMA_30243	-12.5	2.7	0.003	hydroxyacylglutathione hydrolase	GLO4	K01069	Mitochondrion matrix.	S
KLMA_30427	-12.4	3.1	0.001	HDA1 complex subunit 2	HDA2		Nucleus (By similarity).	S
KLMA_10629	-12.4	3.7	0.044	acyl carrier protein	ACP1	K03955	Mitochondrion.	S
KLMA_50039	-12.4	3.7	0.000	uncharacterized protein in HIS3 3'region				S
KLMA_20478	-12.4	5.8	0.000	centromere/microtubule-binding protein CBF5	CBF5	K11131	Nucleus, nucleolus (By similarity). Chromosome, centromere (By similarity). Cytoplasm, cytoskeleton (By similarity).	S
KLMA_40041	-12.4	3.7	0.000	pre-mRNA-splicing factor 18				S
KLMA_40183	-12.4	4.6	0.000	protein transport protein SEC22	SEC22	K08517	Membrane; Single-pass type IV membrane protein (Potential). Endoplasmic reticulum membrane; Single-pass type IV membrane protein (Potential). Golgi apparatus membrane; Single-pass type IV membrane protein (Potential).	S
KLMA_50551	-12.3	3.0	0.000	COP9 signalosome complex subunit 9	CSN9		Cytoplasm (By similarity). Nucleus (By similarity).	S
KLMA_30473	-12.3	2.3	0.000	uncharacterized transporter YBR287W			Membrane; Multi-pass membrane protein (Potential).	S
KLMA_50348	-12.3	3.2	0.000	protein phosphatase methylesterase 1	PPE1	K13617		S

Locus_tag	logFC	logCPM	FDR	Product	UniProt gene	KO number	Localization	Specific[a]
KLMA_30357	-12.3	3.5	0.001	3-ketoacyl-CoA reductase		K10251	Endoplasmic reticulum membrane (By similarity); Single-pass membrane protein (Potential).	S
KLMA_60125	-12.3	2.4	0.007	succinate-semialdehyde dehydrogenase [NADP+]	gabD	K00135		S
KLMA_50411	-12.3	4.3	0.000	hypothetical protein	GAS5		Secreted, cell wall. Membrane; Lipid-anchor, GPI-anchor.	S
KLMA_30298	-12.2	5.1	0.002	ubiquitin-conjugating enzyme E2 13	UBC13	K10580		S
KLMA_20546	-12.2	4.1	0.001	vacuolar protein sorting-associated protein 62	VPS62		Membrane; Single-pass membrane protein.	30X
KLMA_70160	-12.2	2.7	0.000	mediator of RNA polymerase II transcription subunit 7	MED7	K15148	Nucleus (By similarity).	S
KLMA_10805	-12.2	2.1	0.000	uncharacterized abhydrolase domain-containing protein YGR015C			Mitochondrion.	S
KLMA_20445	-12.2	2.1	0.000	adenylyltransferase and sulfurtransferase UBA4	UBA4	K11996	Cytoplasm (By similarity).	S
KLMA_60399	-12.2	2.2	0.003	sporulation protein RMD5	RMD5		Cytoplasm.	S
KLMA_40157	-12.2	3.2	0.000	F-box protein HRT3	HRT3	K10295		S
KLMA_40153	-12.2	3.3	0.010	thiol-specific monooxygenase	fmo1			S
KLMA_40351	-12.2	4.1	0.000	hypothetical protein				S
KLMA_30653	-12.2	3.5	0.003	vacuolar protein sorting-associated protein 71	VPS71	K11663	Nucleus.	S
KLMA_10581	-12.2	3.5	0.002	ubiquinone biosynthesis methyltransferase COQ5	COQ5	K06127	Mitochondrion.	S
KLMA_80109	-12.1	2.7	0.011	frataxin homolog	YFH1		Mitochondrion matrix.	S
KLMA_20319	-12.1	2.5	0.004	CTP-dependent diacylglycerol kinase 1	DGK1		Endoplasmic reticulum membrane; Multi-pass membrane protein. Golgi apparatus membrane; Multi-pass membrane protein. Nucleus membrane; Multi-pass membrane protein.	S
KLMA_20068	-12.1	2.0	0.011	coupling of ubiquitin conjugation to ER degradation protein 1	CUE1	K14022	Endoplasmic reticulum membrane; Single-pass membrane protein (By similarity).	S
KLMA_30659	-12.0	2.2	0.041	probable aminopeptidase YDR415C		K01269		S
KLMA_R514	-12.0	2.0	0.001	Glu-tRNA				30X
KLMA_60410	-12.0	4.2	0.000	coatomer subunit delta	RET2		Cytoplasm (By similarity). Golgi apparatus membrane; Peripheral membrane protein; Cytoplasmic side (By similarity). Cytoplasmic vesicle, COPI-coated vesicle membrane; Peripheral membrane protein; Cytoplasmic side (By	S

Locus_tag	logFC	logCPM	FDR	Product	UniProt gene	KO number	Localization	Specific[a]
							similarity).	
KLMA_60320	-12.0	3.2	0.000	ribose-phosphate pyrophosphokinase 3	PRS3	K00948	Cytoplasm.	S
KLMA_10615	-12.0	4.2	0.000	54S ribosomal protein L23	rplM	K02871		S
KLMA_30562	-12.0	4.0	0.000	UPF0010 protein YMR099C		K01792		S
KLMA_60196	-12.0	4.0	0.005	ras-related protein RSR1	RSR1	K07974	Cell membrane; Lipid-anchor; Cytoplasmic side (Potential).	S
KLMA_60203	-12.0	2.5	0.000	Golgi apparatus membrane protein TVP23	TVP23		Golgi apparatus membrane; Multi-pass membrane protein (By similarity).	S
KLMA_40118	-12.0	4.4	0.000	pre-mRNA-splicing factor SLT11	SLT11		Nucleus (By similarity).	S
KLMA_50117	-11.9	2.6	0.001	gamma-glutamyl phosphate reductase	PRO2	K00147		S
KLMA_20292	-11.9	2.5	0.004	uncharacterized protein YEL137C				S
KLMA_30383	-11.9	3.2	0.002	pH-response regulator protein palF/RIM8	RIM8			S
KLMA_30685	-11.9	3.2	0.000	uncharacterized protein YGL226W		K02263		S
KLMA_20709	-11.9	3.3	0.000	autophagy-related protein 14	ATG14	K08335	Preautophagosomal structure membrane; Peripheral membrane protein (By similarity). Vacuole membrane; Peripheral membrane protein (By similarity).	S
KLMA_30533	-11.9	2.4	0.014	4,5-DOPA dioxygenase extradiol-like protein			Cytoplasm. Nucleus.	S
KLMA_20793	-11.8	1.3	0.021	MTP18 super family				S
KLMA_50088	-11.8	5.0	0.000	uncharacterized protein YBR262C	AIM5		Mitochondrion inner membrane; Single-pass membrane protein (By similarity).	30DS
KLMA_50023	-11.8	6.4	0.000	hypothetical protein				S
KLMA_10816	-11.8	2.4	0.000	ribonucleases P/MRP protein subunit POP7	POP7	K14526	Nucleus.	S
KLMA_60115	-11.8	3.0	0.000	dehydrodolichyl diphosphate synthetase	RER2	K11778	Endoplasmic reticulum membrane; Peripheral membrane protein.	S
KLMA_40237	-11.8	1.8	0.000	putative glycoprotein endopeptidase KAE1	gcp	K01409	Cytoplasm (Potential).	30X
KLMA_40059	-11.8	2.3	0.000	glucose-induced degradation protein 8	GID8		Nucleus. Cytoplasm.	S
KLMA_50406	-11.8	5.4	0.007	peroxiredoxin DOT5	DOT5	K03564	Nucleus. Chromosome, telomere (Potential).	30DS
KLMA_70278	-11.7	4.1	0.001	pyridoxamine 5'-phosphate oxidase homolog			Cytoplasm. Nucleus.	S
KLMA_80124	-11.7	2.4	0.000	RNA polymerase II holoenzyme cyclin-like subunit	SSN8	K15161	Nucleus (Probable).	S
KLMA_40343	-11.7	2.8	0.000	NADH-cytochrome b5 reductase 1	CBR1	K00326	Endoplasmic reticulum membrane; Single-pass membrane protein (By similarity). Mitochondrion outer membrane; Single-pass membrane protein (By similarity).	S
KLMA_40360	-11.7	2.3	0.000	mitochondrial inner membrane magnesium	LPE10		Mitochondrion inner membrane; Multi-pass membrane protein	S

Locus_tag	logFC	logCPM	FDR	Product	UniProt gene	KO number	Localization	Specific[a]
				transporter LPE10			(By similarity).	
KLMA_80369	-11.7	6.4	0.000	isoleucyl-tRNA synthetase	ILS1	K01870	Cytoplasm.	S
KLMA_20344	-11.6	1.1	0.007	mRNA 3'-end-processing protein YTH1	YTH1	K14404	Nucleus (By similarity).	30DS
KLMA_20605	-11.6	2.9	0.000	mitochondrial chaperone BCS1		K08900		S
KLMA_40301	-11.6	1.0	0.001	UPF0067 GAF domain-containing protein YKL069W		K08968	Cytoplasm. Nucleus.	C
KLMA_10114	-11.5	1.7	0.003	phosphatidylinositol transfer protein PDR17	PDR17		Cytoplasm.	S
KLMA_40514	-11.5	2.7	0.000	hypothetical protein				S
KLMA_50619	-11.5	3.4	0.001	protein URE2	URE2	K00799		S
KLMA_70331	-11.5	2.0	0.002	mitochondrial import inner membrane translocase subunit TIM12	TIM12		Mitochondrion inner membrane; Peripheral membrane protein.	30DS
KLMA_10453	-11.5	2.2	0.002	conserved oligomeric Golgi complex subunit 7	COG7		Golgi apparatus membrane; Peripheral membrane protein (By similarity).	S
KLMA_40595	-11.4	2.8	0.000	phosphatidylinositol N-acetylglucosaminyltransferase subunit GPI19	GPI19	K03861	Endoplasmic reticulum membrane; Multi-pass membrane protein (By similarity).	S
KLMA_20705	-11.4	2.1	0.002	hypothetical protein				S
KLMA_70162	-11.4	1.7	0.005	putative prephenate dehydratase	PHA2	K14170	Cytoplasm.	S
KLMA_60314	-11.4	2.6	0.000	putative GTP-binding protein YLF2	engD	K06942		S
KLMA_10482	-11.4	1.9	0.009	serine/threonine-protein kinase BUD32	BUD32	K08851	Cytoplasm (By similarity). Nucleus (By similarity). Chromosome, telomere (By similarity).	S
KLMA_30591	-11.3	2.3	0.006	bolA-like protein 3	AIM1			S
KLMA_10812	-11.3	4.5	0.000	nuclear protein localization protein 4	NPL4	K14015	Cytoplasm, perinuclear region (By similarity). Endoplasmic reticulum membrane; Peripheral membrane protein; Cytoplasmic side (By similarity). Nucleus membrane; Peripheral membrane protein; Cytoplasmic side (By similarity).	S
KLMA_50428	-11.3	3.6	0.000	cell cycle protein kinase DBF2	DBF2	K06684		S
KLMA_50302	-11.3	3.2	0.033	eukaryotic translation initiation factor 3 subunit J	HCR1	K03245	Cytoplasm (By similarity).	S
KLMA_40289	-11.2	4.0	0.000	AP-1 complex subunit sigma-1	APS1		Golgi apparatus. Cytoplasmic vesicle membrane; Peripheral membrane protein; Cytoplasmic side. Membrane, clathrin-coated pit.	S
KLMA_70004	-11.2	2.0	0.000	conserved hypothetical protein				S
KLMA_60422	-11.2	2.6	0.016	prefoldin subunit 4	GIM3	K09550		S
KLMA_60319	-11.2	2.8	0.000	putative uncharacterized				S

Locus_tag	logFC	logCPM	FDR	Product	UniProt gene	KO number	Localization	Specific[a]
				hydrolase YKL033W-A				
KLMA_50412	-11.2	2.3	0.005	1,2-dihydroxy-3-keto-5-methylthiopentene dioxygenase; Acireductone dioxygenase	ADI1	K08967	Cytoplasm. Nucleus.	S
KLMA_60279	-11.2	2.1	0.000	3'(2')5'-bisphosphate nucleotidase	MET22	K01082	Cytoplasm. Nucleus.	S
KLMA_60078	-11.2	2.4	0.002	phosphoserine phosphatase	SER2	K01079		S
KLMA_20279	-11.2	1.6	0.009	uncharacterized membrane protein YBR220C			Membrane; Multi-pass membrane protein.	S
KLMA_30285	-11.2	2.4	0.006	trans-aconitate 3-methyltransferase	TMT1		Cytoplasm (By similarity).	S
KLMA_60096	-11.1	3.2	0.000	exodeoxyribonuclease 1	EXO1	K10746	Nucleus (Potential).	S
KLMA_20376	-11.1	3.6	0.007	eukaryotic translation initiation factor 3 subunit I	TIF34	K03246	Cytoplasm (By similarity).	S
KLMA_10265	-11.1	3.1	0.001	mitochondrial distribution and morphology protein 12	MDM12		Mitochondrion outer membrane; Peripheral membrane protein; Cytoplasmic side (By similarity). Endoplasmic reticulum membrane; Peripheral membrane protein; Cytoplasmic side (By similarity).	S
KLMA_20526	-11.1	2.6	0.019	F-actin-capping protein subunit beta	CAP2	K10365	Cytoplasm, cytoskeleton (By similarity). Nucleus (By similarity).	S
KLMA_20474	-11.1	2.7	0.000	autophagy-related protein 18	ATG18		Preautophagosomal structure membrane; Peripheral membrane protein (By similarity). Vacuole membrane; Peripheral membrane protein (By similarity). Endosome membrane; Peripheral membrane protein (By similarity).	S
KLMA_40196	-11.1	2.2	0.000	protein PTI1	PTI1	K14407	Nucleus.	S
KLMA_40598	-11.0	1.5	0.001	transcription initiation factor TFIID subunit 11	TAF11	K03135	Nucleus.	S
KLMA_50028	-11.0	2.2	0.000	putative 2-hydroxyacid dehydrogenase YPL113C				S
KLMA_50081	-11.0	4.4	0.000	RNA polymerase II-associated protein 1	PAF1	K15174	Nucleus, nucleoplasm.	S
KLMA_40444	-11.0	6.7	0.002	FK506-binding protein 3	FPR3	K14826	Nucleus, nucleolus (By similarity).	S
KLMA_20055	-11.0	0.5	0.037	hypothetical protein				S
KLMA_40078	-11.0	0.5	0.038	v-type ATPase assembly factor PKR1				S
KLMA_30378	-11.0	3.1	0.000	dolichyl-diphosphooligosaccharide--protein glycosyltransferase subunit STT3	STT3	K07151	Endoplasmic reticulum membrane; Multi-pass membrane protein.	S
KLMA_30350	-11.0	2.6	0.003	hsp70/Hsp90 co-chaperone CNS1	CNS1		Cytoplasm.	S

Locus_tag	logFC	logCPM	FDR	Product	UniProt gene	KO number	Localization	Specific[a]
KLMA_R704	-11.0	2.3	0.021	Val-tRNA				S
KLMA_20287	-10.9	2.5	0.000	hypothetical protein			Mitochondrion (Potential).	S
KLMA_20353	-10.9	1.4	0.001	nucleotide exchange factor SIL1	SIL1	K14001	Endoplasmic reticulum lumen (By similarity).	S
KLMA_80270	-10.9	1.8	0.008	37S ribosomal protein RSM28	RSM28		Mitochondrion.	S
KLMA_50346	-10.9	0.7	0.034	UPF0676 protein C1494.01			Cytoplasm. Nucleus.	S
KLMA_80259	-10.9	2.1	0.001	DASH complex subunit ASK1	ASK1	K11566	Nucleus (By similarity). Cytoplasm, cytoskeleton, spindle (By similarity). Chromosome, centromere, kinetochore (By similarity).	S
KLMA_40267	-10.9	2.8	0.001	initiation-specific alpha-1	OCH1	K05528	Endoplasmic reticulum membrane; Single-pass type II membrane protein. Golgi apparatus membrane; Single-pass type II membrane protein.	S
KLMA_40105	-10.9	2.2	0.008	uncharacterized glycosyl hydrolase YBR056W		K01210		S
KLMA_80331	-10.9	1.6	0.001	carrier protein YMC1	YMC1	K15109	Mitochondrion inner membrane; Multi-pass membrane protein (Potential).	S
KLMA_20804	-10.9	1.6	0.014	gatB_Yqey super family	AIM41	K09117	Mitochondrion (By similarity).	S
KLMA_40517	-10.9	1.4	0.012	uncharacterized protein YML079W		K09705		S
KLMA_20629	-10.8	2.2	0.009	6,7-dimethyl-8-ribityllumazine synthase	RIB4	K00794		S
KLMA_40167	-10.8	2.9	0.002	tRNA-splicing endonuclease subunit SEN2	SEN2	K15322		S
KLMA_60382	-10.7	1.3	0.011	probable gluconokinase		K00851	Cytoplasm.	30DS
KLMA_10626	-10.7	2.3	0.001	threonyl-tRNA synthetase	MST1	K01868	Mitochondrion matrix.	S
KLMA_20711	-10.7	0.5	0.043	uncharacterized protein YPR085C	ASA1		Nucleus (By similarity).	S
KLMA_50246	-10.7	3.8	0.007	ribosomal N-lysine methyltransferase 3	RKM3		Nucleus.	S
KLMA_10224	-10.7	0.5	0.006	translation initiation factor eIF-2B subunit beta	GCD7	K03754		S
KLMA_20759	-10.7	1.4	0.005	protein IBD2	IBD2		Cytoplasm, cytoskeleton, spindle pole (By similarity).	S
KLMA_10591	-10.6	3.8	0.014	protein TMA23	TMA23	K14796	Nucleus, nucleolus.	S
KLMA_10138	-10.6	1.6	0.009	vacuolar protein sorting-associated protein 75	VPS75		Nucleus.	S
KLMA_10675	-10.6	1.4	0.014	cytochrome c oxidase assembly protein COX19	COX19		Cytoplasm (By similarity). Mitochondrion intermembrane space (By similarity).	S
KLMA_50525	-10.6	0.1	0.046	transcription initiation factor TFIID subunit 10	TAF10	K03134	Nucleus.	S
KLMA_40349	-10.5	2.1	0.001	ER membrane protein complex subunit 5	EMC5		Endoplasmic reticulum membrane; Multi-pass membrane protein.	S
KLMA_20267	-10.5	5.1	0.000	nuclear	NAB2		Nucleus.	S

Locus_tag	logFC	logCPM	FDR	Product	UniProt gene	KO number	Localization	Specific[a]
				polyadenylated RNA-binding protein NAB2				
KLMA_40306	-10.4	1.6	0.017	ISWI one complex protein 4	IOC4		Nucleus.	S
KLMA_20552	-10.4	3.5	0.045	arginine N-methyltransferase 2	RMT2	K00599	Cytoplasm (By similarity). Nucleus (By similarity).	S
KLMA_70060	-10.4	1.2	0.036	uncharacterized protein YLR063W			Cytoplasm.	S
KLMA_80181	-10.4	3.8	0.003	zuotin	ZUO1	K09522	Cytoplasm.	S
KLMA_20164	-10.4	7.8	0.000	hypothetical protein				S
KLMA_20548	-10.4	2.4	0.012	kpsF-like protein				S
KLMA_10166	-10.4	1.3	0.001	vacuolar protein sorting-associated protein 52	VPS52		Golgi apparatus, trans-Golgi network membrane; Peripheral membrane protein. Endosome membrane; Peripheral membrane protein. Cytoplasm, cytoskeleton.	S
KLMA_50530	-10.4	2.7	0.004	peroxisomal coenzyme A diphosphatase 1	PCD1		Peroxisome.	S
KLMA_70416	-10.4	1.3	0.012	uncharacterized protein YER128W	VFA1		Cytoplasm. Endosome.	S
KLMA_80117	-10.4	1.2	0.006	probable mannosyltransferase KTR5	KTR5	K03854	Membrane; Single-pass type II membrane protein (Probable).	S
KLMA_70078	-10.3	1.9	0.000	central kinetochore subunit CTF3	CTF3	K11501	Nucleus. Chromosome, centromere, kinetochore.	S
KLMA_40056	-10.3	3.7	0.010	GTP-binding protein CIN4	CIN4	K07943		S
KLMA_50618	-10.3	2.5	0.004	J protein JJJ1	JJJ1	K09506	Nucleus (Potential).	S
KLMA_30666	-10.3	1.0	0.029	DNA polymerase eta	RAD30	K03509	Nucleus.	S
KLMA_80379	-10.3	1.3	0.003	dolichyl-P-Man:Man(5)GlcNAc(2)-PP-dolichyl mannosyltransferase	ALG3	K03845	Endoplasmic reticulum membrane; Multi-pass membrane protein (By similarity).	S
KLMA_70277	-10.2	1.8	0.006	PWWP domain-containing protein YLR455W			Nucleus.	S
KLMA_40531	-10.2	6.8	0.000	uncharacterized protein YKL187C			Mitochondrion.	S
KLMA_20309	-10.2	3.6	0.000	CCR4-associated factor 16	CAF16	K12608	Cytoplasm. Nucleus.	S
KLMA_10488	-10.2	4.0	0.001	GTP cyclohydrolase 1	FOL2	K01495		30X
KLMA_60360	-10.2	1.9	0.000	probable endonuclease YGL085W	LCL3		Mitochondrion. Membrane; Single-pass membrane protein (By similarity).	S
KLMA_40449	-10.2	1.0	0.040	epsin-3	ENT3		Cytoplasm. Golgi apparatus, trans-Golgi network membrane; Peripheral membrane protein. Cytoplasmic vesicle, clathrin-coated vesicle membrane; Peripheral membrane protein.	S
KLMA_20772	-10.1	0.2	0.001	hypothetical protein				S
KLMA_70207	-10.1	0.1	0.011	twinfilin-1	TWF1		Cytoplasm, cytoskeleton (By similarity).	S
KLMA_20727	-10.1	1.1	0.036	probable glutamine amidotransferase DUG3	DUG3	K07008	Cytoplasm.	S
KLMA_60400	-10.1	2.6	0.048	SAGA-associated factor 11	SGF11	K11363	Nucleus (By similarity).	S
KLMA_60247	-10.1	2.1	0.003	cytochrome c oxidase-assembly factor	COX23		Mitochondrion intermembrane space (By similarity).	S

Locus_tag	logFC	logCPM	FDR	Product	UniProt gene	KO number	Localization	Specific[a]
				COX23				
KLMA_20281	-10.1	2.7	0.000	FIT family protein SCS3	SCS3		Membrane; Multi-pass membrane protein (Potential).	S
KLMA_70063	-10.0	2.5	0.005	peroxisomal membrane protein import receptor PEX19	PEX19	K13337	Cytoplasm (By similarity). Peroxisome membrane; Lipid-anchor; Cytoplasmic side (By similarity). Endoplasmic reticulum membrane (By similarity).	S
KLMA_20747	-10.0	4.9	0.021	nucleolar protein 13	NOP13		Nucleus, nucleolus.	S
KLMA_10095	-10.0	1.1	0.005	boron transporter 1	BOR1		Cell membrane; Multi-pass membrane protein. Vacuole membrane; Multi-pass membrane protein.	S
KLMA_30500	-9.9	2.4	0.001	forkhead transcription factor HCM1	HCM1	K09413	Cytoplasm. Nucleus.	S
KLMA_60288	-9.9	2.8	0.000	mannan endo-1	DFG5	K08257	Cell membrane; Lipid-anchor, GPI-anchor.	S
KLMA_20532	-9.9	1.4	0.000	peroxisomal targeting signal 2 receptor	PEX7	K13341	Cytoplasm. Peroxisome.	S
KLMA_50567	-9.9	2.0	0.007	T-complex protein 1 subunit zeta	CCT6	K09498	Cytoplasm.	S
KLMA_10725	-9.8	0.4	0.021	DNA repair and recombination protein RAD26	RAD26	K10841	Nucleus (Probable).	S
KLMA_60533	-9.8	1.8	0.037	chromosome segregation in meiosis protein 2	CSM2		Cytoplasm (By similarity). Nucleus (By similarity).	S
KLMA_30523	-9.8	1.6	0.007	riboflavin kinase	FMN1	K00861		S
KLMA_50392	-9.8	1.0	0.010	protein VAB2	VAB2		Cytoplasmic vesicle (By similarity). Vacuole (By similarity). Cytoplasm (By similarity).	S
KLMA_50510	-9.8	2.2	0.001	pre-mRNA-splicing factor CWC15	CWC15	K12863	Nucleus (Probable).	S
KLMA_80269	-9.8	0.9	0.025	tRNA 2'-phosphotransferase	TPT1	K10669		S
KLMA_80351	-9.8	2.9	0.001	hypothetical protein	AIM11		Membrane; Multi-pass membrane protein (Potential).	S
KLMA_80041	-9.7	0.7	0.001	exosome complex exonuclease RRP6	RRP6	K12591	Nucleus, nucleolus.	S
KLMA_80358	-9.7	1.6	0.018	mitochondrial peroxiredoxin PRX1	PRX1	K03386	Mitochondrion.	S
KLMA_10627	-9.7	1.1	0.028	uncharacterized protein YNL040W		K07050		S
KLMA_70128	-9.6	1.1	0.001	uncharacterized protein YBL107C				S
KLMA_40241	-9.6	1.6	0.001	uncharacterized GTP-binding protein YDR336W				S
KLMA_30180	-9.5	2.0	0.023	clathrin light chain	CLC1		Cytoplasmic vesicle membrane; Peripheral membrane protein; Cytoplasmic side. Membrane, coated pit; Peripheral membrane protein; Cytoplasmic side.	S
KLMA_80020	-9.5	1.7	0.004	karyogamy protein KAR9	KAR9		Nucleus. Cytoplasm, cytoskeleton.	S
KLMA_30255	-9.5	4.4	0.008	20S-pre-rRNA D-site endonuclease NOB1	NOB1	K11883	Cytoplasm. Nucleus, nucleolus. Endoplasmic reticulum.	S
KLMA_10282	-9.5	3.3	0.000	pre-rRNA-processing protein PNO1	PNO1	K11884	Cytoplasm. Nucleus, nucleolus (By similarity).	S

Locus_tag	logFC	logCPM	FDR	Product	UniProt gene	KO number	Localization	Specific[a]
KLMA_10228	-9.5	2.3	0.002	U1 small nuclear ribonucleoprotein C homolog	YHC1		Nucleus.	S
KLMA_10722	-9.4	3.5	0.005	probable E3 ubiquitin-protein ligase HUL4	HUL4	K12232	Nucleus (Probable).	S
KLMA_80043	-9.4	0.8	0.046	tRNA A64-2'-O-ribosylphosphate transferase	RIT1	K15463		S
KLMA_30203	-9.4	2.1	0.004	alcohol O-acetyltransferase 1	ATF1	K00664	Membrane; Peripheral membrane protein.	S
KLMA_10342	-9.4	1.1	0.001	dihydrosphingosine 1-phosphate phosphatase LCB3	LCB3	K04716	Endoplasmic reticulum membrane; Multi-pass membrane protein.	S
KLMA_50607	-9.3	0.7	0.006	DNA-dependent ATPase MGS1	MGS1	K07478	Nucleus (Potential).	S
KLMA_50561	-9.3	2.5	0.001	protein ATC1/LIC4	ATC1		Cytoplasm (By similarity). Nucleus (By similarity).	S
KLMA_30159	-9.3	2.5	0.036	54S ribosomal protein L49	MRPL49		Mitochondrion.	S
KLMA_70173	-9.3	1.1	0.028	ran-specific GTPase-activating protein 2	YRB2	K15304	Nucleus.	S
KLMA_40433	-9.3	0.6	0.001	autophagy-related protein 7	ATG7	K08337	Cytoplasm (By similarity).	S
KLMA_10162	-9.2	1.1	0.012	vacuolar protein-sorting-associated protein 60	VPS60	K12198	Endosome membrane; Peripheral membrane protein. Vacuole membrane; Peripheral membrane protein.	S
KLMA_10202	-9.2	1.7	0.003	uncharacterized protein C12G12.12			Membrane; Multi-pass membrane protein (Potential).	S
KLMA_30504	-9.2	5.5	0.000	putative pyridoxal kinase BUD17	BUD17	K00868	Cytoplasm. Nucleus.	S
KLMA_80106	-9.2	1.8	0.010	solute carrier family 25 member 38 homolog		K15118	Mitochondrion inner membrane; Multi-pass membrane protein (By similarity).	S
KLMA_40236	-9.1	1.4	0.029	DASH complex subunit SPC34	SPC34	K11573	Nucleus (By similarity). Cytoplasm, cytoskeleton, spindle (By similarity). Chromosome, centromere, kinetochore (By similarity).	S
KLMA_30358	-9.1	2.2	0.014	cell division control protein 28	CDC28	K04563		S
KLMA_70444	-9.1	6.1	0.000	citrate synthase 3	CIT3	K01647		30DS
KLMA_70264	-9.0	1.5	0.014	origin recognition complex subunit 4	ORC4	K02606	Nucleus.	S
KLMA_10066	-9.0	1.1	0.031	CAP_GLY super family	BIK1		Cytoplasm, cytoskeleton, spindle pole body. Cytoplasm, cytoskeleton, spindle. Cytoplasm.	S
KLMA_60407	-9.0	2.5	0.002	proteasome component PRE4	PRE4	K02736	Cytoplasm. Nucleus.	S
KLMA_10429	-8.9	4.2	0.000	NADH dehydrogenase		K03885		S
KLMA_10316	-8.9	0.5	0.042	uroporphyrinogen-III synthase	HEM4	K01719		S
KLMA_50408	-8.9	8.2	0.000	protein SLG1		K11244		S
KLMA_20823	-8.9	4.2	0.000	uncharacterized transporter YBR287W			Membrane; Multi-pass membrane protein (Potential).	S
KLMA_R706	-8.9	0.2	0.007	Ile-tRNA				S
KLMA_60142	-8.8	2.6	0.030	N-glycosylation protein EOS1	EOS1		Endoplasmic reticulum membrane; Multi-pass membrane protein.	S
KLMA_60166	-8.7	0.6	0.013	sulfiredoxin	SRX1	K12260	Cytoplasm. Nucleus.	S

Locus_tag	logFC	logCPM	FDR	Product	UniProt gene	KO number	Localization	Specific[a]
KLMA_10302	-8.7	3.7	0.041	UPF0399 protein YOR287C	RRP36	K14795	Nucleus, nucleolus (By similarity).	S
KLMA_10688	-8.6	0.0	0.037	protein BIG1	BIG1		Endoplasmic reticulum membrane; Single-pass type I membrane protein (By similarity).	S
KLMA_20655	-8.6	1.4	0.027	polynucleotide 3'-phosphatase	TPP1	K08075	Nucleus (Probable).	S
KLMA_50107	-8.6	0.1	0.006	GLC7-interacting protein 4	GIP4		Cytoplasm (By similarity).	S
KLMA_20560	-8.5	1.8	0.045	vacuolar protein sorting-associated protein 29	VPS29	K07095		S
KLMA_40325	-8.3	5.0	0.000	hypothetical protein				S
KLMA_40623	-8.3	2.2	0.023	delta(12) fatty acid desaturase		K10256	Membrane; Multi-pass membrane protein (Potential).	S
KLMA_50429	-8.3	2.4	0.001	CWF19-like protein DRN1	DRN1		Nucleus.	S
KLMA_40483	-8.3	0.9	0.021	uncharacterized protein YHR202W			Vacuole.	S
KLMA_40588	-8.3	0.9	0.007	histone-lysine N-methyltransferase	DOT1	K11427	Nucleus (By similarity).	S
KLMA_10383	-8.2	6.9	0.001	histone-lysine N-methyltransferase	SET2	K11423	Nucleus (By similarity). Chromosome (By similarity).	S
KLMA_70158	-8.2	2.2	0.005	polyadenylation factor subunit 2	PFS2	K15542	Nucleus (By similarity).	S
KLMA_50602	-8.1	3.2	0.010	PAPA-1 super family conserved domain		K11676		S
KLMA_10201	-8.1	0.4	0.036	e3 ubiquitin-protein ligase complex SLX5-SLX8 subunit SLX5	SLX5		Nucleus, nucleolus.	S
KLMA_60289	-8.0	4.0	0.021	protein BCH1	BUD7		Golgi apparatus, trans-Golgi network membrane; Peripheral membrane protein.	S
KLMA_40430	-8.0	2.1	0.026	ATP-dependent RNA helicase DBP8	DBP8	K14778	Nucleus, nucleolus (By similarity).	S
KLMA_10456	-7.9	5.9	0.000	tRNA-splicing endonuclease subunit SEN34	SEN34	K15323	Nucleus. Endomembrane system; Peripheral membrane protein. Mitochondrion outer membrane; Peripheral membrane protein; Cytoplasmic side.	S
KLMA_80312	-7.8	5.1	0.039	glycyl-tRNA synthetase 1	GRS1	K01880	Isoform Cytoplasmic: Cytoplasm.Isoform Mitochondrial: Mitochondrion matrix.	S
KLMA_40271	-7.8	4.6	0.035	zinc finger protein				S
KLMA_30468	-7.8	3.4	0.005	protoheme IX farnesyltransferase	COX10	K02257	Mitochondrion membrane; Multi-pass membrane protein (By similarity).	S
KLMA_10035	-7.8	3.8	0.035	5',5'''-P-1,P-4-tetraphosphate phosphorylase 2	APA2	K00988		30X
KLMA_70129	-7.8	1.7	0.000	protein SNI2	SRO77			S
KLMA_20627	-7.8	1.2	0.003	peroxisomal biogenesis factor 6	PEX6	K13339		S
KLMA_20406	-7.6	5.8	0.000	nucleoporin SEH1	SEH1	K14299	Nucleus, nuclear pore complex. Cell membrane; Peripheral membrane protein; Cytoplasmic side. Vacuole membrane; Peripheral membrane protein. Cell membrane; Peripheral	S

Locus_tag	logFC	logCPM	FDR	Product	UniProt gene	KO number	Localization	Specific[a]
							membrane protein; Nucleoplasmic side.	
KLMA_10828	-7.6	4.2	0.008	hypothetical protein				S
KLMA_60114	-7.6	1.6	0.001	hexaprenyl pyrophosphate synthetase	COQ1	K05355	Mitochondrion inner membrane; Peripheral membrane protein; Matrix side.	S
KLMA_10832	-7.6	6.9	0.000	dihydroorotate dehydrogenase	URA1	K00226	Cytoplasm.	S
KLMA_40299	-7.4	1.7	0.001	transposon Ty2-LR1 Gag-Pol polyprotein	TY2B-LR1		Cytoplasm. Nucleus (By similarity).	S
KLMA_80279	-7.4	3.5	0.003	ribonucleases P/MRP protein subunit POP3		K14522		S
KLMA_50256	-7.3	1.3	0.017	cyclin-dependent kinase inhibitor FAR1	FAR1	K06652		30DS
KLMA_80142	-7.3	4.8	0.000	carbonic anhydrase	NCE103	K01673	Cytoplasm. Nucleus.	S
KLMA_30654	-7.3	6.0	0.001	carnitine O-acetyltransferase	CAT2	K00624	Isoform Mitochondrial: Mitochondrion inner membrane; Peripheral membrane protein; Matrix side.Isoform Peroxisomal: Peroxisome.	S
KLMA_70305	-7.3	7.2	0.013	copper transport protein CTR1	CTR1		Membrane; Multi-pass membrane protein.	S
KLMA_60262	-7.1	3.0	0.008	UPF0195 protein YHR122W				S
KLMA_40578	-7.1	5.2	0.000	54S ribosomal protein YmL6	YML6		Mitochondrion.	S
KLMA_50155	-7.0	7.3	0.001	actin cytoskeleton-regulatory complex protein SLA1	SLA1		Cell membrane; Peripheral membrane protein; Cytoplasmic side (By similarity). Endosome membrane; Peripheral membrane protein; Cytoplasmic side (By similarity). Cytoplasm, cytoskeleton, actin patch (By similarity).	S
KLMA_40273	-6.9	6.8	0.000	nuclear pore complex subunit	NUP49	K14307	Nucleus, nuclear pore complex. Nucleus membrane; Peripheral membrane protein; Cytoplasmic side. Nucleus membrane; Peripheral membrane protein; Nucleoplasmic side.	S
KLMA_30102	-6.9	3.5	0.003	uncharacterized protein YKL128C	PMU1		Cytoplasm. Nucleus.	30X
KLMA_20791	-6.9	5.5	0.003	iron sulfur cluster assembly protein 1	ISU1	K04488	Mitochondrion matrix (By similarity).	S
KLMA_50036	-6.8	3.6	0.003	isopentenyl-diphosphate Delta-isomerase	IDI1	K01823	Cytoplasm.	S
KLMA_10512	-6.8	7.1	0.003	uncharacterized mitochondrial membrane protein FMP10	FMP10		Mitochondrion membrane; Multi-pass membrane protein (Potential).	S
KLMA_50037	-6.8	3.0	0.006	rRNA methyltransferase	MRM1	K15507	Mitochondrion.	S
KLMA_20540	-6.8	7.0	0.003	proteasome component Y13	PRE9	K02728	Cytoplasm. Nucleus.	S
KLMA_30552	-6.7	4.9	0.000	eukaryotic translation initiation factor 3 subunit A	TIF32	K03254	Cytoplasm (By similarity).	S
KLMA_20648	-6.7	1.3	0.030	uncharacterized protein YMR160W				S
KLMA_20820	-6.7	2.4	0.032	hypothetical protein				30DS

Locus_tag	logFC	logCPM	FDR	Product	UniProt gene	KO number	Localization	Specific[a]
KLMA_40220	-6.6	11.3	0.000	alcohol dehydrogenase 2	ADH2	K13953	Cytoplasm.	30X
KLMA_10829	-6.6	5.6	0.001	hypothetical protein				30DS
KLMA_80069	-6.5	4.7	0.001	alpha-agglutinin	SAG1		Secreted, cell wall. Membrane; Lipid-anchor, GPI-anchor.	S
KLMA_10378	-6.5	2.5	0.002	protein CASP	COY1	K09313	Golgi apparatus membrane; Single-pass type IV membrane protein.	S
KLMA_60085	-6.4	5.8	0.001	uncharacterized kinase YGR205W	TDA10		Cytoplasm. Nucleus.	S
KLMA_40082	-6.2	5.5	0.002	protein ASI1	ASI1		Nucleus inner membrane; Multi-pass membrane protein.	S
KLMA_50552	-6.2	1.0	0.034	uncharacterized protein YDR179W-A				S
KLMA_50218	-6.2	11.0	0.009	protein MBR1				S
KLMA_40453	-6.2	3.2	0.001	tRNA-dihydrouridine synthase 4	DUS4	K05545		S
KLMA_60111	-6.2	1.2	0.005	sorting assembly machinery 35 kDa subunit	SAM35		Mitochondrion outer membrane.	S
KLMA_40624	-6.1	9.6	0.008	alcohol dehydrogenase	adh	K00001		S
KLMA_10518	-6.1	12.9	0.000	inulinase	INU1	K01193	Secreted.	30DS
KLMA_30392	-6.0	1.7	0.003	UPF0657 nucleolar protein YBR141C			Nucleus, nucleolus.	S
KLMA_70303	-6.0	4.9	0.007	probable 6-phosphofructo-2-kinase/fructose-2,6-biphosphatase				30DS
KLMA_80044	-5.8	1.2	0.029	hypothetical protein	AEP2		Mitochondrion (By similarity).	S
KLMA_30136	-5.8	3.3	0.002	putative succinate-semialdehyde dehydrogenase C1002.12c [NADP+]	gabD			S
KLMA_80119	-5.7	11.8	0.000	histone H3	HHT1	K11253	Nucleus (By similarity). Chromosome (By similarity).	30DS
KLMA_30398	-5.6	8.5	0.001	2-deoxyglucose-6-phosphate phosphatase 2	DOG2	K01111		30DS
KLMA_60412	-5.6	10.7	0.000	hexokinase	RAG5	K00844		C
KLMA_50514	-5.6	2.4	0.025	putative ribonuclease YLR143W			Cytoplasm.	S
KLMA_60167	-5.6	12.1	0.000	malate dehydrogenase	MDH1	K00026	Mitochondrion matrix.	30DS
KLMA_70178	-5.5	12.0	0.000	uncharacterized protein YIL057C	RGI1		Cell membrane; Peripheral membrane protein (By similarity).	30DS
KLMA_10736	-5.4	3.1	0.007	actin-like protein	ro-4		Cytoplasm, cytoskeleton (By similarity).	S
KLMA_30610	-5.4	3.8	0.005	calcium-transporting ATPase 1	PMR1	K01537	Golgi apparatus membrane; Multi-pass membrane protein.	S
KLMA_50449	-5.3	7.6	0.000	fungal_trans super family conserved domain				C
KLMA_10248	-5.3	6.0	0.005	probable protein kinase YGL059W	PKP2		Mitochondrion matrix.	S
KLMA_40185	-5.3	4.8	0.000	UPF0363 protein YOR164C	GET4		Cytoplasm.	S
KLMA_30717	-5.3	6.4	0.000	uncharacterized protein YKR096W				S
KLMA_40356	-5.3	6.5	0.029	protein ECM14	ECM14	K08783	Vacuole.	S
KLMA_20033	-5.3	6.9	0.001	cytochrome c oxidase assembly protein	COX15	K02259	Mitochondrion inner membrane; Multi-pass membrane protein.	S

Locus_tag	logFC	logCPM	FDR	Product	UniProt gene	KO number	Localization	Specific[a]
KLMA_50580	-5.3	1.7	0.014	COX15 ribosomal N-lysine methyltransferase 2	RKM2			S
KLMA_30142	-5.2	6.0	0.000	serine/threonine-protein phosphatase PP1-2	GLC7	K06269	Cytoplasm. Nucleus.	C
KLMA_60076	-5.2	2.7	0.004	protein STU2	STU2		Cytoplasm, cytoskeleton, spindle pole body. Cytoplasm, cytoskeleton, spindle.	S
KLMA_30274	-5.2	7.6	0.039	fumarate reductase			Mitochondrion. Cytoplasm.	S
KLMA_40131	-5.1	5.6	0.004	bud site selection protein RAX2	RAX2		Cell membrane; Single-pass type I membrane protein. Bud neck. Bud tip.	S
KLMA_10532	-5.1	7.9	0.034	tryptophan permease	TAT2		Membrane; Multi-pass membrane protein.	S
KLMA_60230	-5.1	5.3	0.018	transcription factor tau 55 kDa subunit	TFC7	K15206	Nucleus.	S
KLMA_10726	-5.0	3.3	0.003	mitochondrial protein PET191	PET191		Mitochondrion.	30X
KLMA_50494	-5.0	3.3	0.013	structure-specific endonuclease subunit SLX4	SLX4	K15079	Nucleus (By similarity).	S
KLMA_30249	-5.0	5.5	0.009	uncharacterized protein YOR051C	ETT1		Nucleus (By similarity).	S
KLMA_50409	-4.9	7.4	0.000	flo11 super family	MUC1	K01178	Secreted, cell wall (Probable). Membrane; Lipid-anchor, GPI-anchor (Potential).	30DS
KLMA_40162	-4.9	2.3	0.034	WD repeat-containing protein YDR128W	MTC5		Vacuole membrane; Peripheral membrane protein.	S
KLMA_80050	-4.8	6.9	0.049	homocysteine S-methyltransferase 2	SAM4	K00547	Cytoplasm. Nucleus.	S
KLMA_10683	-4.8	7.2	0.040	NAD(P)H-dependent D-xylose reductase	XYL1			S
KLMA_30085	-4.8	2.5	0.018	uncharacterized protein YOR296W			Cytoplasm.	S
KLMA_20515	-4.8	6.7	0.000	protein ISD11	ISD11		Mitochondrion.	30DS
KLMA_10437	-4.7	3.2	0.045	D-amino-acid oxidase	DAO1	K00273		S
KLMA_50415	-4.7	3.6	0.006	uncharacterized oxidoreductase YHL021C	AIM17		Mitochondrion.	S
KLMA_80130	-4.5	6.8	0.000	homoisocitrate dehydrogenase	LYS12	K05824	Mitochondrion.	C
KLMA_20830	-4.5	8.8	0.000	lactose permease	LAC12		Membrane; Multi-pass membrane protein.	30DS
KLMA_20294	-4.5	5.9	0.030	rab GDP-dissociation inhibitor	GDI1		Cytoplasm.	S
KLMA_10036	-4.5	5.5	0.001	pantothenate kinase	CAB1	K09680	Cytoplasm. Nucleus.	C
KLMA_30105	-4.4	8.4	0.001	acetolactate synthase	ILV2	K01652	Mitochondrion.	S
KLMA_40155	-4.4	2.6	0.026	ISWI one complex protein 2	IOC2		Nucleus.	S
KLMA_20194	-4.3	4.8	0.018	UPF0613 protein PB24D3.06c			Cytoplasm. Nucleus.	S
KLMA_20061	-4.3	4.4	0.011	nucleoporin NUP188	NUP188	K14311	Nucleus, nuclear pore complex. Nucleus membrane; Peripheral membrane protein; Cytoplasmic side. Nucleus membrane; Peripheral membrane protein; Nucleoplasmic side.	S
KLMA_30047	-4.3	6.8	0.047	phosphomethylpyrimidine kinase THI20	THI20	K00877		S
KLMA_20158	-4.3	10.0	0.000	alcohol dehydrogenase	ADH4	K13953	Mitochondrion matrix.	30X

Locus_tag	logFC	logCPM	FDR	Product	UniProt gene	KO number	Localization	Specific[a]
				4				
KLMA_10257	-4.3	3.9	0.006	ERAD-associated E3 ubiquitin-protein ligase HRD1	HRD1	K10601	Endoplasmic reticulum membrane; Multi-pass membrane protein (By similarity).	30X
KLMA_70189	-4.1	8.6	0.017	protein MMF1	MMF1		Mitochondrion matrix.	30DS
KLMA_50241	-4.1	7.4	0.001	pyridoxamine 5'-phosphate oxidase	PDX3	K00275		C
KLMA_40575	-4.1	7.7	0.032	endopolyphosphatase	PPN1	K06018	Vacuole membrane; Single-pass type II membrane protein.	S
KLMA_20723	-4.1	5.9	0.046	maltose O-acetyltransferase	maa			S
KLMA_20704	-4.1	9.8	0.000	CBM_21 super family	GAC1			30DS
KLMA_30640	-4.0	8.3	0.008	D-amino-acid oxidase	dao1			C
KLMA_10462	-4.0	12.4	0.000	enolase	ENO	K01689	Cytoplasm (By similarity).	S
KLMA_30337	-4.0	6.6	0.043	uncharacterized protein YMR196W				S
KLMA_20537	-4.0	7.6	0.045	PET20 super family	SUE1		Mitochondrion envelope.	S
KLMA_10572	-4.0	5.1	0.034	adenylyl cyclase-associated protein	SRV2		Cytoplasm, cytoskeleton, actin patch.	S
KLMA_10540	-3.9	8.7	0.001	phosphoglycerate kinase	PGK	K00927	Cytoplasm (By similarity).	S
KLMA_80074	-3.9	2.3	0.050	thiamine pathway transporter THI73	THI73		Endoplasmic reticulum membrane; Multi-pass membrane protein. Cell membrane; Multi-pass membrane protein (Probable).	S
KLMA_80059	-3.9	13.4	0.000	glyceraldehyde-3-phosphate dehydrogenase 3	GAP3	K00134	Cytoplasm (By similarity).	S
KLMA_40149	-3.9	9.1	0.000	hypothetical protein				30DS
KLMA_40218	-3.9	13.1	0.000	glyceraldehyde-3-phosphate dehydrogenase 1	GAP1	K00134	Cytoplasm (By similarity).	30DS
KLMA_70406	-3.8	3.4	0.031	protein NBA1	NBA1		Bud neck. Cytoplasm.	S
KLMA_10514	-3.8	10.4	0.000	branched-chain-amino-acid aminotransferase	BAT1	K00826	Mitochondrion matrix.	C
KLMA_40338	-3.8	8.2	0.047	ATP phosphoribosyltransferase	HIS1	K00765	Cytoplasm (By similarity).	S
KLMA_80118	-3.7	11.3	0.000	histone H4	HHF1	K11254	Nucleus (By similarity). Chromosome (By similarity).	S
KLMA_50531	-3.7	9.1	0.018	uncharacterized transporter YLR152C		K07088	Membrane; Multi-pass membrane protein.	30DS
KLMA_70312	-3.6	4.5	0.033	long-chain-fatty-acid--CoA ligase 2	FAA2	K01897	Cytoplasm. Mitochondrion.	S
KLMA_70068	-3.6	10.0	0.018	40S ribosomal protein S29	RPS29	K02980		S
KLMA_80322	-3.6	8.9	0.006	cytochrome c oxidase subunit 7		K02269		30DS
KLMA_50360	-3.6	9.5	0.001	hexose transporter 2	KHT2	K08139	Membrane; Multi-pass membrane protein.	S
KLMA_70443	-3.6	3.9	0.033	probable 2-methylcitrate dehydratase	PDH1	K01720		C
KLMA_50104	-3.5	7.3	0.028	alanyl-tRNA synthetase	ALA1	K01872	Isoform Cytoplasmic: Cytoplasm.Isoform Mitochondrial: Mitochondrion.	S
KLMA_10827	-3.5	5.6	0.006	MFS_1			Membrane; Multi-pass membrane protein.	30DS

Locus_tag	logFC	logCPM	FDR	Product	UniProt gene	KO number	Localization	Specific[a]
KLMA_70044	-3.5	9.8	0.001	sorbitol dehydrogenase 1	SOR1	K00008		30DS
KLMA_30198	-3.5	5.2	0.015	protein transport protein YIP1	YIP1		Endoplasmic reticulum membrane; Multi-pass membrane protein. Golgi apparatus membrane; Multi-pass membrane protein.	S
KLMA_20148	-3.5	8.0	0.008	actin-interacting protein 1	AIP1		Cytoplasm, cytoskeleton. Cytoplasm, cytoskeleton, actin patch.	S
KLMA_60042	-3.5	8.2	0.003	peroxisomal membrane protein PEX21	PEX21		Cytoplasm (By similarity). Peroxisome membrane; Peripheral membrane protein; Cytoplasmic side (By similarity).	30DS
KLMA_60129	-3.4	13.0	0.000	histone H3	HHT1	K11253	Nucleus (By similarity). Chromosome (By similarity).	30DS
KLMA_60128	-3.4	11.4	0.000	histone H4	HHF1	K11254	Nucleus (By similarity). Chromosome (By similarity).	S
KLMA_70118	-3.3	13.0	0.000	guanine nucleotide-binding protein subunit gamma		K07973	Membrane; Peripheral membrane protein (By similarity).	S
KLMA_80013	-3.3	8.0	0.008	uncharacterized dipeptidase C965.12		K01273		S
KLMA_20042	-3.3	8.7	0.003	acetyl-CoA hydrolase	ACH1	K01067	Cytoplasm (By similarity).	30DS
KLMA_20489	-3.3	9.0	0.013	GAL4-like Zn2Cys6 binuclear cluster DNA-binding domain				C
KLMA_40622	-3.3	11.7	0.000	hypothetical protein				C
KLMA_20063	-3.2	10.5	0.002	uncharacterized protein RSN1	RSN1		Membrane; Multi-pass membrane protein (Potential).	S
KLMA_10547	-3.2	8.7	0.005	high-affinity glucose transporter	HGT1		Membrane; Multi-pass membrane protein.	30DS
KLMA_70150	-3.2	5.8	0.045	methionine aminopeptidase 2	MAP2	K01265	Cytoplasm (By similarity).	S
KLMA_40135	-3.2	7.1	0.014	structural maintenance of chromosomes protein 4	SMC4	K06675	Nucleus. Cytoplasm. Chromosome.	S
KLMA_80174	-3.1	8.9	0.019	probable transporter AQR1	AQR1		Membrane; Multi-pass membrane protein.	C
KLMA_10100	-3.1	7.3	0.017	G1/S-specific cyclin CLN1	CCN1			S
KLMA_20821	-3.1	6.6	0.020	aminopeptidase Y	APE3	K01264	Vacuole.	S
KLMA_80225	-3.1	6.3	0.042	alpha-1,2-mannosyltransferase	KTR1	K10967	Golgi apparatus membrane; Single-pass type II membrane protein.	S
KLMA_40412	-3.0	4.2	0.038	uncharacterized protein YER079W				S
KLMA_30172	-3.0	7.0	0.038	UPF0675 protein YJL084C	ALY2		Cytoplasm.	S
KLMA_60379	-3.0	6.5	0.025	recQ-mediated genome instability protein 1	RMI1	K15364	Cytoplasm. Nucleus.	30DS
KLMA_10040	-2.9	19.0	0.000	uncharacterized protein YDR524C-B				30DS
KLMA_20832	-2.9	5.9	0.035	dethiobiotin synthetase	BIO4	K01935		30DS
KLMA_30331	-2.9	6.5	0.028	hypothetical protein				30DS
KLMA_50289	-2.9	9.2	0.007	vacuolar membrane protein YOR292C			Vacuole membrane; Multi-pass membrane protein.	30DS
KLMA_80026	-2.9	7.7	0.021	phosphoacetylglucosamine mutase	PCM1	K01836		S

Locus_tag	logFC	logCPM	FDR	Product	UniProt gene	KO number	Localization	Specific[a]
KLMA_50297	-2.9	6.4	0.039	threonine dehydratase	ILV1	K01754	Mitochondrion.	S
KLMA_20828	-2.9	6.6	0.040	rab proteins geranylgeranyltransferase component A	MRS6			S
KLMA_30029	-2.9	8.3	0.020	anthranilate synthase component 2	TRP3	K01656		S
KLMA_20582	-2.8	10.7	0.001	elongation factor 2	EFT1	K03234	Cytoplasm (By similarity).	S
KLMA_20333	-2.8	9.4	0.006	galactokinase	GAL1	K00849		30DS
KLMA_20324	-2.8	11.0	0.001	mitochondrial DNA replication protein YHM2	YHM2		Mitochondrion inner membrane; Multi-pass membrane protein.	S
KLMA_10558	-2.8	9.6	0.007	D-arabinitol 2-dehydrogenase [ribulose-forming]	ARDH			30DS
KLMA_80221	-2.7	8.2	0.023	ribose-5-phosphate isomerase	RKI1	K01807	Cytoplasm (Potential).	S
KLMA_40045	-2.7	11.5	0.001	ATPase-stabilizing factor 15 kDa protein	STF2		Mitochondrion.	30DS
KLMA_40621	-2.7	8.3	0.032	hypothetical protein				S
KLMA_60392	-2.6	9.4	0.009	uncharacterized protein YPL039W				C
KLMA_30724	-2.6	9.0	0.036	probable pyridoxine biosynthesis protein SNZ3	SNZ3	K06215		S
KLMA_50260	-2.6	9.5	0.016	cytochrome c peroxidase	CCP1	K00428	Mitochondrion matrix (By similarity).	S
KLMA_60075	-2.6	9.4	0.027	pyruvate decarboxylase	PDC1	K01568		S
KLMA_30719	-2.6	7.7	0.046	phosphoenolpyruvate carboxykinase [ATP]	PCK1	K01610		30DS
KLMA_30575	-2.6	5.8	0.049	actin patches distal protein 1	APD1		Cytoplasm. Nucleus.	S
KLMA_40253	-2.5	9.8	0.008	cytochrome c oxidase subunit 6	COX6	K02264	Mitochondrion inner membrane.	S
KLMA_20268	-2.5	10.8	0.006	40S ribosomal protein S2	RPS2	K02981	Cytoplasm. Nucleus, nucleolus.	S
KLMA_20299	-2.5	8.8	0.041	cytochrome c oxidase subunit 6A	COX13	K02266	Mitochondrion inner membrane.	S
KLMA_10179	-2.4	11.2	0.004	glycerol-3-phosphate dehydrogenase [NAD+] 1	GPD1	K00006		S
KLMA_60472	-2.4	9.5	0.020	altered inheritance rate of mitochondria protein 38	RCF2		Mitochondrion membrane; Multi-pass membrane protein.	S
KLMA_20100	-2.3	8.8	0.047	reduced viability upon starvation protein 161	RVS161		Cytoplasm, cytoskeleton.	30DS
KLMA_10425	-2.3	10.2	0.027	pre-mRNA-splicing factor RSE1	RSE1	K12830	Nucleus (By similarity).	S
KLMA_70054	-2.2	10.0	0.033	GTP-binding protein YPT1	YPT1	K07874	Endoplasmic reticulum membrane; Peripheral membrane protein. Golgi apparatus membrane; Peripheral membrane protein. Cytoplasm.	S
KLMA_50529	-2.2	9.5	0.037	HYALURONIC ACID-BINDING PROTEIN 4				S
KLMA_20220	-2.1	13.9	0.000	3-ketoacyl-CoA thiolase	POT1	K00632	Peroxisome.	30DS
KLMA_60499	-2.0	11.2	0.022	serine/threonine-protein phosphatase PP2A-1 catalytic	PPH21	K04382		S

Locus_tag	logFC	logCPM	FDR	Product	UniProt gene	KO number	Localization	Specific[a]
KLMA_50482	-1.8	11.5	0.036	subunit non-classical export protein 2	NCE102		Cell membrane; Multi-pass membrane protein.	30DS
KLMA_40174	-1.8	16.3	0.000	uncharacterized cell wall protein YDR134C				S
KLMA_70062	-1.7	11.5	0.048	covalently-linked cell wall protein 14				S
KLMA_80309	-1.3	12.8	0.029	elongation factor 1-alpha	TEF	K03231	Cytoplasm.	S

[a]Gene expression was significantly (FDR < 0.05) altered under the following conditions: S, 45D-specific down-regulation; C, commonly down-regulated under 30DS, 45D and 30X conditions; 30DS, down-regulated under 45D and 30DS conditions; 30X, down-regulated under 45D and 30X conditions.

Table S15 GO terms enriched in significantly up-regulated genes under 45D condition

GO.ID	Term	Annotated gene[a]	Significant[b]	Expected[c]	P-value[d]	Genes
GO:0034470	ncRNA processing	259	23	7.56	8.4e-07	BUD23, CGR1, CSL4, DBP10, DBP9, DHR2, GRC3, IMP4, LCP5, LSM2, PUS4, RPF2, RRP42, RRP5, RRS1, RTT10, SLX9, SPB1, THG1, TRM9, TUM1, UTP25, UTP6
GO:0042254	ribosome biogenesis	270	23	7.88	1.8e-06	BRX1, BUD23, CAM1, CGR1, CSL4, DBP10, DBP9, DHR2, GRC3, IMP4, LCP5, LSM2, NMD3, RPF2, RPL8B, RPS26A, RRP42, RRP5, RRS1, SLX9, SPB1, UTP25, UTP6
GO:0006364	rRNA processing	191	18	5.58	6.9e-06	BUD23, CGR1, CSL4, DBP10, DBP9, DHR2, GRC3, IMP4, LCP5, LSM2, RPF2, RRP42, RRP5, RRS1, SLX9, SPB1, UTP25, UTP6
GO:0022613	ribonucleoprotein complex biogenesis	317	24	9.26	8.3e-06	BRX1, BUD23, CAM1, CGR1, CSL4, DBP10, DBP9, DHR2, GRC3, IMP4, LCP5, LSM2, NMD3, PKH1, RPF2, RPL8B, RPS26A, RRP42, RRP5, RRS1, SLX9, SPB1, UTP25, UTP6
GO:0016072	rRNA metabolic process	196	18	5.72	1.0e-05	BUD23, CGR1, CSL4, DBP10, DBP9, DHR2, GRC3, IMP4, LCP5, LSM2, RPF2, RRP42, RRP5, RRS1, SLX9, SPB1, UTP25, UTP6
GO:0034660	ncRNA metabolic process	305	23	8.91	1.4e-05	BUD23, CGR1, CSL4, DBP10, DBP9, DHR2, GRC3, IMP4, LCP5, LSM2, PUS4, RPF2, RRP42, RRP5, RRS1, RTT10, SLX9, SPB1, THG1, TRM9, TUM1, UTP25, UTP6
GO:0006396	RNA processing	405	26	11.83	6.3e-05	BUD23, CGR1, CSL4, DBP10, DBP9, DHR2, GRC3, IMP4, LCP5, LSM2, PKH1, PUS4, RPF2, RRP42, RRP5, RRS1, RTT10, SLX9, SPB1, SPP2, SYF2, THG1, TRM9, TUM1, UTP25, UTP6
GO:0000466	maturation of 5.8S rRNA from tricistronic rRNA transcript (SSU-rRNA, 5.8S rRNA, LSU-rRNA)	46	7	1.34	0.00031	BUD23, CSL4, RPF2, RRP42, RRP5, RRS1, UTP6
GO:0000460	maturation of 5.8S rRNA	47	7	1.37	0.00036	BUD23, CSL4, RPF2, RRP42, RRP5,

GO.ID	Term	Annotated gene[a]	Significant[b]	Expected[c]	P-value[d]	Genes
						RRS1, UTP6
GO:0009451	RNA modification	53	7	1.55	0.00076	BUD23, LCP5, PUS4, SPB1, THG1, TRM9, TUM1
GO:0000469	cleavage involved in rRNA processing	39	6	1.14	0.00080	BUD23, CSL4, RRP42, RRP5, RRS1, UTP6
GO:0006231	dTMP biosynthetic process	2	2	0.06	0.00084	CDC21, DCD1
GO:0046073	dTMP metabolic process	2	2	0.06	0.00084	CDC21, DCD1
GO:0034641	cellular nitrogen compound metabolic process	1463	59	42.72	0.00085	ARG82, ASN1, BUD23, CAM1, CAR1, CDC13, CDC21, CDC9, CDD1, CGR1, CSL4, CTF8, DAL1, DAS2, DBP10, DBP9, DCD1, DFR1, DHR2, DNA2, FMP30, GRC3, HIS5, IMP4, KLMA_20616, LCP5, LSM2, MCM4, MEC3, NMD4, OAF3, PCC1, PHR1, PKH1, POL4, PSD1, PUS4, RKR1, RPC19, RPF2, RRN10, RRP42, RRP5, RRS1, RTT10, SLN1, SLX9, SPB1, SPP2, SPT6, SYF2, TAH11, TEL1, THG1, TRM9, TUM1, UNG1, UTP25, UTP6
GO:0090501	RNA phosphodiester bond hydrolysis	40	6	1.17	0.00092	BUD23, CSL4, RRP42, RRP5, RRS1, UTP6
GO:0006139	nucleobase-containing compound metabolic process	1330	54	38.84	0.00158	ARG82, BUD23, CAM1, CDC13, CDC21, CDC9, CDD1, CGR1, CSL4, CTF8, DAL1, DAS2, DBP10, DBP9, DCD1, DFR1, DHR2, DNA2, GRC3, IMP4, KLMA_20616, LCP5, LSM2, MCM4, MEC3, NMD4, OAF3, PCC1, PHR1, PKH1, POL4, PUS4, RKR1, RPC19, RPF2, RRN10, RRP42, RRP5, RRS1, RTT10, SLN1, SLX9, SPB1, SPP2, SPT6, SYF2, TAH11, TEL1, THG1, TRM9, TUM1, UNG1, UTP25, UTP6
GO:0090304	nucleic acid metabolic process	1152	48	33.64	0.00209	ARG82, BUD23, CAM1, CDC13, CDC9, CGR1, CSL4, CTF8, DBP10, DBP9, DHR2, DNA2, GRC3, IMP4, KLMA_20616, LCP5, LSM2, MCM4, MEC3, NMD4, OAF3, PCC1, PHR1, PKH1, POL4, PUS4, RKR1, RPC19, RPF2, RRN10, RRP42, RRP5, RRS1, RTT10, SLN1, SLX9, SPB1, SPP2, SPT6, SYF2, TAH11, TEL1, THG1, TRM9, TUM1, UNG1, UTP25, UTP6
GO:0046483	heterocycle metabolic process	1414	56	41.29	0.00227	ARG82, BUD23, CAM1, CDC13, CDC21, CDC9, CDD1, CGR1, CSL4, CTF8, DAL1, DAS2, DBP10, DBP9, DCD1, DFR1, DHR2, DNA2, GRC3, HIS5, IMP4, KLMA_20616, LCP5, LIPB, LSM2, MCM4, MEC3, NMD4, OAF3, PCC1, PHR1, PKH1, POL4, PUS4, RKR1, RPC19, RPF2, RRN10, RRP42, RRP5, RRS1, RTT10, SLN1, SLX9, SPB1, SPP2, SPT6, SYF2, TAH11, TEL1, THG1, TRM9, TUM1, UNG1, UTP25, UTP6
GO:0009157	deoxyribonucleoside monophosphate biosynthetic process	3	2	0.09	0.00249	CDC21, DCD1
GO:0009162	deoxyribonucleoside monophosphate metabolic process	3	2	0.09	0.00249	CDC21, DCD1
GO:0009176	pyrimidine deoxyribonucleoside	3	2	0.09	0.00249	CDC21, DCD1

GO.ID	Term	Annotated gene[a]	Significant[b]	Expected[c]	P-value[d]	Genes
	monophosphate metabolic process					
GO:0009177	pyrimidine deoxyribonucleoside monophosphate biosynthetic process	3	2	0.09	0.00249	CDC21, DCD1
GO:0006807	nitrogen compound metabolic process	1621	62	47.33	0.00255	ARG82, ASN1, BUD23, CAM1, CAR1, CDC13, CDC21, CDC9, CDD1, CGR1, CSL4, CTF8, DAL1, DAS2, DBP10, DBP9, DCD1, DFR1, DHR2, DNA2, FMP30, GRC3, HIS5, IMP4, KEI1, KLMA_20616, LCP5, LSM2, LYS21, MCM4, MEC3, NIT3, NMD4, OAF3, PCC1, PHR1, PKH1, POL4, PSD1, PUS4, RKR1, RPC19, RPF2, RRN10, RRP42, RRP5, RRS1, RTT10, SLN1, SLX9, SPB1, SPP2, SPT6, SYF2, TAH11, TEL1, THG1, TRM9, TUM1, UNG1, UTP25, UTP6
GO:1901360	organic cyclic compound metabolic process	1454	57	42.46	0.00258	ARG82, BUD23, CAM1, CDC13, CDC21, CDC9, CDD1, CGR1, CSL4, CTF8, DAL1, DAS2, DBP10, DBP9, DCD1, DFR1, DHR2, DNA2, GRC3, HIS5, IMP4, KLMA_20616, LCP5, LIPB, LSM2, MCM4, MEC3, NCP1, NMD4, OAF3, PCC1, PHR1, PKH1, POL4, PUS4, RKR1, RPC19, RPF2, RRN10, RRP42, RRP5, RRS1, RTT10, SLN1, SLX9, SPB1, SPP2, SPT6, SYF2, TAH11, TEL1, THG1, TRM9, TUM1, UNG1, UTP25, UTP6
GO:0006725	cellular aromatic compound metabolic process	1395	55	40.74	0.00294	ARG82, BUD23, CAM1, CDC13, CDC21, CDC9, CDD1, CGR1, CSL4, CTF8, DAL1, DAS2, DBP10, DBP9, DCD1, DFR1, DHR2, DNA2, GRC3, HIS5, IMP4, KLMA_20616, LCP5, LSM2, MCM4, MEC3, NMD4, OAF3, PCC1, PHR1, PKH1, POL4, PUS4, RKR1, RPC19, RPF2, RRN10, RRP42, RRP5, RRS1, RTT10, SLN1, SLX9, SPB1, SPP2, SPT6, SYF2, TAH11, TEL1, THG1, TRM9, TUM1, UNG1, UTP25, UTP6
GO:0000447	endonucleolytic cleavage in ITS1 to separate SSU-rRNA from 5.8S rRNA and LSU-rRNA from tricistronic rRNA transcript (SSU-rRNA, 5.8S rRNA, LSU-rRNA)	23	4	0.67	0.00396	BUD23, RRP5, RRS1, UTP6
GO:0000478	endonucleolytic cleavage involved in rRNA processing	23	4	0.67	0.00396	BUD23, RRP5, RRS1, UTP6
GO:0000479	endonucleolytic cleavage of tricistronic rRNA transcript (SSU-rRNA, 5.8S rRNA, LSU-rRNA)	23	4	0.67	0.00396	BUD23, RRP5, RRS1, UTP6
GO:0090502	RNA phosphodiester bond hydrolysis, endonucleolytic	24	4	0.7	0.00465	BUD23, RRP5, RRS1, UTP6
GO:0000301	retrograde transport, vesicle recycling within Golgi	4	2	0.12	0.00488	COG3, RUD3
GO:0009219	pyrimidine deoxyribonucleotide metabolic process	4	2	0.12	0.00488	CDC21, DCD1
GO:0009221	pyrimidine	4	2	0.12	0.00488	CDC21, DCD1

GO.ID	Term	Annotated gene[a]	Significant[b]	Expected[c]	P-value[d]	Genes
	deoxyribonucleotide biosynthetic process					
GO:0009265	2'-deoxyribonucleotide biosynthetic process	4	2	0.12	0.00488	CDC21, DCD1
GO:0009394	2'-deoxyribonucleotide metabolic process	4	2	0.12	0.00488	CDC21, DCD1
GO:0019692	deoxyribose phosphate metabolic process	4	2	0.12	0.00488	CDC21, DCD1
GO:0046385	deoxyribose phosphate biosynthetic process	4	2	0.12	0.00488	CDC21, DCD1
GO:0009129	pyrimidine nucleoside monophosphate metabolic process	13	3	0.38	0.00559	CDC21, DAS2, DCD1
GO:0009130	pyrimidine nucleoside monophosphate biosynthetic process	13	3	0.38	0.00559	CDC21, DAS2, DCD1
GO:0006284	base-excision repair	14	3	0.41	0.00697	CDC9, POL4, UNG1
GO:0000462	maturation of SSU-rRNA from tricistronic rRNA transcript (SSU-rRNA, 5.8S rRNA, LSU-rRNA)	44	5	1.28	0.00848	BUD23, DHR2, RRP5, RRS1, UTP6
GO:0000956	nuclear-transcribed mRNA catabolic process	63	6	1.84	0.00948	CSL4, KLMA_20616, LSM2, NMD4, PKH1, RRP42
GO:0006402	mRNA catabolic process	63	6	1.84	0.00948	CSL4, KLMA_20616, LSM2, NMD4, PKH1, RRP42

[a]The number of GO term annotated genes in the *K. marxianus* genome.
[b]The number of GO term annotated genes, which were significantly (FDR < 0.05) expressed under the condition.
[c]The expected value of Fisher's exact test.
[d]The P-value of Fisher's exact test.

Table S16 Summary of significantly up-regulated genes under the 45D condition

Locus_tag	logFC	logCPM	FDR	Product	UniProt gene	KO number	Localization	Specific[a]
KLMA_R308	19.1	8.6	0.000	Lys-tRNA				30DS
KLMA_80413	18.1	9.5	0.000	60S ribosomal protein L8-B	RPL8B	K02936	Cytoplasm.	C
KLMA_R519	17.7	7.2	0.000	Gly-tRNA				30DS
KLMA_20492	16.5	6.0	0.000	40S ribosomal protein S26-A	RPS26A	K02976	Cytoplasm.	S
KLMA_R413	16.0	5.5	0.001	Arg-tRNA				S
KLMA_70354	15.6	6.2	0.001	ADP,ATP carrier protein	AAC	K05863	Mitochondrion inner membrane; Multi-pass membrane protein.	30DS
KLMA_10783	15.0	7.0	0.000	sorbose reductase SOU1	SOU1			C
KLMA_R127	15.0	4.9	0.000	Val-tRNA				C
KLMA_R803	15.0	4.5	0.000	Gly-tRNA				S
KLMA_40221	14.8	5.4	0.002	40S ribosomal protein S9	MRPS9		Mitochondrion (Potential).	30X
KLMA_R416	14.8	4.5	0.000	Val-tRNA				C
KLMA_20616	14.7	4.4	0.001	uncharacterized protein YDR370C			Cytoplasm.	30DS
KLMA_30150	14.6	4.1	0.001	uncharacterized phosphatase YNL010W			Cytoplasm. Nucleus.	S
KLMA_R805	14.4	4.0	0.001	Leu-tRNA				30X
KLMA_R322	14.3	4.0	0.000	Gln-tRNA				C

Locus_tag	logFC	logCPM	FDR	Product	UniProt gene	KO number	Localization	Specific[a]
KLMA_R404	14.3	3.8	0.000	Leu-tRNA				S
KLMA_R111	14.0	3.5	0.001	Arg-tRNA				S
KLMA_20293	14.0	4.2	0.001	U6 snRNA-associated Sm-like protein LSm2	LSM2	K12621	Nucleus. Cytoplasm (Probable).	30X
KLMA_R113	13.9	3.4	0.001	Ala-tRNA				S
KLMA_R815	13.9	3.4	0.001	His-tRNA				S
KLMA_R311	13.8	3.3	0.001	Gln-tRNA				S
KLMA_R122	13.6	3.1	0.004	Met-tRNA				S
KLMA_30371	13.5	5.8	0.030	calcium/calmodulin-dependent protein kinase II	CMK2	K00908		30DS
KLMA_30641	13.4	6.2	0.004	probable hydrolase NIT3	NIT3			C
KLMA_R806	13.2	2.7	0.001	Lys-tRNA				S
KLMA_R102	13.0	2.5	0.002	Glu-tRNA				S
KLMA_R411	12.9	2.9	0.002	Leu-tRNA				30X
KLMA_R602	12.8	2.8	0.000	Ala-tRNA				C
KLMA_R220	12.5	2.1	0.001	Met-tRNA				S
KLMA_60474	12.4	4.5	0.001	putative methyltransferase BUD23	BUD23		Cytoplasm. Nucleus.	C
KLMA_20507	12.3	2.3	0.021	uncharacterized protein YGR127W				S
KLMA_20394	12.3	1.8	0.006	actin-related protein 2/3 complex subunit 2	ARC35	K05758	Cytoplasm, cytoskeleton, actin patch.	S
KLMA_R508	12.1	1.6	0.009	Asn-tRNA				S
KLMA_R608	12.1	1.7	0.000	Met-tRNA				30DS
KLMA_R225	12.0	1.5	0.006	Gln-tRNA				S
KLMA_R110	11.8	1.8	0.001	Ala-tRNA				30X
KLMA_R601	11.7	1.4	0.005	Ala-tRNA				S
KLMA_R812	11.6	1.1	0.037	Arg-tRNA				S
KLMA_20496	11.6	2.5	0.005	hypothetical protein		K11098		C
KLMA_50300	11.5	5.9	0.001	hypothetical protein				30X
KLMA_50196	11.5	1.0	0.003	1,3-beta-glucanosyltransferase GAS2	GAS2		Cell membrane; Lipid-anchor, GPI-anchor (By similarity).	S
KLMA_20072	11.5	2.0	0.036	hypothetical conserved protein				S
KLMA_80165	11.2	1.6	0.048	histidinol-phosphate aminotransferase	HIS5	K00817		S
KLMA_60493	11.1	3.8	0.033	homocitrate synthase	LYS21	K01655	Mitochondrion (Potential).	C
KLMA_R525	10.8	5.9	0.001	Leu-tRNA				S
KLMA_30167	10.7	2.1	0.001	hypothetical protein				C
KLMA_R814	10.5	0.1	0.026	Asn-tRNA				S
KLMA_80091	10.3	5.9	0.004	exosome complex component RRP42	RRP42	K12589	Cytoplasm. Nucleus, nucleolus.	30DS
KLMA_20439	9.8	0.1	0.035	protein GRC3	GRC3	K06947	Nucleus, nucleolus (By similarity).	S
KLMA_60403	9.7	6.1	0.000	putative elongation factor 1 gamma homolog	CAM1	K03233	Cytoplasm. Nucleus.	C
KLMA_30374	8.7	3.8	0.006	conserved oligomeric Golgi complex subunit 3	COG3		Golgi apparatus membrane; Peripheral membrane protein; Cytoplasmic side.	S
KLMA_R524	8.6	3.2	0.029	Thr-tRNA				S
KLMA_R406	8.5	9.3	0.000	Thr-tRNA				S
KLMA_30716	8.3	5.0	0.001	polarized growth chromatin-	PCC1		Nucleus (Probable). Chromosome, telomere	S

Locus_tag	logFC	logCPM	FDR	Product	UniProt gene	KO number	Localization	Specific[a]
				associated controller 1			(Probable).	
KLMA_R123	7.9	2.9	0.000	Ala-tRNA				S
KLMA_R117	7.8	1.3	0.039	Val-tRNA				S
KLMA_10516	7.6	4.0	0.019	polygalacturonase	PGU1	K01184		C
KLMA_R521	7.5	5.4	0.000	Thr-tRNA				S
KLMA_R317	7.4	8.7	0.006	Ala-tRNA				S
KLMA_80402	7.3	4.4	0.008	probable 26S proteasome complex subunit SEM1		K10881		30X
KLMA_50617	7.3	6.0	0.000	Golgin IMH1				S
KLMA_20626	7.3	2.9	0.000	mitochondrial DnaJ homolog 2	MDJ2		Mitochondrion inner membrane.	C
KLMA_R226	7.3	6.4	0.006	Ala-tRNA				S
KLMA_70295	7.0	3.2	0.044	mitochondrial import receptor subunit TOM5				S
KLMA_20752	6.8	6.5	0.000	deoxycytidylate deaminase	DCD1	K01493		30DS
KLMA_20051	6.8	4.3	0.000	rRNA-processing protein CGR1	CGR1	K14822	Nucleus, nucleolus (By similarity).	C
KLMA_10151	6.8	2.8	0.044	protein ECM25	ECM25		Cytoplasm.	S
KLMA_30567	6.7	2.8	0.000	uncharacterized protein YMR098C	ATP25		Mitochondrion inner membrane; Peripheral membrane protein; Matrix side (By similarity).	30DS
KLMA_R304	6.5	5.0	0.000	Val-tRNA				S
KLMA_70050	6.4	0.2	0.017	probable metabolite transport protein YFL040W			Membrane; Multi-pass membrane protein.	S
KLMA_R120	6.4	4.6	0.022	Gly-tRNA				S
KLMA_30140	6.3	9.2	0.041	factor RRN10	RRN10	K15221	Nucleus, nucleolus.	S
KLMA_70041	6.2	2.2	0.012	regulator of free ubiquitin chains 1	RFU1		Endosome (By similarity).	S
KLMA_R211	6.1	5.7	0.000	Ala-tRNA				S
KLMA_40596	6.1	6.2	0.004	serine/threonine-protein phosphatase PP-Z1	PPZ1	K01090		S
KLMA_R516	6.1	5.3	0.002	Thr-tRNA				S
KLMA_R208	6.1	3.6	0.001	Leu-tRNA				S
KLMA_10209	6.0	5.0	0.020	ATP-dependent RNA helicase DBP9	DBP9	K14810	Nucleus, nucleolus (By similarity).	S
KLMA_20271	5.9	0.2	0.049	zinc finger DNA binding domain				S
KLMA_R421	5.8	1.8	0.042	Lys-tRNA				S
KLMA_R809	5.8	3.4	0.000	Ser-tRNA				S
KLMA_40375	5.7	4.3	0.002	U3 small nucleolar ribonucleoprotein protein IMP4	IMP4	K14561	Nucleus, nucleolus.	30DS
KLMA_10814	5.7	6.7	0.001	oxidored-like super family			Mitochondrion.	S
KLMA_R804	5.7	5.1	0.014	Thr-tRNA				S
KLMA_R104	5.7	4.5	0.000	Ser-tRNA				S
KLMA_70304	5.7	6.3	0.000	transcription elongation factor SPT6	SPT6	K11292	Nucleus (By similarity).	C
KLMA_R204	5.6	3.2	0.014	Pro-tRNA				S
KLMA_10197	5.6	8.1	0.000	flocculation protein FLO5	FLO5		Secreted, cell wall. Membrane; Lipid-anchor,	30X

Locus_tag	logFC	logCPM	FDR	Product	UniProt gene	KO number	Localization	Specific[a]
							GPI-anchor (Potential).	
KLMA_20221	5.5	4.4	0.002	thiamine transporter	THI72	K03457	Membrane; Multi-pass membrane protein.	S
KLMA_R103	5.4	5.3	0.002	Ala-tRNA				S
KLMA_R115	5.4	2.0	0.045	Thr-tRNA				S
KLMA_50212	5.4	5.2	0.015	tRNA(His) guanylyltransferase	THG1	K10761		S
KLMA_10803	5.3	3.1	0.034	N-acyl-phosphatidylethanolamine-hydrolyzing phospholipase D	FMP30		Mitochondrion membrane; Single-pass membrane protein (Potential).	S
KLMA_50229	5.3	5.6	0.016	putative uridine kinase YDR020C	DAS2		Cytoplasm. Nucleus.	30DS
KLMA_60046	5.3	7.0	0.003	uncharacterized protein YGR237C				30X
KLMA_R811	5.3	4.5	0.000	Thr-tRNA				S
KLMA_R318	5.2	3.4	0.005	Pro-tRNA				S
KLMA_50201	5.2	4.8	0.001	ribonucleases P/MRP protein subunit POP6		K14524		C
KLMA_R124	5.2	6.0	0.000	Asn-tRNA				S
KLMA_R412	5.2	5.0	0.006	Asp-tRNA				S
KLMA_R301	5.2	4.7	0.000	Thr-tRNA				S
KLMA_30657	5.1	5.7	0.000	protein ERD1	ERD1		Endoplasmic reticulum membrane; Multi-pass membrane protein.	S
KLMA_R302	5.0	3.1	0.034	Val-tRNA				S
KLMA_R504	5.0	7.1	0.001	Asp-tRNA				S
KLMA_40508	5.0	2.2	0.045	chromosome transmission fidelity protein 8	CTF8	K11270	Nucleus.	S
KLMA_20313	4.9	1.5	0.030	uncharacterized protein YMR244W			Membrane; Single-pass membrane protein (Potential).	S
KLMA_80396	4.8	5.2	0.034	UPF0596 Golgi apparatus membrane protein YDR367W	KEI1		Golgi apparatus membrane; Multi-pass membrane protein.	S
KLMA_50242	4.8	0.6	0.043	protein RAD61				S
KLMA_R901	4.8	2.9	0.017	Tyr-tRNA				S
KLMA_40579	4.8	4.4	0.000	U3 small nucleolar RNA-associated protein 6	UTP6	K14557	Nucleus, nucleolus.	S
KLMA_60349	4.8	4.5	0.001	spindle pole body component SPC105	SPC105	K11563	Cytoplasm, cytoskeleton, spindle pole body. Nucleus membrane; Peripheral membrane protein; Nucleoplasmic side. Chromosome, centromere, kinetochore.	C
KLMA_30083	4.7	4.4	0.036	regulator of ribosome biosynthesis	RRS1	K14852	Nucleus.	S
KLMA_50574	4.7	4.6	0.026	uncharacterized membrane protein YLR241W			Membrane; Multi-pass membrane protein.	S
KLMA_90008	4.7	1.8	0.029	cytochrome c oxidase subunit 1	COX1	K02256	Mitochondrion inner membrane; Multi-pass membrane protein.	S
KLMA_60269	4.7	4.5	0.011	lysine-rich arabinogalactan protein 19				S

Locus_tag	logFC	logCPM	FDR	Product	UniProt gene	KO number	Localization	Specific[a]
KLMA_10192	4.6	1.2	0.041	allantoinase	DAL1	K01466		S
KLMA_30303	4.6	5.4	0.001	cell division control protein 54	MCM4	K02212	Nucleus (By similarity).	S
KLMA_70154	4.5	3.5	0.006	serine/threonine-protein kinase TEL1	TEL1	K04728	Nucleus (By similarity). Chromosome, telomere (By similarity).	S
KLMA_30711	4.5	2.3	0.031	osmosensing histidine protein kinase SLN1	SLN1	K11231	Cell membrane; Multi-pass membrane protein (Potential).	S
KLMA_60179	4.5	4.5	0.008	probable ATP-dependent RNA helicase DHR2	DHR2	K14781	Nucleus, nucleolus.	30DS
KLMA_10730	4.5	7.3	0.012	mito_carr super family				S
KLMA_50285	4.4	3.6	0.006	nonsense-mediated decay protein 4	NMD4		Cytoplasm (By similarity).	S
KLMA_20751	4.4	5.5	0.001	phosphatidylserine decarboxylase proenzyme 1	PSD1	K01613	Mitochondrion inner membrane.	30DS
KLMA_50024	4.3	5.6	0.001	arginase	CAR1	K01476	Cytoplasm (By similarity).	S
KLMA_10711	4.3	4.8	0.004	hypothetical protein	TAH11	K12414	Cytoplasm. Nucleus.	S
KLMA_50291	4.3	2.8	0.017	rRNA biogenesis protein RRP5	RRP5	K14792	Nucleus, nucleolus.	30DS
KLMA_60236	4.2	4.3	0.025	DNA-directed RNA polymerases I and III subunit RPAC2	RPC19	K03020	Nucleus, nucleolus.	S
KLMA_20604	4.2	4.1	0.004	isoamyl acetate-hydrolyzing esterase	IAH1			S
KLMA_50097	4.2	2.6	0.018	hypothetical protein				S
KLMA_20725	4.2	5.6	0.019	NADPH--cytochrome P450 reductase	NCP1	K00327	Endoplasmic reticulum membrane; Single-pass membrane protein. Mitochondrion outer membrane; Single-pass membrane protein. Cell membrane; Single-pass membrane protein. Microsome.	30DS
KLMA_10363	4.2	6.6	0.001	uncharacterized transcriptional regulatory protein YKR064W	OAF3		Cytoplasm (By similarity). Nucleus (By similarity). Mitochondrion (By similarity).	S
KLMA_50581	4.1	2.8	0.011	octanoyltransferase	LIPB	K03801	Mitochondrion (Probable).	S
KLMA_40600	4.1	5.4	0.027	tRNA (uracil-5-)-methyltransferase TRM9	TRM9	K15444	Cytoplasm. Nucleus.	S
KLMA_40391	4.1	6.9	0.005	malate dehydrogenase	MDH2	K00026	Cytoplasm.	C
KLMA_40320	4.0	6.1	0.009	uncharacterized protein YOL098C		K06972		S
KLMA_50622	4.0	5.7	0.002	exosome complex component CSL4	CSL4	K07573	Cytoplasm. Nucleus, nucleolus.	S
KLMA_30442	4.0	6.2	0.005	F-box protein YDR306C				S
KLMA_30691	4.0	4.9	0.005	conserved hypothetical protein	KEG1		Endoplasmic reticulum membrane; Multi-pass membrane protein.	S
KLMA_50600	4.0	6.0	0.001	uncharacterized protein YNL213C	RRG9		Mitochondrion (By similarity).	S
KLMA_70395	3.9	4.5	0.005	tRNA pseudouridine	PUS4	K03177	Nucleus. Mitochondrion.	C

Locus_tag	logFC	logCPM	FDR	Product	UniProt gene	KO number	Localization	Specific[a]
				synthase 4				
KLMA_80126	3.8	8.1	0.001	uncharacterized protein YIL091C	UTP25	K14774	Nucleus, nucleolus (By similarity).	30DS
KLMA_R224	3.8	5.3	0.003	Gln-tRNA				S
KLMA_60359	3.8	6.7	0.003	spindle assembly checkpoint component MAD1	MAD1	K06679	Nucleus (By similarity).	S
KLMA_60500	3.8	4.7	0.003	probable allantoinase 1				S
KLMA_R105	3.7	5.1	0.011	Leu-tRNA				S
KLMA_40589	3.7	4.3	0.006	uracil-DNA glycosylase	UNG1	K03648	Mitochondrion. Nucleus.	S
KLMA_R209	3.7	4.6	0.049	Gly-tRNA				S
KLMA_10284	3.7	3.4	0.020	hypothetical protein	SPP2		Nucleus (By similarity).	S
KLMA_10366	3.7	5.6	0.014	hypothetical protein				S
KLMA_40529	3.7	7.4	0.046	transcriptional regulatory protein ASH1				S
KLMA_20410	3.7	6.6	0.013	protein transport protein USE1	USE1	K08507	Endoplasmic reticulum membrane; Single-pass type IV membrane protein.	S
KLMA_80011	3.6	6.0	0.004	deoxyribodipyrimidine photo-lyase	PHR1	K01669	Nucleus. Mitochondrion.	30X
KLMA_60322	3.6	3.9	0.027	TEL2-interacting protein 1	TTI1		Cytoplasm. Nucleus (Probable).	S
KLMA_40215	3.6	7.0	0.006	cell division control protein 13	CDC13	K11115	Chromosome, telomere.	30X
KLMA_20803	3.5	4.0	0.031	GRIP domain-containing protein RUD3	RUD3		Golgi apparatus lumen.	S
KLMA_50458	3.5	6.8	0.006	uncharacterized protein YGR111W				30DS
KLMA_10290	3.5	5.3	0.005	IBN_N super family	SXM1		Cytoplasm. Nucleus, nuclear pore complex.	S
KLMA_30020	3.5	5.7	0.017	AP-1 accessory protein LAA1				S
KLMA_20813	3.5	8.9	0.002	tyrosine-protein phosphatase 2	PTP2	K01104	Cytoplasm. Nucleus.	C
KLMA_10418	3.5	5.2	0.009	ribosome biogenesis protein RPF2	RPF2	K14847	Nucleus, nucleolus.	30DS
KLMA_80364	3.5	6.7	0.009	diphthamide biosynthesis protein 3	DPH3	K15455	Cytoplasm (By similarity). Nucleus (By similarity).	S
KLMA_50277	3.5	3.8	0.019	conserved hypothetical protein			Nucleus (Potential).	30X
KLMA_20193	3.5	5.4	0.009	peroxisomal long-chain fatty acid import protein 2	PXA1	K15628	Peroxisome membrane; Multi-pass membrane protein.	30X
KLMA_10277	3.4	4.9	0.012	hypothetical protein				S
KLMA_30272	3.4	5.6	0.014	DUF676 super family[cl10636]			Lipid droplet. Membrane; Single-pass membrane protein (Potential).	S
KLMA_60347	3.4	2.5	0.033	uncharacterized WD repeat-containing protein YPL183C	RTT10		Cytoplasm. Endosome.	S
KLMA_10414	3.4	3.8	0.026	thymidylate synthase	CDC21	K00560	Nucleus.	30DS
KLMA_20779	3.4	7.0	0.007	dihydrofolate reductase	DFR1	K00287		S
KLMA_50131	3.3	6.7	0.015	uncharacterized protein YLR290C			Mitochondrion.	S

Locus_tag	logFC	logCPM	FDR	Product	UniProt gene	KO number	Localization	Specific[a]
KLMA_30560	3.3	6.8	0.011	RING finger protein YMR247C	RKR1		Nucleus.	S
KLMA_30086	3.3	6.7	0.019	meiotically up-regulated gene 14 protein	mug14		Cytoplasm. Nucleus.	S
KLMA_40432	3.3	5.1	0.015	60S ribosomal export protein NMD3	NMD3	K07562	Cytoplasm. Nucleus, nucleoplasm.	30DS
KLMA_20509	3.2	6.5	0.012	pre-mRNA-splicing factor SYF2	SYF2	K12868	Nucleus (By similarity).	S
KLMA_20535	3.2	6.6	0.011	ubiquitin-conjugating enzyme E2-21 kDa		K10689		S
KLMA_30507	3.2	5.1	0.014	ribosome biogenesis protein SLX9	SLX9	K14804	Nucleus, nucleolus (By similarity).	S
KLMA_60277	3.1	5.2	0.014	ATP-dependent RNA helicase DBP10	DBP10	K14808	Nucleus, nucleolus (By similarity).	30DS
KLMA_10031	3.1	4.2	0.026	adoMet-dependent rRNA methyltransferase SPB1	SPB1	K14857	Nucleus, nucleolus (By similarity).	30DS
KLMA_10328	3.1	5.7	0.025	DNA replication ATP-dependent helicase DNA2	DNA2	K10742	Nucleus. Chromosome.	30DS
KLMA_60136	3.0	4.3	0.035	ribosome biogenesis protein BRX1	BRX1	K14820	Nucleus, nucleolus.	30DS
KLMA_20219	3.0	6.7	0.037	BNI1-related protein 1	BNR1			30X
KLMA_50518	3.0	3.8	0.036	ribonuclease MRP protein subunit RMP1		K14532		S
KLMA_10221	3.0	3.7	0.046	DNA damage checkpoint control protein MEC3	MEC3	K02544	Nucleus (Potential).	S
KLMA_30690	3.0	5.9	0.017	ER-localized J domain-containing protein 5	ERJ5		Endoplasmic reticulum membrane; Single-pass type I membrane protein.	S
KLMA_10542	2.9	7.6	0.038	HAD_like super family				S
KLMA_50565	2.9	5.9	0.049	cytidine deaminase	CDD1	K01489		S
KLMA_10541	2.9	7.7	0.034	DNA polymerase IV	POL4	K10981	Nucleus.	S
KLMA_50536	2.9	4.1	0.046	inositol polyphosphate multikinase	ARG82	K00328	Nucleus.	S
KLMA_40337	2.8	6.8	0.039	protein SYG1	SYG1		Cell membrane; Multi-pass membrane protein.	S
KLMA_70281	2.8	10.9	0.019	asparagine synthetase [glutamine-hydrolyzing] 1	ASN1	K01953		S
KLMA_30143	2.7	10.4	0.011	protein YIP4	YIP4		Golgi apparatus membrane; Multi-pass membrane protein.	S
KLMA_10082	2.7	5.1	0.041	protein PLM2	PLM2		Nucleus (Probable).	C
KLMA_70415	2.7	8.2	0.036	U3 small nucleolar ribonucleoprotein protein LCP5	LCP5	K14765	Nucleus, nucleolus.	30DS
KLMA_10608	2.7	6.6	0.045	hypothetical protein				S
KLMA_50322	2.6	9.2	0.038	DNA ligase 1	CDC9	K10747	Isoform Mitochondrial: Mitochondrion.	S

Locus_tag	logFC	logCPM	FDR	Product	UniProt gene	KO number	Localization	Specific[a]
KLMA_30602	2.6	7.7	0.048	acetyl-coenzyme A synthetase 1	ACS1	K01895	Microsome (Potential). Endoplasmic reticulum (Potential).	30X
KLMA_30449	2.5	7.1	0.047	putative thiosulfate sulfurtransferase	TUM1	K01011	Mitochondrion. Cytoplasm.	S
KLMA_80265	2.5	7.3	0.047	probable serine/threonine-protein kinase YOL100W	PKH1			S
KLMA_30555	2.4	11.3	0.003	conserved hypothetical transmembrane protein				30X
KLMA_20427	2.2	10.5	0.030	hypothetical protein				30X

[a]Gene expression was significantly (FDR < 0.05) altered under the following conditions: S, 45D-specific up-regulation; C, commonly up-regulated under 30DS, 45D and 30X conditions; 30DS, up-regulated under 45D and 30DS conditions; 30X, up-regulated under 45D and 30X conditions.

Table S17 Subcellular localization of products of significantly expressed genes

Description	30DS_up		30DS_down		45D_up		45D_down		30X_up		30X_down	
Nucleus	64	40.3%	12	7.8%	33	16.6%	55	10.8%	11	12.4%	3	3.8%
Cytoplasm, nucleus	23	14.5%	14	9.1%	15	7.5%	47	9.3%	6	6.7%	11	13.9%
Membrane	3	1.9%	26	16.9%	9	4.5%	53	10.4%	10	11.2%	8	10.1%
Cytoplasm	15	9.4%	13	8.4%	8	4.0%	66	13.0%	7	7.9%	6	7.6%
Mitochondrion	7	4.4%	8	5.2%	7	3.5%	39	7.7%	4	4.5%	9	11.4%
Peroxisome, ER, golgi (membrane)	1	0.6%	3	1.9%	7	3.5%	30	5.9%	1	1.1%	3	3.8%
Mitochondrion (membrane)	9	5.7%	8	5.2%	6	3.0%	25	4.9%	4	4.5%	2	2.5%
Mitochondrion, nucleus	2	1.3%		0.0%	3	1.5%	1	0.2%	2	2.2%		0.0%
Peroxisome, ER, golgi		0.0%	3	1.9%	2	1.0%	6	1.2%	4	4.5%		0.0%
Cytoplasm (membrane)		0.0%	3	1.9%	1	0.5%	7	1.4%	1	1.1%	1	1.3%
Cytoplasm, mitochondrion		0.0%	2	1.3%	1	0.5%	6	1.2%		0.0%	1	1.3%
Cytoplasm, mitochondrion, nucleus	1	0.6%		0.0%	1	0.5%		0.0%		0.0%		0.0%
Cytoplasm, nucleus (membrane)	1	0.6%		0.0%	1	0.5%	3	0.6%	1	1.1%		0.0%
Cytoplasm, peroxisome, ER, golgi (membrane)		0.0%	1	0.6%	1	0.5%	9	1.8%		0.0%		0.0%
Mitochondrion, peroxisome, ER, golgi (membrane)	1	0.6%	2	1.3%	1	0.5%	2	0.4%	1	1.1%	1	1.3%
Cytoplasm, mitochondrion (membrane)		0.0%		0.0%		0.0%	1	0.2%		0.0%		0.0%
Cytoplasm, mitochondrion, nucleus (membrane)		0.0%		0.0%		0.0%	1	0.2%		0.0%		0.0%
Cytoplasm, mitochondrion, peroxisome, ER, golgi (membrane)	1	0.6%		0.0%		0.0%	1	0.2%		0.0%		0.0%
Cytoplasm, nucleus, peroxisome, ER, golgi		0.0%		0.0%		0.0%	1	0.2%		0.0%		0.0%
Cytoplasm, nucleus, peroxisome, ER, golgi (membrane)		0.0%		0.0%		0.0%	1	0.2%		0.0%		0.0%
Cytoplasm, peroxisome, ER, golgi		0.0%		0.0%		0.0%	1	0.2%		0.0%		0.0%
Nucleus (membrane)		0.0%		0.0%		0.0%	1	0.2%		0.0%		0.0%
Nucleus, peroxisome, ER, golgi (membrane)	1	0.6%		0.0%		0.0%	1	0.2%		0.0%		0.0%
tRNA	7	4.4%	5	3.2%	57	28.6%	4	0.8%	7	7.9%	2	2.5%
Not annotated	23	14.5%	54	35.1%	46	23.1%	147	28.9%	30	33.7%	32	40.5%
Total	159		154		199		508		89		79	

Table S18 HSP and oxidative stress response genes

Heat shock protein genes				
Locus_tag	Product	UniProt	UniProt_gene	KO_number

Heat shock protein genes

Locus_tag	Product	UniProt	UniProt_gene	KO_number
KLMA_10712	heat shock protein SSC1	P12398		K04043
KLMA_10728	peptidyl-prolyl cis-trans isomerase CYP7	P47103	CPR7	K01802
KLMA_10813	heat shock protein homolog SSE1	Q875P5	SSE1	K09485
KLMA_20079	hsp70 nucleotide exchange factor FES1	Q6CNM7	FES1	
KLMA_20282	heat shock protein 60	P19882	HSP60	K04077
KLMA_20459	heat shock protein SSA2	P10592	SSA2	K03283
KLMA_20771	12 kDa heat shock protein	P22943	HSP12	
KLMA_30257	protein SGT1	Q08446	SGT1	K12795
KLMA_30350	hsp70/Hsp90 co-chaperone CNS1	P33313	CNS1	
KLMA_30434	protein interacting with Hsp90 1	P38768	PIH1	
KLMA_30496	TPR repeat-containing protein associated with Hsp90	P25638	TAH1	
KLMA_30546	ribosome-associated complex subunit SSZ1	P38788	SSZ1	
KLMA_30551	vesicular-fusion protein SEC18	P18759	SEC18	K06027
KLMA_30561	co-chaperone protein SBA1	P28707	SBA1	
KLMA_40099	heat shock protein 104	P31539	HSP104	
KLMA_40128	heat shock protein 26	P15992	HSP26	K13993
KLMA_50124	hsp90 co-chaperone AHA1	Q12449	AHA1	
KLMA_50253	cell wall mannoprotein HSP150	Q03178	PIR1	
KLMA_50254	cell wall mannoprotein HSP150	A6ZZG0	PIR1	
KLMA_50255	cell wall mannoprotein HSP150	Q03180	PIR3	
KLMA_50274	heat shock protein SSQ1	Q05931	SSQ1	
KLMA_50344	ATP-dependent molecular chaperone HSC82	P02829	HSP82	K04079
KLMA_50469	HSP70 co-chaperone SNL1			K14017
KLMA_50526	hsp90 co-chaperone Cdc37	P06101	CDC37	K09554
KLMA_50592	heat shock protein SSB	P41770	SSB	K03283
KLMA_60101	heat shock protein 78	P33416	HSP78	K03695
KLMA_60191	heat shock protein 70 homolog LHS1	P36016	LHS1	K09486
KLMA_60248	mitochondrial import receptor subunit TOM70	P07213	TOM70	
KLMA_60484	cell division control protein 48	P25694	CDC48	K13525
KLMA_60511	peptidyl-prolyl cis-trans isomerase D	Q6CL78	CPR6	K05864
KLMA_70283	serine/threonine-protein phosphatase T	P53043	PPT1	K04460
KLMA_80019	probable chaperone protein HSP31	Q04432	HSP31	
KLMA_80087	10 kDa heat shock protein	P38910	HSP10	K04078
KLMA_80278	hsp90 co-chaperone HCH1	P53834	HCH1	
KLMA_80367	heat shock protein SSA3	P09435	SSA3	K03283

Oxidative stress response genes

Locus_tag	Product	UniProt	UniProt gene	KO number	UniProt location
KLMA_10058	glutaredoxin-1	P17695	GRX2	K03676	Cytoplasm. Mitochondrion.
KLMA_10060	selR super family	P25566	MXR2	K00391	
KLMA_10250	YAP1-binding protein 1	P38315	YBP1		Cytoplasm.
KLMA_10673	glutathione peroxidase 2	P38143	GPX2		
KLMA_10682	thioredoxin reductase	Q6HA24	TRR1	K00384	Mitochondrion (Potential).
KLMA_10787	glutathione reductase	Q6HA23	GLR1	K00383	Cytoplasm (By similarity).
KLMA_20243	thioredoxin-3	P25372	TRX3	K03671	Mitochondrion.
KLMA_20370	glutathione synthetase	Q08220	GSH2	K01920	
KLMA_20407	peroxiredoxin HYR1	P40581	HYR1	K00432	Cytoplasm.
KLMA_20553	superoxide dismutase [Mn]	P00447	SOD2	K04564	Mitochondrion matrix.
KLMA_30154	glutamate--cysteine ligase	P32477	GSH1	K11204	
KLMA_30286	monothiol glutaredoxin-3	Q03835	GRX3		
KLMA_30366	monothiol glutaredoxin-5	Q6YFE4	GRX5	K07390	Mitochondrion matrix (By similarity).
KLMA_30632	peroxiredoxin-like protein DDB_G0282517	P34227	PRX1		Mitochondrion.
KLMA_30684	peptide methionine sulfoxide reductase	P40029	MXR1	K07304	
KLMA_40173	peroxiredoxin type-2	P38013	AHP1	K14171	Cytoplasm.
KLMA_40176	metal resistance protein YCF1	P39109	YCF1		Vacuole membrane; Multi-pass membrane protein.
KLMA_40301	UPF0067 GAF domain-containing protein YKL069W	P36088		K08968	Cytoplasm. Nucleus.

Heat shock protein genes					
Locus_tag	Product	UniProt	UniProt_gene	KO_number	
KLMA_40313	superoxide dismutase 1 copper chaperone	Q6CIG2	CCS1		Cytoplasm (By similarity).
KLMA_40574	peroxiredoxin TSA1	P34760	TSA1	K03386	Cytoplasm.
KLMA_50005	glutathione S-transferase 1	P40582	GTT1	K00799	Endoplasmic reticulum membrane; Peripheral membrane protein.
KLMA_50279	glutaredoxin-like protein YLR364W	Q05926	GRX8		Cytoplasm.
KLMA_50406	peroxiredoxin DOT5	P40553	DOT5	K03564	Nucleus. Chromosome, telomere (Potential).
KLMA_50419	catalase T	A6ZV70	CTT1	K03781	Cytoplasm (By similarity).
KLMA_60077	thioredoxin-2	P22803	TRX2	K03671	Cytoplasm. Golgi apparatus membrane; Peripheral membrane protein. Nucleus.
KLMA_60133	monothiol glutaredoxin-7	P38068	GRX7		
KLMA_60401	peroxisomal catalase A	P15202	CTA1	K03781	Peroxisome.
KLMA_70087	superoxide dismutase [Cu-Zn]	Q6CPE2	SOD1	K04565	Cytoplasm (By similarity).
KLMA_70261	D-arabinono-1	Q6CSY3	ALO1	K00107	Mitochondrion membrane (By similarity).
KLMA_80358	mitochondrial peroxiredoxin PRX1	P34227	PRX1	K03386	Mitochondrion.

Table S19 GO terms enriched in significantly up-regulated genes under 30X condition

GO.ID	Term	Annotated gene[a]	Significant[b]	Expected[c]	P-value[d]	Genes
GO:0009062	fatty acid catabolic process	21	7	0.32	1.4e-08	CIT3, FOX2, ICL2, POT1, POX1, PXA1, SOU1
GO:0072329	monocarboxylic acid catabolic process	29	7	0.45	1.7e-07	CIT3, FOX2, ICL2, POT1, POX1, PXA1, SOU1
GO:0044242	cellular lipid catabolic process	38	7	0.59	1.2e-06	CIT3, FOX2, ICL2, POT1, POX1, PXA1, SOU1
GO:0006635	fatty acid beta-oxidation	16	5	0.25	2.8e-06	FOX2, POT1, POX1, PXA1, SOU1
GO:0019395	fatty acid oxidation	17	5	0.26	3.9e-06	FOX2, POT1, POX1, PXA1, SOU1
GO:0034440	lipid oxidation	17	5	0.26	3.9e-06	FOX2, POT1, POX1, PXA1, SOU1
GO:0006631	fatty acid metabolic process	64	8	0.99	4.4e-06	CAT2, CIT3, FOX2, ICL2, POT1, POX1, PXA1, SOU1
GO:0032787	monocarboxylic acid metabolic process	111	10	1.71	5.2e-06	ACS1, ALD4, CAT2, CIT3, FOX2, ICL2, POT1, POX1, PXA1, SOU1
GO:0016042	lipid catabolic process	51	7	0.79	9.7e-06	CIT3, FOX2, ICL2, POT1, POX1, PXA1, SOU1
GO:0044282	small molecule catabolic process	89	8	1.37	5.2e-05	CIT3, DAK1, FOX2, ICL2, POT1, POX1, PXA1, SOU1
GO:0030258	lipid modification	29	5	0.45	6.5e-05	FOX2, POT1, POX1, PXA1, SOU1
GO:0016054	organic acid catabolic process	68	7	1.05	6.6e-05	CIT3, FOX2, ICL2, POT1, POX1, PXA1, SOU1
GO:0046395	carboxylic acid catabolic process	68	7	1.05	6.6e-05	CIT3, FOX2, ICL2, POT1, POX1, PXA1, SOU1
GO:0055114	oxidation-reduction process	160	10	2.47	0.00013	ALD4, CIT3, DAK1, FOX2, MDH2, POT1, POX1, PXA1, SOL3, SOU1
GO:0019541	propionate metabolic process	3	2	0.05	0.00069	CIT3, ICL2

GO.ID	Term	Annotated gene[a]	Significant[b]	Expected[c]	P-value[d]	Genes
GO:0019543	propionate catabolic process	3	2	0.05	0.00069	CIT3, ICL2
GO:0019626	short-chain fatty acid catabolic process	3	2	0.05	0.00069	CIT3, ICL2
GO:0019629	propionate catabolic process, 2-methylcitrate cycle	3	2	0.05	0.00069	CIT3, ICL2
GO:0046459	short-chain fatty acid metabolic process	4	2	0.06	0.00138	CIT3, ICL2
GO:0019752	carboxylic acid metabolic process	345	13	5.32	0.00177	ACS1, ALD4, ARG1, CAT2, CIT3, FOX2, ICL2, LYS21, MDH2, POT1, POX1, PXA1, SOU1
GO:0043436	oxoacid metabolic process	354	13	5.46	0.00223	ACS1, ALD4, ARG1, CAT2, CIT3, FOX2, ICL2, LYS21, MDH2, POT1, POX1, PXA1, SOU1
GO:0019405	alditol catabolic process	5	2	0.08	0.00227	DAK1, SOU1
GO:0006082	organic acid metabolic process	356	13	5.49	0.00235	ACS1, ALD4, ARG1, CAT2, CIT3, FOX2, ICL2, LYS21, MDH2, POT1, POX1, PXA1, SOU1
GO:0016052	carbohydrate catabolic process	63	5	0.97	0.00259	DAK1, GLK1, PGU1, SOL3, SOU1
GO:0006083	acetate metabolic process	6	2	0.09	0.00337	ACS1, ALD4
GO:0016233	telomere capping	6	2	0.09	0.00337	CDC13, POL12
GO:0046174	polyol catabolic process	7	2	0.11	0.00467	DAK1, SOU1
GO:0007155	cell adhesion	8	2	0.12	0.00617	FLO5, HSP12
GO:0022610	biological adhesion	8	2	0.12	0.00617	FLO5, HSP12
GO:0019321	pentose metabolic process	10	2	0.15	0.00972	SOL3, SOU1
GO:0044712	single-organism catabolic process	282	10	4.35	0.00983	CIT3, DAK1, FOX2, GLK1, ICL2, POT1, POX1, PXA1, SOL3, SOU1

[a]The number of GO term annotated genes in the *K. marxianus* genome.

[b]The number of GO term annotated genes, which were significantly (FDR < 0.05) expressed under the condition.

[c]The expected value of Fisher's exact test.

[d]The P-value of Fisher's exact test.

Table S20 Summary of significantly up-regulated genes under the 30X condition

Locus_tag	logFC	logCPM	FDR	Product	UniProt gene	KO number	Localization	Specific[a]
KLMA_30482	18.3	7.9	0.000	glyoxalase super family protein				30DS
KLMA_80413	18.3	9.5	0.000	60S ribosomal protein L8-B	RPL8B	K02936	Cytoplasm.	C
KLMA_40373	17.4	7.0	0.001	hypothetical protein	OM45		Mitochondrion outer membrane.	30DS
KLMA_10783	17.1	7.0	0.000	sorbose reductase SOU1	SOU1			C
KLMA_30641	16.4	6.2	0.002	probable hydrolase NIT3	NIT3			C
KLMA_50300	16.4	5.9	0.000	hypothetical protein				45D
KLMA_10180	15.8	7.3	0.015	argininosuccinate synthase	ARG1	K01940	Cytoplasm.	30DS
KLMA_10331	15.8	5.3	0.000	6-phosphogluconolactonase 3	SOL3	K01057	Cytoplasm. Nucleus.	S
KLMA_10267	15.4	5.2	0.000	SAP super family	AIM34		Mitochondrion membrane; Single-pass membrane protein (By similarity).	30DS
KLMA_10225	15.2	5.3	0.000	GTP-binding nuclear protein GSP1/Ran	GSP1	K07936	Nucleus (By similarity).	30DS
KLMA_40221	15.0	5.4	0.008	40S ribosomal protein S9	MRPS9		Mitochondrion (Potential).	45D

Locus_tag	logFC	logCPM	FDR	Product	UniProt gene	KO number	Localization	Specific [a]
KLMA_20293	13.3	4.2	0.008	U6 snRNA-associated Sm-like protein LSm2	LSM2	K12621	Nucleus. Cytoplasm (Probable).	45D
KLMA_60474	13.2	4.5	0.003	putative methyltransferase BUD23	BUD23		Cytoplasm. Nucleus.	C
KLMA_60493	13.1	3.8	0.040	homocitrate synthase	LYS21	K01655	Mitochondrion (Potential).	C
KLMA_R127	13.1	4.9	0.001	Val-tRNA				C
KLMA_R416	12.0	4.5	0.000	Val-tRNA				C
KLMA_20460	11.9	1.4	0.037	uncharacterized mitochondrial carrier YPR011C		K14684	Mitochondrion inner membrane; Multi-pass membrane protein.	S
KLMA_R411	11.5	2.9	0.016	Leu-tRNA				45D
KLMA_20496	11.2	2.5	0.021	hypothetical protein		K11098		C
KLMA_R602	11.1	2.8	0.001	Ala-tRNA				C
KLMA_30167	11.0	2.1	0.002	hypothetical protein				C
KLMA_20617	10.7	0.9	0.005	SAM50-like protein SpAC17C9.06				30DS
KLMA_R322	10.4	4.0	0.025	Gln-tRNA				C
KLMA_R805	10.3	4.0	0.046	Leu-tRNA				45D
KLMA_R110	10.2	1.8	0.011	Ala-tRNA				45D
KLMA_60403	10.1	6.1	0.000	putative elongation factor 1 gamma homolog	CAM1	K03233	Cytoplasm. Nucleus.	C
KLMA_10516	10.0	4.0	0.002	polygalacturonase	PGU1	K01184		C
KLMA_20220	9.9	13.9	0.000	3-ketoacyl-CoA thiolase	POT1	K00632	Peroxisome.	S
KLMA_80402	8.4	4.4	0.010	probable 26S proteasome complex subunit SEM1		K10881		45D
KLMA_20263	8.4	8.4	0.000	acyl-coenzyme A oxidase	POX1	K00232	Peroxisome (By similarity).	S
KLMA_50012	8.0	8.0	0.000	potassium-activated aldehyde dehydrogenase	ALD4	K00128	Mitochondrion matrix.	S
KLMA_70429	7.8	4.5	0.001	mitochondrial 2-methylisocitrate lyase	ICL2	K01637	Mitochondrion matrix.	S
KLMA_10740	7.7	2.7	0.016	esterase_lipase super family				S
KLMA_70444	7.5	6.1	0.000	citrate synthase 3	CIT3	K01647		S
KLMA_40391	7.3	6.9	0.000	malate dehydrogenase	MDH2	K00026	Cytoplasm.	C
KLMA_20771	6.9	5.7	0.001	12 kDa heat shock protein	HSP12			S
KLMA_20626	6.7	2.9	0.001	mitochondrial DnaJ homolog 2	MDJ2		Mitochondrion inner membrane.	C
KLMA_20009	6.7	5.2	0.005	hypothetical protein	ADY2	K07034	Cell membrane; Multi-pass membrane protein. Vacuole membrane; Multi-pass membrane protein.	S
KLMA_70304	6.5	6.3	0.000	transcription elongation factor SPT6	SPT6	K11292	Nucleus (By similarity).	C
KLMA_30511	5.7	4.1	0.033	ATP-dependent RNA helicase DBP3	DBP3	K14811	Nucleus, nucleolus (By similarity).	30DS
KLMA_20345	5.6	9.4	0.006	protein FUN14				30DS
KLMA_50277	5.3	3.8	0.001	conserved hypothetical protein			Nucleus (Potential).	45D
KLMA_70346	5.3	3.1	0.042	DNA polymerase alpha subunit B	POL12	K02321	Nucleus.	30DS
KLMA_10197	5.2	8.1	0.001	flocculation protein FLO5	FLO5		Secreted, cell wall. Membrane; Lipid-anchor, GPI-anchor (Potential).	45D
KLMA_30654	5.2	6.0	0.037	carnitine O-acetyltransferase	CAT2	K00624	Isoform Mitochondrial: Mitochondrion inner membrane; Peripheral membrane protein; Matrix side.Isoform	S

Locus_tag	logFC	logCPM	FDR	Product	UniProt gene	KO number	Localization	Specific [a]
KLMA_60323	5.2	8.3	0.000	uncharacterized transporter YHL008C			Peroxisomal: Peroxisome. Membrane; Multi-pass membrane protein (Probable).	S
KLMA_70426	5.2	7.7	0.000	peroxisomal hydratase-dehydrogenase-epimerase	FOX2	K14729	Peroxisome.	S
KLMA_50201	5.1	4.8	0.006	ribonucleases P/MRP protein subunit POP6		K14524		C
KLMA_20587	5.1	4.8	0.025	ammonia transport outward protein 3	ATO3	K07034	Cell membrane; Multi-pass membrane protein.	S
KLMA_40214	5.1	2.6	0.013	SUR7 family protein FMP45	FMP45		Cell membrane; Multi-pass membrane protein.	S
KLMA_30101	5.0	5.8	0.003	uncharacterized protein YMR107W	SPG4			S
KLMA_50023	5.0	6.4	0.001	hypothetical protein				S
KLMA_30656	5.0	5.7	0.001	ribosomal RNA-processing protein 17	RRP17	K14851	Nucleus, nucleolus.	S
KLMA_40173	4.9	10.7	0.000	peroxiredoxin type-2	AHP1	K14171	Cytoplasm.	30DS
KLMA_20193	4.7	5.4	0.002	peroxisomal long-chain fatty acid import protein 2	PXA1	K15628	Peroxisome membrane; Multi-pass membrane protein.	45D
KLMA_10715	4.7	5.6	0.048	sorbose reductase homolog SOU2	SOU2			S
KLMA_10051	4.7	6.7	0.001	glucokinase-1	GLK1	K00844		S
KLMA_20051	4.6	4.3	0.016	rRNA-processing protein CGR1	CGR1	K14822	Nucleus, nucleolus (By similarity).	C
KLMA_60074	4.6	5.6	0.002	dicarboxylic amino acid permease	DIP5	K03293	Membrane; Multi-pass membrane protein.	S
KLMA_70395	4.5	4.5	0.004	tRNA pseudouridine synthase 4	PUS4	K03177	Nucleus. Mitochondrion.	C
KLMA_60262	4.5	3.0	0.050	UPF0195 protein YHR122W				30DS
KLMA_60046	4.5	7.0	0.040	uncharacterized protein YGR237C				45D
KLMA_60204	4.4	7.2	0.004	ribosomal RNA-processing protein 8	RRP8	K14850	Nucleus, nucleolus. Chromosome, telomere (Potential).	30DS
KLMA_20219	4.4	6.7	0.007	BNI1-related protein 1	BNR1			45D
KLMA_60349	4.3	4.5	0.007	spindle pole body component SPC105	SPC105	K11563	Cytoplasm, cytoskeleton, spindle pole body. Nucleus membrane; Peripheral membrane protein; Nucleoplasmic side. Chromosome, centromere, kinetochore.	C
KLMA_70361	4.1	4.4	0.017	conserved hypothetical protein	TEC1	K09450	Nucleus.	S
KLMA_60172	4.1	7.2	0.010	ribosomal RNA-processing protein 14	RRP14		Nucleus, nucleolus.	30DS
KLMA_30602	4.0	7.7	0.005	acetyl-coenzyme A synthetase 1	ACS1	K01895	Microsome (Potential). Endoplasmic reticulum (Potential).	45D
KLMA_80142	4.0	4.8	0.013	carbonic anhydrase	NCE103	K01673	Cytoplasm. Nucleus.	S
KLMA_30555	3.9	11.3	0.000	conserved hypothetical transmembrane protein				45D
KLMA_70145	3.9	5.4	0.016	conserved hypothetical membrane protein	ywtG		Cell membrane; Multi-pass membrane protein (Potential).	S

Locus_tag	logFC	logCPM	FDR	Product	UniProt gene	KO number	Localization	Specific [a]
KLMA_20435	3.9	5.3	0.011	KH domain-containing protein YLL032C			Cytoplasm.	S
KLMA_20658	3.8	3.3	0.037	uncharacterized membrane protein YMR155W			Membrane; Multi-pass membrane protein.	S
KLMA_70170	3.8	7.6	0.017	ribonucleoside-diphosphate reductase large chain 1	RNR1	K10807	Cytoplasm.	30DS
KLMA_60246	3.8	4.1	0.026	cytoplasmic tRNA 2-thiolation protein 2	NCS2	K14169	Cytoplasm (By similarity).	S
KLMA_50161	3.6	7.6	0.040	dihydroxyacetone kinase 1	DAK1	K00863		S
KLMA_80011	3.5	6.0	0.017	deoxyribodipyrimidine photo-lyase	PHR1	K01669	Nucleus. Mitochondrion.	45D
KLMA_40215	3.4	7.0	0.028	cell division control protein 13	CDC13	K11115	Chromosome, telomere.	45D
KLMA_80196	3.4	8.8	0.015	beta-1,3-glucanosyltransferase	GAS1		Cell membrane; Lipid-anchor, GPI-anchor. Secreted, cell wall.	S
KLMA_70240	3.4	6.3	0.038	G2/mitotic-specific cyclin-4	CLB4			S
KLMA_30360	3.4	7.3	0.023	protein TOS1	TOS1		Secreted (Potential).	S
KLMA_40245	3.4	5.9	0.038	pleiotropic ABC efflux transporter of multiple drugs	PDR5		Cell membrane; Multi-pass membrane protein.	S
KLMA_20088	3.2	6.2	0.044	myosin-1	MYO1	K10352		S
KLMA_10082	3.2	5.1	0.043	protein PLM2	PLM2		Nucleus (Probable).	C
KLMA_80261	3.0	10.4	0.012	uncharacterized protein YMR031C	EIS1		Cytoplasmic granule (By similarity). Cell membrane; Peripheral membrane protein; Cytoplasmic side (By similarity).	S
KLMA_20427	2.8	10.5	0.013	hypothetical protein				45D
KLMA_20813	2.8	8.9	0.047	tyrosine-protein phosphatase 2	PTP2	K01104	Cytoplasm. Nucleus.	C
KLMA_40079	2.5	10.7	0.016	uncharacterized endoplamic reticulum membrane				30DS
KLMA_40174	1.3	16.3	0.004	uncharacterized cell wall protein YDR134C				S

[a]Gene expression was significantly (FDR < 0.05) altered under the following conditions: S, 30X-specific up-regulation; C, commonly up-regulated under 30DS, 45D and 30X conditions; 30DS, up-regulated under 30X and 30DS conditions; 45D, up-regulated under 30X and 45D conditions.

Table S21 GO terms enriched in significantly down-regulated genes under 30X condition

GO.ID	Term	Annotated gene[a]	Significant[b]	Expected[c]	P-value[d]	Genes
GO:1901605	alpha-amino acid metabolic process	154	9	2.12	0.00020	ARO10, ARO8, BAT1, FOL2, GAD1, HIS2, HOM2, LYS12, ppr1
GO:0019752	carboxylic acid metabolic process	345	13	4.75	0.00056	ALD5, ARO10, ARO8, BAT1, BIO3, FOL2, GAD1, HIS2, HOM2, LYS12, PDH1, PDX3, ppr1
GO:0009085	lysine biosynthetic process	13	3	0.18	0.00064	ARO8, HOM2, LYS12
GO:0044283	small molecule biosynthetic process	263	11	3.62	0.00069	ALD5, ARO10, ARO8, BAT1, BIO3, FOL2, HIS2, HOM2, LYS12, PDX3, ppr1
GO:0043436	oxoacid metabolic process	354	13	4.88	0.00072	ALD5, ARO10, ARO8, BAT1, BIO3, FOL2, GAD1, HIS2, HOM2, LYS12, PDH1, PDX3, ppr1
GO:0006082	organic acid metabolic process	356	13	4.9	0.00076	ALD5, ARO10, ARO8, BAT1, BIO3, FOL2, GAD1, HIS2, HOM2, LYS12, PDH1, PDX3, ppr1

GO.ID	Term	Annotated gene[a]	Significant[b]	Expected[c]	P-value[d]	Genes
GO:0016053	organic acid biosynthetic process	191	9	2.63	0.00098	ALD5, ARO8, BAT1, BIO3, FOL2, HIS2, HOM2, LYS12, ppr1
GO:0046394	carboxylic acid biosynthetic process	191	9	2.63	0.00098	ALD5, ARO8, BAT1, BIO3, FOL2, HIS2, HOM2, LYS12, ppr1
GO:0006553	lysine metabolic process	15	3	0.21	0.00100	ARO8, HOM2, LYS12
GO:1901607	alpha-amino acid biosynthetic process	119	7	1.64	0.00106	ARO8, BAT1, FOL2, HIS2, HOM2, LYS12, ppr1
GO:0044282	small molecule catabolic process	89	6	1.23	0.00122	ALD5, ARO10, BAT1, GAD1, PDH1, ppr1
GO:0009066	aspartate family amino acid metabolic process	60	5	0.83	0.00125	ARO10, ARO8, BAT1, HOM2, LYS12
GO:0044281	small molecule metabolic process	645	18	8.88	0.00153	ALD5, APA2, ARO10, ARO8, BAT1, BIO3, CAB1, FOL2, FPS1, GAD1, HIS2, HOM2, KLMA_40628, LYS12, PDH1, PDX3, gcp, ppr1
GO:0006555	methionine metabolic process	38	4	0.52	0.00167	ARO10, ARO8, BAT1, HOM2
GO:0016054	organic acid catabolic process	68	5	0.94	0.00219	ARO10, BAT1, GAD1, PDH1, ppr1
GO:0046395	carboxylic acid catabolic process	68	5	0.94	0.00219	ARO10, BAT1, GAD1, PDH1, ppr1
GO:0044272	sulfur compound biosynthetic process	69	5	0.95	0.00234	ARO10, ARO8, BAT1, BIO3, HOM2
GO:0009081	branched-chain amino acid metabolic process	20	3	0.28	0.00238	ARO10, BAT1, HOM2
GO:0009063	cellular amino acid catabolic process	43	4	0.59	0.00265	ARO10, BAT1, GAD1, ppr1
GO:0006558	L-phenylalanine metabolic process	6	2	0.08	0.00269	ARO10, ARO8
GO:0006570	tyrosine metabolic process	6	2	0.08	0.00269	ARO10, ARO8
GO:0009083	branched-chain amino acid catabolic process	6	2	0.08	0.00269	ARO10, BAT1
GO:1902221	erythrose 4-phosphate/phosphoenolpyruvate family amino acid metabolic process	6	2	0.08	0.00269	ARO10, ARO8
GO:0008652	cellular amino acid biosynthetic process	142	7	1.96	0.00294	ARO8, BAT1, FOL2, HIS2, HOM2, LYS12, ppr1
GO:0000096	sulfur amino acid metabolic process	45	4	0.62	0.00313	ARO10, ARO8, BAT1, HOM2
GO:0009067	aspartate family amino acid biosynthetic process	49	4	0.67	0.00428	ARO8, BAT1, HOM2, LYS12
GO:0006520	cellular amino acid metabolic process	241	9	3.32	0.00489	ARO10, ARO8, BAT1, FOL2, GAD1, HIS2, HOM2, LYS12, ppr1
GO:0006551	leucine metabolic process	8	2	0.11	0.00494	ARO10, BAT1
GO:0034599	cellular response to oxidative stress	52	4	0.72	0.00530	GAD1, KLMA_40301, SCH9, ppr1
GO:1901566	organonitrogen compound biosynthetic process	292	10	4.02	0.00551	ARO8, BAT1, BIO3, CAB1, FOL2, HIS2, HOM2, LYS12, PDX3, ppr1
GO:0009097	isoleucine biosynthetic process	9	2	0.12	0.00629	BAT1, HOM2
GO:0019509	L-methionine salvage from methylthioadenosine	9	2	0.12	0.00629	ARO8, BAT1
GO:0043102	amino acid salvage	9	2	0.12	0.00629	ARO8, BAT1
GO:1901606	alpha-amino acid catabolic process	29	3	0.4	0.00698	ARO10, GAD1, ppr1
GO:0006895	Golgi to endosome transport	10	2	0.14	0.00780	ENT5, SFT2
GO:0071267	L-methionine salvage	10	2	0.14	0.00780	ARO8, BAT1
GO:0006979	response to oxidative stress	59	4	0.81	0.00831	GAD1, KLMA_40301, SCH9, ppr1
GO:0006549	isoleucine metabolic process	11	2	0.15	0.00945	BAT1, HOM2
GO:0019878	lysine biosynthetic process via aminoadipic acid	11	2	0.15	0.00945	ARO8, LYS12

[a]The number of GO term annotated genes in the *K. marxianus* genome.

[b]The number of GO term annotated genes, which were significantly (FDR < 0.05) expressed under the condition.

[c]The expected value of Fisher's exact test.

[d]The P-value of Fisher's exact test.

Table S22 Summary of significantly down-regulated genes under the 30X condition

Locus_tag	logFC	logCPM	FDR	Product	UniProt gene	KO number	Localization	Specific[a]
KLMA_50503	-18.5	8.5	0.000	aspartate-semialdehyde dehydrogenase	HOM2	K00133		S
KLMA_30481	-17.9	7.6	0.000	glyoxalase super family protein				S
KLMA_50017	-16.8	7.0	0.004	(2R,3R)-2,3-butanediol dehydrogenase	BDH2	K00004	Cytoplasm. Nucleus.	S
KLMA_10235	-16.4	6.8	0.000	WW domain-containing protein YFL010C				S
KLMA_80090	-15.8	6.2	0.005	uncharacterized protein YGL146C				S
KLMA_20536	-15.3	4.8	0.000	yjgF_YER057c_UK114_family				C
KLMA_20195	-14.8	5.0	0.001	acetyltransferases	ppr1			S
KLMA_60491	-14.6	7.1	0.001	60S acidic ribosomal protein P1-beta	RPP1B	K02942	Cytoplasm.	S
KLMA_70093	-14.6	4.6	0.004	carboxypeptidase S	CPS1		Vacuole membrane; Single-pass membrane protein.	45D
KLMA_50500	-14.6	4.1	0.011	epsin-like protein	ENT5		Cytoplasm. Endosome membrane; Peripheral membrane protein.	C
KLMA_30124	-14.4	4.7	0.025	succinate dehydrogenase [ubiquinone] cytochrome b subunit		K00236	Mitochondrion inner membrane; Multi-pass membrane protein (By similarity).	S
KLMA_30672	-14.3	6.0	0.000	probable metabolite transport protein C1271.09			Membrane; Multi-pass membrane protein (Potential).	30DS
KLMA_30556	-14.2	4.7	0.000	glutamate decarboxylase	GAD1	K01580		45D
KLMA_70443	-14.2	3.9	0.000	probable 2-methylcitrate dehydratase	PDH1	K01720		C
KLMA_50308	-14.0	6.1	0.000	glycylpeptide N-tetradecanoyltransferase	NMT1	K00671	Cytoplasm (By similarity).	S
KLMA_80414	-13.6	3.7	0.034	single-stranded nucleic acid-binding protein	SBP1		Cytoplasm. Nucleus, nucleolus.	45D
KLMA_10035	-13.5	3.8	0.016	5',5'''-P-1,P-4-tetraphosphate phosphorylase 2	APA2	K00988		45D
KLMA_10233	-13.4	4.5	0.000	hypothetical protein				45D
KLMA_60021	-13.2	3.7	0.040	carboxypeptidase S	CPS1	K01293	Vacuole membrane; Single-pass membrane protein.	S
KLMA_70403	-13.2	3.3	0.040	40S ribosomal protein MRP10	MRP10		Mitochondrion (By similarity).	45D
KLMA_10726	-13.2	3.3	0.000	mitochondrial protein PET191	PET191		Mitochondrion.	45D
KLMA_20149	-12.9	3.7	0.009	chromatin structure-remodeling complex subunit RSC7	NPL6	K11761	Nucleus.	S
KLMA_60068	-12.9	4.1	0.044	mitochondral 37S ribosomal protein S27	RSM27		Mitochondrion.	45D
KLMA_40106	-12.8	4.7	0.001	uncharacterized protein YDR210W				45D
KLMA_70126	-12.7	3.1	0.019	uncharacterized protein YJR080C	AIM24		Mitochondrion (By similarity).	45D
KLMA_40044	-12.5	4.7	0.009	ethanolamine-phosphate cytidylyltransferase	ECT1	K00967	Cytoplasm. Nucleus.	45D

Locus_tag	logFC	logCPM	FDR	Product	UniProt gene	KO number	Localization	Specific[a]
KLMA_20546	-12.2	4.1	0.014	vacuolar protein sorting-associated protein 62	VPS62		Membrane; Single-pass membrane protein.	45D
KLMA_R514	-12.0	2.0	0.015	Glu-tRNA				45D
KLMA_40237	-11.8	1.8	0.007	putative glycoprotein endopeptidase KAE1	gcp	K01409	Cytoplasm (Potential).	45D
KLMA_40301	-11.6	1.0	0.009	UPF0067 GAF domain-containing protein YKL069W		K08968	Cytoplasm. Nucleus.	C
KLMA_20702	-11.5	3.7	0.046	small nuclear ribonucleoprotein Sm D2	SMD2	K11096	Nucleus.	S
KLMA_10757	-11.3	2.0	0.016	probable 26S protease subunit YTA6	YTA6	K01509		S
KLMA_60545	-10.7	5.4	0.031	hypothetical protein				S
KLMA_40392	-10.2	5.8	0.001	uncharacterized vacuolar membrane protein YNL305C	BXI1	K06890	Endoplasmic reticulum membrane; Multi-pass membrane protein. Vacuole membrane; Multi-pass membrane protein. Mitochondrion membrane; Multi-pass membrane protein.	30DS
KLMA_10488	-10.2	4.0	0.012	GTP cyclohydrolase 1	FOL2	K01495		45D
KLMA_40266	-10.2	1.6	0.025	conserved hypothetical protein		K13621		S
KLMA_10549	-10.1	6.2	0.027	1,4-alpha-glucan-branching enzyme	GLC3	K00700		S
KLMA_40374	-8.9	5.3	0.019	negative regulator of RAS-cAMP pathway	MKS1		Nucleus.	S
KLMA_60402	-8.9	6.6	0.034	pisatin demethylase	PDAT9	K00493		45D
KLMA_20165	-8.5	5.5	0.009	adenylate kinase 1	ADK1	K00939	Cytoplasm, cytosol (By similarity). Mitochondrion intermembrane space (By similarity).	S
KLMA_30338	-8.3	5.1	0.002	protein ICY2				S
KLMA_40404	-8.1	8.8	0.000	aldehyde dehydrogenase 5	ALD5	K00128	Mitochondrion matrix.	S
KLMA_30142	-7.4	6.0	0.000	serine/threonine-protein phosphatase PP1-2	GLC7	K06269	Cytoplasm. Nucleus.	C
KLMA_30640	-7.3	8.3	0.000	D-amino-acid oxidase	dao1			C
KLMA_40220	-6.8	11.3	0.001	alcohol dehydrogenase 2	ADH2	K13953	Cytoplasm.	45D
KLMA_10257	-6.3	3.9	0.001	ERAD-associated E3 ubiquitin-protein ligase HRD1	HRD1	K10601	Endoplasmic reticulum membrane; Multi-pass membrane protein (By similarity).	45D
KLMA_20831	-6.0	1.1	0.044	adenosylmethionine-8-amino-7-oxononanoate aminotransferase	BIO3	K00833		30DS
KLMA_30102	-5.6	3.5	0.044	uncharacterized protein YKL128C	PMU1		Cytoplasm. Nucleus.	45D
KLMA_40260	-5.6	3.1	0.006	hypothetical protein				30DS
KLMA_50151	-5.3	6.1	0.025	aromatic amino acid aminotransferase 1	ARO8		Cytoplasm.	30DS
KLMA_20158	-5.1	10.0	0.000	alcohol dehydrogenase 4	ADH4	K13953	Mitochondrion matrix.	45D
KLMA_80411	-4.7	4.7	0.001	glycerol uptake/efflux facilitator protein	FPS1	K03441	Membrane; Multi-pass membrane protein (Probable).	S
KLMA_60412	-4.5	10.7	0.000	hexokinase	RAG5	K00844		C
KLMA_50248	-4.4	8.0	0.001	cAMP-dependent protein kinase type 3	TPK1	K04345	Cytoplasm. Nucleus.	S
KLMA_40480	-4.4	6.3	0.004	serine/threonine-protein	SCH9	K08286		S

Locus_tag	logFC	logCPM	FDR	Product	UniProt gene	KO number	Localization	Specific[a]
				kinase SCH9				
KLMA_50449	-4.3	7.6	0.013	fungal_trans super family conserved domain				C
KLMA_40622	-4.3	11.7	0.000	hypothetical protein				C
KLMA_10404	-4.2	5.7	0.013	zinc/iron permease	ATX2	K14715	Golgi apparatus membrane; Multi-pass membrane protein.	S
KLMA_40628	-4.2	4.9	0.008	NADPH-dependent methylglyoxal reductase GRE2				S
KLMA_10436	-4.1	2.6	0.030	histidinol-phosphatase	HIS2	K04486		S
KLMA_10514	-4.1	10.4	0.000	branched-chain-amino-acid aminotransferase	BAT1	K00826	Mitochondrion matrix.	C
KLMA_20489	-4.0	9.0	0.007	GAL4-like Zn2Cys6 binuclear cluster DNA-binding domain				C
KLMA_20152	-3.8	4.7	0.016	probable ADP-ribose 1''-phosphate phosphatase YML087W				S
KLMA_30404	-3.7	4.9	0.016	family of serine hydrolases 1	FSH1		Cytoplasm. Nucleus.	S
KLMA_50338	-3.7	4.7	0.018	uncharacterized protein YPL245W		K09384	Cytoplasm. Nucleus.	S
KLMA_70134	-3.7	6.8	0.019	protein transport protein SFT2	SFT2		Golgi apparatus membrane; Multi-pass membrane protein.	30DS
KLMA_20282	-3.7	10.7	0.005	heat shock protein 60	HSP60	K04077	Mitochondrion matrix.	S
KLMA_20597	-3.7	5.7	0.016	transaminated amino acid decarboxylase	ARO10	K12732	Cytoplasm.	30DS
KLMA_R530	-3.6	5.1	0.048	Gln-tRNA				30DS
KLMA_40627	-3.6	6.0	0.019	siderophore iron transporter ARN1	GEX1		Cell membrane; Multi-pass membrane protein. Vacuole membrane; Multi-pass membrane protein.	S
KLMA_10036	-3.5	5.5	0.025	pantothenate kinase	CAB1	K09680	Cytoplasm. Nucleus.	C
KLMA_40128	-3.5	10.1	0.001	heat shock protein 26	HSP26	K13993		30DS
KLMA_80174	-3.4	8.9	0.034	probable transporter AQR1	AQR1		Membrane; Multi-pass membrane protein.	C
KLMA_50241	-3.3	7.4	0.021	pyridoxamine 5'-phosphate oxidase	PDX3	K00275		C
KLMA_80130	-3.3	6.8	0.028	homoisocitrate dehydrogenase	LYS12	K05824	Mitochondrion.	C
KLMA_30496	-3.3	6.0	0.046	TPR repeat-containing protein associated with Hsp90	TAH1		Cytoplasm. Nucleus.	30DS
KLMA_40075	-3.1	4.8	0.050	uncharacterized membrane protein YMR126C	DLT1		Membrane; Multi-pass membrane protein (Potential).	S
KLMA_30284	-3.1	8.0	0.031	cytochrome c	CYCK	K08738	Mitochondrion intermembrane space.	S
KLMA_60392	-2.7	9.4	0.026	uncharacterized protein YPL039W				C

[a]Gene expression was significantly (FDR < 0.05) altered under the following conditions: S, 30X-specific down-regulation; C, commonly down-regulated under 30DS, 45D and 30X conditions; 30DS, down-regulated under 30X and 30DS conditions; 45D, down-regulated under 30X and 45D conditions.

CHAPTER 5

Essentiality of respiratory activity for pentose utilization in thermotolerant yeast *Kluyveromyces marxianus* DMKU 3-1042

5.1 Abstract

By random integrative mutagenesis with a *kan*MX4 cassette in *Kluyveromyces marxianus* DMKU 3-1042, we obtained three mutants of *COX15*, *ATP25* and *CYC3* encoding a cytochrome oxidase assembly factor (singleton), a transcription factor required for assembly of the Atp9p subunit of mitochondrial ATP synthase and cytochrome *c* heme lyase, respectively, as mutants lacking growth capability on xylose and/or arabinose. They exhibited incapability of growth on non-fermentable carbon sources, such as acetate or glycerol, and thermosensitiveness. Their biomass formation in glucose medium was reduced, but ethanol yields were increased with a high ethanol level in the medium, compared to those of the parental strain. Experiments with respiratory inhibitors showed that *cox15* and *cyc3*, but not *atp25*, were able to grow in glucose medium containing antimycin A and that the *atp25* mutant was KCN-resistant. Activities of NADH and ubiquinol oxidases in membrane fractions of each mutant became a half of that of the parent and negligible, respectively, and their remaining NADH oxidase activities were found to be resistant to KCN. Absolute absorption spectral analysis revealed that the peak corresponding to $a+a_3$ was very small in *atp25* and negligible in *cox15* and *cyc3*. These findings suggest that the *K. marxianus* strain possesses an alternative KCN-resistant oxidase that is located between primary dehydrogenases and the ubiquinone pool and that the respiratory activity is essential for utilization of pentoses.

5.2 Introduction

Shrinking availability of fossil resources dictate the necessity to explore alternative raw materials for fuel production in the future. Abundant

lignocelluloses as plant biomass have been expected to become such materials, though technology for efficient biochemical transformation to fuel must be developed (Wackett 2008). Xylose is the main monomer of hemicelluloses as components of lignocelluloses and the second most abundant sugar in nature. The efficient conversion of this 'wood sugar' to ethanol is thus critical for utilization of lignocelluloses as economically sustainable materials.

Yeast uptake xylose via transporters by either a facilitated diffusion mechanism or proton symport mechanism (Jojima et al. 2010). In the traditional baker's yeast *Saccharomyces cerevisiae*, xylose is poorly taken up probably by nonspecific hexose transporter in facilitated diffusion, and their affinity for xylose is one to two orders of magnitude lower than that for glucose (Kötter and Ciriacy 1993). Therefore, xylose uptake usually occurs after depletion of hexose sugars in the medium, as in the case of recombinant xylose-fermenting *S. cerevisiae* strains (Matsushika et al. 2009; Karhumaa et al. 2007; Gárdonyi et al. 2003). In naturally xylose-fermenting yeasts, xylose can be imported through active transporters with a high affinity for xylose (Jojima et al. 2010). However, since this transport system consumes 1 mol of ATP for each proton co-transported with xylose, it is likely that ATP will become insufficient, resulting in reduction of cell growth under anaerobic or microaerobic conditions (Weusthuis et al. 1993).

The mitochondrial respiratory chain, which forms membrane potentials to produce ATP by ATPase as a multi-complex, consists of vital components to transfer electrons, including cytochromes bearing heme groups of types *a*, *b* and *c* as a prosthetic group. Heme contains an iron atom that is embedded inside a porphyrin ring system and coordinated to four nitrogen atoms. The biosynthesis of heme is a multistep process that starts by the formation of a porphyrin ring from succinyl-CoA and glycine (Moraes et al. 2004). Even partial deficiencies in some enzymes involved in the biosynthetic pathway of heme result in defective respiratory activities and subsequently reduction of ATP (Moraes et al. 2004). Problems in the assembly of ATPase or respiratory components also hamper respiratory activity (Zeng et al. 2008; Moraes et al. 2004).

Naturally xylose-fermenting yeasts utilize different transport systems under different conditions. For example, *Kluyveromyces marxianus* possesses activities

of both active transport and facilitated diffusion systems of xylose under aerobic conditions but only that of the facilitated diffusion system of xylose under microaerophilic conditions (Spencer-Martins 1994). In *Candida succiphila,* only a single high-affinity transporter is active in a xylose medium, while a low-affinity transporter is active in a glucose medium (Spencer-Martins 1994). *Spathaspora passalidarum* also expresses different xylose transport systems under anaerobic and aerobic conditions (Nguyen et al. 2006). In spite of such diversity, it is likely that the utilization capability of xylose in most yeasts is low under anaerobic conditions.

K. marxianus has been adopted by industries for a relatively broad range of applications from biomass production to bioremediation (Fonseca et al. 2008; Lane and Morrissey 2010) due to advantages of its traits such as rapid growth, thermotolerance, secretion of the enzyme inulinase and production of ethanol from various carbon sources (Nonklang et al. 2008; Lertwattanasakul et al. 2011; Rodrassamee et al. 2011). A particularly attractive application of this yeast is high-temperature fermentation and bioconversion of hemicellulose. In addition, like *Kluyveromyces lactis*, its glucose repression effect is not as severe as that of *S. cerevisiae* (Rodrussamee et al. 2011; Lertwattanasakul et al. 2011). However, as a disadvantage, *K. marxianus* may have a relatively strong respiration activity during fermentation compared to that of *Saccharomyces cerevisiae*, and the respiratory activity becomes strong when it is grown on pentose, resulting in low production of ethanol (Lertwattanasakul et al., unpublished data). Therefore, elucidation of the pentose metabolism of *K. marxianus* and its further improvement are crucial for application of the yeast to ethanol production from pentose.

In this study, in order to identify key factors involved in pentose metabolism, we mutagenized *K. marxianus* DMKU 3-1042 as one of type strains by a random *kan*MX4-insertion mutagenesis and screened mutants that are unable to assimilate xylose and/or arabinose as a sole carbon source. The mutant analysis allowed us to understand not only key genes for pentose assimilation but also the organization and physiological activity of the respiratory chain in *K. marxianus*. This knowledge would lead us to identify targets for metabolic engineering of *K. marxianus* for improvement of ethanol productivity from pentose sugars.

5.3 Materials and methods

5.3.1 Materials

Oligonucleotide primers were synthesized by Proligo Japan (Tokyo). A DNA sequencing kit (ABI PRISM® BigDye® Terminator v3.1 Cycle Sequencing Kit) was purchased from Applied Biosystems Japan (Kyoto, Japan). Other chemicals were all of analytical grade.

5.3.2 Strains, media and culture conditions

Yeast strains used in this work were *K. marxianus* DMKU 3-1042 strain, deposited in the NITE Biological Resource Center (NBRC) under the deposit number NITE BP-283 (Limtong et al. 2007) and its mutant derivatives. Media used were YP (1% w/v yeast extract and 2% w/v peptone) supplemented with different carbon sources: YPD, with 2% w/v glucose; YPX, with 2% w/v xylose; and YPA, with 2% w/v arabinose. If required, 1 mM potassium cyanide (KCN), 10 μM antimycin A (AA) or 20 μM carbonyl cyanide *m*-chlorophenylhydrazone (CCCP) was added to the media. Cells grown in YPD medium at 30°C for 18 h were inoculated into a 30-ml batch culture medium in a 100-ml Erlenmeyer flask and incubated under a shaking condition of 160 rpm at 30°C or 45°C.

5.3.3 Genetic and molecular biological techniques

General procedures for nucleic acid analyses followed standard protocols (Ausubel et al. 1993). TAIL-PCR reaction was performed as described previously (Charoensuk et al. 2011). DNA sequences were determined by ABI Prism 310 (Perkin Elmer, USA) and examined via BLAST analysis (Altschul et al. 1990). Genomic yeast DNA was extracted as described previously (Sambrook and Russell 2001).

5.3.4 Untargeted integration mutagenesis, screening and characterization of mutants

A *kan*MX4-PCR-amplified fragment (20 μg DNA) was transformed into *K. marxianus* DMKU 3-1042 (Antunes et al. 2000). Transformants were obtained and replica-plated after colonies had formed on YPD supplemented with 150 μg/mL of G418 sulfate (Geneticin, Nacalai Tesque). Colonies unable to grow on xylose and/or arabinose as a carbon source were subjected to further investigation. For identification of the locus of *kan*MX4-fragment integration, TAIL-PCR was employed using genomic DNA isolated from transformants as a template (Charoensuk et al. 2011) with specific primer sets (Table 5.1). The fragments obtained were purified and subjected to nucleotide sequencing (Sanger et al. 1977). The resultant data were analyzed by a BLAST search.

5.3.5 Complementation of *kan*MX4-insertion mutants with DNA fragments of the target gene and drug-resistance gene

For the complementation test of *COX15*-, *ATP25*- and *CYC3*-disrupted mutant strains, double transformation with amplified DNA fragments of the corresponding target gene and the *ble*^{R} encoding zeomycin resistance gene was performed. Primers were designed to anneal at approximately 2,000 bp away from each coding region of the target genes. Target genes were amplified by PCR using genomic DNA of the parental strain as a template with corresponding primer sets (Table 5.1). The *ble*^{R} gene was amplified by PCR from pSH65 (Güldener et al. 2002) DNA as a template with a primer set (Table 5.1). The PCR products were recovered by ethanol precipitation, and 50−400 ng of the products of each target gene and *ble*^{R} was mixed and transformed using the LiAc method (Antunes et al. 2000) into the corresponding disrupted-mutant strain. Transformants were then obtained on 2% YPD agar plates containing 100 □g/ml of zeomycin after incubation at 30°C. For the complementation test, three independent colonies were cultivated in 2% YPD medium at 30°C overnight and subjected to a spot test (Rodrussamee et al. 2011). After washing the cells with deionized water, the

suspended cells (1 x 10^7 cells/ml) were 10-fold sequentially diluted and then spotted onto agar plates of 3% YPD and 3% YPX. The plates were incubated at 30°C for 48 h.

5.3.6 Analytical methods

Cell growth was determined by means of periodical optical density (660 nm) measurement. Concentrations of glucose, ethanol and glycerol during fermentation were determined at 35°C by an HPLC system (Lertwattanasakul et al. 2011). NADH and ubiquinol oxidase activities were measured as described previously (Lertwattanasakul et al. 2009; Sootsuwan et al. 2008).

Table 5.1 Primers used in this study

Name	Sequence 5'→3'	Remark
COX15F	5′-GGTATGACTGACGTTGCGGA-3′	To amplify *COX15* gene for complementation
COX15R	5′-TACATGCCTGGTGCCTTCTC-3′	
ATP25F	5′-TCTGACATTTCTCACGAGGGC-3′	To amplify *ATP25* gene for complementation
ATP25R	5′-CCGACATTTGGCATACCACC-3′	
CYC3F	5′-AGTTGCGTTACAACGTTCACTG-3′	To amplify *CYC3* gene for complementation
CYC3R	5′-ACTCGATTCCTCCAGCTCCA-3′	
bleF	5′-TCTGTACAGACGCGTGTACG-3′	To amplify *ble*^{r} gene as a selective marker
bleR	5′-AACTAATTACATGATATCGA-3′	
KanMX-KpnI5'	5′-GATGGTACCCAGCTGAAGCTTCGTACGC-3′	To amplify *kan*MX4 gene as a selective marker for random integrative mutagenesis
KanMX-KpnI3'	5′-CATGGTACCGCATAGGCCACTAGTGGATCTG-3′	
KanMX-100-IV	5′-AGGAGGGTATTCTGGGC-3′	To amplify and sequence the flanking regions of *kan*MX4 insertion site
KanMX-1381-IV	5′-TGCGAAGTTAAGTGCGC-3′	
KanMX-322-IV	5′-TGCTCGCAGGTCTGCAGCGAGGA-3′	
KanMX-216-IV	5′-ACGGGCGACAGTCACATCATGCC-3′	
KanMX-1135-IV	5′-AGTCGGAATCGCAGACCGATACC-3′	
KanMX-1485-IV	5′-GGTCGCTATACTGCTGTCGATTC-3′	

5.4 Results

5.4.1 Isolation and characterization of pentose utilization-defective mutants

To isolate pentose utilization-defective mutants of *K. marxianus* DMKU 3-1042, random integration mutagenesis with a *kan*MX4 cassette was applied. About 9,000 transformants were screened by replica-plating onto YP medium containing xylose or arabinose as a sole carbon source. Three isolated mutants, MYA003, MYA037 and MYA042, had lost their ability to grow on these media (Table 5.2). Integration sites of *kan*MX4 in the mutants were identified by TAIL-PCR followed by nucleotide sequencing. The results indicated that MYA003, MYA037 and MYA042 have an insertion of the mutagenic fragment into the ORFs on chromosomes 2, 3 and 8, respectively, which encode proteins homologous to ScCox15, ScAtp25 and ScCyc3 of *S. cerevisiae*, respectively (Table 5.2). Due to their high identity as described below, these homologous proteins were named KmCox15, KmAtp25 and KmCyc3. The insertion points of *kan*MX4 in MYA003, MYA037 and MYA042 were found to correspond to positions between Ser-92 and Lys93 of KmCox15, Asn-342 of KmAtp25 and Lys-20 of KmCyc3, respectively.

Table 5.2 Identification of *kan*MX4-insertion sites of mutants isolated by TAIL-PCR and nucleotide sequencing

Name	Disrupted gene	Gene product		Insertion position	Function	Remark
		nt	aa			
MYA003	*COX15*	1,479	492	Ser-92/ Lys93	Cytochrome oxidase assembly factor singleton	Stable
MYA037	*ATP25*	1,704	567	Asn-342	Required for Atp9 ring assembly (component of F_o-ATP synthase)	Stable
MYA042	*CYC3*	864	287	Lys-20	Holocytochrome-*c* synthase (cytochrome *c* heme lyase)	Stable

KmCox15, which consists of 492 amino acid residues, shares 68% identity (91% coverage) with ScCox15, which is an integral membrane protein that functions as a cytochrome oxidase assembly protein in *S. cerevisiae*. Like

ScCox15, KmCox15 bears a Cox15-CtaA (pfam02628) domain, which is required for cytochrome oxidase assembly. For example, Cox15 and CtaA are required for cytochrome *c* oxidase assembly in yeast and cytochrome aa_3 oxidase assembly in *Bacillus subtilis*, respectively (Marchler-Bauer et al. 2011). KmAtp25, which has 567 amino acid residues, shares 57% identity (100% coverage) with ScAtp25, which is required for expression and assembly of the Atp9p subunit of the mitochondrial ATPase in *S. cerevisiae* (Zeng et al. 2008). KmAtp25 and ScAtp25 bear mRNA stabilization (pfam13929) and oligomerization (pfam02410) domains (Marchler-Bauer et al. 2011). KmCyc3 with a length of 287 amino acid residues shares 58% identity (98% coverage) with ScCyc3, a cytochrome *c* heme lyase required for the attachment of heme *c* to apo-cytochrome *c* in *S. cerevisiae* (Moraes et al. 2004; Dumont et al. 1991). Both proteins bear a cytochrome *c*/*c*1 heme lyase domain (pfam01265; Marchler-Bauer et al. 2011). These findings suggest that KmCox15, KmAtp25 and KmCyc3 have a crucial function in the formation of complexes I, III and IV in the mitochondrial respiratory chain.

To further verify the disrupted genes of the three mutants, we reintroduced the DNA fragments of their corresponding genes together with those of the bleomycin-resistant gene as a selective marker, which were PCR-amplified from the genomic DNA of the parental *K. marxianus* and plasmid pSH65 (Güldener et al. 2002), respectively, into their genomes and confirmed restoration of growth of all three mutants on xylose (data not shown). These results clearly indicated that only a single integration event of the *kan*MX4 fragment had occurred in each mutant.

5.4.2 Growth and fermentation ability of pentose utilization-defective mutants

To clarify the effects of disruption of *COX15*, *ATP25* and *CYC3*, we examined the growth of the three mutants in comparison with that of the parental strain in YP media containing various sugars and organic acids at 30°C under a shaking condition. All three mutants were found to have completely lost their ability to utilize xylose or arabinose as a sole carbon source. Moreover, these mutants were no longer able to utilize non-fermentable substrates such as acetate and glycerol (data not shown).

To further examine their effects, we compared the growth and ethanol production of the three mutants with those of the parental strain in YPD medium at 30°C and 45°C under a shaking condition (Fig. 5.1). At 30°C, glucose was completely exhausted and the amount of ethanol reached the maximum level within the first 6 h in all of the cultures except for that of the *cyc3* mutant (12 h; Fig. 5.1a). Biomass formation of the three mutants was about 50% lower than that of the parental strain. Ethanol production was maintained at almost a constant level throughout the fermentation period of the three mutants, but the level gradually decreased in the case of the parental strain. The enhanced ethanol content in the cultures of the three mutants might to some extent be due to the diminution of ethanol re-assimilation of the three mutants. At 45°C, glucose utilization rate was dramatically decreased in *cox15* and *atp25* compared to that of the parental strain and glucose was not consumed at all in *cyc3* (Fig. 5.1b). However, the maximum ethanol concentrations of the *cox15* and *atp25* mutants were nearly 2-times higher than that of the parental strain. It is noteworthy that all of the three mutants showed reduction in growth rate and biomass yield at the elevated temperature compared to those of the parental strain (Fig. 5.1b and data not shown).

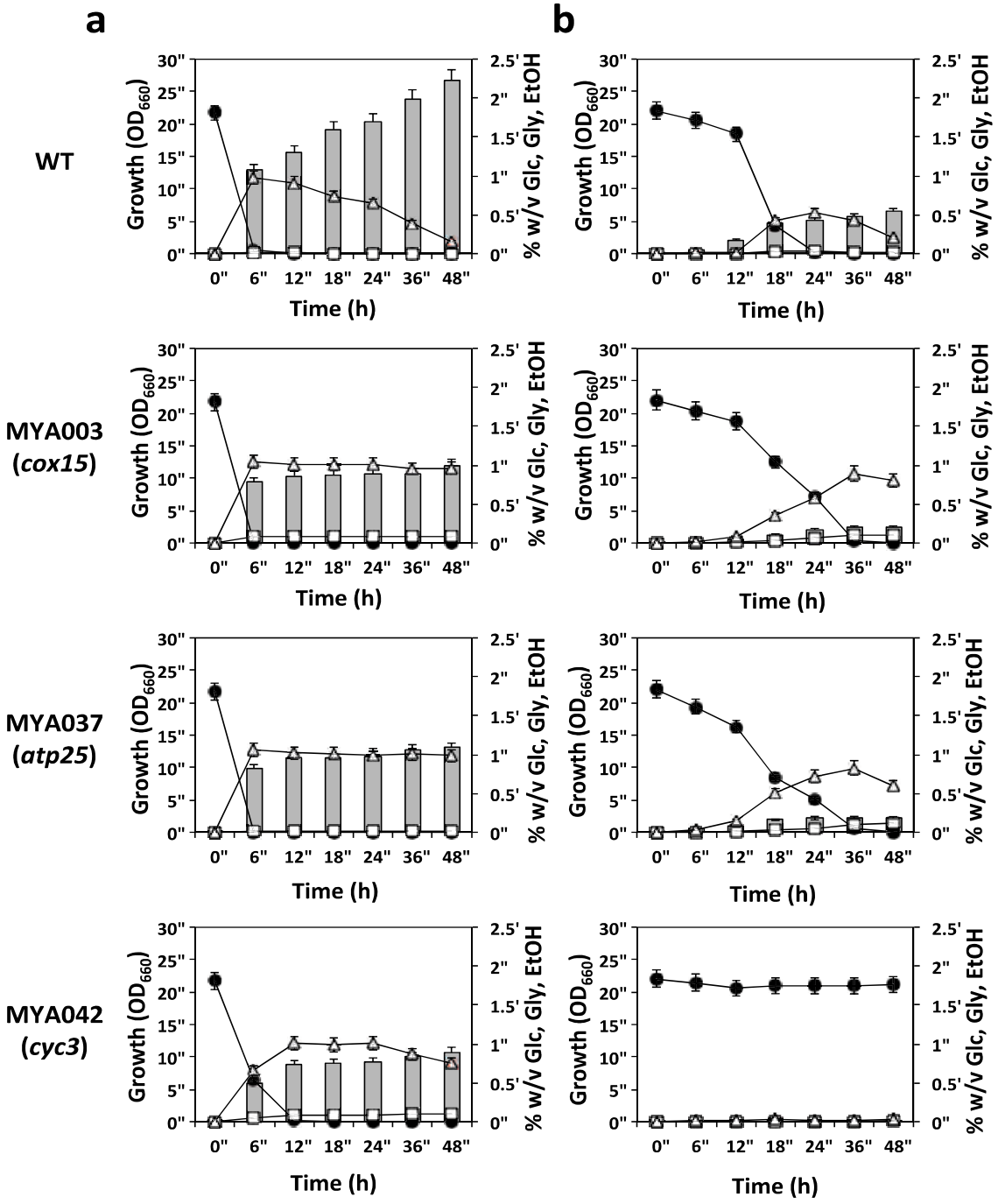

Fig. 5.1 Growth and ethanol productivity of mutants isolated and the parental strain. Cells grown in YPD medium at 30°C for 18 h were inoculated into 30-ml YPD medium in a 100-ml Erlenmeyer flask and incubated at 30°C (a) and 45°C (b) under a shaking condition (160 rpm). Initial OD_{660} was adjusted to 0.1. *Columns* represent cell growth and *closed circles*, *open squares* and *open triangles* represent amounts of glucose, glycerol and ethanol in the medium, respectively. *Bars* represent the ±SD for triplicate experiments.

5.4.3 Effects of respiratory inhibitors on cell growth and ethanol production in the wild-type strain

To obtain supporting evidence of the phenotypes of the three mutants, we examined the effects of two inhibitors of the respiratory chain: potassium cyanide (KCN), which inhibits the terminal oxidase, antimycin A, which blocks the electron transport from bc_1 complex to cytochrome *c*, and carbonyl cyanide *m*-chlorophenylhydrazone (CCCP), which eliminates the proton gradient across the mitochondrial membrane. The experiments were performed with the wild-type strain in YPD and YPX media at 30°C under a shaking condition (Fig. 5.2). As expected, the addition of antimycin A or CCCP caused a dramatic decrease in cell growth in the YPD medium (Fig. 5.2a). On the other hand, KCN had only a weak effect on cell growth in the YPD medium. The maximum ethanol concentration was obtained at 12 h in all cultures, and assimilation of ethanol was observed in the presence of KCN or in the absence of respiratory inhibitors, though there was some leakage of ethanol assimilation in the case with CCCP (Fig. 5.2a). In the YPX medium, cell growth was dramatically inhibited in the presence of KCN and no growth was observed in the presence of antimycin A or CCCP (Fig. 5.2b). Taken together, these results suggest that xylose assimilation in *K. marxianus* absolutely requires respiratory activity and/or oxidative phosphorylation but that glucose assimilation is sufficiently supported by the ethanol fermentation pathway.

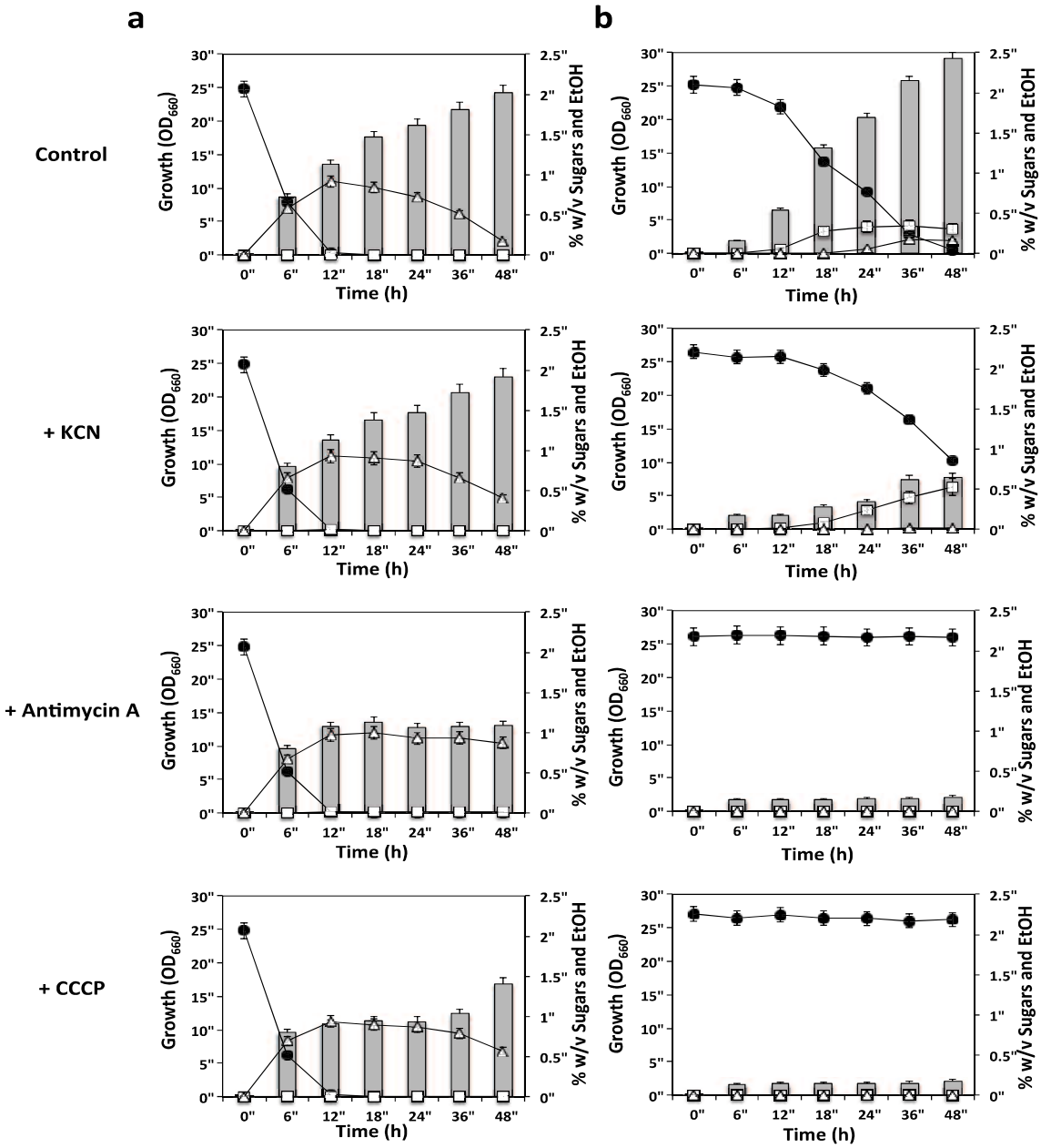

Fig. 5.2 Growth and ethanol productivity of the wild-type *K. marxianus* in the presence of respiratory inhibitors. Cells grown in YPD medium at 30°C for 18 h were inoculated into 30-ml YPD (a) or YPX (b) medium in a 100-ml Erlenmeyer flask and incubated at 30°C under a shaking condition (160 rpm). Initial OD_{660} was adjusted to 0.1. Inhibitors were added 6 h after the inoculation; 1 mM potassium cyanide (KCN), 10 μM antimycin A (AA) or 20 μM carbonyl cyanide *m*-chlorophenylhydrazone (CCCP). Columns represent cell growth and closed circles, open squares and open triangles represent amounts of glucose, glycerol and ethanol in the medium, respectively. Bars represent the ±SD for triplicate experiments.

5.4.4 Respiratory activities and low-temperature reduced-minus-oxidized difference spectra

Since products of *COX15* and *CYC3* are essential for the assembly of cytochrome oxidase and the attachment of heme *c* to apo-cytrochrome *c*, respectively, it was assumed that their inactivation would influence the respiration function of cells. To test this assumption, we determined the respiratory activities of NADH and ubiquinol oxidases in membrane fractions and also examined the effect of KCN on the activities.

In the parent as a control, NADH oxidase activities were found to be 0.033 ± 0.000 units/mg of protein and 0.013 ± 0.001 units/mg of protein in the absence and presence of KCN, respectively, and ubiquinol oxidase activities were 0.038 ± 0.005 units/mg of protein and 0.000 units/mg of protein in the absence and presence of KCN, respectively (Table 5.3). Since KCN specifically blocks cytochrome *c* oxidase, its effect is reflected as a reduction of activity of terminal oxidase. Thus, these results suggest that a KCN-insensitive alternative oxidase (AOX) exists in the respiratory chain of *K. marxianus* and that it is located between the primary dehydrogenases and ubiquinone pool. This localization of AOX in *K. marxianus* appears to be different from those in other yeasts (Veiga et al. 2000; 2003). On the other hand, all three mutants showed a half level of and similar level of NADH oxidase activity in the absence and presence of KCN, respectively, to those of the parent and exhibited no detectable ubiquinol oxidase activity. Consistent with the suggested location of AOX in the parent, the ubiquinol oxidase activity was abolished in *cox15* and *cyc3*.

Table 5.3 Effect of potassium cyanide on respiratory activities in mutants isolated and its parental strain

Strain	Oxidase activity (unit mg protein^{-1})			
	NADH KCN (−)	Ubiquinol KCN (−)	NADH KCN (+)[a]	Ubiquinol KCN (+)[a]
WT	0.033 ± 0.000	0.038 ± 0.005	0.013 ± 0.001	0
cox15	0.014 ± 0.001	0	0.014 ± 0.001	ND
atp25	0.017 ± 0.002	0	0.016 ± 0.000	ND
cyc3	0.015 ± 0.003	0	0.013 ± 0.001	ND

Data are the average ± SD of the mean of the analyses in triplicate
ND not determined
[a] 1 mM KCN

To further examine the characters of the mutants, especially *atp25*, which showed NADH and ubiquinol oxidase activities similar to those of *cox15* and *cyc3*, low-temperature reduced-minus-oxidized difference spectra were obtained (Fig. 5.3). The peak areas of cytochromes c/c_1 were reduced by about 20 and 30% in *atp25* and *cyc3*, respectively, but showed almost no change in *cox15*. The peak areas of cytochrome *b* were reduced by about 20 and 40% in *cox15* and *cyc3*, respectively, but showed almost no change in *atp25*. Interestingly, the peak of $a+a_3$ was almost absent in *cox15* and *cyc3* and was very small in *atp25*. These reductions of the $a+a_3$ peak were consistent with the negligible level of ubiquinol oxidase in all three mutants. These findings suggest that the absence of ubiquinol oxidase in all three mutants is due to reduction of the amounts of cytochromes, especially cytochrome $a+a_3$.

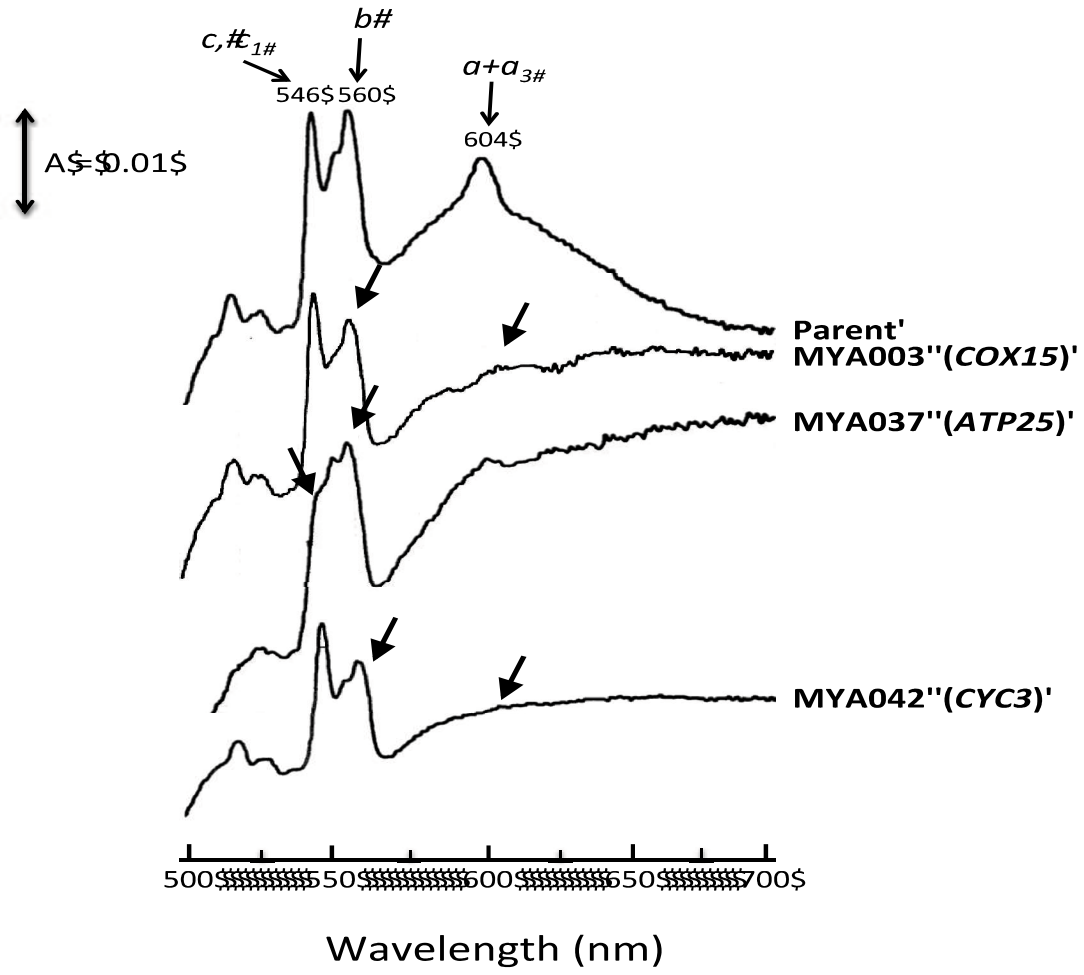

Fig. 5.3 Absolute absorption spectra of membrane fractions of mutants isolated and the parental strain. Cells of *cox15*, *atp25*, *cyc3* and the parent were grown at 30°C in YPD medium until the early stationary phase. The membrane fraction was then prepared at a final protein concentration of 10 mg/ml as described previously (Lertwattanasakul et al. 2009). Low-temperature reduced-minus-oxidized difference spectra were taken between a portion of the membrane fraction reduced with sodium dithionite and the other portion oxidized with potassium ferricyanide (Hatefi 1985). The difference spectrum was recorded and the absorption maxima of the α-bands of cytochromes a+a_3, b and c+c_1 are indicated.

5.5 Discussion

Efficient fermentative conversion of pentose to ethanol is one of crucial issues in the utilization of cellulosic biomass. Although *Scheffersomyces stipitis* is known to have such an efficient conversion ability, the range of fermentation temperatures is up to 25−26°C due to its relatively high thermosensitiveness (Slininger et al. 1990). On the other hand, *K. marxianus* is applicable for high-temperature fermentation around 40°C, but its ability for pentose fermentation is relatively low (Rodrussamee et al. 2011). As the first step to overcome this problem by understanding the background of the pentose metabolism, we attempted random insertion mutagenesis with *kan*MX4 into the genome of *K. marxianus* and obtained 3 pentose utilization-defective mutants. Detailed analysis of these mutants allows us to speculate that the defectiveness of pentose metabolism by disruption of *cox15*, *atp25* or *cyc3* is due to the insufficient reoxidation of reduced cofactors. All of these mutations are thought to have crucial effects on the amount of functional cytochromes, causing almost complete dysfunction of the respiratory activity in *K. marxianus.*

In yeast, Cox15 together with ferredoxin and ferredoxin reductase is involved in the first of the two steps of heme *a* synthesis from heme *o* (Barros et al. 2001; Glerum et al. 1997). An *S. cerevisiae cox15* mutant that is deficient in assembly and function of cytochrome oxidase has no heme *a* (Tzagoloff et al. 1993). This evidence is consistent with our findings that the *K. marxianus cox15*-disrupted mutant exhibited no absorption signal of cytochrome a+a_3 and no ubiquinol oxidase activity (Fig. 5.3; Table 5.3). Additionally, the mutant exhibited a slight reduction of the spectral signal of cytochrome *b*. Similar spectral defects have been found in the *P. stipitis cox5* mutant, which lacks terminal oxidase activity and cyanide-sensitive respiration ability (Freese et al. 2011).

In the *S. cerevisiae atp25* mutant, active F_1 ATPase is synthesized but is unable to combine with the larger proton-translocating F_o portion because of the blockage of its assembly, in which Atp25 is involved (Zeng et al. 2008). The *K. marxianus atp25* mutant showed a severe reduction in growth possibly due to a defect in the formation of F_1 F_o ATPase complex. In addition, the mutant showed a

very low spectral signal of cytochrome a+a_3, a slightly reduced signal of cytochrome *c* and sensitivities to antimycin A and SHAM (Figs. 5.3 and 5.4), which have not been reported in the *S. cerevisiae atp25* mutant. The growth phenotype of the mutant may be due to combined defects of assembly of the F_1 F_o ATPase complex and activity of the respiratory chain.

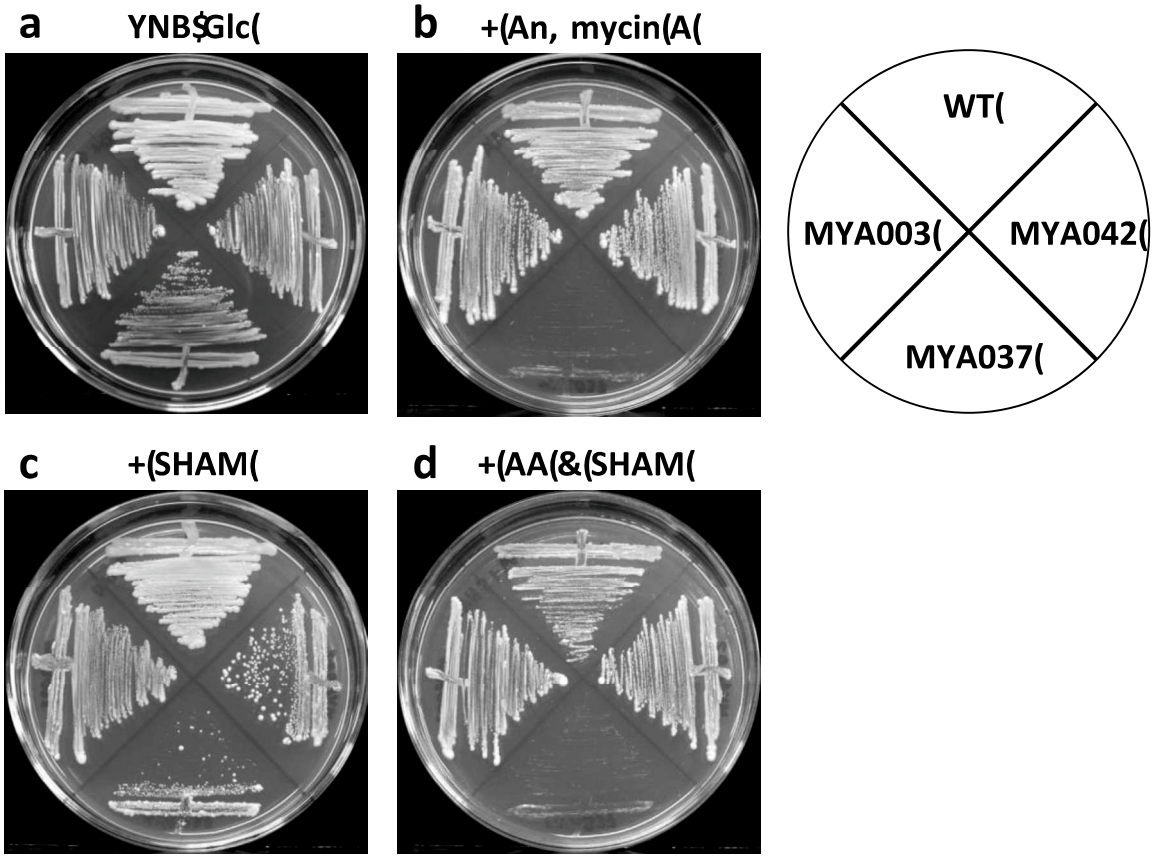

Fig. 5.4 Effects of respiratory inhibitors on cell growth of mutants isolated and the parent. Cells of *cox15*, *atp25*, cyc3 and the parent were grown in YNB-Glc (2%) medium. a No inhibitor added; b antimycin A (5 μM); c SHAM, salicylhydroxamic acid (4 mM); d antimycin A (5 μM) and SHAM (4 mM).

S. cerevisiae Cyc3 as a cytochrome *c* heme lyase catalyzes the attachment of heme *c* to apocytochrome *c* (Dumont et al. 1987). It may play a critical role in the translocation process of the respective cytochrome to the mitochondrial compartment since the import of apocytochrome *c* into mitochondria is impaired in the *cyc3* null mutant (Dumont et al. 1991). Interestingly, in addition to reduction in

the spectral signal of the cytochrome *c* content, the *K. marxianus cyc3* mutant showed a greatly reduced signal of cytochrome *b* and no signal of cytochrome $a+a_3$ (Fig. 5.3). These phenotypes were similar to those of the *cyc1* mutant of *P. stipitis*, which has no signals of cytochromes *c* and $a+a_3$ but retains that of cytochrome *b* (Shi et al. 1999). Therefore, it is likely that no electron flow through cytochrome *c* oxidase occurs in the *K. marxianus cyc3* mutant as in the *P. stipitis cyc1* mutant.

The data presented here demonstrate that Cox15, Atp25 and Cyc3 are not essential for the survival of *K. marxianus* cells on fermentable substrates such as glucose. However, defective mutations of genes for these proteins caused deleterious effects on the assimilation of non-fermentable substrates, so that they are incapable of growing on xylose or arabinose as a carbon source. This incapability may be due to impaired respiratory activity because all three mutants of *cox15*, *cyc3* and *atp25* lost ubiquinol oxidase activity. Therefore, it is thought that respiratory activity is essential for the assimilation of these pentose sugars as found in recombinant *S. cerevisiae* expressing *XYL1*, *XYL2* and *XYL3* derived from *P. stipitis* (Jin et al. 2004). On the other hand, the coincidence of impaired respiration and defect of pentose assimilation in these mutants may correspond to the fact that the uptake of xylose and arabinose through a high-affinity glucose transporter(s) requires ATP (Hahn-Hägerdal et al. 2007) and the fact that redox imbalance that causes accumulation of NADH occurs in the process of xylose and arabinose catabolism (Jeffries 2006). Notably, although the three mutants are thought to retain an active AOX system, it is not clear whether its activity is sufficient to clear the redox imbalance or not.

K. marxianus possesses four Adh isozymes, which exhibit different cellular localizations and play distinctive roles in cells (Lertwattanasakul et al. 2007; 2009). Of these, the cytosolic Adh1 and Adh2 are responsible for the conversion of acetaldehyde to ethanol, though only the *ADH1* gene is expressed in xylose or glycerol media (unpublished data). The yeast would thus recognize xylose as a non-fermentable carbon source. Taken together with findings in this study, it is thought that the reoxidation of NADH, which is generated from xylitol

dehydrogenase, by Adh1 for ethanol synthesis is insufficient to allow *K. marxianus* cells to grow on xylose.

On the basis of results of analyses of absolute absorption spectra and respiratory activity and experiments with inhibitors, it is likely that both *cox15* and *cyc3* lack the functional terminal oxidase but retain a KCN-insensitive AOX activity and that the AOX activity is not sensitive to antimycin A. Therefore, it is thought that the AOX is located between primary dehydrogenases and the ubiquinone pool in *K. marxianus* (Fig. 5.5). Its location on the respiratory chain is quite surprising because all of the AOXs reported previously in yeasts and plants are located after the ubiquinone pool. However, the AOX in *K. marxianus* seems to be divergent from SHAM-sensitive terminal oxidases (STO) previously found in many yeasts including *S. stipitis* (Jeppsson et al. 1995; Veiga et al. 2000; 2003; Shi et al. 2002) because a homology search using known AOX primary sequences from *S. stipitis*, *C. albicans, Yarrowia lipolytica, C. tropicalis* and *Debaryomyces hansenii* returns no hit on the *K. marxianus* whole genome database. Notably, experiments with SHAM in the *atp25* mutant indicate the existence of an STO in *K. marxianus*, which is contradictory to the report by Veiga et al. (2000) based on the measurement of oxygen consumption in the presence of 3.2 mM KCN. This might be due to the difference in method or concentration of the respiratory inhibitor used for analysis. In addition, the STO activity level in *K. marxianus* might be too low to be detected by their method. Further study with mutants isolated will lead to an understanding of the respiratory chain in *K. marxianus.*

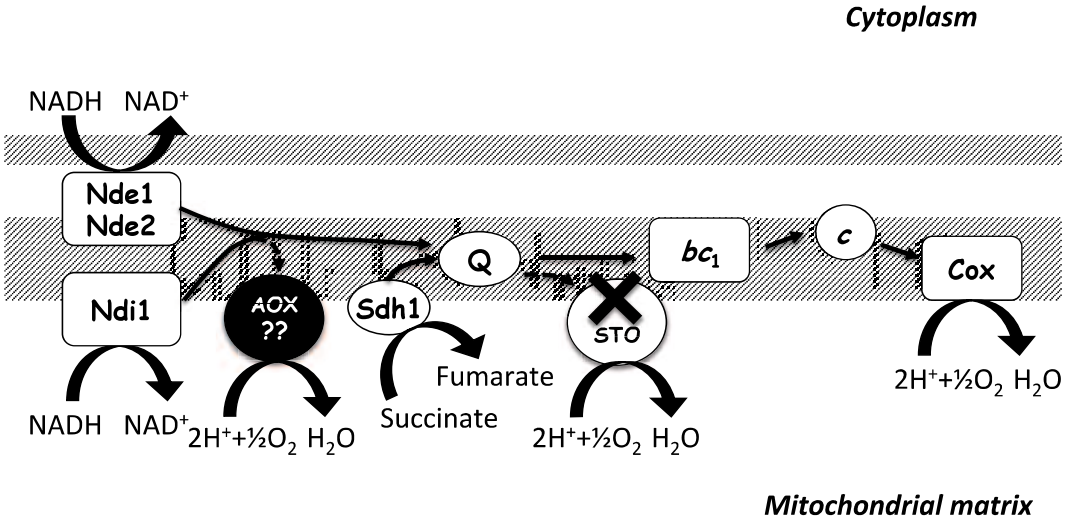

Fig. 5.5 A proposed model of the respiratory chain of *K. marxianus* DMKU 3-1042. *Abbreviations:* Nde1 and 2, external NADH dehydrogenase; Ndi1, internal NADH dehydrogenase; AOX, alternative oxidase; Sdh1, succinate dehydrogenase; Q, ubiquinone; STO, SHAM-sensitive terminal oxidase; bc_1, bc_1 complex; *c*, cytochrome *c*; Cox, cytochrome *c* oxidase.

REFERENCES

Abdel-Banat BM, Nonklang S, Hoshida H, Akada R (2010) Random and targeted gene integrations through the control of non-homologous end joining in the yeast *Kluyveromyces marxianus*. Yeast 27:29–39

Abranches J, Mendonça-Hagler LC, Hagler AN, Morais PB, Rosa CA (1997) The incidence of killer activity and extracellular proteases in tropical yeast communities. Can J Microbiol 43:328–336

Ahuatzi D, Herrero P, de la Cera T, Moreno F (2004) The glucose-regulated nuclear localization of hexokinase 2 in *Saccharomyces cerevisiae* is Mig1-dependent. J Biol Chem 279:14440–14446

Aiba H, Adhya S, de Crombrugghe B (1981) Evidence for two functional gal promoters in intact *Escherichia coli* cells. J Biol Chem 256:11905–11910

Alexa A, Rahnenfuhrer J (2000) topGO: enrichment analysis for gene ontology. R package version 2

Almeida JRM, Runquist D, Sànchez i Nogué V, Lidén G, Gorwa-Grauslund M (2011) Stress-related challenges in pentose fermentation to ethanol by the yeast *Saccharomyces cerevisiae*. Biotechnol J 6:286–299

Alms GR, Sanz P, Carlson M, Haystead TAJ (1999) Reg1p targets protein phosphatase 1 to dephosphorylate hexokinase II in *Saccharomyces cerevisiae*: characterizing the effects of a phosphatase subunit on the yeast proteome. EMBO J 18:4157–4168

Altschul SF, Gish W, Miller W, Myers EW, Lipman DJ (1990) Basic local alignment search tool. J Mol Biol 215:403–410

Altschul SF, Madden TL, Schäffer AA, Zhang J, Zhang Z, Miller W, Lipman DJ (1997) Gapped BLAST and PSI-BLAST: a new generation of protein database search programs. Nucleic Acids Res 25:3389−3402

Anderson PJ, McNeil K, Watson K (1986) High-efficiency carbohydrate fermentation to ethanol at temperatures above 40°C by *Kluyveromyces marxianus* var. *marxianus* isolated from sugar mills. Appl Environ Microbiol 51:1314–1320

Antunes DF, de Souza Jr CG, de Morais Jr MA (2000) A simple and rapid method for lithium acetate-mediated transformation of *Kluyveromyces marxianus* cells. World J Microbiol Biotechnol 16:653−654

Aoki-Kinoshita KF, Kanehisa M (2007) Gene annotation and pathway mapping in KEGG. Methods Mol Biol 396:71−91

Ashrafi K, Lin SS, Manchester JK, Gordon JI (2000) Sip2p and its partner Snf1p kinase affect aging in *S. cerevisiae.* Genes Dev 14:1872–1885

Ausubel FM, Brent R, Kingston RE, Moore DD, Seidman JG, Smith JA, Struhl K (1993) Current Protocol in Molecular Biology. New York: Greene Publishing Associates/Wiley Interscience

Bakker BM, Overkamp KM, van Maris AJ, Kötter P, Luttik MA, van Dijken JP, Pronk JT (2001) Stoichiometry and compartmentation of NADH metabolism in *Saccharomyces cerevisiae*. FEMS Microbiol Rev 25:15−37

Banat IM, Nigam P, Singh D, Marchant R, McHale AP (1998) Review: Ethanol production at elevated temperatures and alcohol concentrations: part I - yeasts in general. World J Microbiol Biotechnol 14:809–821

ACKNOWLEDGEMENTS

I express my deepest gratitude to my supervisors, Prof. Dr. Mamoru Yamada, for creative guidance, attentive supervision and encouragement throughout this research. Besides, he also provides good opportunities and good suggestions, which are valuable to my future career. Your vast knowledge and enthusiastic attitude towards science have been encouraging and motivating.

Beside my advisor, I would like to thank Assist. Prof. T. Kosaka, Prof. Dr. K. Matsushita and Assoc. Prof. T. Yakushi for their helpful discussion and valuable advice.

I am particularly grateful to Dr. Masayuki Murata, Dr. Naoko Fujimoto, Dr. Noppon Lertwattanasakul, Dr. Kannikar Charoensuk, Dr. Nadchanok Rodrussamee, Dr. Sukanya Nitiyon, Mochamad Nurcholis, M.Agr., and members of Josei laboratory who study in Yamaguchi University for their valuable comments, discussion, suggestions and friendship during my study in Yamaguchi University.

I am extremely thankful to the Directorate General of Resources for Science, Technology and Higher Education (DIKTI) scholarship, Ministry of Research, Technology and Higher Education of Indonesia, Brawijaya University, Indonesia for financial support and Department of Biological Chemistry, Yamaguchi University for providing laboratory facilities.

Finally, I greatly appreciate to my parents, my family and my friends for their understanding, encouragement and powerful support.

Suprayogi

Graduate School of Medicine
Yamaguchi University
Japan

Bao WG, Guiard B, Fang ZA, Donnini C, Gervais M, Passos FML, Ferrero I, Fukuhara H, Bolotin-Fukuhara M (2008) Oxygen-dependent transcriptional regulator Hap1p limits glucose uptake by repressing the expression of the major glucose transporter gene RAG1 in *Kluyveromyces lactis*. Eukaryot Cell 7:1895–1905

Bardwell l, Cook JG, Zhu-Shimoni JX, Voora D, Thorner J (1998) Differential regulation of transcription: Repression by unactivated mitogen-activated protein kinase Kss1 requires the Dig1 and Dig2 proteins. Proc Natl Acad Sci USA 95:15400–15405

Barros MH, Carlson CG, Glerum DM, Tzagoloff A (2001) Involvement of mitochondrial ferredoxin and Cox15p in hydroxylation of heme O. FEBS lett 492:133−138

Bera AK, Ho NW, Khan A, Sedlak M (2011) A genetic overhaul of *Saccharomyces cerevisiae* 424A(LNH-ST) to improve xylose fermentation. J Ind Microbiol Biotechnol 38:617–626

Bergdahl B, Sandström AG, Borgström C, Boonyawan T, van Niel EW, Gorwa-Grauslund MF (2013) Engineering yeast hexokinase 2 for improved tolerance toward xylose-induced inactivation. PLoS One 8:e75055

Billard P, Menart S, Blaisonneau J, Bolotin-Fukuhara M, Fukuhara H, Wésolowski-Louvel M (1996) Glucose uptake in *Kluyveromyces lactis*: role of the HGT1 gene in glucose transport. J Bacteriol 178:5860−5866

Bothast RJ, Schlicher MA (2005) Biotechnological processes for conversion of corn into ethanol. Appl Microbiol Biotechnol 67:19–25

Breitkreutz A, Choi H, Sharom JR, Boucher L, Neduva V, Larsen B, Lin ZY, Breitkreutz BJ, Stark C, Liu G, Ahn J, Dewar-Darch D, Reguly T, Tang X, Almeida R, Qin ZS, Pawson T, Gingras AC, Nesvizhskii AI, Tyers M (2010) A global protein kinase and phosphatase interaction network in yeast. Science 328 (5981):1043–1046

Burda P and Aebi M (1998) The *ALG10* locus of *Saccharomyces cerevisiae* encodes the α–1,2 glucosyltransferase of the endoplasmic reticulum: the terminal glucose of the lipid-linked oligosaccharide is required for efficient N-linked glycosylation. Glycobiology 8 (5):455–462

Butler G, Rasmussen MD, Lin MF, Santos MA, Sakthikumar S, Munro CA, Rheinbay E, Grabherr M, Forche A, Reedy JL, Agrafioti I, Arnaud MB, Bates S, Brown AJ, Brunke S, Costanzo MC, Fitzpatrick DA, de Groot PW, Harris D, Hoyer LL, Hube B, Klis FM, Kodira C, Lennard N, Logue ME, Martin R, Neiman AM, Nikolaou E, Quail MA, Quinn J, Santos MC, Schmitzberger FF, Sherlock G, Shah P, Silverstein KAT, Skrzypek MS, Soll D, Staggs R, Stansfield I, Stumpf MPH, Sudbery PE, Srikantha T, Zeng Q, Berman J, Berriman M, Heitman J, Gow NAR, Lorenz MC, Birren BW, Kellis M, Cuomo CA (2009) Evolution of pathogenicity and sexual reproduction in eight *Candida* genomes. Nature 459:657−662

Cáceres AJ, Portillo R, Acosta H, Rosales D, Quiñones W, Avilan L, Salazar L, Dubourdieu M, Michels PA, Concepción JL (2003) Molecular and biochemical characterization of hexokinase from *Trypanosoma cruzi*. Mol Biochem Parasitol 126:251–262

Cao J, Barbosa JM, Singh NK, Locy RD (2013) GABA shunt mediates thermotolerance in *Saccharomyces cerevisiae* by reducing reactive oxygen production. Yeast 30:129−144

Carlson M (1987) Regulation of sugar utilization in *Saccharomyces* species. J Bacteriol 169 (11):4873–4877

Carlson M (1999) Glucose repression in yeast. Curr Opin Microbiol 2 (2):202–207

Carlson M and Botstein D (1983) Organization of the *SUC* gene family in *Saccharomyces*. Mol Cell Biol 3:351–359

Carrasco C, Baudel HM, Sendelius J, Modig T, Roslander C, Galbe M, Hahn-Hägerdal B, Zacchi G, Lidén G (2010) SO2-catalyzed steam pretreatment and fermentation of enzymatically hydrolyzed sugarcane bagasse. Enzyme Microb Technol 46:64–73

Cassart JP, Georis I, Ostling J, Ronne H, Vandenhaute J (1995) The MIG1 repressor from *Kluyveromyces lactis*: cloning, sequencing and functional analysis in *Saccharomyces cerevisiae*. FEBS Lett 371 (2):191–194

Charoensuk K, Irie A, Lertwattanasakul N, Sootsuwan K, Thanonkeo P, Yamada M (2011) Physiological importance of cytochrome c peroxidase in ethanologenic thermotolerant *Zymomonas mobilis*. J Mol Microbiol Biotechnol 20:70–82

Chen W, Guéron M (1992) The inhibition of bovine heart hexokinase by 2-deoxy-D-glucose-6-phosphate: characterization by ^{31}P NMR and metabolic implications. Biochimie 74:867–873

Chen XJ, Wésolowski-Louvel M, Fukuhara H (1992) Glucose transport in the yeast *Kluyveromyces lactis*. II. Transcriptional regulation of the glucose transporter gene RAG1. Mol Gen Genet 233:97−105

Christensen AD, Kádár Z, Oleskowicz-Popiel P, Thomsen MH (2011) Production of bioethanol from organic whey using *Kluyveromyces marxianus*. J Ind Microbiol biotechnol 38 (2):283–289

Chu S and Majumdar A (2012) Opportunities and challenges for a sustainable energy future. Nature 488:294–301

Chua PR and Roeder GS (1998) Zip2, a meiosis-specific protein required for the initiation of chromosome synapsis. Cell 93 (3):349–359

Codón AC, Gasent-Ramírez JM, Benítez T (1995) Factors which affect the frequency of sporulation and tetrad formation in *Saccharomyces cerevisiae* baker's yeasts. Appl Environ Microbiol 61:630−638

Cook JG, Bardwell L, Kron SJ, Thorner J (1996) Two novel targets of the MAP kinase Kss1 are negative regulators of invasive growth in the yeast *Saccharomyces cerevisiae*. Genes Dev 10 (22):2831–2848

Crabeel M, Huygen R, Verschueren K, Messenguy F, Tinel K, Cunin R, Glansdorff N (1985) General amino acid control and specific arginine repression in *Saccharomyces cerevisiae*: physical study of the bifunctional regulatory region of the *ARG3* gene. Mol Cell Biol 5 (11):3139–3148

Crabeel M, Messenguy F, Lacroute F, Glansdorff (1981) Cloning arg3, the gene for ornithine carbamoyltransferase from *Saccharomyces cerevisiae*: expression in *Escherichia coli* requires secondary mutations; production of plasmid β-lactamase in yeast. Proc Natl Acad Sci USA 78 (8):5026–5030

Delcher AL, Bratke KA, Powers EC, Salzberg SL (2007) Identifying bacterial genes and endosymbiont DNA with Glimmer. Bioinformatics 23:673−679

Demeke MM, Dietz H, Li Y, Foulquié-Moreno MR, Mutturi S, Deprez S, Den Abt T, Bonini BM, Liden G, Dumortier F, Verplaetse A, Boles E, Thevelein JM (2013) Development of a D-xylose fermenting and inhibitor tolerant industrial *Saccharomyces cerevisiae* strain with high performance in lignocellulose hydrolysates using metabolic and evolutionary engineering. Biotechnol Biofuels 6:89

Demirbas A (2009) Production of biodiesel from algae oils. Energy Source Part A 31:163–168

Demirbas MF (2011) Biofuels from algae for sustainable development. Appl Energy 88:3473–3480

Derisi JL, Iyer Vr, Brown PO (1997) Exploring the metabolic and genetic control of gene expression on a genomic scale. Science 278:680–686

DeVit MJ and Johnston M (1999) The nuclear exportin Msn5 is required for nuclear export of the Mig1 glucose repressor of *Saccharomyces cerevisiae.* Curr Biol 9 (21):1231–1241

DeVit MJ, Waddle JA, Johnston M (1997) Regulated nuclear translocation of the Mig1 glucos repressor. Mol Biol Cell 8:1603–1618

Dietrich FS, Voegeli S, Brachat S, Lerch A, Gates K, Steiner S, Mohr C, Pöhlmann R, Luedi P, Choi S, Wing RA, Flavier A, Gaffney TD, Philippsen P (2004) The *Ashbya gossypii* genome as a tool for mapping the ancient *Saccharomyces cerevisiae* genome. Science 304:304−307

Domitrovic T, Kozlov G, Freire JCG, Masuda CA, da Silva Almeida M, Montero-Lomeli M, Atella GC, Matta-Camacho E, Gehring K, Kurtenbach E (2010) Structural and functional study of Yer067w, a new protein involved in yeast metabolism control and drug resistance. PloS One 5 (6):e11163

dos Santos VC, Bragança CRS, Passos FJV, Passos FML (2013) Kinetics of growth and ethanol formation from a mix of glucose/xylose substrate by *Kluyveromyces marxianus* UFV-3. Antonie van Leeuwenhoek 103:153–161

Dujon B, Sherman D, Fischer G, Durrens P, Casaregola S, Lafontaine I, De Montigny J, Marck C, Neuvéglise C, Talla E, Goffard N, Frangeul L, Aigle M, Anthouard V, Babour A, Barbe V, Barnay S, Blanchin S, Beckerich JM, Beyne E, Bleykasten C, Boisramé A, Boyer J, Cattolico L, Confanioleri F, De Daruvar A, Despons L, Fabre E, Fairhead C, Ferry-Dumazet H, ~~et al~~ Groppi A, Hantraye F, Hennequin C, Jauniaux N, Joyet P, Kachouri R, Kerrest A, Koszul R, Lemaire M, Lesur I, Ma L, Muller H, Nicaud JM, Nikolski M, Oztas S, Ozier-Kalogeropoulos O, Pellenz S, Potier S, Richard GF, Straub ML, Suleau A, Swennen D, Tekaia F, Wesolowski-Louvel M, Westhof E, Wirth B, Zeniou-Meyer M, Zivanovic I, Bolotin-Fukuhara M, Thierry A, Bouchier C, Caudron B, Scarpelli C, Gaillardin C, Weissenbach J, Wincker P, Souciet JL (2004) Genome evolution in yeasts. Nature 430:35−44

Dumont ME, Cardillo TS, Hayes MK, Sherman F (1991) Role of cytochrome *c* heme lyase in mitochondrial import and accumulation of cytochrome *c* in *Saccharomyces cerevisiae*. Mol Cell Biol 11 (11):5487−5496

Dumont ME, Ernst JF, Hampsey DM, Sherman F (1987) Identification and sequence of the gene encoding cytochrome c heme lyase in the yeast *Saccharomyces cerevisiae*. EMBO J 6 (1):235−241

Entian KD (1986) Glucose repression: a complex regulatory system in yeast. Microbiol Sci 3 (12):366–371

Eshaq FS, Ali MN, Mohd MK (2010) *Spirogyra* biomass a renewable source for biofuel (bioethanol) production. Int J Eng Sci Technol 2:7045–7054

Faga BA, Wilkins MR, Banat IM (2010) Ethanol production through simultaneous saccharification and fermentation of switchgrass using *Saccharomyces cerevisiae* D_5A and thermotolerant *Kluyveromyces marxianus* IMB strains. Bioresour Technol 101:2273–2279

Farrell AE, Plevin RL, Turner BT, Jones AD, O'hare M, Kammen DM (2006) Ethanol can contribute to energy and environmental goals. Science 311:506–508

Flores CL, Rodríguez C, Petit T, Gancedo C (2000) Carbohydrate and energy-yielding metabolism in non-conventional yeasts. FEMS Microbiol Rev 24:507–529

Fonseca GG, Gombert AK, Heinzle E, Wittmann C (2007) Physiology of the yeast *Kluyveromyces marxianus* during batch and chemostat cultures with glucose as the sole carbon source. FEMS Yeast Res 7 (3):422–435

Fonseca GG, Heinzle E, Wittmann C, Gombert AK (2008) The yeast *Kluyveromyces marxianus* and its biotechnological potential. Appl Microbiol Biotechnol 79:339–354

Foukis A, Stergioua P, Theodoroua LG, Papagianni M, Papamichael EM (2012) Purification, kinetic characterization and properties of a novel thermo-tolerant extracellular protease from *Kluyveromyces marxianus* IFO 0288 with potential biotechnological interest. Biores Technol 123:214–220

Freese S, Passoth V, Klinner U (2011) A mutation in the *COX5* gene of the yeast *Scheffersomyces stipitis* alters utilization of amino acids as carbon source, ethanol formation and activity of cyanide insensitive respiration. Yeast 28:309–320

Fukuhara H (2006) *Kluyveromyces lactis* - A retrospective. FEMS Yeast Res 6:323–324

Gancedo JM (1998) Yeast carbon catabolite repression. Microbiol Mol Biol Rev 62 (2):334–361

Gancedo JM, Gancedo C (1986) Catabolite repression mutants of yeast (Catabolite repression; *Saccharomyces cerevisiae*; yeast mutants). FEMS Microbiol Rev 32:179–187

Gárdonyi M, Jeppsson M, Liden G, Gorwa-Grauslund MF, Hahn-Hägerdal B (2003b) Control of xylose consumption by xylose transport in recombinant *Saccharomyces cerevisiae*. Biotechnol Bioeng 82 (7):818–824

Glerum DM, Muroff I, Jin C, Tzagoloff A (1997) *COX15* codes for a mitochondrial protein essential for the assembly of yeast cytochrome oxidase. J Biol Chem 272 (30):19088–19094

González-Siso MI, Freire-Picos MA, Ramil E, González-Domínguez M, Rodríguez Torres A, Cerdán ME (2000) Respirofermentative metabolism in *Kluyveromyces lactis*: insights and perspectives. Enzyme Microb Technol 26:699–705

Gonzalez-Siso MI, Garcia-Leiro A, Tarrio N, Cerdan ME (2009) Sugar metabolism, redox balance and oxidative stress response in the respiratory yeast *Kluyveromyces lactis*. Microb Cell Fact 8:46

Goshima T, Tsuji M, Inoue H, Yano S, Hoshino T, Matsushika A (2013) Bioethanol production from lignocellulosic biomass by a novel *Kluyveromyces marxianus* strain. Biosci Biotechnol Biochem 77:1505–1510

Gough SBD, Nigam P, Marchant R, McHale AP (1997) Production of ethanol from molasses at 45°C using alginate-immobilized *Kluyveromyces marxianus* imb3. Bioprocess Biosyst Eng 16 (6):389–392

Gray KA, Zhao L, Emptage M (2006) Bioethanol. Curr Opin Chem Bio 10:141–146

Groeneveld P, Stouthamer AH, Westerhoff HV (2009) Super life – how and why 'cell selection' leads to the fastest-growing eukaryote. FEBS J 276:254–270

Güldener U, Heinisch J, Köhler GJ, Voss D, Hegemann, JH (2002) A second set of *lox*P marker cassettes for Cre-mediated multiple gene knockouts in budding yeast. Nucl Acids Res 30 (6):e23

Hahn-Hägerdal B, Galbe M, Gorwa-Grauslund MF, Lidén G, Zacchi G (2006) Bio-ethanol – the fuel of tomorrow from the residues of today. Trends in Biotechnol 24:549−556

Hahn-Hägerdal B, Karhumaa K, Fonseca C, Spencer-Martins I, Gorwa-Grauslund MF (2007) Towards industrial pentose-fermenting yeast strains. Appl Microbiol Biotechnol 74:937–953

Hamacher T, Becker J, Gárdonyi M, Hanh-Hägerdal B, Boles E (2002) Characterization of the xylose-transporting properties of yeast hexose transporters and their influence on xylose utilization. Microbiology 148:2783–2788

Hatefi Y (1985) The mitochomdrial electron transport and oxidative phosphorylation system. Ann Rev Biochem 54:1015−1069

Hector RE, Dien BS, Cotta MA, Qureshi N (2011) Engineering industrial *Saccharomyces cerevisiae* strains for xylose fermentation and comparison for switchgrass conversion. J Ind Microbiol Biotechnol 38:1193–1202

Heredia MF, Heredia CF (1988) *Saccharomyces cerevisiae* acquires resistance to 2-deoxyglucose at a very high frequency. J Bacteriol 170:2870–2872

Hong J, Wang Y, Kumagai H, Tamaki H (2007) Construction of thermotolerant yeast expressing thermostable cellulase genes. J Biotech 130 (2):114–1123

Hori A, Yoshida M, Shibata T, Ling F (2009) Reactive oxygen species regulate DNA copy number in isolated yeast mitochondria by triggering recombination-mediated replication. Nucleic Acids Res 37:749–761

Hoshida H, Murakami N, Suzuki A, Tamura R, Asakawa J, Abdel-Banat BM, Nonklang S, Nakamura M, Akada R (2014) Non-homologous end joining-mediated functional marker selection for DNA cloning in the yeast *Kluyveromyces marxianus*. Yeast 31:29–46

Hsu TC, Guo GL, Chen WH, Hwang WS (2010) Effect of dilute acid pretreatment of rice straw on structural properties and enzymatic hydrolysis. Bioresour Technol 101:4907–4913

Jablonowski D, Schaffrath R (2007) Zymocin, a composite chitinase and tRNase killer toxin from yeast. Biochem Soc Trans 35:1533–1537

Jeffries TW (2006) Engineering yeasts for xylose metabolism. Curr Opin Biotechnol 17 (3):320−326

Jeffries TW, Grigoriev IV, Grimwood J, Laplaza JM, Aerts A, Salamov A, Schmutz J, Lindquist E, Dehal P, Shapiro H, Jin YS, Passoth V, Richardson PM (2007) Genome sequence of the lignocellulose-bioconverting and xylose-fermenting yeast *Pichia stipitis*. Nat Biotechnol 25:319−326

Jeong H, Lee DH, Kim SH, Kim HJ, Lee K, Song JY, Kim BK, Sung BH, Park JC, Sohn JH, Koo HM, Kim JF (2012) Genome sequence of the thermotolerant yeast *Kluyveromyces marxianus* var. *marxianus* KCTC 17555. Eukaryotic Cell 11:1584–1585

Jeppsson H, Alexander NJ, Hahn-Hägerdal B (1995) Existence of cyanide-isensitive respiration in the yeast *Pichia stipitis* and its possible influence on product formation during xylose utilization. Appl Environ Microbiol 61 (7):2596−2600

Jiang R and Carlson M (1996) Glucose regulates protein interactions within the yeast SNF1 protein kinase complex. Genesdev 10:3105–3115

Jin YS, Laplaza JM, Jeffries TW (2004) *Saccharomyces cerevisiae* engineered for xylose metabolism exhibits a respiratory response. Appl Environ Microbiol 70 (11):6816−6825

Jojima T, Omumasaba CA, Inui M, Yukawa H (2010) Sugar transporters in efficient utilization of mixed sugar substrates: current knowledge and outlook. Appl Microbiol Biotechnol 85 (3):471−480

Kahar P, Taku K, Tanaka S (2011) Enhancement of xylose uptake in 2-deoxyglucose tolerant mutant of *Saccharomyces cerevisiae*. J Biosci Bioeng 111:557–563

Karhumaa K, Garcia Sanchez R, Hahn-Hägerdal B, Gorwa-Grauslund MF (2007) Comparison of the xylose reductase-xylitol dehydrogenase and the xylose isomerase pathways for xylose fermentation by recombinant *Saccharomyces cerevisiae*. Microb Cell Fact 6:5

Keleher CA, Redd MJ, Schultz J, Carlson M, Johnson AD (1992) Ssn6-Tup1 is a general repressor of transcription in yeast. Cell 68:709–719

Kim SR, Park YC, Jin, YS, Seo JH (2013) Strain engineering of *Saccharomyces cerevisiae* for enhanced xylose metabolism. Biotechnol Adv 31:851–861

Kita K, Okada S, Sekino H, Imou K, Yokoyama S and Amano T (2010) Thermal pretreatment of wet microalgae harvest for efficient hydrocarbon recovery. Appl Energy 87:2420–2423

Klein CJL, Olsson L, Nielsen J (1998) Glucose control in *Saccharomyces cerevisia*: the role of *MIG1* in metabolic function. Microbiology 144:13–24

Kötter P, Ciriacy M (1993) Xylose fermentation by *Saccharomyces cerevisiae*. Appl Microbiol Biotechnol 38:776−783

Kuser PR, Krauchenco S, Antunes OA, Polikarpov I (2000) The high resolution crystal structure of yeast hexokinase PII with the correct primary sequence provides new insights into its mechanism of action. J Biol Chem 275:20814–20821

Kwast KE, Lai LC, Menda N, James DT III, Aref S, Burke PV (2002) Genomic analyses of anaerobically induced genes in *Saccharomyces cerevisiae*: functional roles of Rox1 and other factors in mediating the anoxic response. J Bacteriol 184:250–265

Lachance MA (1998) *Kluyveromyces* van der Walt emend. van der Walt. In: The Yeasts. A Taxonomic Study. Elsevier, Amsterdam

Lachance MA (2011) *Kluyveromyces* van der Walt. In The Yeasts. A Taxonomic Study. 5th edition, Edited by Kurtzman CP, Fell JW, Boekhout T: Elsevier, Amsterdam 471–481

Lane MM, Morrissey JP (2010) *Kluyveromyces marxianus*: A yeast emerging from its sister's shadow. Fungal Biol Rev 24:17−26

Laslett D, Canback B (2004) ARAGORN, a program to detect tRNA genes and tmRNA genes in nucleotide sequences. Nucleic Acids Res 32: 11−16

Leclerc M, Chemardin P, Arnaud A, Ratomahenina R, Galzy P, Gerbaud C, Raynal A, Guérineau M (1987) Comparison of the properties of the purified beta-glucosidase from the transformed strain of *Saccharomyces cerevisiae* TYKF2 with that of the donor strain *Kluyveromyces fragilis* Y610. Biotechnol Appl Biochem 9:410–422

Lertwattanasakul N, Kaewta S, Limtong S, Thanonkeo P, Yamada M (2007) Comparison of the gene expression patterns of alcohol dehydrogenase isozymes in the thermotolerant yeast *Klueyveromyces marxianus* and their physiological functions. Biosci Biotechnol Biochem 71 (5):1170–1182

Lertwattanasakul N, Shigemoto E, Rodrussamee N, Limtong S, Thanonkeo P, Yamada M (2009) The crucial role of alcohol dehydrogenase Adh3 in *Kluyveromyces marxianus* mitochondrial metabolism. Biosci Biotechnol Biochem 73 (12):2720−2726

Lertwattanasakul N, Rodrussamee N, Suprayogi, Limtong S, Thanonkeo P, Kosaka T, Yamada M (2011) Utilization capability of sucrose, raffinose and inulin and its less-sensitiveness to glucose repression in thermotolerant yeast *Kluyveromyces marxianus* DMKU 3-1042. AMB Express 1:20

Lertwattanasakul N, Suprayogi, Murata M, Rodrussamee N, Limtong S, Kosaka T, Yamada M (2013) Essentiality of respiratory activity for pentose utilization in thermotolerant yeast *Kluyveromyces marxianus* DMKU 3-1042. Antonie Leeuwenhoek 103:933–945

Lertwattanasakul N, Kosaka T, Hosoyama A, Suzuki Y, Rodrussamee N, Matsutani M, Murata M, Fujimoto N, Suprayogi, Tsuchikane K, Limtong S, Fujita N, Yamada M (2015) Genetic basis of the highly efficient yeast *Kluyveromyces marxianus*: complete genom sequence and transcriptome analyses. Biotechnol Biofuels 8:47

Limtong S, Sringiew C, Yongmanitchai W (2007) Production of fuel ethanol at high temperature from sugar cane juice by a newly isolated *Kluyveromyces marxianus*. Bioresour Technol 98:3367–3374

Linde M, Galbe M, Zacchi G (2007) Simultaneous saccharification and fermentation of steam-pretreated barley straw at low enzyme loadings and low yeast concentration. Enzyme Microb Technol 40:1100–1107

Linde M, Jakobsson EL, Galbe M, Zacchi G (2008) Steam inretreatment of dilute H_2SO4-impregnated wheat straw and SSF with low yeast and enzyme loadings for bioethanol production. Biomass Bioenergy 32:326–332

Llorente B, Malpertuy A, Blandin G, Artiguenave F, Wincker P, Dujon B (2000) Genomic exploration of the hemiascomycetous yeasts: 12. *Kluyveromyces marxianus* var. *marxianus*. FEBS Lett 487:71–75

Lobo Z, Maitra PK (1977) Resistance to 2-deoxyglucose in yeast: a direct selection of mutants lacking glucose-phosphorylating enzymes. Mol Gen Gent 157:297–300

Lowry OH, Rosebrough NJ, Farr AL, Randall RJ (1951) Protein measurement with the Folin phenol reagent. J Biol Chem 193:265–275

Lu S, Li L, Zhou G (2010) Genetic modification of wood quality for second-generation biofuel production. GM Crops 1:230–236

Luftiyya L, Johnston M (1996) Two zinc-finger-containing repressors are responsible for glucose repression of *SUC2* expression. Mol Cell Biol 16:4790–4797

Lulu L, Ling Z, Dongmei W, Xiaolian G, Hisanori T, Hidehiko K, Jiong H (2003) Identification of a xylitol dehydrogenase gene from *Kluyveromyces marxianus* NBRC1777. Mol Biotechnol 53:159−169

Marchler-Bauer A, Lu S, Anderson JB, Chitsaz F, Derbyshire MK, DeWeese-Scott C, Fong JH, Geer LY, Geer RC, Gonzales NR, Gwadz M, Hurwitz DI, Jackson JD, Ke Z, Lanczycki CJ, Lu F, Marchler GH, Mullokandov M, Omelchenko MV, Robertson CL, Song JS, Thanki N, Yamashita RA, Zhang D, Zhang N, Zheng C, Bryant SH (2011) CDD: a Conserved Domain Database for the functional annotation of proteins. Nucleic Acids Res 39 (D):225−229

Marres CA, de Vries S, Grivell LA (1991) Isolation and inactivation of the nuclear gene encoding the rotenone-insensitive internal NADH: ubiquinone oxidoreductase of mitochondria from *Saccharomyces cerevisiae*. Eur J Biochem 195:857–862

Martin M, Heredia CF (1977) Characterization of a phophatase specific for 2-deoxyglucose-6-phosphate in a yeast mutant. FEBS Lett 83:245–248

Martins DB, de Souza CG Jr, Simões DA, de Morais MA Jr (2002) The β-galactosidase activity in *Kluyveromyces marxianus* CBS6556 decreases by high concentrations of galactose. Curr Microbiol 44:379–382

Matsushika A, Inoue H, Murakami K, Takimura O, Sawayama S (2009) Bioethanol production performance of five recombinant strains of laboratory and industrial xylose-fermenting *Saccharomyces cerevisiae*. Bioresour Technol 100:2392–2398

Matsutani M, Hirakawa H, Yakushi T, Matsushita K (2010) Genome-wide phylogenetic analysis of *Gluconobacter, Acetobacter*, and *Gluconacetobacter*. FEMS Microbiol Lett 315:122−128

Mokranjac D, Sichting M, Popov-Celeketic D, Berg A, Hell K, Neupert W (2005) The import motor of the yeast mitochondrial TIM23 preprotein translocase contains two different J proteins, Tim14 and Mdj2. J Biol Chem 280 (36):31608–31614

Moraes CT, Diaz F, Barrientos A (2004) Defects in the biosynthesis of mitochondrial heme *c* and heme *a* in yeast and mammals. Biochim Biophy Acta 1659 (2−3):153−159

Moreno F and Herrero P (2002) The hexokinase 2-dependent glucose signal transduction pathway of *Saccharomyces cerevisiae*. FEMS Microbiol Rev 26:83–90

Moriya Y, Itoh M, Okuda S, Yoshizawa AC, Kanehisa M: KAAS (2007) an automatic genome annotation and pathway reconstruction server. Nucleic Acids Res 35(Suppl 2):W182−W185

Mussatto SI, Dragone G, Guimarães PMR, Silva JPA, Lívia MC, Carneiro LM, Roberto IC, Vicente A, Domingues L, Teixeira JA (2010) Technological trends, global market, and challenges of bio-ethanol production. Biotechnol Adv 28 (6):817–830

Naik SN, Goud VV, Rout PK, Dalai AK (2010) Production of first and second generation biofuels: A comprehensive review. Renewable Sustainable Energy Rev 14:578–597

Nehlin JO, Carlberg M, Ronne H (1991) Control of yeast *GAL* genes by MIG1 repressor: a transcriptional cascade in the glucose response. EMBO J 10 (11):3373–3377

Nehlin JO, Ronne H (1990) Yeast MIG1 repressor is related to the mammalian early growth response and Wilms' tumour finger proteins. EMBO J 9 (9):2891–2898

Nguyen NH, Suh SO, Marshall CJ, Blackwell M (2006) Morphological and ecological similarities: wood-boring beetles associated with novel xylose-fermenting yeasts, *Spathaspora passalidarum* gen. sp. nov. and *Candida jeffriesii* sp. nov. Mycol Res 110 (10):1232−1241

Niederacher D, Entian KD (1991) Characterization of Hex2 protein, a negative regulatory element necessary for glucose repression in yeast. Eur J Biochem 200:311–319

Nonklang S, Abdel-Banat BM, Cha-aim K, Moonjai N, Hoshida H, Limtong S, Yamada M, Akada R (2008) High-temperature ethanol fermentation and transformation with linear DNA in the thermotolerant yeast *Kluyveromyces marxianus* DMKU 3-1042. Appl Environ Microbiol 74:7514–7521

Oda Y, Nakamura K (2009) Production of ethanol from the mixture of beet molasses and cheese whey by a 2-deoxyglucose-resistant mutant of *Kluyveromyces marxianus*. FEMS Yeast Res 9 (5):742–748

Öhgren, K, Bura R, Saddler J, Zacchi G (2007) Effect of hemicellulose and lignin removal on enzymatic hydrolysis of steam pretreated corn stover. Bioresour Technol 98:2503–2510

Ostling J and Ronne H (1998) Negative control of the Mig1p repressor by Snf1p-dependent phosphorylation in the absence of glucose. Eur J Biochem 252:162–168

Pal R, Tewari S, Rai JPN (2009) Metals sorption from aqueous solutions by *Kluyveromyces marxianus*: process optimization, equilibrium modeling and chemical characterization. Biotechnol J 4 (10):1471–1478

Pas M, Piskur B, Sustaric M, Raspor P (2007) Iron enriched yeast biomass-a promising mineral feed supplement. Bioresour Technol 98 (8):1622–1628

Peláez R, Herrero P, Moreno F (2010) Functional domains of yeast hexokinase 2. Biochem J 432:181–190

Pemberton LF and Blobel G (1997) Characterization of the Wtm proteins, a novel family of *Saccharomyces cerevisiae* transcriptional modulators with roles in meiotic regulation and silencing. Mol and Cell Biol 17 (8):4830–4841

Polevoda B, Martzen MR, Das B, Phizicky EM, Sherman F (2000) Cytochrome *c* methyltransferase, Ctm1p, of yeast. J Biol Chem 275 (27):20508–20513

Popp J, Lakner Z, Harangi-Rákos M, Fári M (2014) The effect of bioenergy expansion: Food, energy, and environment. Renew Sust Energ Rev 32 :559–578

Prior C, Mamessier P, Fukuhara H, Chen XJ, Wesolowski-Louvel M (1993) The hexokinase gene is required for transcriptional regulation of the glucose transporter gene *RAG1* in *Kluyveromyces lactis*. Mol Cell Biol 13:3882–3889

Raimondi S, Uccelletti D, Amaretti A, Leonardi A, Palleschi C, Rossi M (2010) Secretion of *Kluyveromyces lactis* Cu/Zn SOD: strategies for enhanced production. Appl Microbiol Biotechnol 86:871–878

Rajoka MI (2007) Kinetic parameters and thermodynamic values of β-xylosidase production by *Kluyveromyces marxianus*. Bioresour Technol 98 (11):2212–2219

Ralser M, Wamelink MM, Struys EA, Joppich C, Krobitsch S, Jakobs C, Lehrach H (2008) A catabolic block does not sufficiently explain how 2-deoxy-D-glucose inhibits cell growth. Proc Natl Acad Sci USA 105:17807–17811

Rémond C, Aubry N, Cronier D, Noel S, Martel F, Roge B, Rakotoarivonina H, Debeire P, Chabbert B (2010) Combination of ammonia and xylanase pretreatments: Impact on enzymatic xylan and cellulose recovery from wheat straw. Bioresour Technol 101:6712–6717

Richard P, Toivari MH, Penttilä M (1999) Evidence that the gene YLR070c of *Saccharomyces cerevisiae* encodes a xylitol dehydrogenase. FEBS Lett 457:135–138

Robinson MD, McCarthy DJ, Smyth GK (2010) edgeR: a Bioconductor package for differential expression analysis of digital gene expression data. Bioinformatics 26:139−140

Rocha SN, Abrahão-Neto J, Cerdán ME, Gombert AK, González-Siso MI (2011) Heterologous expression of a thermophilic esterase in *Kluyveromyces* yeasts. Appl Microbiol Biotechnol 89:375–385

Rocha SN, Abrahão-Neto J, Cerdán ME, González-Siso MI, Gombert AK (2010) Heterologous expression of glucose oxidase in the yeast *Kluyveromyces marxianus*. Microb Cell Fact 9:4 DOI: 10.1186/1475–2859–9–4

Rodicio R, Heinisch JJ (2013) Yeast on the milky way: genetics, physiology and biotechnology of *Kluyveromyces lactis*. Yeast 30:165–177

Rodrussamee N, Lertwattanasakul N, Hirata K, Suprayogi, Limtong S, Kosaka T, Yamada M (2011) Growth and ethanol fermentation ability on hexose and pentose sugars and glucose effect under various conditions in thermotolerant yeast *Kluyveromyces marxianus*. Appl Microbiol Biotechnol 90:1573–1586

Rothfels K, Tanny JC, Molnar E, Friesen H, Commisso C, Segall J (2005) Components of the ESCRT pathway, *DFG16*, and *YGR122w* are required for Rim101 to act as a corepressor with Nrg1 at the negative regulatory element of the *DIT1* gene of *Saccharomyces cerevisiae*. Mol Cell Biol 25 (15):6772–6788

Rubio-Texeira M (2006) Endless versatility in the biotechnological applications of *Kluyveromyces* LAC genes. Biotechnol Adv 24:212–225

Salzberg SL, Delcher AL, Kasif S, White O (1998) Microbial gene identification using interpolated Markov models. Nucleic Acids Res 26:544−548

Sambrook J & Russell DW (2001) *Molecular Cloning, a laboratory manual 3rd ed.* Cold Spring Harbor Laboratory, Cold Spring Harbor

Sanger F, Nicklen S, Coulson AR (1977) DNA sequencing with chain-terminating inhibitors. Proc Natl Acad Sci USA 74:5463–5467

Sarkar N, Ghosh SK, Bannerjee S, Aikat K (2012) Bioethanol production from agricultural wastes: An overview. Renew Energy 37:19–27

Sassner P, Galbe M, Zacchi G (2005) Steam pretreatment of *Salix* with and without SO_2 impregnation for production of bioethanol. Appl Biochem Biotechnol 121(124):1101– 1117

Saxena RC, Adhikari DK, Goyal HB (2009) Biomass-based energy fuel through bio-chemical routes: A review. Renew Sust Energy Rev 13 (1):167–178

Schaffrath R, Breunig KD (2000) Genetics and molecular physiology of the yeast *Kluyveromyces lactis*. Fungal Genet Biol 30:173–190

Schuurmans JM, Boorsma A, Lascaris R, Hellingwerf KJ, Teixeira de Mattos MJ (2008) Physiological and transcriptional characterization of *Saccharomyces cerevisiae* strains with modified expression of catabolic regulators. FEMS Yeast Res 8:26–34

Scott EM, Pillus L (2010) Homocitrate synthase connects amino acid metabolism to chromatin functions through Esa1 and DNA damage. Genes Dev 24:1903−1913Singh D, Nigam P, Banat IM, Marchant R, McHale AP (1998) Review: Ethanol production at elevated temperatures and alcohol concentrations: Part II-Use of *Kluyveromyces marxianus* IMB3. World J Microbiol Biotechnol 14:823-834Sols A, Crane RK (1954) Substrate specificity of brain hexokinase. J Biol Chem 210:581–595

Shi NQ, Cruz JC, Sherman F, Jeffries TW (2002) SHAM-sensitive alternative respiration in the xylose-metabolizing yeast *Pichia stipitis*. Yeast 19:1203−1220

Shi NQ, Davis B, Sherman F, Cruz J, Jeffries TW (1999) Disruption of the cytochrome *c* gene in xylose-utilizing yeast *Pichia stipitis* leads to higher ethanol production. Yeast 15:1021−1030

Singh A and Olsen SI (2011) Critical analysis of biochemical conversion, sustainability and life cycle assessment of algal biofuels. Appl Energy 88:3548–3555

Singh A, Nigam PS, Murphy JD, (2011) Mechanism and challenges in commercialisation of algal biofuels. Bioresource Technol 102:26–34

Slininger PJ, Bothast RJ, Ladisch MR, Okos MR (1990) Optimum pH and temperature conditions for xylose fermentation by *Pichia stipitis*. Biotechnol Bioeng 35:727−731

Snoek ISI, Steensma HY (2006) Why does *Kluyveromyces lactis* not grow under anaerobic conditions? Comparison of essential anaerobic genes of *Saccharomyces cerevisiae* with the *Kluyveromyces lactis* genome. FEMS Yeast Res 6:393−403

Sootsuwan K, Lertwattansakul N, Thanonkeo P, Matsushita K, Yamada M (2008) Analysis of the respiratory chain in ethanologenic *Zymomonas mobilis* with a cyanide-resistant *bd*-type ubiquinol oxidase as the only terminal oxidase and its possible physiological roles. J Mol Microbiol Biotechnol 14:163−175

Spencer-Martins I (1994) Transport of sugars in yeasts - implications in the fermentation of lignocellulosic materials. Bioresour Technol 50:51–57

Sreenath HK, Jeffries TW (1999) 2-deoxyglucose as a selective agent for derepressed mutants of *Pichia stipitis*. Appl Biochem Biotechnol 77:211–222

Stanke M, Schöffmann O, Morgenstern B, Waack S (2006) Gene prediction in eukaryotes with a generalized hidden Markov model that uses hints from external sources. BMC Bioinformatics 7:62

Stanke M, Waack S (2003) Gene prediction with a hidden Markov model and a new intron submodel. Bioinformatics 19:ii215–ii225

Steizt TA (1971) Structure of yeast hexokinase-B. I. Preliminary x-ray studies and subunit structure. J Mol Bio 61:695–700

Suzuki T, Hoshino T, Matsushika A (2014) Draft genome sequence of *Kluyveromyces marxianus* strain DMB1, isolated from sugarcane bagasse hydrolysate. Genome Announcements 2:e00733–14

Szulczyk KR, McCarl BA, Cornforth G (2010) Market penetration of ethanol. Renew Sust Energy Rev 14:394–403

Tanino T, Hotta A, Ito T, Ishii J, Yamada R, Hasunuma T, Ogino C, Ohmura N, Ohshima T, Kondo A (2010) Construction of a xylose-metabolizing yeast by genome integration of xylose isomerase gene and investigation of the effect of xylitol on fermentation. Appl Microbiol Biotechnol 88:1215–1221

Tarrio N, Becerra M, Cerdan ME, Gonzalez-Siso MI (2006a) Reoxidation of cytosolic NADPH in *Kluyveromyces lactis*. FEMS Yeast Res 6:371–380

Tatusov RL, Fedorova ND, Jackson JD, Jacobs AR, Kiryutin B, Koonin EV, Krylov DM, Mazumder R, Mekhedov SL, Nikolskaya AN, Rao BS, Smirnov S, Sverdlov AV, Vasudevan S, Wolf YI, Yin JJ, Natale DA (2003) The COG database: an updated version includes eukaryotes. BMC Bioinformatics 4:41

Thompson JD, Higgins DG, Gibson TJ (1994) CLUSTALW: improving the sensitivity of progressive multiple sequence alignment through sequence weighting, position-specific gap penalties and weight matrix choice. Nucleic Acids Res 22:4673–4680

Treitel MA and Carlson (1995) Repression by SSN6-TUP1 is directed by MIG1, a repressor/activator protein. Proc Natl Acad Sci USA 92 (8):3132–3136

Treitel MA, Kuchin S, Carlson M (1998) Snf1 protein kinase regulates phosphorylation of the Mig1 repressor in *Saccharomyces cerevisiae*. Mol Cell Biol 18:6273–6280

Tsukahara K and Sawayama S (2005) Liquid fuel production using microalgae. J Jpn Pet Inst 48:251–259

Tzagoloff A, Nobrega M, Gorman N, Sinclair P (1993) On the functions of the yeast *COX10* and *COX11* gene products. Biochem Mol Biol Int 31 (3):593–598

Tzamarias D and Struhl K (1994) Functional dissection of the yeast Cyc8-Tup1 transcriptional co-repressor complex. Nature 369 (6483):758–761

Tzamarias D and Struhl K (1995) Distinct TPR motifs of Cyc8 are involved in recruiting the Cyc8-Tup1 corepressor complex to differentially regulated promoters. Genes Dev 9 (7):821–831

Vallier LG, Carlson M (1994) Synergistic release from glucose repression by mig1 and ssn mutations in *Saccharomyces cerevisiae*. Genetics 137:49–54
van Dijken JP, Scheffers WA (1986) Redox balances in the metabolism of sugars by yeasts. FEMS Microbiol Rev 32:199–224
van Ooyen AJ, Dekker P, Huang M, Olsthoorn MM, Jacobs DI, Colussi PA, Taron CH (2006) Heterologous protein production in the yeast *Kluyveromyces lactis*. FEMS Yeast Res 6:381–392
Vasallo MDC, Puppo MC, Palazolo GG, Otero MA, Beress L, Wagner JR (2006) Cell wall proteins of *Kluyveromyces fragilis*: surface and emulsifying properties. LWT-Food Sci Technol 39 (7):729–739
Veiga A, Arrabaça JD, Loureiro-Dias MC (2000) Cyanide-resistant respiration is frequent, but confined to yeasts incapable of aerobic fermentation. FEMS Microbiol Lett 190:93−97
Veiga A, Arrabaça JD, Loureiro-Dias MC (2003) Cyanide-resistant respiration, a very frequent metabolic pathway in yeasts. FEMS Yeast Res 3:239−245
Vemuri GN, Eiteman MA, McEwen JE, Olsson L, Nielsen L, Nielsen J (2007) Increasing NADH oxidation reduces overflow metabolism in *Saccharomyces cerevisiae*. Proc Natl Acad Sci USA 104:2402–2407
Wackett LP (2008) Biomass to fuels via microbial transformation. Curr Opin Chem Biol 12:187−193
Walker GM (2011) 125th Anniversary review: Fuel alcohol: Current production and future challenges. J Inst Brew 117:3–22
Watanabe S, Saleh AB, Pack SP, Annaluru N, Kodaki T, Makino K (2007) Ethanol production from xylose by recombinant *Saccharomyces cerevisiae* expressing protein engineered $NADP^+$-dependent xylitol dehydrogenase. J Biotechnol 130 (3):316–319
Westermann B, Neupert W (1997) Mdj2p, a novel DnaJ homolog in the mitochondrial inner membrane of the yeast *Saccharomyces cerevisiae*. J Mol Biol 272 (4):477–483
Westman JO and Franzén CJ (2015) Current progress in high cell density yeast bioprocesses for bioethanol production, Review. Biotechnol J 10:1185–1195
Weusthuis RA, Adams H, Scheffers WA, Vandijken JP (1993) Energetics and kinetics of maltose transport in *Saccharomyces cerevisiae* -a continuous-culture study. Appl Environ Microbiol 59:3102−3109
Wick AN, Drury DR, Nakada HI, Wolfe JB (1957) Localization of the primary metabolic block produced by 2-deoxyglucose. J Biol Chem 224:963–969
Wilson WA, Hawley SA, Hardie DG (1996) Glucose repression/derepression in budding yeast: SNF1 protein kinase is activated by phosphorylation under derepressing conditions, and this correlates with a high AMP:ATP ratio. Curr Biol 6:1426–1434
Wiselolgel A (1996) Biomass feedstock resources and composition in: Wyman C (Ed) handbook on bioethanol production and utilization. Taylor and Francis Washington DC pp 108–118
Wood V, Gwilliam R, Rajandream MA, Lyne M, Lyne R, Stewart A, Sgouros J, Peat N, Hayles J, Baker S, Basham D, Bowman S, Brooks K, Brown D, Brown S, Chillingworth T, Churcher C, Collins M, Connor R, Cronin A, Davis P, Feltwell T, Fraser A, Gentles S, Goble A, Hamlin N, Harris D,

Hidalgo J, Hodgson G, Holroyd S, Hornsby T, Howarth S, Huckle EJ, Hunt S, Jagels K, James K, Jones L, Jones M, Leather S, McDonald S, McLean J, Mooney P, Moule S, Mungall K, Murphy L, Niblett D, Odell C, Oliver K, O'Neil S, Pearson D, Quail MA, Rabbinowitsch E, Rutherford K, Rutter S, Saunders D, Seeger K, Sharp S, Skelton J, Simmonds M, Squares R, Squares S, Stevens K, Taylor K, Taylor RG, Tivey A, Walsh S, Warren T, Whitehead S, Woodward J, Volckaert G, Aert R, Robben J, Grymonprez B, Weltjens I, Vanstreels E, Rieger M, Schafer M, Muller-Auer S, Gabel C, Fuchs M, Fritz C, Holzer E, Moestl D, Hilbert H, Borzym K, Langer I, Beck A, Lehrach H, Reinhardt R, Pohl TM, Eger P, Zimmerman W, Wedler H, Wambutt R, Purnelle B, Goffeau A, Cadieu E, Dreano S, Gloux S, Lelaure V, Mottier S, Galibert F, Aves SJ, Xiang Z, Hunt C, Moore K, Hurst SM, Lucas M, Rochet M, Gaillardin C, Tallada VA, Garzon A, Thode G, Daga RR, Cruzado L, Jimenez J, Sanchez M, del Rey F, Benito J, Dominguez A, Revuelta JL, Moreno S, Armstrong J, Forsburg SL, Cerrutti L, Lowe T, McCombie WR, Paulsen I, Potashkin J, Shpakovski GV, Ussery D, Barrell BG, Nurse P (2002) The genome sequence of *Schizosaccharomyces pombe*. Nature 415:871−880

Workman WE, Day DF (1984) The cell wall-associated inulinase of *Kluyveromyces fragilis*. Antonie van Leeuwenhoek 50: 349–353

Yoshida K and Blobel G (2001) The karyopherin Kap142p/Msn5p mediates nuclear import and nuclear export of different cargo proteins. J Cell Biol 152 (4):729–740

Zaldivar J, Nielsen J, Olsson L (2001) Fuel ethanol production from lignocellulose: a challenge for metabolic engineering and process integration. Appl Microbiol Biotechnol 56 (1):17–34

Zeng X, Barros MH, Shulman T, Tzagoloff A (2008) *ATP25*, a new nuclear gene of *Saccharomyces cerevisiae* required for expression and assembly of the Atp9p subunit of mitochondrial ATPase. Mol Biol Cell 19:1366−1377

Zhang B, Zhang L, Wang D, Gao X, Hong J (2011) Identification of a xylose reductase gene in the xylose metabolic pathway of *Kluyveromyces marxianus* NBRC1777. J Ind Microbiol Biotechnol 38:2001−2010

Zoppellari F and Bardi L (2013) Production of bioethanol from effluents of the dairy industry by *Kluyveromyces marxianus*. N Biotechnol 30 (6):607–613

ACKNOWLEDGEMENTS

I express my deepest gratitude to my supervisors, Prof. Dr. Mamoru Yamada, for creative guidance, attentive supervision and encouragement throughout this research. Besides, he also provides good opportunities and good suggestions, which are valuable to my future career. Your vast knowledge and enthusiastic attitude towards science have been encouraging and motivating.

Beside my advisor, I would like to thank Assist. Prof. T. Kosaka, Prof. Dr. K. Matsushita and Assoc. Prof. T. Yakushi for their helpful discussion and valuable advice.

I am particularly grateful to Dr. Masayuki Murata, Dr. Naoko Fujimoto, Dr. Noppon Lertwattanasakul, Dr. Kannikar Charoensuk, Dr. Nadchanok Rodrussamee, Dr. Sukanya Nitiyon, Mochamad Nurcholis, M.Agr., and members of Josei laboratory who study in Yamaguchi University for their valuable comments, discussion, suggestions and friendship during my study in Yamaguchi University.

I am extremely thankful to the Directorate General of Resources for Science, Technology and Higher Education (DIKTI) scholarship, Ministry of Research, Technology and Higher Education of Indonesia, Brawijaya University, Indonesia for financial support and Department of Biological Chemistry, Yamaguchi University for providing laboratory facilities.

Finally, I greatly appreciate to my parents, my family and my friends for their understanding, encouragement and powerful support.

Suprayogi

Graduate School of Medicine
Yamaguchi University
Japan

SUMMARY

Basic study on thermotolerant yeast *Kluyveromyces marxianus* DMKU 3-1042 toward efficient conversion of cellulosic biomass to ethanol

High-temperature fermentation technology with thermotolerant microbes has been expected to reduce the cost of conversion of biomass to useful materials. Bioethanol from cellulosic biomass is an environment-friendly alternative to fossil fuels but materials derived from such biomass contain various sugars including glucose, which inhibits the assimilation of other sugars via the glucose-repression mechanism. Thermotolerant ethanologenic yeast *Kluyveromyces marxianus* is capable of fermenting various sugars including xylose but exhibits the glucose repression to hamper the utilization of other sugars. In this study, four research topics in the yeast were performed: 1) isolation and characterization of spontaneous mutants bearing glucose repression-defectiveness, 2) isolation and characterization of *kan*MX4-inserted mutants bearing glucose repression-defectiveness, 3) determination of complete genome sequence and analysis of transcriptome and 4) analysis of assimilation of xylose and/or arabinose via a random *kan*MX4 insertion mutagenesis.

To acquire glucose repression-defective mutants, 33 isolates as 2-deoxyglucose (2-DOG)-resistant mutants were isolated and characterized on their sugar consumption abilities and cell growth and ethanol accumulation along with cultivation time. As a result, they were classified into three groups. The first group (3 isolates) utilized glucose and xylose in similar patterns along with cultivation to those of the parental strain, presumably due to reduction of the uptake of 2-DOG or enhancement of its export. The second group (29 isolates) showed greatly delayed utilization of glucose, presumably by reduction of the uptake or initial catabolism of glucose. The last group, only one isolate, showed enhanced utilization ability of xylose in the presence of glucose. Further analysis revealed that the isolate had a single nucleotide mutation to cause amino acid substitution (G270S) in *RAG5* encoding hexokinase and exhibited very low activity of the enzyme.

2-DOG-resistant mutants were also isolated from randomly *kan*MX4-inserted mutants. Analysis of the sugar utilization ability revealed that there were two categories of the intragenically *kan*MX4-inserted mutants including the *mig1* mutant as a control. One group showed enhanced utilization of xylose in the presense of glucose, presumably due to a defect in the glucose-repression mechanism, and the other group showed delayed utilization of glucose, probably by reduction of the uptake or initial catabolism of glucose. Considering the possible functions of the disrupted genes in these mutants, it is assumed that *K. marxianus* has undiscovered mechanisms for glucose repression and complex regulation for the uptake or initial catabolism of glucose.

The complete genome sequence of *K. marxianus* DMKU 3-1042 as one of the most thermotolerant strains in the same species has been determined. Comparison of its genomic information with those of other yeasts and transcriptome analysis revealed that the yeast bears beneficial properties of

temperature resistance, wide-range bioconversion ability and production of proteins. The transcriptome analysis clarified distinctive metabolic pathways under three different growth conditions, static culture, high temperature and xylose medium, in comparison to the control condition of glucose medium under a shaking condition at 30°C. Interestingly, the yeast appears to overcome the issue of reactive oxygen species, which tend to accumulate under all three conditions. This study provides many gene resources for the ability to assimilate various sugars in addition to species-specific genes in *K. marxianus*, and the molecular basis of its attractive traits for industrial applications including high-temperature fermentation.

In order to identify key factors involved in pentose metabolism, *K. marxianus* DMKU 3-1042 was mutagenized by a random *kan*MX4-insertion mutagenesis and screened mutants that were unable to assimilate xylose and/or arabinose as a sole carbon source. Consequently, three mutants of *COX15*, *ATP25* and *CYC3* encoding a cytochrome oxidase assembly factor (singleton), a transcription factor required for assembly of the Atp9p subunit of mitochondrial ATP synthase and cytochrome *c* heme lyase, respectively, were obtained. They exhibited incapability of growth on non-fermentable carbon sources, such as acetate or glycerol, and thermosensitiveness. Their biomass formation in glucose medium was reduced, but ethanol yields were increased with a high ethanol level in the medium, compared to those of the parental strain. Experiments with respiratory inhibitors showed that *cox15* and *cyc3*, but not *atp25*, were able to grow in glucose medium containing antimycin A and that the *atp25* mutant was KCN-resistant. Activities of NADH and ubiquinol oxidases in membrane fractions of all mutants became a half of that of the parent and negligible, respectively, and their remaining NADH oxidase activities were found to be resistant to KCN. Absolute absorption spectral analysis revealed that the peak corresponding to $a+a_3$ was very small in *atp25* and negligible in *cox15* and *cyc3*. These findings suggest that the *K. marxianus* strain possesses an alternative KCN-resistant oxidase that is located between primary dehydrogenases and the ubiquinone pool and that the respiratory activity is essential for utilization of pentose.

LIST OF PUBLICATIONS

This thesis is based on the following four studies, which are referred to in chapter 2, 3, 4 and 5.

1. A *Kluyveromyces marxianus* 2-deoxyglucose-resistant mutant with enhanced activity of xylose utilization

Suprayogi, Minh T. Nguyen, Noppon Lertwattanasakul, Nadchanok Rodrussamee, Savitree Limtong, Tomoyuki Kosaka, Mamoru Yamada

International Microbiology, in press

(CHAPTER 2)

2. Characteristics of *kan*MX4-inserted mutants that exhibit 2-deoxyglucose resistance in thermotolerant yeast *Kluyveromyces marxianus*

Suprayogi, Mochamad Nurcholis, Masayuki Murata, Noppon Lertwattanasakul, Tomoyuki Kosaka, Nadchanok Rodrussamee, Savitree Limtong, Mamoru Yamada

The Open Biotechnology Journal, in press

(CHAPTER 3)

3. Genetic basis of the highly efficient yeast *Kluyveromyces marxianus:* complete genome sequence and transcriptome analyses

Noppon Lertwattanaskul, Tomoyuki Kosaka, Akira Hosoyama, Yutaka Suzuki, Nadchanok Rodrussamee, Minenosuke Matsutani, Masayuki Murata, Naoko

Fujimoto, Suprayogi, Keiko Tsuchikane, Savitree Limtong, Nobuyuki Fujita, Mamoru Yamada

Biotechnology for Biofuels 2015, 8 (47):1-14 DOI: 10.1186/s13068-015-0227-x

(CHAPTER 4)

4. Essentiality of respiratory activity for pentose utilization in thermotolerant yeast *Kluyveromyces marxianus* DMKU 3-1042

Noppon Lertwattanaskul, Suprayogi, Masayuki Murata, Nadchanok Rodrussamee, Savitree Limtong, Tomoyuki Kosaka, Mamoru Yamada

Antonie van Leeuwenhoek 2013, 103 (4):933-945 DOI: 10.1007/s10482-012-9874-0

(CHAPTER 5)